Universität für Bodenkultur Wien

Towards a Structure-Function Link of Microbial Succession:

A Characterization of the Fungal Community during Beech Litter Decay and Optimization of a phylum-specific rRNA Capture Technique.

Doctoral thesis of

DI SANDRA MOLL, BEd

Aimed academic degree:

Doctor of Natural Resources and Life Sciences

(Dr.nat.techn.)

Matrikelnummer: 0240113

Study ID number: H788 915

Main advisor: Univ.Prof.Dr. Joseph Strauss

Advisory team member: Assoc. Prof. Dr. Katja Sterflinger-Gleixner

University: University of Natural Resources and Life Sciences Vienna

Department of Applied Genetics and Cell Biology

Tulln, Austria- August 2016

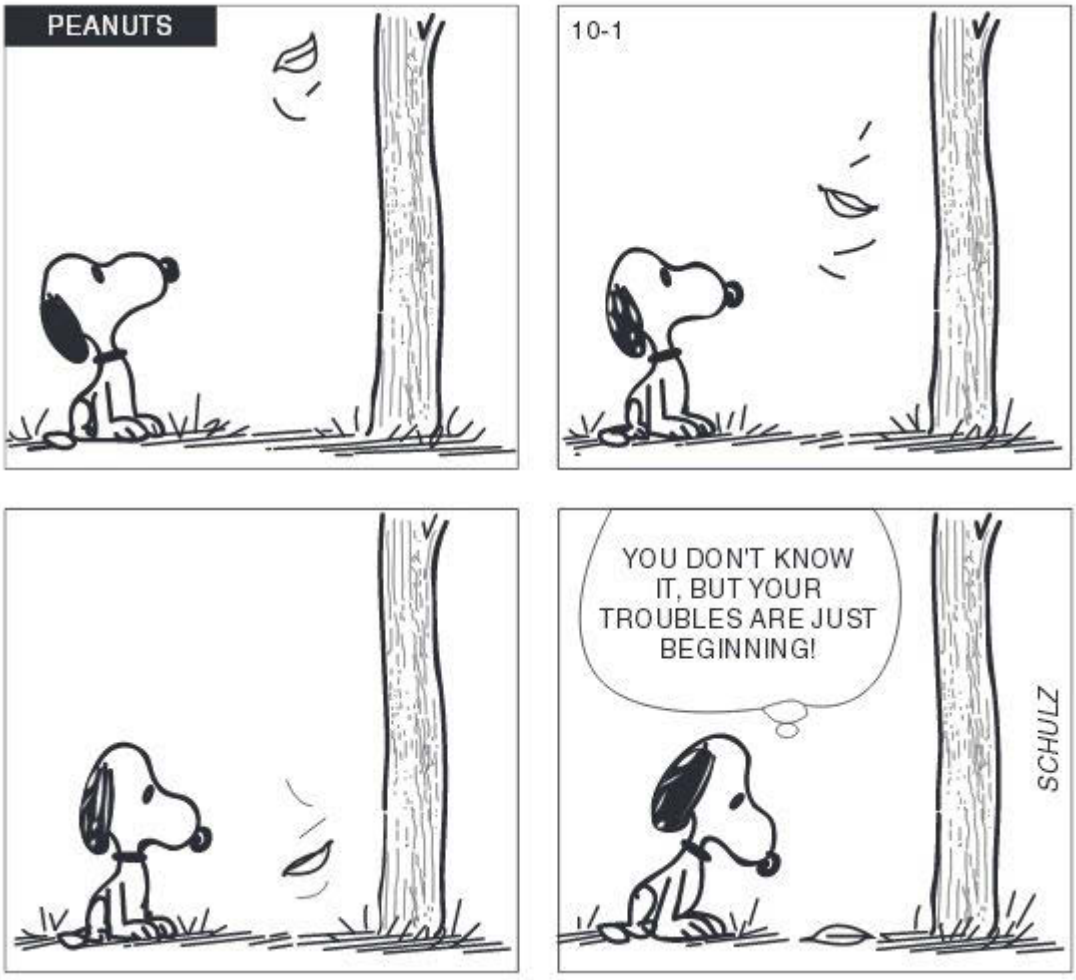

Figure 1: Snoopy's view of decomposition and soil organic matter formation, as published in 'Soil Microbiology, Ecology, and Biochemistry', Third Edition 2007, Paul E.A. (Editor), Elsevier Academic Press.

DANKSAGUNG

Der Entstehungsprozess dieser im Jahre 2008 gestarteten Arbeit war mit einigen Rückschlägen und kreativen Pausen gemeinsam mit wissenschaftlicher und persönlicher Weiterentwicklung durchwachsen. Ich verdanke die Chance und Motivation zur Fertigstellung meinem Betreuer Joseph, der mich in den 10 Jahren unserer Zusammenarbeit in vielerlei Hinsicht geprägt und mir immer geholfen hat, an mich zu glauben. Er bietet einen unerschöpflichen Pool an Inspiration und ist für mich bewundernswert sowohl auf menschlicher als auch wissenschaftlicher Ebene. Ich bin dankbar für eine anstrengende und doch lustige gemeinsame Zeit mit vielen KollegInnen innerhalb der AG Strauss- insbesondere Aga, Christoph und Stefan- und für die Zusammenarbeit mit WissenschafterInnen an der BOKU, am AIT, an der Universität Wien und am BFW. Danke an das ehemalige "Team Brehmstraße" besonders Dragana und Markus für eure Unterstützungen, sowie dem gesamten Team von MICDIF.

Diese Arbeit wäre immer noch unvollendet ohne die Hilfe meiner Familie: meine Eltern und Schwiegereltern – ohne Euch hätte ich nichts von alledem geschafft. Ich bin dankbar für die viele Zeit und Unterstützung die ich von euch allen bekommen habe, damit ich diese Arbeit verfassen konnte! Meinem Mann Herwig, der mit mir gemeinsam unsere Welt zusammenhält sowie unseren Kindern Edmund und Liselotte danke für die Abwechslung, Herausforderung und Freude die ihr mir täglich bietet.

ABSTRACT

Highly diverse fungal decomposer communities are at the center of terrestrial litter decomposition, however little is known about the successional involvement of different fungi and bacteria within this process. Additionally, improved methods for tracking nutrient use pathways are needed to conquer the lack of knowledge in understanding exactly which microbial taxa are actively contributing to nutrient flow.

In this study a characterization of the fungal community on Austrian beech litter from four different locations was conducted in a laboratory microcosm experiment, using a combined approach of RFLP typing and clone library sequencing. Richness and diversity methods as well as taxonomic analysis lead to a complete description of fungal species on Austrian beech litter based on molecular data. The highly uneven fungal community was dominated by *Ascomycota*. Most assigned genera are known to be associated with litter decomposition, and were not specific for a particular location. One location showed a significantly different fungal community from the other three locations, possibly because of environmental and nutrient differences. Fungal diversity and richness were shown to increase quickly during the first two weeks of incubation, which lead to a possible underrepresentation of rare species. In a mesocosm experiment, fungi dominated decomposition especially on high nutrient litter. From the same inoculum, very distinctive microbial communities evolved on nutritionally different beech litters within only two weeks. However eventually, the relative involvement of fungi versus bacteria during litter decomposition went down to the same ratio in all locations. Temperature stress did not induce drastic changes in the microbial community. The further development of the PhyloTrap method, using rRNA as a target molecule, was another task of this study. This method is a promising tool to gain futher insight into nutrient acquisition pathways and community shift patterns. Experimental conditions were optimized with the goal to separate a mix of pure culture RNAs by specific probes and increase the yield and purity of the obtained SSU RNA. The use of different probes- on various phylogenetic levels- will allow for phylogenetic separation of an environmental RNA sample in the future. Together with the application of stable isotope substrates and subsequent detection in the RNA this method will be able to answer multiple questions in microbial ecology.

Keywords: microbial ecology; fungi; litter decomposition; phylogenetic separation; SSU rRNA;

ZUSAMMENFASSUNG

Die Funktion von Ökosystemen wäre undenkbar ohne den Laubstreuabbau durch mikrobielle Gemeinschaften, wobei Mikropilze eine wichtige Rolle spielen. Die genaue Abfolge von Pilzen und Bakterien innerhalb der Abbauprozesse ist jedoch nur schlecht verstanden. Um die mikrobielle Arbeitsteilung innerhalb der Nährstoffkreisläufe genauer zu beschreiben werden neue Methoden benötigt, speziell wenn es um die Vernetzung von Diversität und Funktion geht. In dieser Arbeit wurde zunächst die Mikropilzdiversität in Laubstreuproben ermittelt, welche sich in Abhängigkeit von Nährstoffangebot sowie Fortschritt des Abbaus dynamisch anpasst. Durch RFLP und Sequenzierung wurde die Pilzgemeinschaft in Buchenstreu vier verschiedener Standorte in Österreich mit Hilfe molekularer Daten beschrieben. Artenvielfalt und Diversität der Standorte wurde verglichen und an verschiedenen Zeitpunkten dargestellt. Innerhalb der Pilzgemeinschaft war die Ausgewogenheit der Arten sehr gering, aufgrund einer ausgeprägten Dominanz an Ascomyceten. Es traten allgemein an allen Standorten typische Spezies mit Bedeutung im Streuabbau auf. Ein Standort fiel im Vergleich zu den anderen 3 Standorten durch eine sehr spezielle Zusammensetzung der Mikropilze auf, vermutlich aufgrund unterschiedlicher Umwelt- und Nährstoffbedingungen. Innerhalb der ersten zwei Wochen der Inkubation stiegen sowohl die Anzahl der verschiedenen Pilzspezies (Artenvielfalt) als auch die Häufigkeit der einzelnen Arten (Pilzdiversität) rasch an. Versuche in Mesokosmen zeigten, dass sich auf steriler Laubstreu mit unterschiedlicher Ressourcenverfügbarkeit sich aus dem selben Inokulum innerhalb von nur zwei Wochen unterschiedliche mikrobielle Gemeinschaften. Im Laufe des Abbaus wurde jedoch ein immer ähnlicheres Verhältnis Pilze/Bakterien für alle Standorte erreicht. Der Streuabbau war insbesondere unter hohem Ressourcenangebot stark pilzdominiert. Temperaturstress zeigte keine wesentliche Veränderung der mikrobiellen Gemeinschaftsverhältnisse auf Basis von DNA-Analysen.

Die Weiterentwicklung einer Methode zur Detektion metabolischer Aktivitäten in phylogenetisch aufgetrennten Proben (PhyloTrap) war ein weiterer Teil dieser Arbeit. Ribosomale RNA soll dabei künftig als Markermolekül dienen, um assimilatorische Aktivität, z.B. beim Abbau von Laubstreu, mit Hilfe stabiler Isotope anzuzeigen. Die experimentellen Bedingungen wurden für die Anwendung bakterieller sowie eukaryotischer Sonden optimiert, um eine gemischte Probe wieder in die Bakterien- und Pilz RNA aufzutrennen. Hauptaugenmerk galt dabei der Spezifität der Sonden sowie der Maximierung der Ausbeute. Das Potential dieser Methode liegt in der dualen Aussagekraft des funktionellen Biomarkers SSU-rRNA. Sowohl assimilatorische

Aktivität (Einbau der Markersubstanz) als auch phylogenetische Auflösung ermöglichen dann einen direkten Rückschluß auf die Diversitätsstruktur und die damit zusammenhängende Aktivität in komplexen mikrobiellen Ökosystemprozessen.

Keywords: Mikrobielle Ökologie; Mikropilze; Streuabbau; phylogenetische Marker; SSU rRNA;

TABLE OF CONTENTS

DESIGN OF THE STUDY

The objective of this study was the characterization of microbial communities in early beech litter decay under different litter nutrient ratios, and to improve a novel phylogenetic separation method (the "PhyloTrap") for targeting active microbial communities. Fungal richness and diversity from four different beech litter locations was evaluated and a taxonomic characterization based on molecular sequencing data was achieved from a combined approach of Restriction Fragment Length Polymorphism (RFLP) and clone library construction. First, the undisturbed fungal community of each sample was described taxonomically, following a comparison of biodiversity and richness parameters between locations and time points up to 14 days. The same four sampling locations were used within the framework of the MICDIF project (FWF-project S100, see page 3) *„Linking microbial diversity and ecosystem functions across scales and interfaces",* where sterilized and re-inoculated beech litter samples from a mesocosm study were produced over a time course of 15 months. MICDIF mesocosm samples were used to examine the contribution of fungi and bacteria to beech litter decomposition over the time course via Real time- PCR. With the idea to further investigate functionally active species within the decomposer network, a magnetic bead- based phylogenetic separation method for ribosomal SSU RNA was adapted for the use with fungal specific probes. This method, in combination with the application of stable isotope labelled substrates and subsequent nano-SIMS mass spectrometry, has the potential to determine which species are successively active as decomposition progresses.

The specific research questions of this work were:

1. Which fungal species are present on beech litter from four different sites in Austria?
2. Does the richness and diversity of the fungal beech litter community show any impact of sampling location- and therefore nutrient ratios?
3. Is there a succession of fungal species during the onset of beech litter decay?
4. Does the involvement of microbes on four different beech litter samples change during decomposition?
5. How does temperature stress alter fungal/bacterial involvement in different beech litter samples?
6. Is it possible to separate fungal and bacterial SSU RNA from mixed RNA samples with a hybridization method based on microbeads?

Ad.1 To find out which fungal species were present on the native unsterilized beech litter, samples from four different forest locations in Austria were used. A molecular genotyping approach employing a combination of Restriction Fragment Length Polymorphism (RFLP) and clone library construction together with sequencing generated the data to answer this question. See 3.1. for a detailed list of the assigned fungal species. Most of them involved known litter endophytes or saprophytes.

Ad.2 Taxonomic analysis and an array of methods to describe richness and diversity were employed to obtain a detailed characterization of the fungal community from four different locations. See 3.1.for detailed results. Even though all samples were characterized as highly uneven, one sampling site (SW) showed a very different fungal community than the other locations.

Ad.3 Changes in community composition, richness and diversity at the start of decomposition were detected in a small-scale laboratory microcosm experiment, unsterilized beech litter samples from four different locations were incubated at room temperature and 60% water content for 2 and 14 days respectively. Taxonomic characterization after fungal clone library sequencing showed a trend towards a higher species richness, together with decreasing dominant species with incubation time. There was clearly a succession in the remarkably small time frame of only two weeks.

Ad.4 To find out if the microbial community was changing during 15 months of decomposition in a mesocosm experiment, the fungal/bacterial ratio over the time course was assessed via quantitative Real-time PCR. All four litter types showed very different F/B ratios at the beginning of the experiment, but the ratios changed with time, until they eventually reached the same ratio at the end of the experiment. This means that the involvement of microbes was indeed changing during the course of the experiment.

Ad.5 By quantitative Real-Time PCR, the fungal/bacterial involvement in beech litter decomposition after temperature stress did not show drastic changes compared to the unstressed conditions. Frost stress caused a slight decrease in F/B ratios.

Ad.6 A magnetic bead-based method using biotinylated oligos was finetuned and optimized. A specific capture of fungal and bacterial SSU rRNA from a mixed RNA sample was successful using hybridization with two specific probes.

THE MICDIF PROJECT

The MICDIF project (Nationales Forschungsnetzwerk FWF S 100) "*Linking microbial diversity and ecosystem functions across scales and interfaces*" was a multi-disciplinary project which started in 2007 with the aim to unravel links between community structure and ecosystem functioning. It consisted of 8 individual projects and involved several research groups and universities in Austria and Switzerland (Richter, 2006). One of the project goals was to examine the influences of ecological stoichiometry, i.e. elemental composition of resources, on microbial community shifts and metabolism changes. Conceptual ideas on how to implement ecological stoichiometry to ecosystem ecology were published in an early synthesis paper (Hall *et al.*, 2011). A review publication on the possible adaptations of terrestrial microbial decomposer communities to stoichiometric resource imbalances summarizes the main findings of MICDIF and puts them in a broad ecological context (Mooshammer *et al.*, 2014b).

The project started with a baseline experiment on microbial stoichiometry in pure cultures (E0), which produced insights into nutrient-related dynamics on microbial carbon-use efficiency (Keiblinger *et al.*, 2010) in four microbial species. Based on macromolecular composition data from the E0 project, a model was developed to predict the microbial biomass stoichiometry response to resource changes by trade-offs among cellular components (Franklin *et al.*, 2011). The next level of the project involved co-culture experiments of a fungus and a bacterium growing on beech litter, and results suggested 'cheating' behavior of bacteria during litter decomposition (Schneider *et al.*, 2010). Central experiments of MICDIF were based on nutritionally distinct beech litter sampled at four different locations in Austria. Effects of the different beech litter nutrient chemistry were shown in experimentally grown hyporheic biofilms (Hall *et al.*, 2012), as well as in litter decomposition experiments. The early phase of litter decomposition was shown to be accompanied by fast and major changes in the microbial community by PFLA experiments (Brandstatter *et al.*, 2013). Enzyme activity patterns were shown to be directly linked to microbial community composition in a tree girdling experiment, which explains the link between nutrient availability differences and seasonal changes within the decomposition process (Kaiser *et al.*, 2010). The development of a novel ^{15}N isotope pool dilution assay (Wanek *et al.*, 2010) was crucial for the finding that not only the rates of gross protein depolymerization by extracellular enzymes, but also the N demand of the microbial community controls N mineralization to ammonium. That is because within the N limited process of litter decomposition, rather than complete mineralization before assimiliation (i.e. the M-I-T route mineralization-immobilization

turnover), microbes seem to prefer a more direct route and take up released amino acids directly (Wanek *et al.*, 2010), (Wanek *et al.*, 2011). A similar isotope pool dilution assay was developed using ^{13}C Glucose as a tracer, which allowed for calculation of gross rates of glucose production through glucan depolymerization and microbial glucose consumption rates (Leitner *et al.*, 2012). In the main MICDIF experiment (E1), four beech litter types with different C:N:P stoichiometry were sterilized and re-inoculated with the same starting community. A mesocosm decomposition experiment was conducted over the course of 15 months. Samples of these mesocosms were distributed to different research groups addressing various research questions. For example, it was demonstrated that gross N and P cycling processes were influenced by C:nutrient ratios (Mooshammer *et al.*, 2012) because homeostatic microbes maintain their elemental composition regardless of their resources, forcing them to adjust their nutrient mineralization and immobilization patterns to compensate litter nutrient ratio changes. This metabolic flexibility of microbial communites was suggested to be facilitated by adjustments of microbial nitrogen use efficiency (NUE)(Mooshammer *et al.*, 2014a). Microbial succession within the litter decomposition experiment was assessed by a metaproteomic approach, showing that litter C:N:P stoichiometry has an influence on both microbial community structure and activity (Schneider *et al.*, 2012), revealing fungi as key players in terms of main extracellular enzyme production. A following MICDIF experiment mimicking climate change events (E2) resulted in short-to medium term changes of microbial functions, but not on a community compositon level (Keiblinger *et al.*, 2012). The main goals of MICDIF, to investigate input stoichiometry effects on microbial communities, were achieved both directly (microbial community structure change) and indirectly (metabolism and enzyme activity change). The overall project design was complex, however the outcome takes our understanding of decomposition a few steps closer to eventually *'link microbial diversity and ecosystem function across scales and ecosystems'.*

The results discussed in this study were produced within the framework of MICDIF. Litter samples were collected for all research groups in 2009. Some of the experiments in this study involved litter samples in their native, unsterilized state ('native litter experiments'), subsamples of the mesocosm decomposition experiment were produced for all research groups and involved sterilized and re-inoculated litter. Mesocosms were maintained under the supervision of Dr.Ieda Hämmerle at the University of Vienna. Litter stoichiometry data used for data interpretation in this study were provided by Dr.Katharina Keiblinger (Institute of Soil Research, BOKU) .

1 INTRODUCTION

Litter decomposition is a tremendously important ecosystem process involving a high diversity of organisms and stands out as a key mechanism in the global balance between carbon sequestration and mineralization. The importance of fungi in the process of litter decomposition is emphasized by emerging research (Schneider *et al.*, 2012, Amend *et al.*, 2015). Their ability to break down biopolymers like lignin, cellulose and hemicellulose is crucial for nutrient cycling within the ecosystem (Dashtban *et al.*, 2010, Makela *et al.*, 2014). These compounds are structurally highly complex, making them inaccessible to plants and microorganisms. The breakdown of dead plant material into accessible forms is facilitated by fungi, being able to tolerate high C:N ratios in their substrate. Especially at the very beginning of decomposition, these initial decay steps are crucial as they provide substrates for other species in the decomposer community. This represents a key feature of carbon cycling, which is ultimately critical for the global climate(Chapin III *et al.*, 2002).

1.1 Ecosystems and communities

Ecology has a very broad definition: ranging from abundance and distribution of organisms, to their interactions with the environment. Ecologists needed a way to make their scientific life more convenient, so they started to introduce the concepts of ECOSYSTEMS and COMMUNITIES, chopping the global ecology into bite-size pieces, making it easier to study specific processes and dynamics. An ecosystem can range in size by several orders of magnitude- it can be a river, a forest, a tree, a bunch of leaves on the forest floor, or the Earth as a whole. It involves all organisms and the abiotic pools within the boundaries of the system. An ecosystem process describes energy and material transfers between the pools, and can be studied at various scales, according to the researcher's choice (Chapin III *et al.*, 2011b). The term 'ecosystem' has first been mentioned by Sir Arthur G. Tansley in 1935, printed in the famous journal 'Ecology', where he stated that the organisms could …..

'….not be separated from their special environment, with which they form one physical system.'(Tansley, 1935)

Essential abiotic, physical components of a terrestrial ecosystem include water, atmosphere, climate, soil and rocks. Biological components of ecosystems include plants, animals and decomposers. The abiotic and biotic components of an ecosystem are connected in a network. Ecosystems cycle energy and matter, and they are

influenced by their environment, which results in a wide spectrum of different ecosystems (Jørgensen, 2008). They are open, complex systems that are hierarchically organized. The initial energy input is the starting point for the trophic-dynamic model of ecosystem structure (Lindeman, 1942): energy flows into an ecosystem in the form of sunlight, is captured by plants as the primary producers, and passed on to the next trophic levels with losses due to respiration (Cotgreave & Forseth, 2002), up to Herbivores and finally to top consumers (Carnivores). These trophic chains can be seen as pathways for energy flow within ecosystems, with Decomposers returning energy back into the system. This is emphasizing that energy flow and biogeochemical nutrient cycling are the major components of an ecosystem network, which is maintained by decomposer communities.

A big question in ecology is: why are species found in one area and not in others? A well-known hypothesis first written by Lourens Baas-Becking in 1934 claims that '*Everything is everywhere, but, the environment selects*' (Baas Becking, 1934). Even though there are now more and more studies questioning this general paradigm, environmental factors are known to perform as filters in community assembly. Every habitat has a characteristic set of features, like temperature or nutrient availability, and therefore hosts unique combinations of organisms. All trophically similar organisms living in one particular habitat are referred to as the COMMUNITY, consisting of all the populations within the habitat (Morris & Blackwood, 2007). For example, all *Aspergillus* species found in a soil sample form the *Aspergillus* population, and all fungal populations combined form the fungal community. Because all these fungi are interacting in different ways, communities have their own properties that make them more than the sum of its individual organisms. This concept also implies that anything that affects one species will very likely also affect many others within the community. Ecologists like to approach this by making comparisons and defining patterns.

Within the ecosystem network, community organisms may interact through processes like mutualism, parasitism, predation and competition. Processes involving direct transfer of energy or matter are called direct effects, whereas indirect effects describe the interactions between components without direct energy or matter transfer (Krivtsov, 2008). According to this, classic predation can be called a direct effect, but mutualism and competition are always indirect. There are numerous theories on how the community structure- the numbers and kinds of organisms present in a community- is assembled. In a changing environment, like decomposing litter, succession is an important factor.

1.1.1 Succession and life history traits

The change in community structure within a habitat through time is called succession. On decomposing plant litter, a habitat that can be considered low in readily available nutrients, resources are used up quickly and the dynamics of litter chemical composition during decomposition lead to constantly changing resource conditions (Berg & McClaugherty, 2014). Hand in hand with these nutrient dynamics goes community succession, as some species are gradually less adapt to the new conditions, whereas others find it gradually more suitable (Morris & Blackwood, 2007). On a temporal scale, nutrient availability changes during decomposition, and species with different 'life history TRAITS' are supported successively due to their respective growth and reproduction patterns. These traits determine how quickly a species can get to a site, how fast it grows, or how long it survives. Commonly used is the model of r- and K-selection as reviewed in (Reznick *et al.*, 2002):

- r-strategists ('growth strategists') are adapted to environments with variable climate conditions and high resource levels, showing highly variable population sizes, low resource use efficiency, rapid maturation, early reproduction, short life span, and high productivity.
- K-strategists (competitive strategists), exhibit the opposite characteristics, favoring more stable conditions, due to higher competitive ability they are dominant in unbalanced resource conditions, but have lower maximum growth.

  (Morris & Blackwood, 2007)

Therefore, growth strategists would be expected to maximize their growth under optimal resource conditions (for example at the beginning of litter decomposition), succeeded by competitive strategists in later stages of decomposition with less favorable nutrient availabilities i.e. later stages of litter decay (Keiblinger *et al.*, 2010).

1.2 Statistics in ecology

Because ecological biodiversity studies are dealing with very large communities and comparisons between habitats, treatments, or spatial and temporal patterns, it is convenient to work with empirical subsamples. For example, the number of species in a number of subsites will be recorded and taken as a proxy for the total number of species in the entire area. Biodiversity studies usually create huge datasets, and it gets more and more complicated the more influence factors, treatment conditions, or time points are introduced. With the use of subsamples, the possibility of undersampling

grows, and statistical methods are needed to describe how efficiently the real communities were represented. When it comes to data analysis, there are a lot of statistical tools to calculate and describe all the different information that can be drawn from subsamples representing a community, including diversity indices, species richness estimators, rarefaction curves, rank abundance curves, or accumulation curves (Hughes *et al.*, 2001). Some methods solely use the species information and can be used to compare sites and their respective species compositions. Other methods use both species data and environmental variables of the sites, and are able to investigate the influence of different environmental factors on community patterns (Kindt & Coe, 2005). Before import into statistical programs, species matrices or environmental matrices have to be created with the collected data, according to the program manuals. Using these matrices, models can be created by linear or multiple regression analysis to predict patterns about how explanatory variables (i.e. nutrient ratio or site elevation) influence fungal diversity. Biodiversity differences between sites can be assessed by distance matrices and clustering. A very useful exploratory method in multivariate ecological datasets is PCA, principal component analysis (Ramette, 2007), where variables are ordinated two-dimensionally making it easier to look at complicated multidimensional relationships.

1.3 Description of community composition

In order to investigate ecosystem dynamics and influences of different biotic and abiotic factors, ecologists need to be able to compare communities. But, how to describe a community? Some of the words that are encountered in community studies on a regular basis include species richness, species evenness, and species diversity. All of these terms are needed to get an idea of the nature of a community, but it is crucial to understand the different meanings. Basically, diversity already includes information about richness and evenness. In simple words, species richness is the number of species, and species evenness is the similarity in species abundance within a community.

Two kinds of data can be used in richness and diversity studies (Gotelli & Colwell, 2010): Incidence data (each detected species is simply noted as being present) or abundance data (the abundance of each species in each sample is noted).

1.3.1 Richness metrics

The easiest way possible to describe a community is to simply note the present species and list them- the actual **species richness** (Peet, 1974). **Figure 2** shows how richness and number of individuals in a sample are related:

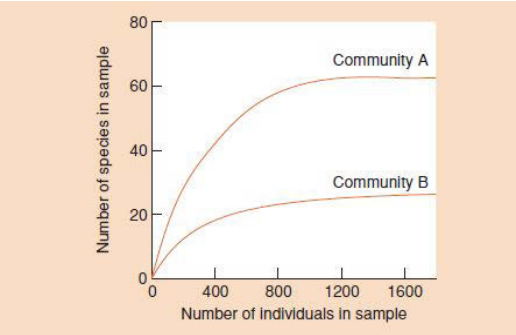

Figure 2: Relationship between species richness and the number of individual organisms, from (Begon et al., 2005).

In Figure 2, two communities with different richness are shown. The curve of Community B flattens out much earlier than Community A, and Community A takes much longer until the species count reaches the asymptote. Species Richness of Community A is therefore much higher than species richness of Community B.

When dealing with genetic techniques to describe microbial diversity, empirical samples are used to estimate the actual diversity. This means that rather than noting all individuals in a community, we use a few subsamples to get an idea of the actual species richness or diversity - an imperfect representation of the ecological community (Maurer & McGill, 2010). This produces a few constraints for molecular ecologists, as rare species tend to remain undetected, and therefore introduce a so-called undersampling bias. Statistical methods are employed to determine if sampling was sufficient to represent the actual community.

1.3.1.1 Species accumulation curves and rarefaction

When comparing different samples, a problem concerning sample size arises: larger samples usually have a higher number of individuals, and therefore probably higher species richness than smaller samples. Larger samples are more likely to pick up rare species. Small samples have common species and few rare species[1]. This relationship between the number of observed species and sampling effort can be used to gain

[1] Ganter Homepage, http://ww2.tnstate.edu/ganter/index.html, retrieved 04/27/2015

information about the total diversity of the sampled community. One way to show this is a species accumulation curve as shown in **Figure 3**:

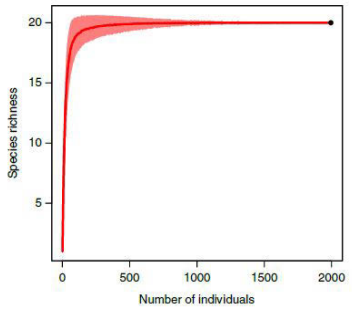

Figure 3: Species accumulation curve, from (Gotelli & Chao, 2013). The x-axis is the number of individuals sampled; the y axis shows the number of species observed.

Usually, the curve is steepest in the early part of the collection, as common species are detected quickly. Continued sampling leads to detection of more individuals, and the curve keeps rising, but eventually becomes shallower: more sampling is required to detect rare species. The curve will flatten out asymptotically representing the true species richness. The actual community richness is represented by the asymptote, and this is why the shape of the accumulation curve gives us an idea about how well the communities have been sampled.

For comparison of species richness between different communities, corrections for different sample sizes can be achieved by using the construction of **rarefaction curves** (Hurlbert, 1971). Rarefaction means interpolation of a biodiversity sample to a smaller number of individuals, it is calculated 'backward' from the endpoint of an observed accumulation curve (Colwell *et al.*, 2004). It gives us an idea how species richness would look like if the sample was smaller. An example how a rarefaction curve and species accumulation curve of actual data could look is given in **Figure 4**:

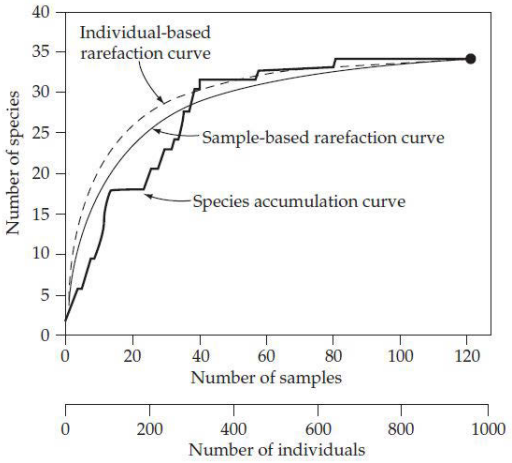

Figure 4: Species accumulation and rarefaction curves, taken from (Gotelli & Colwell, 2010). The jagged line represents a species accumulation curve for 121 soil samples yielding 952 individual tree seedlings, from a plot of Costa Rican rainforest (Butler & Chazdon, 1998). The smooth solid line is the sample-based rarefaction curve for the same data set, representing the statistical expectation of the species accumulation curve. The dashed line is the individual-based rarefaction curve for the same data set.

The principal use of rarefaction curves is to compare species richness among empirical samples with different total individual counts. Richness of rarefied references samples can only be compared at the sample size of the *smallest* reference sample. This means that quite often, data for larger samples have to be discarded in order to make comparisons. A new approach has been published recently to overcome this problem: The combination of rarefaction curves (interpolation) and extrapolation generates species accumulation curves for sample comparison regardless of their individual sample sizes (Colwell *et al.*, 2012). Using this approach, smaller samples can be extrapolated (based on nonparametric asymptotic estimators, see 1.3.1.2) to be compared with the reference sample for larger samples in the dataset.

1.3.1.2 Nonparametric asymptotic estimators

Clearly, sampling data can only show which species are present in a sample. However the mere fact that a species is not encountered in the sample, does not necessarily mean that it is truly absent from the community. The term 'false absence' can be used to describe an incident where a species is present but was not detected (Gotelli & Colwell, 2010). Ecologists have some statistical methods at their disposal to address this issue, estimating how many species remain undetected in a sample. As explained by (Gotelli & Chao, 2013), in an abundance-based sampling approach with N^* total individuals each belonging to one of S distinct species, we take a reference sample with n individuals, drawn at random. In this reference sample, S_{obs} species are

observed. f_0 is the number of undetected species. In our example, $S_{obs} + f_0 = S$. The true, underlying abundance and species richness *S* is unknown, but can be estimated.

In contrast to interpolation of species diversity data by rarefaction (see 1.3.1.1), it is also possible to extrapolate species diversity (Colwell & Coddington, 1994) out to the asymptote of the species accumulation curve. According to (Gotelli & Chao, 2013), three basic strategies can be used to estimate the asymptote: parametric curve fitting (for example Michaelis-Menten equation), fitting to a species abundance distribution (such as log distribution), and nonparametric estimators. These are based on the concept that rare species carry the most information about undetected species (Gotelli & Chao, 2013). Based on this assumption, these estimators add a term to the observed richness S_{obs} that is derived from species represented by only one or two individuals (singletons and doubletons) (Gotelli & Colwell, 2010). The Chao1, ACE (abundance based coverage estimator), and jackknife estimators can be used for abundance data, whereas Chao2, ICE (incidence-based coverage estimator) and another set of jackknife estimators can be applied to incident based data. All these nonparametric estimators can be calculated by various statistical programs, like EstimateS (Colwell, 2013), and help to estimate the minimum number of species in the community. They are crucial to reduce undersampling bias by estimating the number of undetected species.

These tools were implemented in EstimateS 9 to calculate extrapolation from a reference sample. For this purpose, the required "target richness" that estimates the asymptotic number of species (including undetected species) is Chao1 for individual-based data and Chao2 for sample-based data (Colwell *et al.*, 2012).

1.3.2 Diversity metrics

Some species in a community are rare and others common. This sounds like stating the very obvious, but it is the crucial difference between richness and diversity. It is the reason why richness metrics (1.3.1) - simply the number of different species- don’t give the full picture. Taking abundance of the species (the number of individuals per species) into account, it shows that less even communities are actually less diverse than their richness alone would indicate (Maurer & McGill, 2010). To describe diversity, calculated diversity indices like Simpson index and Shannon index are used. They estimate how even individuals are distributed among the different species (=evenness or equitability).

1.3.2.1 Rank- abundance curves

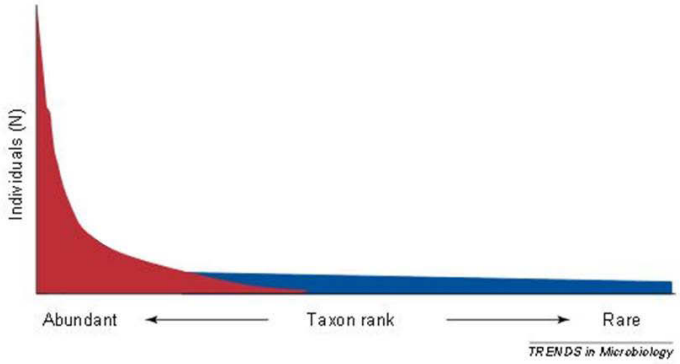

Figure 5: Rank-abundance curve, modified from (Pedros-Alio, 2006). Red shows the abundant fraction, blue shows the rare fraction of biodiversity.

Rank- abundance curves compare communities based on the detected species and their respective abundances. The x-axis shows species from most to least abundant, and the y axis shows the abundance of each type observed (**Figure 5**). The most abundant species take rank 1, the second most abundant rank 2, and so on, until the rarest species of all. The plot given in **Figure 5** shows a pattern that also applies to diverse soil fungal decomposer communities: a few species in the sample are abundant, but most are rare, represented by the long tail on the rank-abundance curve (Hughes et al., 2001). A steeper slope in rank-abundance diagrams represents higher dominance of common species in the community: a sharp drop in relative abundance (Begon et al., 2014).

1.3.2.2 Diversity indices

$$D = \frac{1}{\sum_{i=1}^{S} p_i^2},$$

Equation 1: Simpson index D.
In this equation, p is the proportion (n/N) of individuals of one particular species found (n) divided by the total number of individuals found (N), S is the number of species (=richness). Taken from (Begon *et al.*, 2005).

Simpson index D (Equation 1) was proposed by Edward H. Simpson as a mathematical means to show how likely it was that two species taken from a sample represent the same type (Simpson, 1949). It measures the strength of dominance, giving more weight to dominant species. The **proportion p** of each species relative to the total number of species is calculated and squared. The squared proportions for **all species (S)** are summed, and the reciprocal is taken. For Simpson index D, a few rare species will not affect the diversity much.

Simpson index gets smaller when the diversity of the community increases. It is zero when there is no dominance, and 1 when there is maximum dominance i.e. only one species in the sample (Sagar & Sharma, 2012).

Simpson index is often expressed as the **Inverse Simpson Index** 1/D so that the index will increase as diversity increases.

$$H = -\sum_{i=1}^{S} P_i \ln P_i$$

Equation 2: Shannon's diversity index. p_i is the proportion (n/N) of individuals of one particular species found (n) divided by the total number of individuals found (N) for the i^{th} species. S is the number of species (=richness). Taken from (Begon *et al.*, 2005).

Shannon's diversity index H, or Shannon entropy, was shown by Claude Shannon (Shannon & Weaver, 1949) and it is the most commonly used index in ecological studies. It shows the uncertainty in predicting the species identity of an individual that is randomly taken from the sample. The proportion p of species *i* relative to the total number of species is calculated, and then multiplied by the natural logarithm of this proportion. The resulting product is summed across all species (S), and multiplied by -1. Shannon index is an information statistic index assuming that all species are present in a sample. Shannon index will be zero if there is only one species in the sample (Sagar & Sharma, 2012). If the number of species increases, H increases.

Both Shannon and Simpson indices as well as species richness are incorporated into the Hill numbers (Hill, 1973), sometimes called the 'effective number of species'(Chao *et al.*, 2014). The Hill numbers are defined by their order q controlling the sensitivity of the measure to species relative abundance (Gotelli & Chao, 2013). The diversity profile curve can be plotted as a function of q, see Figure 6:

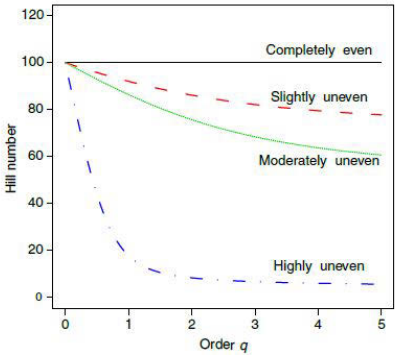

Figure 6: Diversity profiles for communities of differing evenness, from (Gotelli & Chao, 2013).

1.3.2.3 Phylogenetic, taxonomic, and functional diversity

For traditional diversity metrics, some assumptions are made, one of them being 'all species are equally different from one another and receive equal weighting'. This

ignores aspects of phylogenetic or functional diversity: a community of closely related species is 'less phylogenetically diverse' than a community of distantly related species; the same can be said for functionally divergent species (Gotelli & Chao, 2013). If needed, species can be weighted by a measure of their taxonomic classification, phylogeny, or function.

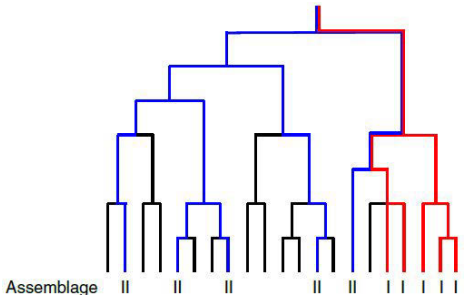

Figure 7: Phylogenetic diversity in species composition, from (Gotelli & Chao, 2013). The common ancestor of the whole community is at the top, the 21 species are shown at the bottom of this branching diagram. Assemblage I is shown in red and consists of five closely related species. Assemblage II is shown in blue and consists of five species sharing a much older common ancestor. Time is measured in the vertical axis.

Phylogenetic diversity can be shown with a branching diagram or cladogram that shows evolutionary relationships as in Figure 7, explained by (Gotelli & Chao, 2013): all other things being equal, Assemblage II is considered more phylogenetically diverse than the community of closely related species

Cladistic diversity (CD) is defined as the total number of taxa or nodes in a taxonomic tree of all species in the community (Vane-Wright *et al.*, 1991). Phylogenetic diversity (PD) is defined as the sum of the branch lengths of a phylogenetic tree connecting all species in the community (Faith *et al.*, 2009). Both CD and PD do not consider abundances. The quadratic entropy and phylogenetic entropy are diversity measures that take both phylogeny and species abundances into account (Gotelli & Chao, 2013).

1.3.3 Biotic similarity

The concept of diversity can also be applied to the comparison of multiple communities. Biotic similarity quantifies how similar two or more sites are in their species composition and abundance distribution (Gotelli & Chao, 2013). Lots of different similarity measures are available as explained in (Jost *et al.*, 2010). Among the most widely used ones are the Jaccard index and the Sørensen index, as well as the Horn overlap measure (Horn, 1966) and the Morisita-Horn similarity measure.

Whittaker (Whittaker, 1972) proposed three levels of diversity: α- diversity: richness in a specific community (i.e. in a sample). β- diversity: change (turnover) in species richness

between communities of two distinct habitats (i.e. how assemblages change across a range of samples). γ- diversity: total diversity across a large geographic area or landscape (Lynch & Neufeld, 2015).

1.3.4 The software application EstimateS

The bioinformatics software application EstimateS (Statistical Estimation of Species Richness and Shared Species from Samples) was developed by Robert K. Colwell from the University of Connecticut, USA. It is an open software package specifically designed for the calculation of various biodiversity estimators, indices and statistics, and highly cited in all kinds of biological studies (Colwell & Elsensohn, 2014). It can be accessed at http://purl.oclc.org/estimates.

EstimateS computes a large number of biodiversity statistics for each level of rarefaction (explained in 1.3.1.1), using a resampling framework that randomly selects sampling units until all individuals in the reference sample have been accumulated (Colwell, 2013). Indices and Estimators are shown for each level of accumulation, from a single individual up to the full reference sample, and shown as means of the number of randomizations that can be specified by the user.

1.4 The Element Cycles

Major nutrients like Carbon, Nitrogen and Phosphorus move through ecosystems in intertwined biogeochemical cycles, wherein both biotic and abiotic components are included to maintain growth and reproduction of living organisms. In order to keep up energy flow through ecosystems, mineral nutrients must always be supplied by a balanced cycle within the ecosystem. Therefore natural ecosystems are never in equilibrium; however they can be at steady state which means that even though there are fluxes, the net pool values remain the same (Agren & Andersson, 2012). Liebig's Law of the Minimum (Liebig, 1840) tells us that low quantities of any essential nutrient can cause stress and decrease productivity, so the cycling of all nutrients is important in understanding ecosystem dynamics. Cycling generally occurs on different time scales, the slow external geological cycle, and faster biological and internal cycling (Rayner & Boddy, 1988). Most ecosystems depend mainly on quick internal cycling done by microbes, where nutrients are returned through decomposition processes, rather than fresh inputs of nutrients (Morris & Blackwood, 2007).

Small or large scale changes by anthropogenic influences cause different effects on ecosystem processes. Environmental phenomena like acid rain (Galloway & Likens, 1981) and global warming show that there is indeed a close link between ecology at the ecosystem level and global scale environmental problems (Agren & Andersson, 2012). But it is impossible to say exactly how these influences are going to change our ecosystems in the future. Modelling approaches are used to develop possible scenarios of global change, for example identifying land use change as the biggest influence on terrestrial ecosystems (Sala *et al.*, 2000), but uncertainties arise because of unpredictable interactions between the possible drivers of change. However ecosystems are the basic building blocks of global nutrient cycles and understanding their complexity is absolutely necessary to get an idea of the Earth's function.

1.4.1 The Carbon Cycle

1.4.1.1 Global Carbon Cycle

The global Carbon cycle describes the transfer of Carbon among the atmosphere, oceans, land, and biota, by a long-term cycle (weathering of rocks and sedimentation of

marine carbonates) and a short-term cycle (terrestrial components, plants, soil biota, and soil organic matter). A picture of the global carbon cycle including anthropogenic carbon inputs is shown in **Figure 8**.

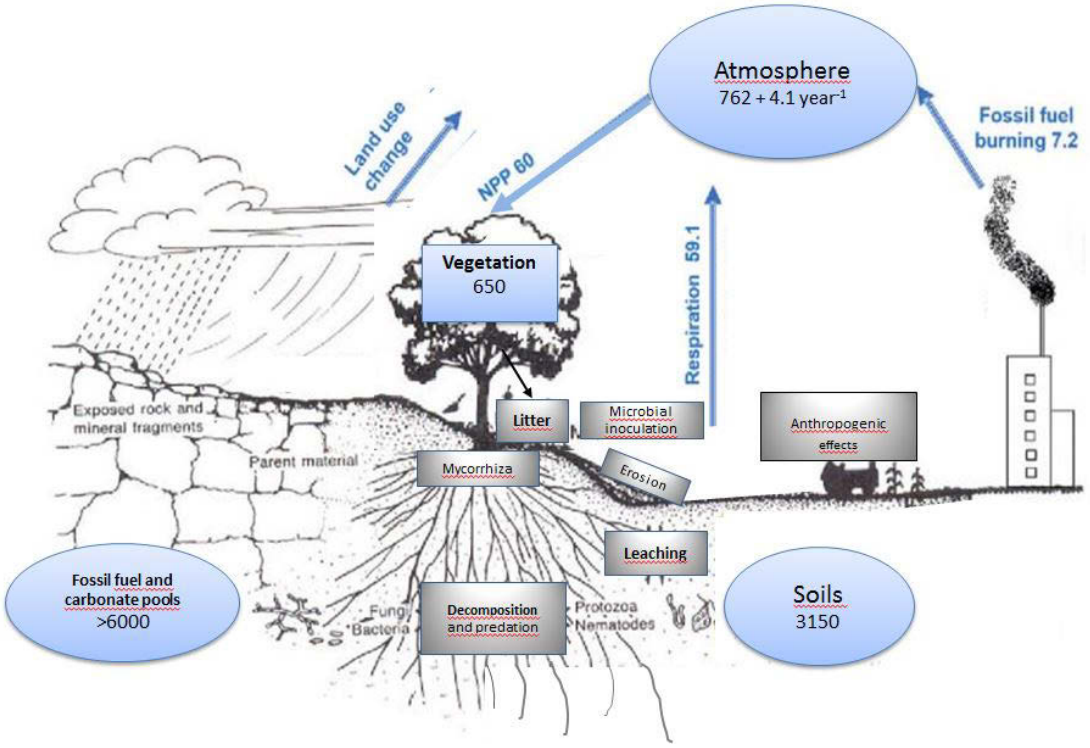

Figure 8: The global carbon cycle, modified from (Morris & Blackwood, 2014). Values are shown in Pg. One Pentagram (Pg) = 10^{15} g.

Geochemical processes in the long-term cycle are critical on scales from thousands to millions of years, and although they are influenced by biological factors, they are very slow compared to anthropogenic effects (Chapin III *et al.*, 2011b).

The short- term cycle is dominated by photosynthesis, respiration, and organic matter formation. These processes are driven by metabolism of organisms. Anthropogenic perturbations on the short-term C cycle are responsible for the third largest C flux to the atmosphere (Chapin III *et al.*, 2011b) and have a very high climate change potential due to the production of so- called greenhouse gases (Horwath, 2007).

The relatively small but dynamic C pool of the atmosphere depends mainly on the two gases carbon dioxide (CO_2) and methane (CH_4). The net increase in atmospheric CO_2 concentrations of +4,1 Pg per year (Morris & Blackwood, 2014) is a result of imbalances between anthropogenic sources and the carbon storage in carbon sinks. Although vegetation, soils and oceans have increased CO_2 capture rates, these sink functions are not sufficient to remove all the excess carbon from the atmosphere (Chapin III *et al.*, 2011b).

Increased atmospheric methane levels are also caused by human activities. Although methane accounts for much lower amounts within the carbon budget, it does have a large global warming potential (Agren & Andersson, 2012). CH_4 is produced by microbial decomposition of organic matter in the absence of oxygen- examples of methanogenic habitats include rice paddies, wetlands, ruminant stomachs, and waste disposal sites (Horwath, 2007). Fossil fuels also contribute significantly to CH_4 emissions. Sinks for Methane are atmospheric removal by hydroxyl radicals (to water and CO_2), and soil microbial oxidation (Chapin III *et al.*, 2011b).

The capture and storage of C on a global level is called Carbon sequestration. It depends on natural sinks or reservoirs that accumulate and store carbon compounds, including oceans, photosynthesis by plants, and soils. These natural sinks must be maintained and well cared for; any human intervention to reduce the sources or enhance the sinks of greenhouse gases are referred to as climate change mitigation (IPCC, 2014). Soil organic matter (SOM) represents a big reservoir of Carbon within the global carbon cycle, and Carbon sequestration in soils offers a natural strategy to reduce excess atmospheric carbon (Lal, 2004),(Johnson *et al.*, 2007). Thus, the understanding of decomposition processes in terrestrial ecosystems is necessary to fully appreciate the natural C sink abilities of soils and to exploit the contribution of soil microbes to mitigate climate change (Bailey *et al.*, 2002).

1.4.1.2 Terrestrial C cycling

In terrestrial ecosystems, C is bound either in plants, consumers, decomposers, or fresh or decomposing organic matter, as shown in Figure 9.

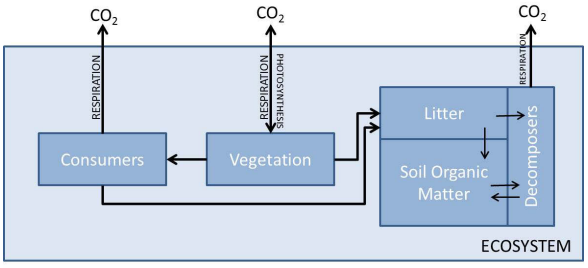

Figure 9: Terrestrial Carbon Cycle components, modified from (Aber & Melillo, 2001).

Carbon available for autotrophic plant uptake is in the atmosphere as CO_2. It is fixed by photosynthesis, starting with absorption of sunlight, converting inorganic CO_2 into organic C. The total energy fixed is called gross primary production (GPP). Net primary production (NPP) shows what is left after the autotrophs have used parts of the GPP for their own respiration (Agren & Andersson, 2012). The overall exchange of CO_2 between

ecosystems and the atmosphere (see Figure 9) reflects the balance between photosynthesis by autotrophic plants, and total respiration. This balance is called net ecosystem exchange (NEE), taking heterotrophic respiration into account, which is mainly decomposer respiration by bacteria and fungi (Agren & Andersson, 2012).

Net ecosystem production (NEP, see Figure 10) includes all carbon losses over the ecosystem boundary, respiratory as well as others. NEP is therefore the net carbon balance of a forest as a whole (Agren & Andersson, 2012).

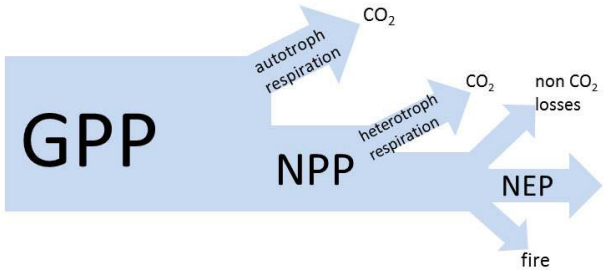

Figure 10: Carbon fluxes in an ecosystem, modified from (Agren & Andersson, 2012). GPP = gross primary production; NPP = net primary production, (GPP minus autotrophic respiration, usually about 50% of GPP); NEP = net ecosystem production (includes non-respiratory C losses through fire, methane uptake and emission, DOC (dissolved organic carbon) transfers, erosion losses)

NEP of different ecosystems varies depending on plant species, soil type, and climate zones (Horwath, 2007).There are forest ecosystems where NEP=0, i.e. carbon is at a steady-state and photosynthesis is balanced by respiration. Old-growth forests had long been assumed to be carbon neutral, however recent studies have shown that in undisturbed forests between 15-800 years old, NEP is positive, which means they are acting as carbon sinks (Luyssaert *et al.*, 2008).

Only a small amount of NPP is grazed by herbivore consumers and passed on to higher trophic levels. All ecosystem production ultimately becomes detritus (Berg & McClaugherty, 2014) and gets decomposed or stored as humus (Figure 9). Decomposition of NPP by microorganisms and soil fauna leads to the production of persistent soil humic substances, making the terrestrial biosphere the largest organic carbon reservoir (Chapin III *et al.*, 2011b). Soil microbial decomposer communities are therefore crucial in maintenance of the C budget, as well as SOM accumulation (see more in 1.5). SOM can persist for thousands of years (Paul *et al.*, 2001) and is important for soil fertility, determines soil structure, water-holding capacity and ion exchange (Aber & Melillo, 2001). Upon interaction and protection with mineral soil particles (Gentsch *et al.*, 2015), SOM ultimately provides a huge carbon sink for long-term carbon storage.

1.4.2 The Nitrogen Cycle

1.4.2.1 Global Nitrogen Cycle

Ecosystem productivity is largely dependent on the availability of **Nitrogen**. It is the key element for biological activity, as it is required for nucleic acids as well as amino acids and enzymes. Nitrogen is the most abundant element; the total amount of N is more than the total mass of Carbon, Oxygen, Phosphorus and Sulphur combined- but strikingly, about 99% are not available to most living organisms (Galloway *et al.*, 2003) as nonreactive N_2 in the atmosphere. Before humans started to interfere with the N cycle, it used to be a limiting factor for biodiversity and functioning of many ecosystems (Vitousek *et al.*, 1997) and was virtually entirely controlled by microbes.

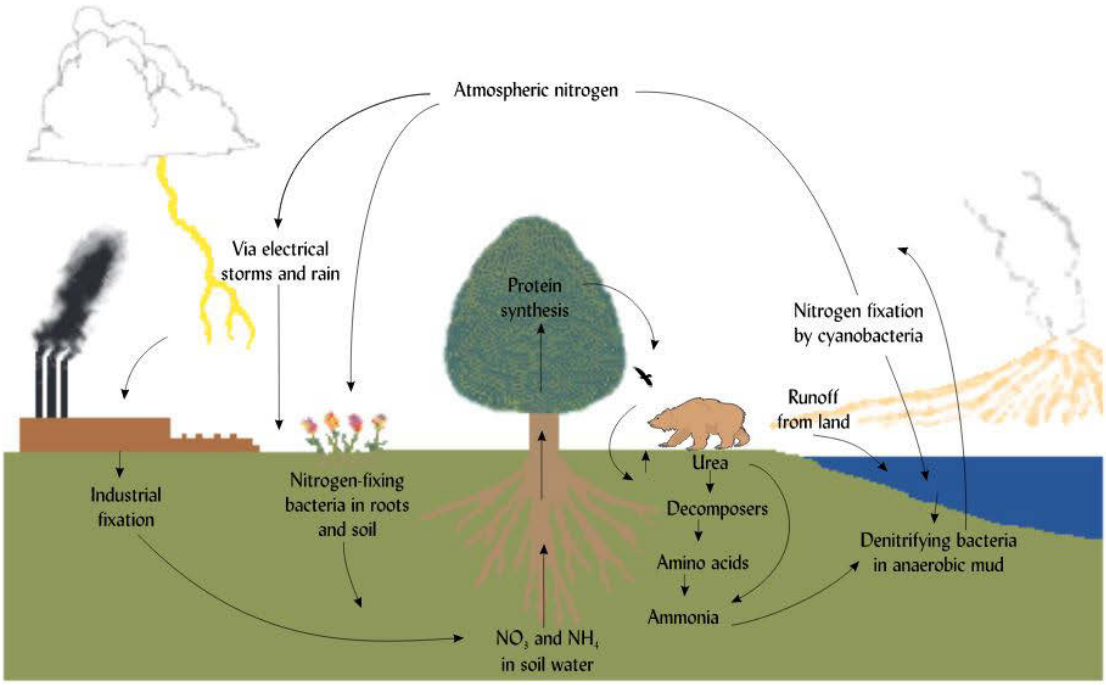

Figure 11: Simplified Nitrogen Cycle, from (Vitousek *et al.*, 1997).

In the absence of human influences, biological N_2 fixation (BNF) by microbes and lightning would be the only ways of new reactive N entering the cycle (Fowler *et al.*, 2013). However food production in the modern world would not be possible without fertilizer, provided through industrially fixed nitrogen by the Haber-Bosch process. In 2010, the industrially fixed N by Haber-Bosch (120 Tg $year^{-1}$) was double the amount of natural terrestrial sources (Fowler *et al.*, 2013). Other human activities (fossil fuel combustion, electricity production, increased BNF by legume and rice cultivation)

produce further reactive N, which means that the overall anthropogenic N deposition has doubled the global amount of N cycling in the last century (Fowler *et al.*, 2013).

The reactive nitrogen gas emissions of NO_x (NO and NO_2), N_2O and NH_3, have continued to rise in the last decades, and are predicted to increase further over the next decades (Galloway *et al.*, 2013). As a result, N accumulates in the environment, because only denitrification is cycling unreactive N_2 back to the atmosphere. Numerous environmental problems are caused by these increased reactive N pools, including human health problems, acidification and biodiversity loss in lakes, coastal water pollution, acid rain, and greenhouse effects and global climate change (Galloway *et al.*, 2013). Compared to the global amount of Nitrogen in the atmosphere, organic Nitrogen pools in soils and terrestrial vegetation are very small. But in contrast to Carbon, N is mainly cycled within terrestrial ecosystems, the annual throughput about 4 times greater than inputs and losses (Chapin III *et al.*, 2011b). Therefore, microbial communities are the key drivers of the N cycle.

1.4.2.2 Biological Nitrogen Fixation

Nitrogen takes nine different forms in soil, each with a different oxidative state. The N cycle is driven by microbial transformations between these forms, namely reduction and oxidation steps catalyzed by diverse, multispecies interactions (Falkowski *et al.*, 2008).

The first enzyme in the series of Nitrogen conversion steps is Nitrogenase, a highly conserved heterodimeric enzyme complex which facilitates biological nitrogen fixation (BNF). Plants rely on Nitrogen uptake in the form of Ammonium (NH_4^+) or Nitrate (NO_3^-), provided by BNF (Lam *et al.*, 1996). BNF is restricted to prokaryotic Bacteria and Archaea known as diazotrophs, expressing the *nif* genes for conversion of N_2 to NH_3. This reaction is the only biological process providing reactive Nitrogen for the N cycle.

Diazotrophic bacteria can generate fixed N in a wide variety of environments due to their different lifestyles including obligate aerobes (e.g. *Azotobacter*, *Anabaena*), microaerophilic (e.g. *Azospirillum*, *Oscillatoria*), facultative aerobic (e.g. *Klebsiella*, *Enterobacter*, *Rhodobacter*), and obligate anaerobes (e.g. *Clostridium*, *Chromatium*), as well as their diverse energy sources (phototrophs, lithotrophs, and heterotrophs) (Bottomley & Myrold, 2007). Within the Archaea, diazotrophs have only been identified in the methanogenic Euryarchaeota (Leigh, 2000).

Diazotrophs are found in different habitats including free-living in soils and water, associative symbioses with grasses and symbiotic associations in termite guts,

actinorhizal associations with woody plants, cyanobacterial symbioses with plants, and root-nodule symbioses with legumes (Dixon & Kahn, 2004).

BNF is energetically very expensive: not only are 16 ATP molecules needed to provide the eight electrons to reduce 1 N_2 molecule to 2 NH_3 (Bottomley & Myrold, 2007), but also at least 20 genes and their products are involved in the synthesis and regulation of nitrogenase, and the catalytic process of N_2 fixation (Cheng, 2008).

$$N_2 + 8e^- + 8H^+ + 16MgATP \longrightarrow 2NH_3 + H_2 + 16MgADP + 16P_i$$

Equation 3: Stoichiometry of Dinitrogen reduction under optimal conditions.

Additionally, Nitrogenase is extremely sensitive to oxygen, and is quickly denatured in aerobic environments. Some strategies, like symbiotic nitrogen-fixing root nodules, help to reduce the oxygen concentration within the nodule providing a microaerobic environment (Dixon & Kahn, 2004).

NH_3, the main product of N_2 fixation, has to be prevented from accumulation within the cell for two main reasons. First, ammonia is toxic to cells upon accumulation. Therefore most diazotrophs combine glutamine synthetase (GS) and glutamate synthetase (GOGAT) to assimilate NH_3 as Glutamine (Merrick & Edwards, 1995), which requires additional ATP and adds to the energy burden of the N_2 fixing process (Bottomley & Myrold, 2007). Second, feedback inhibition of nitrogenase synthesis through high intracellular Glutamine levels has to be avoided (Arcondeguy *et al.*, 2001).

Because of this very high energy demand of BNF, it is not surprising that the expression of *nif g*enes is tightly regulated in response to nitrogen and oxygen status, as well as sufficient energy sources (Dixon & Kahn, 2004), making sure that the environment meets the physiological requirements for nitrogenase activity, and unnecessary consumption of energy is avoided. In *Azotobacter vinelandii,* the NifL–NifA system has been shown to serve as a regulator system to this end (Martinez-Argudo *et al.*, 2004).

The major factor limiting BNF is the energy supply. Free-living diazotrophs in soils are therefore fixing more N_2 if they are able to produce their own energy by photosynthesis (e.g. Cyanobacteria in rice paddies, or biological soil crusts in arid environments) (Bottomley & Myrold, 2007). Facultative and obligately anaerobic heterotrophic N-fixers are found on decaying wood, where they depend on cellulolytic and ligninolytic fungi for their C supply, or during the decomposition of litter with high C/N ratios (Bottomley & Myrold, 2007). Associative N_2-fixing bacteria (*Azospirillum*, *Herbaspirillum*, *Burkholderia*) use root secretions of grasses as their C source in soil, and they can

either invade the root tissues without forming a specialized symbiotic structure, or live in the rhizosphere (Reinhold-Hurek & Hurek, 1998).

Symbiosis is a very interesting way N-fixing prokaryotes can compensate the energy cost of BNF. Rhizobia (e.g. *Rhizobium, Mesorhizobium, Sinorhizobium*) can transform from free-living bacteria into bacteroids, forming characteristic root nodules in legumes (pea, beans, soybean, alfalfa, clover) (Bottomley & Myrold, 2007). Rhizobia modify their metabolism in order to receive energy from the plant for BNF, and at the same time supply N for the host plant (Nelson & Sadowsky, 2015). Actinorhizal symbioses involve nonleguminous plants and the actinobacterium *Frankia*, also forming nitrogen-fixing root nodules. Rhizobial and actinorhizal nodulation may involve similar mechanisms and orthologous genes, but they differ in their evolutionary origin (Svistoonoff *et al.*, 2014).

1.4.2.3 Terrestrial N cycling

Despite being crucial for plant growth, only trace amounts of nitrogen are readily available in the soil. BNF is the sole entry pathway of N into the reactive N cycle in the soil. But there is another way to get Nitrogen moving. Key is the microbially facilitated process of N mineralization: the decomposition or oxidation of organic matter into inorganic plant-accessible forms. Nitrogen compounds in plant litter and soil represent a major source of N (Schulten & Schnitzer, 1997), but it has to become bioavailable first. Decomposer microbes are able to produce extracellular enzymes in order to depolymerize proteins (Schimel & Bennett, 2004), generating oligopeptides and amino acids available for microbial uptake (Jan *et al.*, 2009). This represents the so-called 'new paradigm' of N cycling, as presented by (Schimel & Bennett, 2004), highlighting exoenzyme mediated depolymerization of N polymers as the main control on N cycling (Figure 12): it regulates how fast N from litter polymers becomes bioavailable.

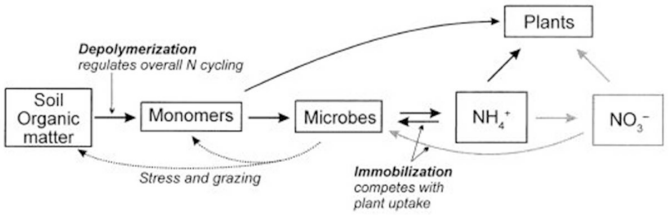

Figure 12: The ‚new paradigm' of the soil N cycle, from (Schimel & Bennett, 2004).

Mineralization is often regarded as the opposite of N immobilization, which describes the assimilation of inorganic N compounds by microbes. Immobilization makes the N inaccessible for plants and is sometimes also called demineralization (Robertson &

Groffman, 2007). The balance between N mineralization and immobilization is regulated by several mechanisms, like environmental and biological controls, some of them are described in 1.5.

On an ecosystem level, N availability and plant N uptake along a gradient from organic N to NH_4 to NO_3^- determine dominant soil processes: if mineralization, immobilization, or nitrification occurs (Schimel & Bennett, 2004). According to this, amino acids in N-limited ecosystems (e.g. tundra) would be completely used up with no considerable mineralization; whereas in agricultural soils with high N availability, competition for ammonium becomes low, creating a NO_3^- dominated environment with active nitrifiers.

However resource imbalances also occur within terrestrial ecosystems, and this has recently been shown to determine how much of the available Nitrogen is used for microbial growth, and how much is released to the environment as inorganic N (mineralization). This partitioning of organic N uptake can be expressed as Microbial nitrogen use efficiency (NUE) (Mooshammer *et al.*, 2014a):

$$NUE = \frac{U_N - M_N}{U_N} = \frac{G_N}{U_N}$$

Equation 4: Microbial Nitrogen Use Efficiency (NUE) expresses the fraction of consumed organic Nitrogen that is not released to the environment as inorganic N. U_N =total amount of organic N uptake; M_N = N Mineralization (release of inorganic N into the environment), G_N = growth (N incorporated into microbial biomass).

Nitrification is the microbial oxidation of Ammonium (produced by mineralization) to less reduced forms ($NH_4^+ \rightarrow NO_2^- \rightarrow NO_3^-$) mainly by autotrophic bacteria. This process is ecologically very important in terms of nitrate leaching. Nitrate as an Anion can easily be transported out of rooting zones by water and lost from soil ecosystems- as opposed to the Cation Ammonium which can stick to clay surfaces or minerals (Robertson & Groffman, 2007).

Autotrophic Nitrification is a two-step process carried out by bacteria, and the oxidation of the respective nitrogen compounds serves as their energy source. Ammonia oxidizing Proteobacteria include the *Nitrosococcus*, *Nitrosomonas,* and *Nitrosospira* clusters with a total of 14 species (Koops & Pommerening-Roser, 2001). In most soils, nitrite produced by ammonia oxidizers does not accumulate but is quickly oxidized to nitrate by nitrate oxidizers (Robertson & Groffman, 2007), carried out in soils by the genera *Nitrobacter* and *Nitrospira* (Koops & Pommerening-Roser, 2001).

Heterotrophic Nitrification is carried out by a variety of different organisms, including fungi and bacteria. It is not linked to cellular growth; the organisms cannot use the compounds as energy source (Robertson & Groffman, 2007). Bacteria include *Arthrobacter, Aerobacter, Streptomyces,* and *Pseudomonas* species; the fungus *Aspergillus flavus* is a well-studied heterotrophic nitrifier (Koops & Pommerening-Roser, 2001). Heterotrophic nitrification by these species may be an important process in some soils, however they rarely dominate the soil nitrifier community (De Boer & Kowalchuk, 2001).

Nitrification in soils is mostly regulated by ammonium supply, and nitrifiers are poor competitors for ammonium against plants and heterotrophs. Thus the balance between mineralization and immobilization is an indicator if nitrification can occur: low decomposition and high N-immobilization by plants or heterotrophs will result in low nitrification rates (Robertson & Groffman, 2007).

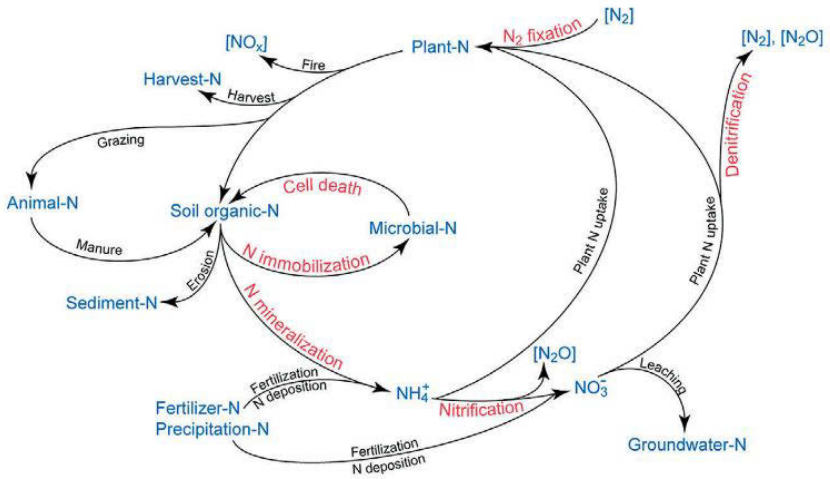

Figure 13: Terrestrial nitrogen cycle, from (Robertson & Groffman, 2015). Soil microbe mediated processes appear in red.

Denitrification is the dissimilatory reduction of soil NO_3^- to N gases (NO, N_2O, N_2) by facultative anaerobic heterotrophic bacteria and has also been described since the 1990s in fungi. It is the major pathway of fixed N to be returned to the atmosphere and therefore represents an important N cycle process under oxygen limiting conditions.

The expression of bacterial genes coding for denitrifying enzymes as well as the respective enzyme activities are highly sensitive to O_2 (Zumft, 1997). Each reduction step is catalyzed by individual enzymes: dissimilatory nitrate reductase, dissimilatory nitrite reductase, nitric oxide reductase, and nitrous oxide reductase, finally releasing N_2 to the atmosphere as shown in Figure 14. Because bacterial denitrification reactions are coupled to the synthesis of ATP receiving reducing equivalents from the respiratory

chain, energy demands can be met under oxygen limitation and thus bacterial denitrification is called anaerobic respiration (Zumft, 1997).). *Pseudomonas* and *Alcaligenes* are examples for bacterial denitrifiers in soils.

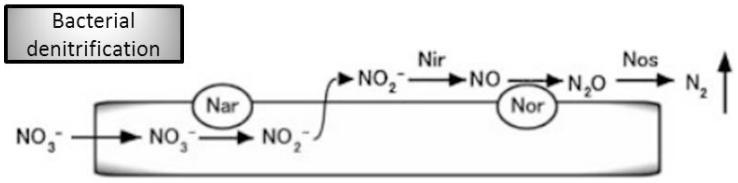

Figure 14: Denitrification process in Bacteria, showing the cellular location and names of responsible enzymes. Modified from (Takaya, 2009). Nar=Nitrate Reductase, Nir=Nitrite Reductase, Nor=Nitric Oxide Reductase, Nos= nitrous oxide Reductase.

Denitrification had been considered a bacterial trait for a long time, but since fungi had been shown to exhibit denitrifying activities (Shoun & Tanimoto, 1991), the view of fungal contribution to the N cycle has changed. Model systems for this so-called hypoxic (oxygen-limited) denitrification are *Fusarium oxysporum* and *Cylindrocarpon tonkinense (Shoun et al., 2012).* As shown in Figure 15, fungi involve Nar, Nir and Nor like bacteria, but are lacking Nos and hence produce N_2O (Takaya, 2009).

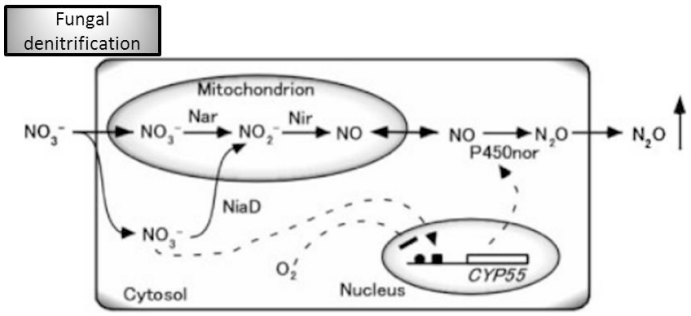

Figure 15: Denitrification in Fungi, showing the cellular location and names of responsible enzymes. Modified from (Takaya, 2009). Nar=Nitrate Reductase, Nir=Nitrite Reductase, P450nor= cytochromeP450nor, NiaD=gene product of *niaD* (*niaD* has been shown to complement NO_3^- growth deficiency (Fujii & Takaya, 2008) and contribute to N_2O production via NO_3^- assimilation(Takaya, 2009))

Fungal denitrification partly takes place in the mitochondria (Kobayashi *et al.*, 1996), which is interesting because the classic view of mitochondria is aerobic ATP production and high sensitivity to oxygen absence (Tielens *et al.*, 2002). However when O_2 is insufficiently available, some fungal mitochondria are able to use other terminal electron acceptors like NO_3^- or NO_2^- in the cytochrome system. Fungal denitrification is overall an energy-yielding process, but in contrast to bacteria, not all three reductases involved are linked to the respiratory system (Takaya *et al.*, 2003). The dissimilatory Nar and Nir share the mitochondrial respiratory chain with cytochrome oxidase in a 'hybrid

respiration' system (Takaya *et al.*, 2003). But the unique fungal P450nor receives electrons directly from NADH to reduce NO to N_2O, and together with its cytosolic rather than membrane bound location, this shows that fungal cytochrome P450nor is not connected to the respiratory chain (Nakahara *et al.*, 1993). The reaction probably serves as a detoxifying mechanism protecting the cells from NO radical damage.

The fact that the final product of fungal denitrification is N_2O rather than N_2, implies that fungi can contribute significantly to N_2O emissions of soils which recently has gained more and more attention (Butterbach-Bahl *et al.*, 2013). N_2O is a potent greenhouse gas and also causes processes in the upper atmosphere that result in destruction of the ozone layer (Baker & Conrad, 2011), making the regulation of its production even more interesting. In a grassland soil, up to 89% of N_2O emissions have been attributed to fungi (Laughlin & Stevens, 2002), and it has been shown that land use could have an influence on the amount of fungal N_2O emissions by selection of crops with different formate levels in the rhizosphere (Ma *et al.*, 2008).

Other N gas sources from soil include Codenitrification (Laughlin & Stevens, 2002), DNRA (Silver *et al.*, 2001), or Nitrifier-denitrification; but although some of these processes might be important in specific ecosystems, they are negligible for most litter decomposition dynamics.

1.4.2.4 Controls on terrestrial N cycling processes

Generally, nutrient cycle reactions are always controlled by availability of their respective substrate. Other important general controls include oxygen availability, temperature, energy and water supply. In soils, water filled pore space (WPS) is a determinant of denitrification activity. Following rainfall, O_2 becomes less available and nitrate is used instead for respiration (Robertson & Groffman, 2007), causing denitrification levels to rise. On decomposing plant litter, denitrification may also be an important process due to oxygen limitation.

Other controls on denitrification are represented by C and NO_3 availability, and therefore denitrification rates depend on the type of ecosystem. Carbon is generally stimulating denitrification due to the heterotrophic lifestyle of most denitrifiers. Nitrate can only be generated by nitrification which depends on oxygen, but in order for denitrification to occur, the generated nitrate has to diffuse into less oxygenated areas of the soil (Robertson & Groffman, 2007).

Nitrate levels in soil are very unstable and only represent a 'snapshot in time'. Many factors are affecting the Nitrate status, including among others soil temperatures,

moisture, and soil properties. Soils with finer structures (clay, silt) generally have higher Nitrate levels than sandy soils which are more prone to leaching. Excessive rainfall can pulse denitrification activity due to increased anaerobic conditions (Groffman, 2012). The three fates of Nitrate in soils are therefore:

- Assimilation (by plants or microorganisms)
- Leaching
- Denitrification.

The variable pattern of nitrate cycling processes is defined by so- called 'hot moments' (brief periods of high reaction rates) and 'hot spots' (small areas with significantly higher reaction rates), as reviewed in (McClain *et al.*, 2003). Rainfall, freeze-thaw events, and other environmental factors are controlling decomposition and therefore all nutrient cycles and availabilities in natural ecosystems.

1.5 Terrestrial plant litter decomposition

Decomposition is the transformation of organic matter into increasingly stable forms, and includes physical, chemical, and biological mechanisms (Berg & McClaugherty, 2014). The fate of plant residues deposited on the soil surface is to be degraded and decomposed, providing energy for microbial decomposer communities. Why is it important to understand decomposition? The two major carbon- transforming processes (see 1.4.1) on the planet are decomposition and photosynthesis. Whereas photosynthesis is well understood (Janna Olmos & Kargul, 2015), decomposition is less well studied. However factors that increase the rate of decomposition could serve to increase the amount of carbon based gases in the atmosphere, so increased knowledge of decomposition processes could help gain valuable insight into global carbon emission scenarios. Furthermore, soils have the potential to act as major carbon sinks, and this process could be used to sequester carbon emissions avoiding high amounts to be circled in the atmosphere (Berg & McClaugherty, 2014, Lal, 2004).

One reason why decomposition is rather difficult to unravel, is the irregular biochemistry of decomposition. In terrestrial ecosystems, most of the NPP (see 1.4.1.2) enters decomposition as plant litter, but the breakdown of this litter is determined by a range of factors on different spatial and temporal scales, and additionally a lot of feedback mechanisms. Climate, abiotic soil characteristics, litter quality, activity and composition of soil microbial communities, and top-down and bottom-up controls by predation and

competition (Wardle & Lavelle, 1997) are all playing their part in this sophisticated symphony of nature.

When trying to understand how decomposition works, it helps to 'think like a microbe' (Robertson & Groffman, 2007): Microbes simply want to grow and meet their needs, not help other organisms or even the ecosystem. So decomposers use the C and N produced by their exoenzymes as an energy source and for their own growth. As a by-product, they release (i.e. mineralize) nutrients. Depending on how much of the N is used for their own growth, and depending on the detritus C:N ratio, net mineralization or immobilization occurs. The regulation of NUE (effective immobilization of organic N into microbial biomass) has been proposed to be a strategy of microbial communities to cope with resource variability as it is associated with litter decomposition (Mooshammer *et al.*, 2014a).

The overall process of decomposition is responsible for the formation of humic substances with tremendous importance for soil fertility and long-term carbon storage. Plant litter (i.e. the NPP, see 1.4.1.2) represents the primary input of organic carbon into soils for soil organic matter (SOM) formation (Kögel-Knabner, 2002). It decomposes in the soil, releasing CO_2 to the atmosphere, in a process called soil respiration. These amounts account for about half of the CO_2 released from ecosystems to the atmosphere (Chapin III *et al.*, 2011a).

Most decomposition occurs in the litter layer and in the organic O-horizon and mineral A- horizon of the soil (Chapin III *et al.*, 2011a). See a generalized flowchart of litter decay in Figure 16:

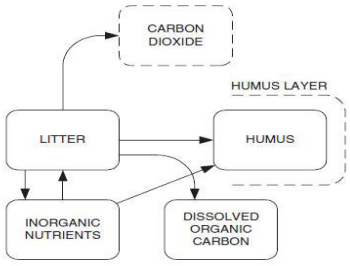

Figure 16: Transformation of litter by decay, from (Berg & McClaugherty, 2014). Decomposition starts with plant litter (detritus) and produces carbon gases and humus.

Litter is shed from the plant, and the decomposition process starts. It includes leaching, fragmentation by soil animals, changes in litter chemical composition, and synthesis of new organic compounds (Chapin III *et al.*, 2011a). The gradual decomposition leads to the formation of soil organic matter (SOM), a complex mixture of organic material, of unrecognizable original identity. The initial chemical composition of litter differs among

plant species (Berg & McClaugherty, 2014), but generally the groups of compounds all belong to major classes.

For the ecosystem, decomposition results in:

- mineralization of organic matter into CO_2 and mineral nutrients
- transformation of organic matter into recalcitrant complex organic compounds, soil organic matter and subsequently humus formation.

Three phases are distinguished until humus is formed: early stage, late stage, and humus-near stage (Berg & McClaugherty, 2014). In early stages of decomposition, sugars, amino acids, low molecular weight phenolics, and some nutrients are dissolved and lost from litter in a process called leaching, which supports the growth of fast growing microorganisms (r-strategists, see 1.1.1). The early stage is heavily influenced by climate and rainfall. Later in decomposition, lignocellulosic biomass is degraded more slowly. Slow growing species and the production of extracellular enzymes (K-strategists, see 1.1.1) are dominating factors for degradation of the recalcitrant substances in the leaf litter. Litter mass loss is regarded as the sum of leaching and production of CO_2 by microorganisms during decomposition (Berg & McClaugherty, 2014).

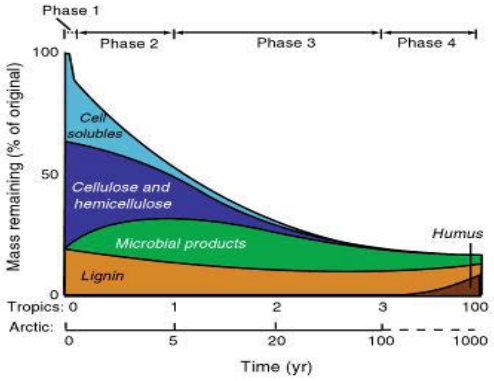

Figure 17: Time course of leaf-litter decomposition, from (Chapin III *et al.*, 2011a).

Entire food webs are based on decomposition: the processes described above are primarily carried out by bacteria and fungi. The different phases and their associated substrates are affiliated with different groups of microorganisms. Due to a wide selection of intermediate products, a high diversity of microbial populations are stimulated successively as litter mass loss is progressing (Berg & McClaugherty, 2014). This change in community composition over time is called microbial succession.

There are a lot of processes involved in microbial succession within decomposer communities, like synergistic or competitive effects. Dead microorganisms become a

substrate for decomposition (Berg & McClaugherty, 2014). Ultimately C/N ratio of plant residues decides if N is mineralized or immobilized, and therefore shapes the community.

1.5.1 Fungal decomposition of leaf litter

When leaves are shed from trees, they represent a generous resource of nutrients for soil and wood decay fungi. There are basically two arrival modes prior to colonization: arrival as propagules or as migratory mycelium (Rayner & Boddy, 1988). Spores from the air or dispersed by animals, as well as dormant structures like chlamydospores or sclerotium, find a great substrate for germination. Sporulation is often induced by environmental cues such as moisture or temperature. Leaf litter provides not only sugars and other easily available nutrients, but also recalcitrant macromolecules including polysaccharides (cellulose, hemicellulose, chitin, peptidoglycan), proteins, and lignin as carbon sources for decay fungi, and they can be utilized to different extents by different fungi (Rayner & Boddy, 1988). As the key players in litter decay, fungi can be considered ecosystem engineers: they make leaf litter nutrients available to other functional groups (Lonsdale *et al.*, 2008).

The fungal lifestyle of hyphal growth makes it easy for fungi to transport nutrients from locations with better nutrient availability through the hyphal network to areas with low nutrients (Paustian & Schnurer, 1987), facilitating growth into new areas and exploring new litter and soil habitats, even traversing dry, nutrient-poor spaces between moist microhabitats. Bacteria, the other main group of decomposers, are left behind on these terms.

Another major advantage of fungi is their ability to produce extracellular enzymes (Lundell *et al.*, 2010). For example, fungi are the main producers of these enzymes on decaying beech litter (Schneider *et al.*, 2012). Extracellular enzymes facilitate plant cell wall deconstruction, and the released soluble substrates are available for microbial assimilation. The most prominent soil fungal extracellular enzymes include Glucosidases, Cellulases, Hydrolases, Peptidases, Phosphatases, Phenol oxidases, and Peroxidases (Sinsabaugh *et al.*, 2008).

Cellulose and hemicellulose (xylan, heteroxylans, glucomannans) represent the major carbohydrate resources in litter. Filamentous ascomycete fungi have a very interesting regulatory system regarding their production of cell wall hydrolases, called carbon catabolite repression (Guerriero *et al.*, 2015). But not only cellulose has to be degraded-fungi must also somehow tackle the lignin in order to get more of the delicious cellulose

(Talbot & Treseder, 2012), for two main reasons. First, it is often structurally necessary because lignin protects cellulosic layers. Second, parts of the cellulose or hemicelluloses is bound to lignin in the so-called ligno-cellulose- or lignin-polysaccharide-complex (Kögel-Knabner, 2002). However lignin itself is not a very appealing carbon source because of its complex structure. Whereas cellulose has a repeating polymer structure, lignin is a complex and random polymer - a single enzyme cannot attack all of the different bonds (Forsythe *et al.*, 2013). Furthermore, lignin provides structural rigidity by its three-dimensional structure consisting of phenyl-propane units. The primary building units of lignin are the cinnamyl alcohols: coniferyl alcohol, sinapyl alcohol, and p-coumaryl alcohol (Kögel-Knabner, 2002).

Historically, wood decay fungi were classified due to their appearance and ability to degrade lignin: **white rot** degrade all components of plant material, and **brown rot** basidiomycetes leave lignin more or less intact (Hori *et al.*, 2013). Although newer research (Riley *et al.*, 2014) suggests different wood decay strategists, this is still a widely accepted classification. The term **soft rot** was introduced to describe softening of wood (polysaccharide degradation) by ascomycetes and deuteromycetes, but it has been shown later that they also degrade lignin to some extent (Nilsson *et al.*, 1989).
The model organism for white rot and lignin degradation is the basidiomycete *Phanaerochaete chrysosporium,* (Martinez *et al.*, 2004). Other model organisms include the ascomycete *Trichoderma reesei* for soft rot and cellulose degradation (Martinez *et al.*, 2008), and the brown rot basidiomycete *Postia placenta* (Martinez *et al.*, 2009).

1.5.2 Ecological stoichiometry

The balance of nutrients is often just as important as total quantities in explaining patterns of nutrient absorption and production. Ecological stoichiometry refers to the use of nutrient elemental ratios to predict nutrient cycling dynamics and biomass production. Animals are able to keep their elemental composition more or less constant, even if their resource changes- which is called Homeostasis. Other organisms ‘are what they eat’ (in certain bounds of course)- they display no homeostasis. The stoichiometry of non-homeostatic organisms may be 1:1 linear with the change of resource stoichiometry, or may diverge from the 1:1 line (Sterner & Elser, 2002). Differences in resource stoichiometry might therefore be reflected by changes in mineralization and nutrient release patterns, and subsequently changes in decomposition rate.

Applied to decomposition in natural ecosystems, Figure 18 shows how C:N ratios decline from wood to leaf litter to soil organic matter. Declining C:N ratios mean less

available C, and therefore increased C limitation, and decreasing N limitation (Mooshammer *et al.*, 2014a). Microbial growth can be limited by C or N availability, or both. For homeostatic organisms, stoichiometric imbalances between resource and biomass C:N lead to growth limitations.

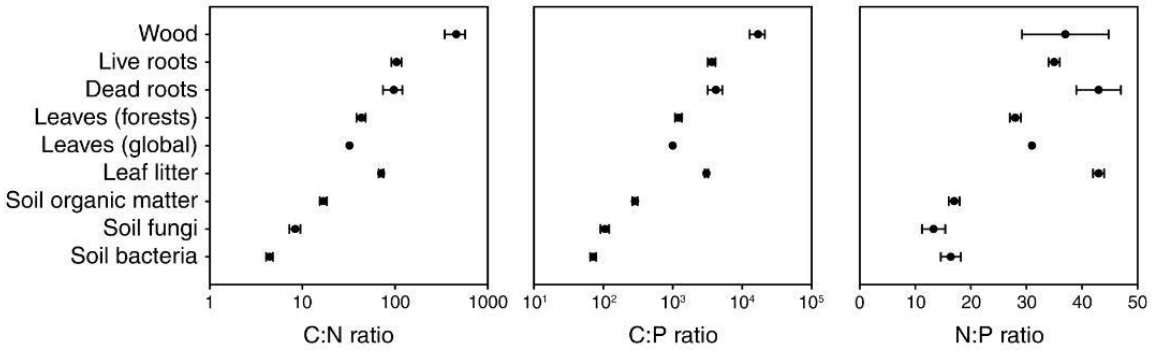

Figure 18: C:N:P ratios of different natural materials from alive to dead, towards SOM and soil decomposers. Figure from (Zechmeister-Boltenstern *et al.*, 2015)

Fungi typically require less nitrogen per unit biomass than bacteria. The elemental C:N ratio for fungi is 10 (35:1 (Rayner & Boddy, 1988)), and the C:N ratio of bacteria is 4 (Chapin III *et al.*, 2011a). This could explain why fungal:bacterial ratios are typically higher in soils with high C:N ratios. But is there a general pattern in soil-microbial systems?

The Redfield ratio, proposed by marine biologist Albert C. Redfield, refers to the constant elemental ratio of marine biomass of C:N:P = 106:16:1(Redfield, 1934). This ratio, conserved across a huge variety of regions globally, is a fundamental tool for ocean biogeochemistry due to its predictive use. For terrestrial systems, the issue of finding a 'magic ratio' was a little more complex, however a global scale soil elemental ratio of 186:13:1 has been proposed (Cleveland & Liptzin, 2007). Plant litter exhibits even wider C:N:P ratios of 1166:20:1 (Mooshammer *et al.*, 2014a). Even though elemental concentrations differ for individual phylogenetic groups, the general soil microbial biomass seems to stay at 60:7:1(Cleveland & Liptzin, 2007). These stoichiometric imbalances between decomposer communities and their resources have recently been shown to be compensated by N mineralization; C:N homeostasis has also been demonstrated for microbial decomposer communities on organic and mineral soil and plant litter as resources (Mooshammer *et al.*, 2014a).

The chemical composition of litter differs among plant species (Berg & McClaugherty, 2014), and the often used term 'litter quality' refers to the nutrient quality, i.e. the C:N and C:P ratios of the litter, and also the speed of decomposition. This dynamically defines the communities decomposing the litter as well as decomposition rates.

1.6 Fungal Taxonomy

The use of taxonomic ranks dates back historically to Carl von Linné, who started using binomial nomenclature (genus name + species name) for natural organisms in the 18th century. Today the taxonomic nomenclature uses a hierarchical system, which means that larger taxons include all lower taxons within them (Cotgreave & Forseth, 2002). The rank denotes a level within a taxonomic hierarchy- a nested set of categories- and this system helps to express evolutionary relationships among organisms. Figure 19 shows an example of taxonomic classification for the fungus *Aspergillus nidulans*, using Linnaean hierarchy:

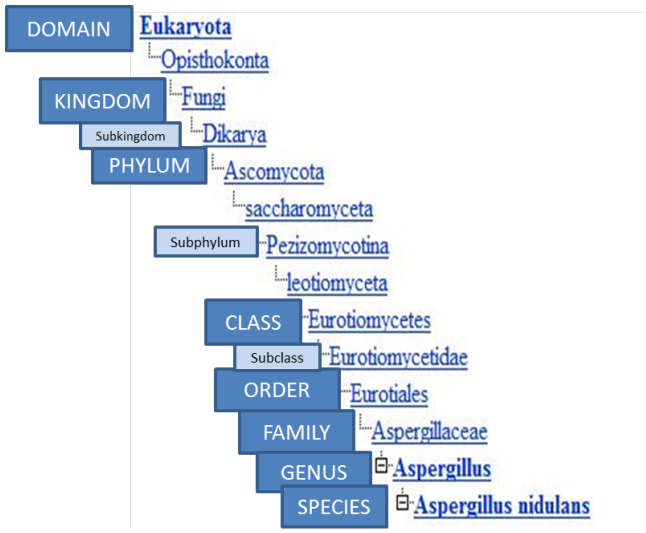

Figure 19: Taxonomic classification of Aspergillus nidulans, full lineage retrieved from http://www.ncbi.nlm.nih.gov/taxonomy on 05/18/2015.

From the simple listing and naming organisms in early science, to the development of taxonomic naming systems, to microscopy, to theories on evolution and genetics, it was a long way to the use of molecular techniques to describe species, for example by PCR amplification of ribosomal genes (White *et al.*, 1990b). The three-domain system proposed by (Woese *et al.*, 1990), based on rRNA data, was a ground-breaking study that resulted in the well-known rooted three-domains tree, dividing life into Bacteria, Archaea and Eukaryota. Although this view was never accepted by all scientists, and newer studies even suggest only two domains (Williams *et al.*, 2013), this is still a basic system of domains based on molecular data.

Interestingly, fungi are phylogenetically closer related to Animalia than to Plantae (Nikoh *et al.*, 1994, James *et al.*, 2006), although they had originally been placed into

1.6 Fungal Taxonomy

The use of taxonomic ranks dates back historically to Carl von Linné, who started using binomial nomenclature (genus name + species name) for natural organisms in the 18th century. Today the taxonomic nomenclature uses a hierarchical system, which means that larger taxons include all lower taxons within them (Cotgreave & Forseth, 2002). The rank denotes a level within a taxonomic hierarchy- a nested set of categories- and this system helps to express evolutionary relationships among organisms. Figure 19 shows an example of taxonomic classification for the fungus *Aspergillus nidulans*, using Linnaean hierarchy:

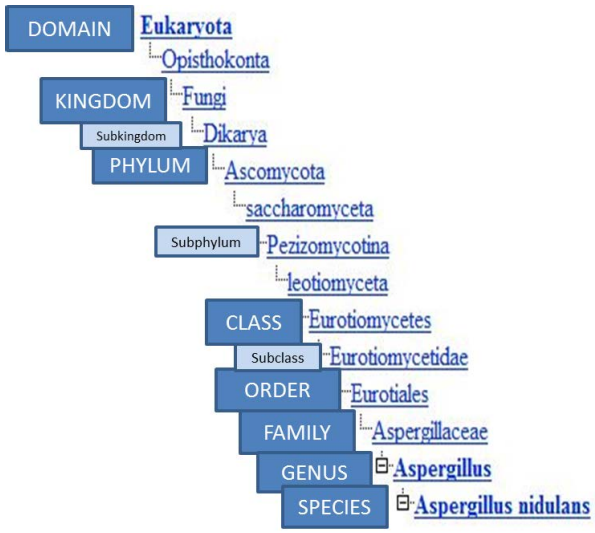

Figure 19: Taxonomic classification of Aspergillus nidulans, full lineage retrieved from http://www.ncbi.nlm.nih.gov/taxonomy on 05/18/2015.

From the simple listing and naming organisms in early science, to the development of taxonomic naming systems, to microscopy, to theories on evolution and genetics, it was a long way to the use of molecular techniques to describe species, for example by PCR amplification of ribosomal genes (White *et al.*, 1990b). The three-domain system proposed by (Woese *et al.*, 1990), based on rRNA data, was a ground-breaking study that resulted in the well-known rooted three-domains tree, dividing life into Bacteria, Archaea and Eukaryota. Although this view was never accepted by all scientists, and newer studies even suggest only two domains (Williams *et al.*, 2013), this is still a basic system of domains based on molecular data.

Interestingly, fungi are phylogenetically closer related to Animalia than to Plantae (Nikoh *et al.*, 1994, James *et al.*, 2006), although they had originally been placed into

the same kingdom as plants in a very preliminary two-kingdom theory comprising only of Plantae and Animalia (Hagen, 1996).

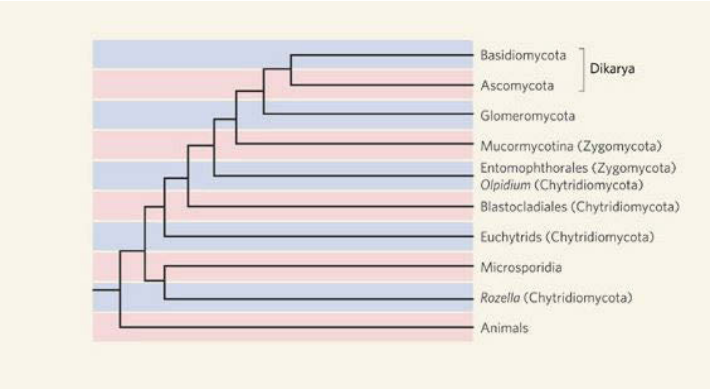

Figure 20: Phylogenetic tree of the fungi, from (Bruns, 2006). This tree shows evolutionary relations between the traditional fungal phyla. Ascomycota and Basidiomycota are united as Dikarya. Their closest relative is the Glomeromycota (arbuscular mycorrhizal fungi). Together with Animalia, Fungi emerged from within the clade of Ophistokonta (Adl *et al.*, 2005).

Throughout history, other two-, three-, four- and five-kingdom systems have been proposed and revised, with the fungi representing their own kingdom since Robert Whittaker in 1969 (Whittaker, 1969). The six- kingdom theory by Cavalier- Smith has been revised and reinstated for several years (Cavalier-Smith, 2004). Recently the newest hierarchy based on the Catalogue of Life (http://www.catalogueoflife.org/) has been developed as an extension to the six-kingdom schema (Cavalier-Smith, 1998) and proposes a two-superkingdom, seven-kingdom classification (Ruggiero *et al.*, 2015): the superkingdoms Prokaryota and Eukaryota, and the seven kingdoms Archaea, Bacteria, Protozoa, Chromista, Fungi, Plantae, and Animalia.

Within the kingdom of the fungi, one subkingdom, seven phyla, ten subphyla, 35 classes, 12 subclasses, and 129 orders are recognized (Hibbett *et al.*, 2007). The phyla Ascomycota and Basidiomycota are grouped together in the subkingdom of Dikarya- also called the 'higher fungi', whereas the other 5 phyla ("Zygomycetes" and "chytrids") are often referred to as 'basal fungal lineages' (McLaughlin *et al.*, 2009). A phylogenetic tree of the Ascomycota and Basidiomycota are shown in Figure 21.

.

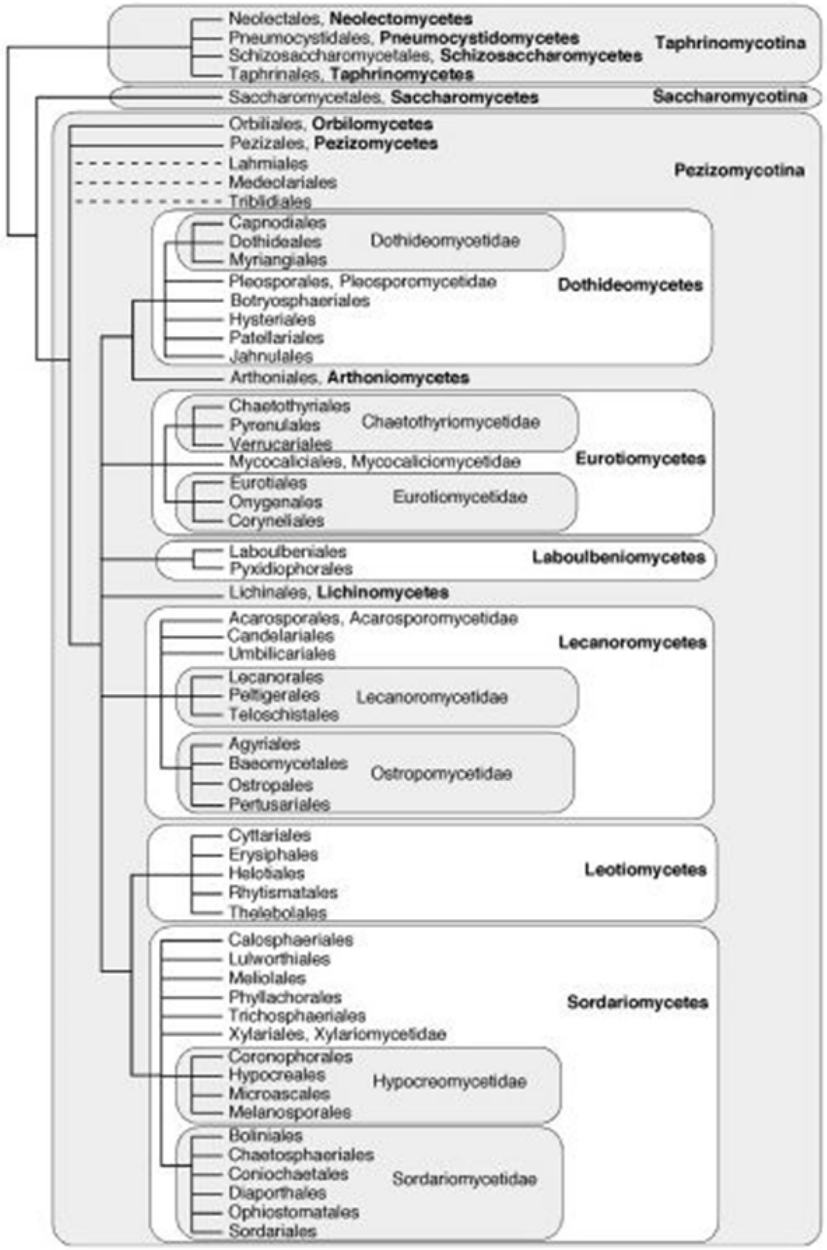

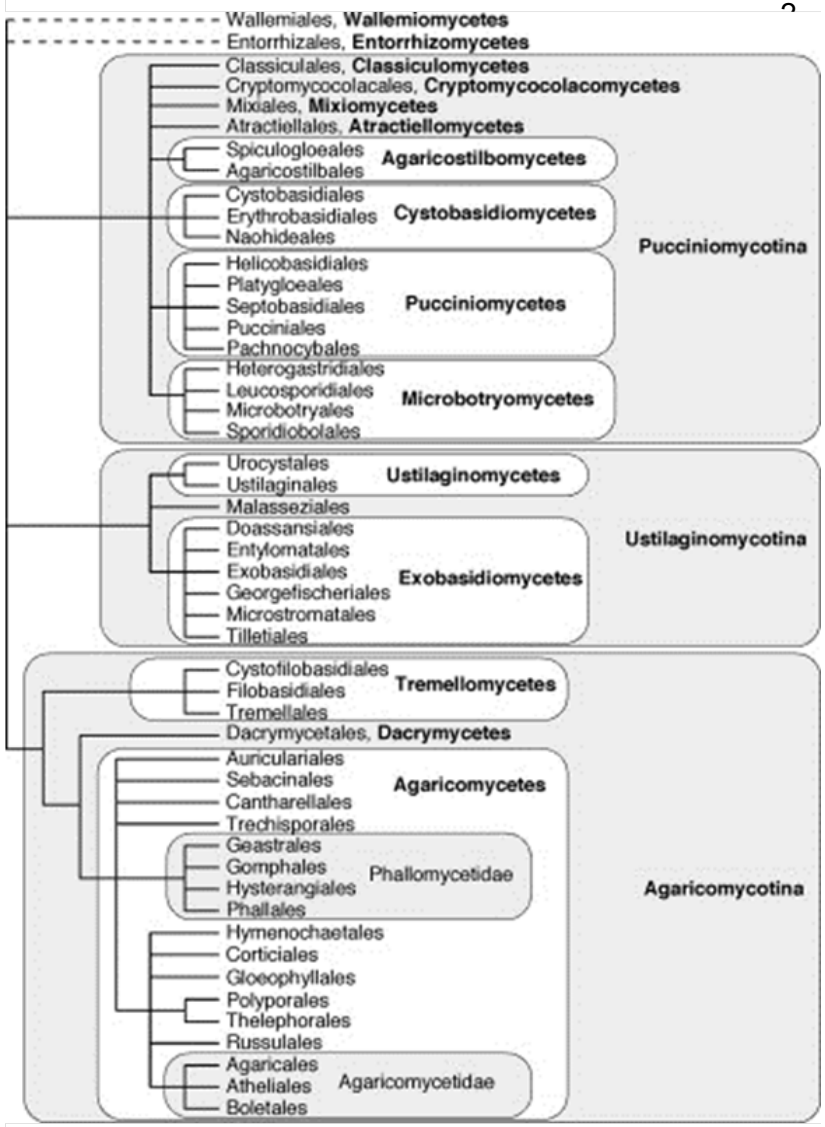

Figure 21: **Phylogeny and classification of *Ascomycota* (left) and *Basidiomycota* (right), from (Hibbett *et al.*, 2007)**

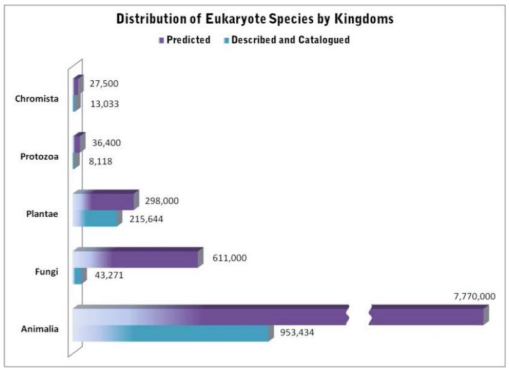

Figure 22: Distribution of species by kingdom, from (Census of Marine Life, 2011). Numbers of predicted and described species from (Mora *et al.*, 2011).

As shown in Figure 22, there are still 93% of the estimated fungal species unknown, based on the models proposed by (Mora *et al.*, 2011). On the mission to search for missing fungi, molecular methods have been a huge help. Environmental studies have revealed unknown major clades of Fungi. One of these clades, for a long time known from molecular sequences only, was a basal clade within the Ascomycota and thus important in understanding the evolution of this phylum. It was initially called Soil Clone Group I (SCGI) (Porter *et al.*, 2008) and described with an impressive ecological distribution in soils and rhizosphere of various ecosystems. A few years later this class was described and named Archaeorhizomycetes (Rosling *et al.*, 2011), and phylogenetically placed within the Taphrinomycotina. Thousands of sequences were already available before this class of fungi was even named or cultured, which proves the enormous potential of culture-independent research in ecology.

1.7 Ribosomal markers in microbial ecology

Since cultivation techniques are not only labor intensive, but insensitive to many naturally occurring microbial species, molecular techniques (i.e. culture-independent methods) have been introduced to provide a more suitable way for describing microbial diversity and function sufficiently. Various fingerprinting techniques (RAPD, DGGE, microarrays,…) have been used in different approaches, most of them based on an initial DNA or RNA extraction step followed by detection of a molecular marker (e.g. by PCR). A cell's total RNA pool consists of 82-90% rRNA, which is mostly ribosome associated (Nomura *et al.*, 1984). Small subunit ribosomal RNA (SSU rRNA) has been used extensively in microbial ecology as a phylogenetic marker due to its ubiquity and low evolutionary rate. In addition, several databases are available specifically for SSU rRNA data which makes this marker the most powerful for use in diversity studies.

Within bacterial and eukaryotic cells, SSU rRNAs serve as a part of the ribosome complex, together with other rRNAs and proteins. Millions of ribosomes are readily available in the cytoplasm where they perform protein synthesis from mRNAs. Every cell contains multiple copies of the necessary rRNA genes to be able to produce enough ribosomes. The eukaryotic rRNA cistron contains 18S, 28S and 5.8S rRNA genes which are transcribed together as a precursor rRNA molecule. Figure 23 shows the posttranslational modifications occurring within the nucleus of eukaryotic cells, producing the rRNA molecules needed for assembly of ribosomes.

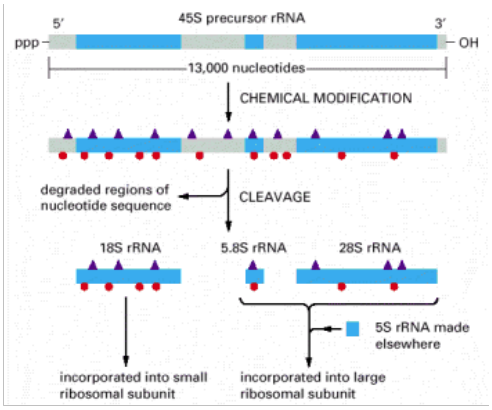

Figure 23: Processing of eukaryotic rRNA molecules in the nucleus, from (Alberts *et al.*, 2002)**.**

In Figure 24, the assembly of small and large ribosomal subunits are shown. Procaryotic and eukaryotic SSU rRNAs differ in their S- values (Svedberg unit), which refers to their sedimentation rate in an ultracentrifuge: 16S prokaryotic rRNA and 18S eukaryotic rRNA. Large subunit (LSU) sequences are also available in most databases for 28S (eukaryotic) and 23S (prokaryotic) rRNA sequences.

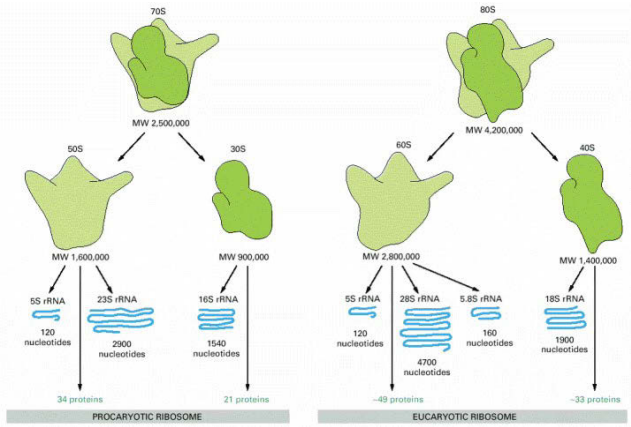

Figure 24: Structural comparison of procaryotic and eukaryotic ribosomes, from (Alberts *et al.*, 2002).

Depending on the level of resolution needed for a study, SSU rRNA can be used as a valuable and robust phylogenetic marker in prokaryotic as well as eukaryotic systems,

both on the DNA and RNA level. For fungi, both LSU and SSUs might not provide enough resolution if identification down to the species level is desired. Therefore, the ITS (internal transcribed spacer) region has been proposed as the primary fungal barcode marker (Schoch *et al.*, 2012). Fungal ITS1 and ITS2 are hypervariable regions within the rRNA gene as shown in Figure 25. Since they are not part of the structural rRNAs transcribed from this gene, they vary in both sequence and length and can therefore provide species level identification for most fungal groups. Universal fungal ITS primer sequences are available (Gardes & Bruns, 1993), but it must be kept in mind that even though most fungal groups are targeted, some might not be covered by this approach.

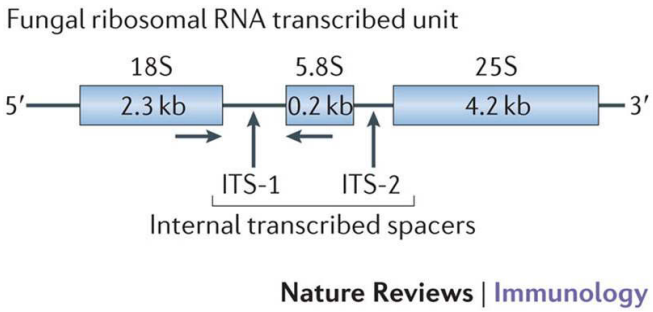

Figure 25: Location oft he ITS (internal transcribed spacer) regions within the polycistronic fungal rRNA gene, from (Underhill & Lliev, 2014).

1.8 Linking fungal diversity with function: the PhyloTrap method

Many methods in microbial community are based on the same molecule: DNA. This is mainly due to the fact that most of the employed methods and phylogenetic markers are established for the work with DNA samples, and it is straightforward and easy to work with. However DNA does not give many insights into activity of certain microbial groups, but represents all possible life stages (active, growing, dormant, and recently deceased). Depending on the research question, this might be a major disadvantage because fungal spores and other dormant, inactive life stages of bacteria (Jones & Lennon, 2010) not actively contributing to processes in their environment are detected, and thus painting a completely different picture of the microbial community. rRNA analyses are commonly used to identify active populations within a mixed community, however this might still not be enough to appropriately link community structure to ecosystem function quantitatively (Blazewicz *et al.*, 2013). Because of the relationship of rRNA concentration and growth, it is usually assumed that rRNA concentration and activity are related. However exoenzyme production or defense mechanisms are crucial activities in microbial communities, but are not defined by growth (Blazewicz *et al.*,

2013). Metaproteomics comes one step closer, but lacks evidence of enzyme activities. A very promising tool is therefore the application of stable isotopes which provide direct proof of activity. This coupling of metabolic activity (isotope incorporation) and rRNA analysis makes it possible to address a major gap in understanding microbial communities. Similar to the bacterial rRNA isolation published a while ago (MacGregor *et al.*, 2002), the idea was to combine stable isotope labelling on RNA basis and subsequent measure of ^{13}C and ^{15}N tracer incorporation, with the specific capture of rRNA of different phylogenetic origin. This method could be used to determine active carbon and nitrogen assimilating fungal and bacterial phyla (or even classes) because the isotopic ratio of stable isotopes ($\delta^{13}C$) of the carbon source has been shown to be reflected in total RNA and SSU rRNA of *E.coli* pure cultures (MacGregor *et al.*, 2002).

In vivo incorporation of substrates such as ^{13}C glucose or ^{15}N- nitrate, together with the use of SSU rRNA as diversity (sequence-based phylogenetic separation) as well as functional (isotope incorporation) biomarker, has the potential to gain insight into C and N flow in natural microbial communities.

In my diploma thesis “Linking fungal Diversity with Function: Development of a species-specific rRNA capturing System” (Böck, 2008), the PhyloTrap method was developed and its capability of highly specific SSU- rRNA separation on different phylogenetic levels was shown for pure culture RNA of a bacterial (*R.terrigena*) and three fungal species (*A.nidulans, S.pulverulentum, T.harzianum*).

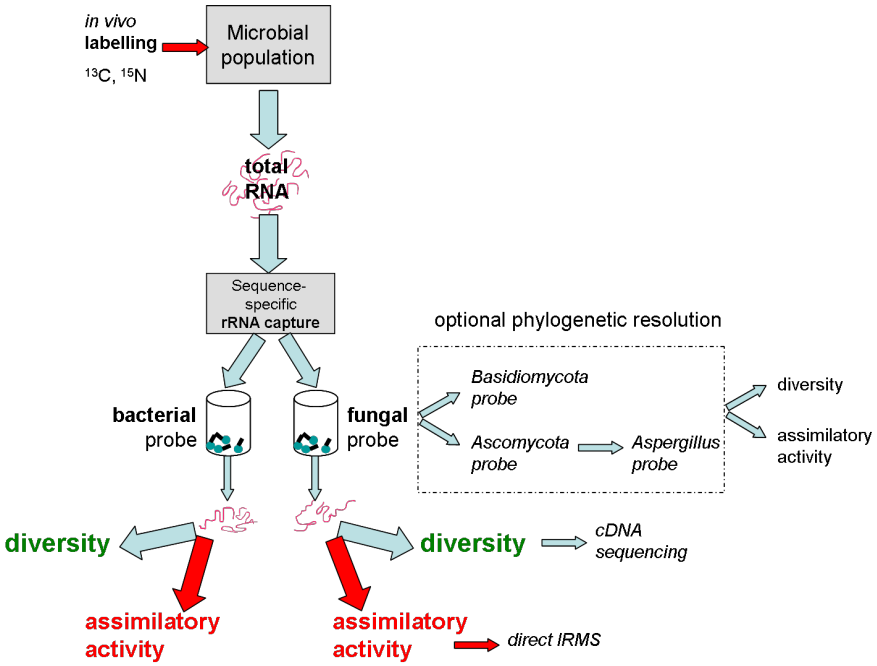

Figure 26: Conceptual development of the ‘PhyloTrap’, a magnetic- bead- based rRNA capture method with labelling of assimilatory active species. Figure from (Böck, 2008).

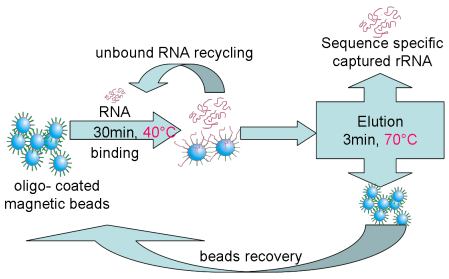

Figure 27: Final flowchart of the rRNA capturing method, as developed in (Böck, 2008).

This stringent protocol, as developed in my diploma thesis, provides exclusion of bacterial RNA and sequence- specific rRNA isolation from three fungal species with a eukaryotic probe targeting the 18S rRNA subunit of nearly all eukarya. However total RNA yield was not only too low, but also contaminated with an unknown, high-N chemical compound (most likely Guanidinium-thiocyanate from QIAquick cleaning procedure), that made IRMS measurements of the enriched rRNA unsatisfying. Therefore, the method had to be refined and developed further in order to address purification and RNA yield issues as discussed in detail in (Böck, 2008).

1.8.1 Improving rRNA yield with LNA probes

In order to improve the oligonucleotide-probe based PhyloTrap technique, it was important to increase target rRNA-probe hybridization. LNAs (locked nucleic acids) are oligonucleotides with increased binding affinity, containing one or more LNA monomers with structurally rigid modifications. The latter are very similar to native nucleic acids, but have an extra bridge connecting the 2' and 4' carbons which locks the furanose ring in the 3'-endo structural conformation (Koshkin *et al.*, 1998), see Figure 28.

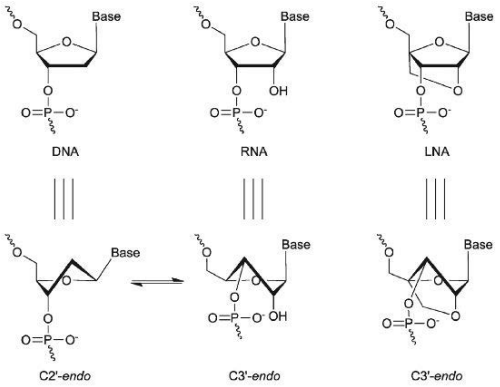

Figure 28: Structures of DNA, RNA and LNA monomers and their furanose conformation, from (Campbell & Wengel, 2011).

It has been reported that oligonucleotides containing one or more LNA monomers can considerably increase the melting temperature (T_m) of a LNA/RNA duplex, while also offering high discrimination between match vs. mismatch pairings (Campbell & Wengel, 2011). Therefore, the use of LNA enhanced probes was chosen to increase rRNA yield for the previously developed PhyloTrap technique within this project. Using both a universal eukaryotic and a bacterial probe, different hybridization conditions were subject to optimization:

- Hybridization time
- Hybridization temperature
- Formamide concentration in hybridization buffer
- Washing conditions
- Elution temperature

All the above were supposed to be optimized with regards to maximum specificity and yield of rRNA, as well as beads and probe reusability and minimum chemical contaminations in the rRNA eluate.

2 MATERIALS AND METHODS

2.1 Leaf litter methods

2.1.1 Leaf litter sampling sites

	Achenkirch (AC)	Ossiach (OS)	Klausenleopoldsdorf (KL)	Schottenwald (SW)
Latitude Longitude	47°35′N 11°39′E	46° 40' N 14° 40' E	48°07′N 16°03′E	48°14′N 16°15′E
location	Tyrol, Austria	Carinthia,Austria	Lower Austria, Austria	Vienna, Austria
Forest type	Spruce (*Picea abies*) , beech *(Fagus sylvatica*)	Spruce (*Picea abies*), beech (*Fagus sylvatica*)	Beech (*F.sylvatica*)	Beech(*F.sylvatica*)
Elevation asl	895	889	510	370
Soil type	Rendzic leptosol/ chromic cambisol	Orthodystric cambisol	Dystric cambisol over sandstone	Dystric cambisol over sandstone
Soil texture	Loam		Loam-loamy clay	Silty loam
Soil pH 0-7 cm	6.4		4.6	4.4

Table 1: Litter sampling sites and soil characteristics as described in (Wanek *et al.*, 2010) and (Schneider *et al.*, 2012)

2.1.2 Leaf litter sampling

Freshly fallen beech leaf litter was collected at four different locations in fall 2007 in Austria: Achenkirch (AC), Ossiach (OS), Klausenleopoldsdorf (KL) and Schottenwald (SW). The exact collection dates differed for the sampling sites and were chosen to obtain leaf litter at similar developmental stages. For details on sampling see (Wanek *et al.*, 2010) and (Schneider *et al.*, 2012). After transfer to the laboratory, litter was chopped to pieces (0.2-1 cm), thoroughly mixed per sampling site and air-dried.

2.1.3 Litter biochemistry[2]

Elemental composition of litter was determined before the start of decomposition experiments. Detail on the chemical analysis can be found in (Schneider *et al.*, 2012).

[2] Litter chemical analysis were done by Dr. Katharina Keiblinger, Institute for Soil Research, Department of Forest and Soil Sciences, University of Natural Resources and Life Sciences (BOKU), Peter Jordanstrasse 82, 1190 Vienna, Austria.

Samples were dried in an oven at 105 ºC for 24 h and ground to a fine homogeneous powder with a mill (MM2000, Retsch). The total carbon (C) and nitrogen (N) contents of the litter were analysed from the respective samples with an integrated oxidation and detection device (LECO CN2000, Leco Corp.). For determination of the elements P, K, and Mn, ground samples were wet acidic oxidized with H_2SO_4 and HNO_3 (Henschler, 1988) in a microwave oven (CEM MARS Express) and analysed by inductively coupled plasma atomic emission spectrometry (Vista Pro, Varian, Darmstadt, Germany).

2.1.4 DNA Extraction from litter samples

Dry litter samples were ground in liquid nitrogen using a prechilled mortar and pestle. Ground frozen powder was transferred into a 15 ml Greiner tube to the 2 ml mark. 6ml of DNA Extraction buffer were added, and after vigorous vortexing, the samples were incubated at 65°C for 30 minutes. Then, the DNA was extracted by addition of 6 ml Phenol and vortexing. After 5-10 min, for centrifugation, the samples were split into 2 ml aliquots and centrifuged at 4°C and 13.000 rpm. The upper liquid phases were pooled in 15ml Greiner tubes again. For the second extraction step, Chloroform-Isoamylalcohol (CI) was added. After another 5-10 minutes, phase separation was again obtained by centrifugation at 4°C and 13.000 rpm. The liquid phase was transferred into a new tube. RNase was added and samples were incubated at 37°C for 30 min. Afterwards, samples were split into 2 ml eppis, 0,8 vol Isopropanol was added for precipitation. The samples were incubated at -20°C overnight. The next day, samples were centrifuged at RT for 20 min at 13.000 rpm. The pellet was washed with 70% Ethanol and air dried, and finally dissolved in 100 µl H_2O. The split samples were pooled again.

2.2 Native litter community methods

Using 2 grams of the finely chopped, dried and unsterilized litter, microcosms were set up in 15ml Greiner tubes at room temperature with a water content of 60% and incubated at room temperature for two weeks. Details on sampling and litter locations can be found in 2.1. The use of microcosms was explained in detail here (Inselsbacher *et al.*, 2009). A total of 8 microcosms were produced: each of the 4 locations was sampled at 2 days and 2 weeks after start of the experiment. 4 litter samples were taken as a ‘baseline’ at start of the experiment, called timepoint ‘0 days’. To get an idea of the ‘native’ undisturbed fungal community on the litter becoming active upon increase of the water content, fungal SSU/partial LSU gene clone libraries were constructed for each location and time point, yielding a total of 12 libraries (4 locations, three time points).

Water content was maintained at 60 % fresh weight by regular addition of sterile deionised water. DNA was extracted from samples as explained in 2.1.4 for molecular genotyping.

2.2.1 PCR with fungal specific primers for ITS region

DNA samples from litter were generated as described in 2.1.4. To clean them from PCR inhibiting substances, the DNA was purified using the QIAquick® PCR purification kit according to manufacturer's instructions. Fungal ITS region and partial LSU were amplified with the primers ITS1F and TW13 using REDTaq™. ITS1F(Gardes & Bruns, 1993), is specific for fungi, and TW13 is an universal eukaryotic primer (Taylor & Bruns, 1999). While the ITS region provides excellent resolution down to the species level, the partial LSU region provides good resolution at higher taxonomic levels when sufficiently identified ITS reference data in public databases are missing (Klaubauf *et al.*, 2010a, Urban *et al.*, 2008). PCR contitions were as described in Klaubauf *et al.* (2010a) except that REDTaq ReadyMix PCR Reaction Mix (Sigma-Aldrich) was used. PCR reactions were analyzed by agarose gel electrophoresis.

Premix calculation per sample:

REDTaq™ Ready Mix™		12.5 µl
DNA sample 1:1000	3 µl	
ITS1F (pF)		1 µl
TW13 (pR)		1 µl
dH2O		6,5 µl
		25 µl

Temperature program:

1	80°C		preheating
2	95°C	2:30	Initial denaturation
3	94°C	0:30	
4	**54°C**	0:30	Annealing
5	72°C	0:45	Repeat 3-5 **35** times
6	72°C	5:00	
7	12°C	Hold	

Table 2: PCR Temperature Program for amplification of ITS region

2.2.2 Clone library production from litter samples

For each litter sample, a clone library of ITS1F/TW13 PCR products (described in 2.2) was generated in pGEM®-T Easy vectors system (Promega) carrying the lacZ gene for blue/white selection of positive clones.

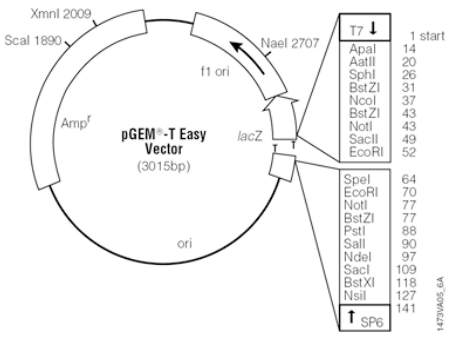

Figure 29: pGEM-T Easy Vector (Promega)

Ligation reaction:

2x rapid ligation buffer
for T4 DNA ligase..... 5 µl
pGEM-T easy Vector..... 1 µl
PCR product..... 3 µl
T4 DNA ligase..... 1 µl

The ligation reaction was incubated overnight at 4°C.

50 µl of competent cells were incubated with 2 µl ligation reaction on ice for 20 min. Heat shock was performed at 42°C for 50 sec, followed by incubation on ice for 2 min. Then 950 µl LB broth were added to the cells, and the tube was incubated at 37°C with shaking for 1 h. Cells were plated on LB/Ampicillin/X-Gal/IPTG plates and incubated overnight at 37°C. Putative positive white colonies, each containing one distinct product derived from one single fungal species, were selected. For each library, 96 independent clones were picked and resuspended in 200 µl LB+amp in deep well plates. Plates were sealed with a breathable membrane, and incubated at 37°C for 4 hours. Afterwards, 5µl of bacterial suspension were resuspended in 40 µl H_2O and cooked at 95°C for 7 min. 3,5 µl of this cell lysate were directly used for PCR reaction as described in 2.2. The rest of the uncooked bacterial cells were covered with 200 µl 40% glycerol and frozen at -80°C.

REDTaq Ready Mix	10 µl
ITS1F (pF)	2 µl
TW13 (pR)	2 µl
dH_2O	2,5 µl
cell lysate	3,5 µl

PCR reactions were analyzed by agarose gel electrophoresis. PCR products were directly subjected to RFLP analysis.

2.2.3 RFLP analysis and selection of clones

PCR products from clone libraries generated as described in 2.2.2 were directly digested with the enzymes *AluI* and *Hha I* (Fermentas) in the 96 well plates. 5 units of enzyme were used per well.

Restriction enzyme premix:

Alu I	50 µl
Hha I	50 µl
Tango buffer	200 µl
H_2O	700 µl

10 µl of this premix were added to the PCR products and incubated at 37°C for 2 hours, then 10 min at 70°C. Fragments were analysed on a 2% Agarose gel. Based on visual analysis of RFLP patterns, representative clones for each pattern were picked for sequencing. Sequencing was performed by AGOWA GmbH (Berlin, Germany).

2.2.4 Bioinformatic analysis

Sequences obtained from fungal clone libraries as described in 2.2.3 were analysed with Vector NTI® Advance 11 for Windows. Using the primer sequences of ITS1F and TW13 as reference, ab1 sequences were trimmed. Contigs were generated from forward and reverse sequences in ContigExpress Project. Primer orientation was checked. Mended contig sequences were checked for chimeras by Bellerophon (Huber *et al.*, 2004) and subjected to nucleotide BLAST searches (Basic local alignment search tool) at http://blast.ncbi.nlm.nih.gov/. Multiple alignments of sequences were created for easier overview of sequence similarity.

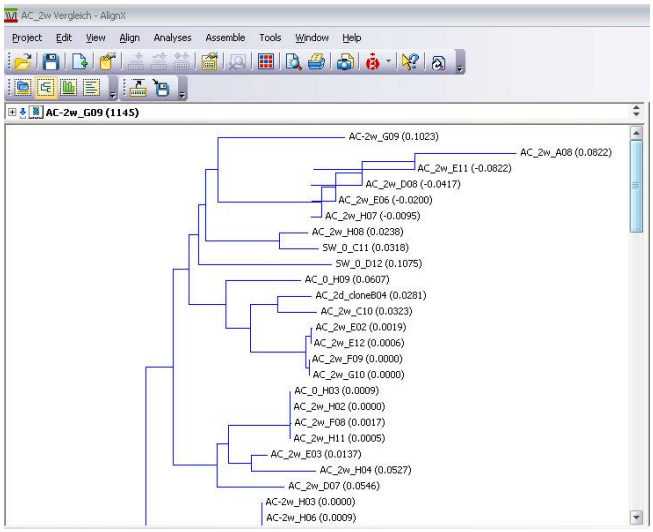

Figure 30: Example of multiple sequence alignment for Achenkirch (AC) litter samples, created with AlignX in Vector NTI® Advance 11 for Windows.

Blast searches were done systematically with full and partial sequences, using the ITS4 primer sequence location to find the 5' end of the LSU region: (1) whole sequence, (2)from start to ITS4 (ITS region), and (3) from ITS4 to the end (LSU region).

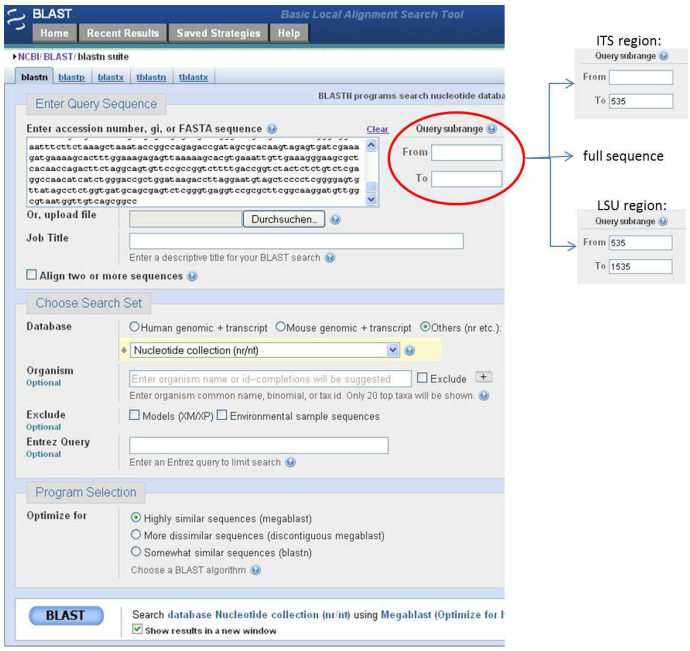

Figure 31: BLAST search window for different query subranges, according to ITS or LSU regions within the sequence.

The taxonomic results were compared for consistency. Potential chimeric sequences were discarded. Taxonomic identification of the clones was mostly based on the partial blastn search results: for identification down to the species level, a high % identity of ITS sequences was preferred, whereas the partial LSU region was used for higher taxonomic level identification.

In cases in which sequences could not be identified to a certain taxonomic level, the lowest common affiliation of reliable reference sequences was taken. Cut-off for distinct species was set to 97 % for the ITS region (Hughes et al., 2009) and 99 % for the LSU region, unless BLAST results for two closely related sequences gave distinct hits to well characterised strains. Chimeric sequences were excluded from further analyses.

Sequences were deposited at GenBank (Benson *et al.*, 2003) under the following accession numbers:

AC_0	JF424278 - JF424358
AC_2	JF449454 - JF449493
AC_14	JF449494 - JF449563
OS_0	JF449639 - JF449665
OS_2	JF449666 - JF449703
OS_14	JF449704 - JF449748
KL_0	JF449564 - JF449587
KL_2	JF495179 - JF495259
KL_14	JF449588 - JF449638
SW_0	JF449749 - JF449776
SW_2	JF449777 - JF449847
SW_14	JF449848 - JF449892

Figure 32: GenBank accession numbers of sequences obtained by fungal clone libraries.

2.2.5 Statistic data processing: EstimateS

Obtained data from each clone library were used to calculate species richness and diversity indices and estimates, applying the software EstimateS Version 9.1.0 (Colwell, 2013). Statistical data evaluation and plotting was done using SPSS and Excel for Windows.

EstimateS requires different data input formats depending on the analyses needed. Format 1 was used to compute Biodiversity Statistics for each sample individually, and Format 3 was used to compute Shared Species Statistics for all samples pairwise.

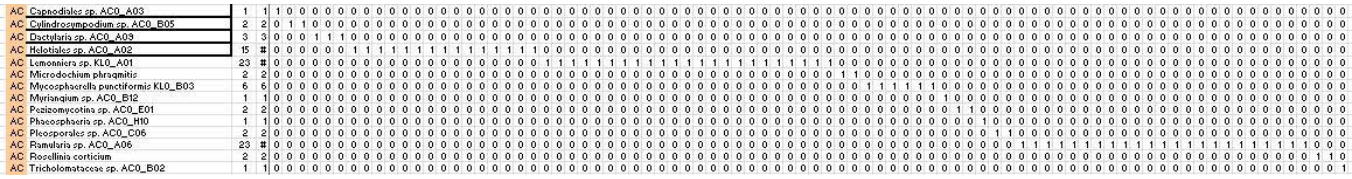

Figure 33: Example for Beech litter clone library data AC -0 days (Achenkirch) in file format 1 for EstimateS data input. Species (rows) by Samples (columns). Each clone was treated as a sample.

OSSIACH: 26 species, 3 samples (0, 2, 14 days)		
species#	sample#	abundance
OSSIACH		
26	3	
1	1	2
2	1	2
3	1	1
4	1	1
5	1	63
5	2	61
5	3	18
6	1	1
6	2	1
6	3	1
7	1	3
7	2	4
7	3	2
8	2	1
9	2	3
9	3	4
10	2	7
10	3	5
11	2	1
12	2	1
12	3	1
13	3	2
14	3	1
15	3	1
16	3	1
17	3	7
18	3	1
19	3	1
20	3	1
21	3	1
22	3	1
23	3	1
24	3	1
25	3	1
26	3	1
-1	-1	-1

Figure 34: Example for Beech litter clone library data OS (Ossiach) in file format 3 for EstimateS data input. Species, Sample, Abundance triplets: the first column contains the species number, the second the sample number, and the third the number of individuals (abundance) of that species in that sample. The example contains shared species data for 26 species (rows) in 3 samples (0, 2 and 14 days respectively, named sample 1, 2 and 3 in column 2).

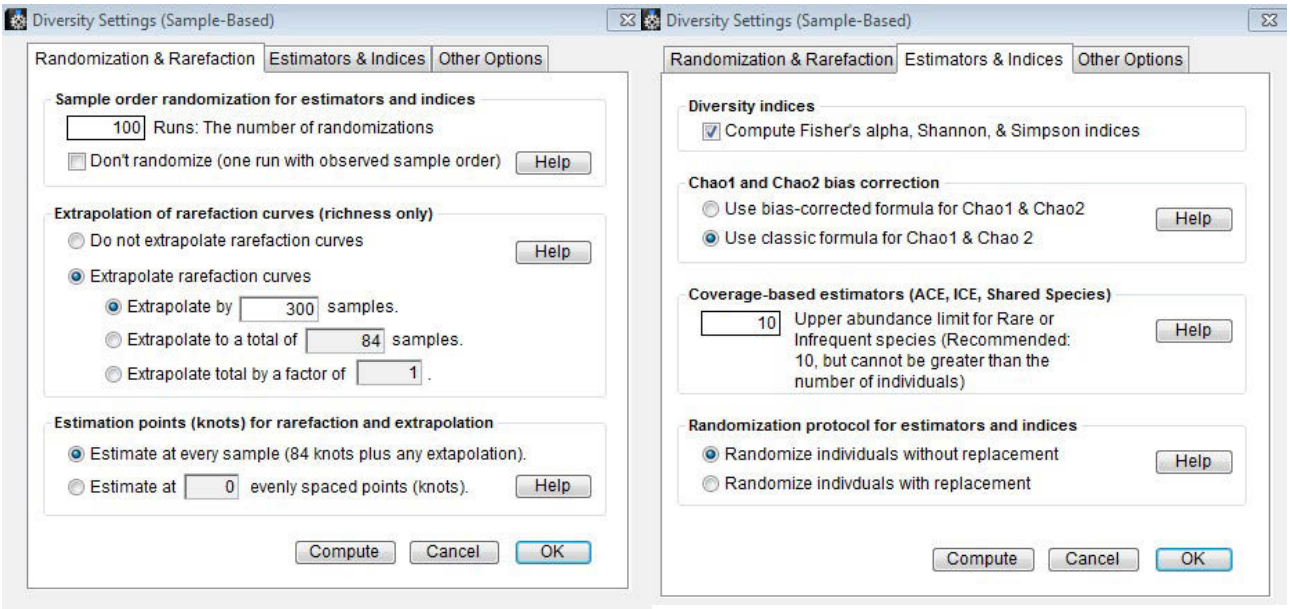

Figure 35: Diversity Statistics Settings used for sample-based data analysis. These settings were used to calculate Diversity Indices and Estimators, Rarefaction curves, and Extrapolation for each sample (location and time point) individually, using File Format 1. This example shows the sample AC_0, with 84 clones (samples) analyzed, randomized 100 times, and extrapolated to a total of 300 samples.

Finally, data was exported into Excel for further data processing.

2.2.6 UniFrac Principal Component Analysis

UniFrac (Lozupone *et al.*, 2006) was used to compare the phylogenetic structures of the fungal communities from soils the four litter samples at different sampling time points. Sequences were aligned with the MUSCLE (Edgar, 2004) algorithm in MEGA5 (Tamura *et al.*, 2011), and a maximum likelihood tree was calculated from the aligned partial LSU sequences. The ITS-region was excluded, since it cannot be unambiguously aligned over such a broad phylogenetic distance. A sequence from a fungus of uncertain affiliation (RELIS_K1_B08, Acc. Nr. JF519027) was used as outgroup but excluded from further analyses. Data were weighted for abundance and normalized for branch length to perform UniFrac Principal Coordinates Analysis (Lozupone *et al.*, 2006).

2.2.7 Materials

Buffers
DNA Extraction buffer: TRIS 0.2 M , SDS 1% , EDTA 1 mM
Reagents
Chloroform-Isoamyl Alcohol (24:1): 48 ml chloroform
2 ml isoamyl alcohol
store at 4°C
Roti®- Phenol (Roth)
Isopropanol
Ethanol 75%
Glycerol (Roth)

Materials
QIAquick® PCR Purification Kit (QIAGEN), containing: QIAquick Spin Columns
Buffer PB
Buffer PE (concentrate)
Buffer EB
Collection Tubes (2 ml)

REDTaq™ ReadyMix™ PCR Reaction Mix with $MgCl_2$ (Sigma)

pGEM®-T Easy Vector System (Promega),containing:
pGEM®-T Easy Vector
Control Insert DNA
T4 DNA Ligase
2x rapid ligation buffer
96-well-plates
96-deepwell-plates
breathable membrane for 96-well-plates
15 ml Greiner tubes

Primer sequences

Primer	Sequence (5'-3')	Target	Gene	T_m	Reference
ITS1F	CTTGGTCATTTAGAGGAAGTAA	Fungal ITS	18S	54°C	(Gardes & Bruns, 1993)
TW13	GGTCCGTGTTTCAAGACG	Univ.eukaryotic	LSU	54°C	https://nature.berkeley.edu/brunslab/

More information on the used primers can be found on https://nature.berkeley.edu/brunslab/ as well as in (White *et al.*, 1990a) and (Gardes & Bruns, 1993).

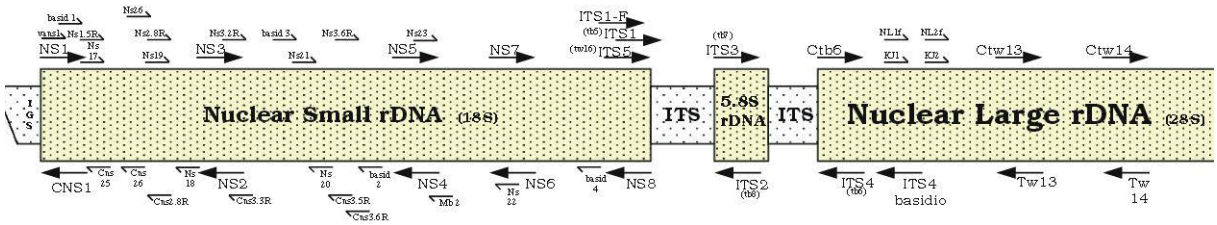

Figure 36: Primer map including ITS1F and TW13 primers used in the experiment, from https://nature.berkeley.edu/brunslab/

Media:

LB Medium:	NaCl	10g
	Peptone	10g
	Yeast extract	5g
	(Agar)	10g
	To 1 l with ddH_2O, autoclave	

Ampicillin stock solution was filter- sterilized and stored at 4°C.
LB-amp: 1 ml of 100 mg/ml amp-stock was added to the autoclaved medium.
X-Gal
IPTG: 100 mM stock
IPTG/X-Gal plates: X- Gal and IPTG were spread over the surface of LB-amp plates.

Restriction enzymes:

HhaI 10 U/µl (Fermentas International Inc, Ontario, Canada)
5'...GCG↓C...3'
3'...C↑GCG....5'
Source : *Haemophilus haemolyticus*
Supplied with: 10x Buffer Tango™

AluI 10 U/µl (Fermentas International Inc, Ontario, Canada)
5'...AG↓CT...3'
3'...TC↑GA....5'
Source: *Arthrobacter luteus*
Supplied with: 10x Buffer Tango™

2.3 Beech litter mesocosm experiments (E1 and E2)

2.3.1 Litter preparation and mesocosm setup

Beech litter from four different locations was prepared as explained in 2.1. After transfer to the laboratory, litter was chopped to pieces (0.2-1 cm), thoroughly mixed per sampling site and air-dried at 40°C for 48 hours. Litter was sterilized by γ –radiation and inoculated with a soil-litter suspension as explained in (Wanek *et al.*, 2011). The inoculum was generated from material harvested at the Klausenleopoldsdorf location. 60g of each inoculated litter type were placed into PVC mesocosms (height 10cm, diameter 12.5cm, perforated plastic grid bottom, micromesh cloth on top) and kept at 15°C. The litter water content was maintained at 60%. For each harvest time point, 5 mesocosms per litter type were established (n=5).

2.3.1.1 Setup and harvest time points E1

Beech litter from AC, OS, KL, and SW was collected and processed as described above. Harvest time points for Experiment 1 (E1):

Harvest I: 2 weeks (14 days)

Harvest II 3 months (97 days)

Harvest III 6 months (181 days)

Harvest IV 15 months (475 days)

20 mesocosms total were mounted per harvest time point (i.e. 4 locations, 5 replicates each) for E1.

DNA was extracted from samples as described in 2.1.4.

2.3.1.2 Setup and harvest timepoints E2: temperature perturbation

Beech litter from OS, KL, and SW was processed for a mesocosm experiment as described above in 2.3.1.

Stress treatments were introduced to mimic climate change events, as described in detail in (Keiblinger *et al.*, 2012).

- Heat treatment: short period at 30°C
- Frost treatment: short period at -4°C

Stress treatments took 14 days, with temperature gradually increasing or decreasing for 4 days, 6 days at the stressful temperature, and then a 4 days decrease/increase to the initial temperature of 15°C.

The treatments started 14 days before Harvest II of E1 (see above). This means that samples for E1-II, E2-H-II and E2-F-II were harvested simultaneously. After 6 months (harvest III) another set of E2 samples was harvested. DNA was extracted from samples as described in 2.1.4.

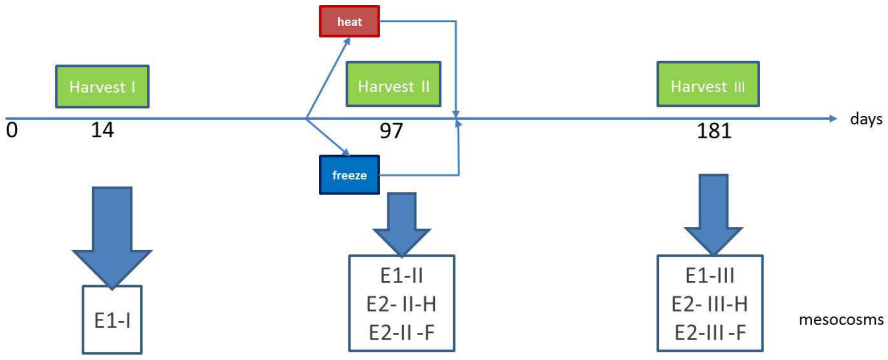

Figure 37: Scheme showing mesocosm setup and harvest time points of E1 and E2 experiments.

2.3.2 Fungal-specific RFLP analysis of E1 replicas

RFLP analysis was performed on the extracted litter DNA samples from time point 2 weeks with primers ITS1F-ITS4 targeting fungi. PCR was performed in triplicates for 30 cycles. The triplicates were pooled before performing RFLP analysis. Digested samples were analysed on a 2% Agarose gel.

Restriction enzymes for RFLP:

5'	G	G↓	C	C	3'	
3'	C	C↑	G	G	5'	BsuRI (HaeIII) was used at 37°C in R buffer
5'	A	G↓	C	T	3'	
3'	T	C↑	G	A	5'	AluI was used at 37°C in Tango buffer

2.3.3 Fungal specific T-RFLP analysis of E1 replicas

T-RFLP analysis was performed on the extracted litter DNA samples from time point 2 weeks with primers ITS1F-fam and ITS4 targeting fungi. The cycling conditions were as follows: initial denaturation at 95 °C for 2'30", 30 cycles of 94 °C for 30", 54 °C for 30"

and 72 °C for 45", and a final extension at 72 °C for 5'. All PCRs were carried out in triplicate.

10 µl	2x PCR-Mix
2 µl	ITS1F-FAM
2 µl	ITS4
5 µl	H_2O, BSA, DMSO, MgCl2
1 µl	DNA (1:10 dilution)

Triplicates were pooled and checked on a gel. Pooled PCR products were digested with restriction endonuclease *Bsu*RI in a 20µl restriction reaction (10 µl PCR product) and purified with the QIAquick PCR Purification Kit. 5µl of purified product was mixed with 15µl HiDi-Formamide and 0,3µl GeneScan™ 500 ROX™ Size Standard and denatured at 95°C for 2min. Detection of FAM-labelled terminal restriction fragments was done by capillary electrophoresis using an ABI 3100 automatic DNA sequencer at BOKU (Ulrike Vavra). T-RFLPs were transformed into numerical data using GenoTyper 3.7 NT software. These raw data were normalized and binned according to (Abdo *et al.*, 2006).

5µl	purified restriction reaction
15µl	HIDI formamide
0,3µl	internal size standard (ROX500)
20 µl	

Sequencer settings:
Standard: ROX 500
Label: FAM
Injection time: 10s

Sequencing results were edited using GeneScan program, and converted to txt. Next, the programs Perl and R were used to generate FilteringAndBinning document, and finally a ClusBinMatrix.

2.3.4 Real-time PCR of litter DNA

Real-time PCR was performed on the extracted litter DNA samples with primers targeting bacteria (primer pair: 101F, 537R) and fungi (primer pair: NSI1 , 5.8S) for all samples, as described in (Inselsbacher *et al.*, 2010). All reactions were run in triplicates. As standards for bacteria and fungi, pure culture genomic DNAs of known concentrations were used (*Cadophora finlandia, Pseusomonas fluorescens*). For further calculations, results of [ng/µl] concentrations are shown as ratio of fungi:bacteria.

Premix calculation per sample:

IQ™SYBR®-Green Supermix	12.5 µl
DNA sample 1:500	10 µl
pF	1 µl
pR	1 µl
BSA	0,5 µl (0.2 mg/ml)
	25 µl

Temperature program:

1	80°C		preheating
2	95°C	3:00	Initial denaturation
3	94°C	0:10	
4	**60/66°C**	0:30	Annealing
5	72°C	0:30	Repeat 3-5 **40** times
6	12°C	hold	

Table 3: PCR Temperature Program for real-time PCR

PCR reactions were analyzed by agarose gel electrophoresis.

2.3.5 Materials

Buffers

DNA Extraction buffer: TRIS 0.2 M
SDS 1%
EDTA 1 mM

Reagents

Chloroform-Isoamyl Alcohol (24:1): 48 ml chloroform
2 ml isoamyl alcohol
store at 4°C

Roti®- Phenol (Roth)
Isopropanol
Ethanol 75%
Glycerol (Roth)
BSA

Materials
AluI (10 U/µL) (Thermo Scientific) with Tango buffer
BsuRI (HaeIII) (10 U/µL) (Thermo Scientific) with R buffer
HiDi-Formamide (Applied Biosystems)
QIAquick PCR Purification Kit (Quiagen)
GeneScan™ 500 ROX™ Size Standard (Applied Biosystems)
ABI 3100 automatic DNA sequencer
IQ TMSYBR®-Green Supermix (BIO-Rad)
iCycler iQ5 Multicolor Real Time PCR Detection System (BIO-Rad)

Primer sequences

Primer	Sequence (5'-3')	Target	Gene	T_m (°C)	Reference
ITS1F	CTTGGTCATTTAGAGGAAGTAA	fungi	18S	54	(Gardes & Bruns, 1993)
ITS4	TCCTCCGCTTATTGATATGC	fungi	18S	54	(White *et al.*, 1990a)
NSI1	GATTGAATGGCTTAGTGA	fungi	18S	60	(Martin & Rygiewicz, 2005)
5.8S	CGCTGCGTTCTTCATCG	fungi	5.8S	60	(Inselsbacher *et al.*, 2010)
101F	ACTGGCGGACGGGTGAGTAA	bacteria	16S	66	(Inselsbacher *et al.*, 2010)
537R	CGTATTACCGCGGCTGCTGG	bacteria	16S	66	(Schmalenberger *et al.*, 2001)

2.4 Phylotrap methods

2.4.1 Culture of fungi and bacteria

Aspergillus nidulans spores are stored at -80°C in the strain collection. For reactivation they were plated on complete medium with 1% Glucose and ammonium as nitrogen source. Plates were incubated at 37°C.Reactivated strains were grown on minimal medium with appropriate supplements and a N source. Spores were harvested with a spatula and vortexed in 0,1% TWEEN solution. Spore count was determined with a chamber. For *A.nidulans* liquid culture, 10^6 spores were inoculated in 200 ml liquid Minimal Medium in 1 L Erlenmeyer flasks, and incubated overnight at 37°C with 180 rpm. *Raoultella terrigena* was grown in 50 ml liquid culture (LB- medium) overnight at 30°C.

2.4.1.1 Materials

Media

Minimal medium (MM):	carbon source (Glucose 1%) 20 ml salt solution/L (see below) pH 6.8 with NaOH (optional: 15 g agar-agar) up to 1 litre with deionized water, autoclave
Complete medium (CM):	carbon source (usually glucose 1%) 20 ml salt solution (see below) 1.5 g casoaminoacids 2 g peptone 1 g yeast extract pH 6.8 with NaOH (optional: 15 g agar-agar) up to 1 litre with deionized water, autoclave
Nitrogen source for CM:	100x stock solution of Ammonium tartrate (9.2 g / 100 ml H_2O)
Salt solution:	26 g KCl 26 g $MgSO_4$ $7H_2O$ 76 g KH_2PO_4 50 ml trace-element solution (see below) 2 ml of chloroform for sterility up to 1 litre with dH_2O
Trace element solution:	40 mg sodiumborate 400 mg $CuSO_4$ $5H_2O$ 714 mg $FeSO_4$ $7H_2O$ 728 mg $MgSO_4$ $7H_2O$ 800 mg sodiummolybdate 8 mg $ZnSO_4$ $7H_2O$ up to 1 liter with H_2O, autoclave

LB Medium:	NaCl	10g
	Peptone	10g
	Yeast extract	5g
	(Agar)	10g
	To 1 l with ddH_2O, autoclave	

Reagents
TWEEN 20 for molecular biology (Sigma- Aldrich, St. Louis, MO, USA)

Strains

Aspergillus nidulans wt fawn
Raoultella terrigena

2.4.2 RNA extraction from *A.nidulans* and *R.terrigena* pure cultures

A.nidulans mycelia were grown overnight at 37°C in liquid medium, then harvested by filtration, ground to a fine powder in liquid nitrogen with a pre-chilled mortar and pestle and subsequently frozen in liquid nitrogen. For maximum RNA yield, up to 0,1 mg of ground material were used per sample. 1ml TRIzol®- Reagent was added to the tubes and mixed by vortexing. After 5 minutes at room temperature and repeated vortexing, tubes were centrifuged at 13.000 rpm for 15 minutes at 4°C to precipitate the mycelia. The supernatant was transferred to a new tube. By addition of 400 µl chloroform, phases are separated. RNA partitions to the aqueous phase, DNA to the interphase, and proteins to the organic phase. Repeated vortexing and incubation at room temperature for 10 minutes ensures that the entire RNA can migrate into the aqueous phase. Phase separation was done by 15 min centrifugation at 4°C and 13.000 rpm The upper, aqueous phase was transferred into a new tube. RNA was precipitated by addition of 250 µl isopropanol and incubation for another 20 minutes. After centrifugation (30 min, 13.000 rpm), supernatant was discarded. The RNA pellet was washed with 1 ml 70% ethanol to get rid of salts. Finally, the air- dried RNA pellet was dissolved in 50-100 µl H_2O. Samples were stored at -80°C.

Raoultella terrigena cultures were grown overnight in LB medium at 30°C. 1,5 ml of ON-culture were centrifuged at 12,000g for 10 min. The pellet was washed with 300 µl of saline, and resuspended in 400 µl of 0,12 M sodium phosphate buffer, pH 7,2. 50 µl of 5% SDS and 50 µl of proteinase K (0,5 mg/ml) were added for cell lysis, followed by incubation at 37°C for 20 min. Next, 500 µl of PEG 8000 (12,5% w/v) in 1 % potassium phosphate were added. After vortexing, the tubes were centrifuged at 12.000g for 10 min. The supernatant containing the RNA was carefully transferred to a new tube without touching the pellet containing DNA and cell debris. RNA was precipitated by adding 0,1 vol 3M sodium acetate and 1 vol isopropanol and incubation at -20°C for ~1

hour. Samples were centrifuged at 12,000g for 20 min at 4°C. The supernatant was discarded and the pellet was washed in 70% ethanol. After centrifugation at 12.000g for 10 min, the pellet was dried by inverting onto tissue paper. The RNA was dissolved in 100 µl water. To reduce PEG leftovers in the RNA samples, RNeasy kit (Qiagen) RNA cleanup procedure was performed according to manufacturer's instructions. Additionally, on- column DNase digest with RNase free DNase was done at the point indicated in manufacturer's protocol due to a quite high DNA contamination level.

DNase incubation mix:
1,5 µl of RNase free DNase I
8 µl 10xDNase I buffer
72 µl water

80 µl DNase incubation mix were added directly to the spin column membrane. After incubation at RT for 30 min, 350 µl of buffer RW1 were added and tubes spinned for 15s. The rest of the protocol was done according to the manufacturer. RNA samples were stored at -80°C.

2.4.3 RNA quantitation by UV- spectrophotometry

The relationship between the absorption of UV light by RNA and its concentration in the sample was used to determine RNA concentration in samples. A_{260}=1 corresponds to the RNA concentration 40 µg/ml.

[RNA]µg/ml = A_{260} x dilution x 40

Proteins absorb at 280 nm, thus A_{260}/A_{280} shows the purity of the RNA sample. A pure sample of RNA has an A_{260}/A_{280} ratio of 2.0 ±0,1, so the ratio of RNA samples should be between 2.0 and 2.4. A lower ratio indicates protein contamination. RNA samples are diluted 1:50 in TE buffer and measured in a 100 µl quartz cuvette. Absorption of TE buffer is used as blank.

2.4.4 Phylotrap initial protocol

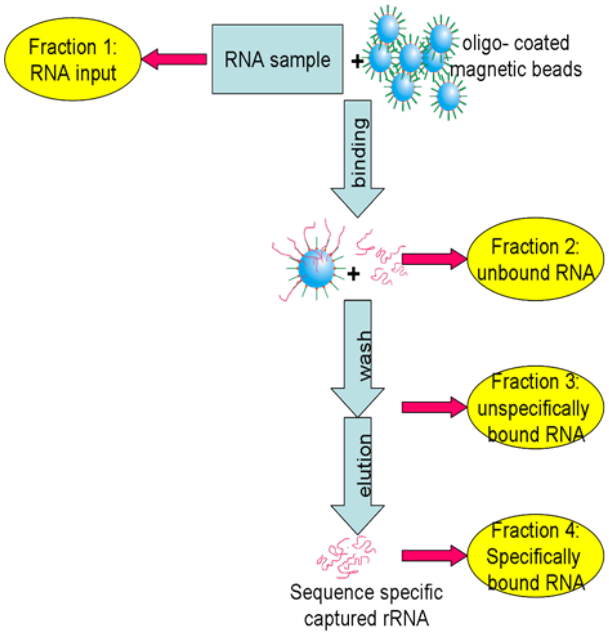

Figure 38: Flow chart of indirect sequence- specific rRNA capture with magnetic beads and obtained fractions 1-4 that were analyzed after the experiment, as developed in (Böck, 2008).

Bead coating: For RNA applications, 100 µl Dynabeads were washed twice with SolutionA for 2 minutes, and then with Solution B. For immobilization of the probe on the beads, beads were washed with 2xB&W buffer and resuspended in 1xB&W buffer to a final concentration of 5 µg/ml (twice the original volume). Biotinylated oligos (200 pmol) are added to the beads and incubated at RT for 15 minutes using gentle rotation. After immobilization, beads were washed 2-3 times with 1xB&W buffer and used for downstream applications or stored at 4°C.

RNA pre- treatment: Mix sample RNA (10 µg), Hybridization buffer (5xSSC, 0,1% N-laurylsarcosine, 0,1% NaCl, 0,02% SDS) and Formamide (15%) to a final volume of 450 µl. Incubate at 70°C for 10 min, then 30 min at RT. The mixture was divided: 200 µl were taken (→ Fraction 1: RNA input), 200 µl were used for the capturing step.

RNA capture: Add 200 µl RNA mixture to 1mg of probe- coated beads and incubate at 40°C for 30 min with agitation. Supernatant → Fraction 2

Washing step: Wash the beads with 0,5x SSC. Supernatant = Fraction 3: wash.

Elution: add 200 µl DEPC- water and incubate for 10 min at RT. Then incubate at 70°C for 3 min. Supernatant = Fraction 4: Eluate.

2.4.5 RNA precipitation

RNA of all 4 fractions (200 µl) was precipitated by adding 10 µg of yeast-tRNA (Invitrogen), 1 volume isopropanol and 0,1 volume 3M Na-Acetate. Pellet was washed with 3 volumes 70% ethanol, and resuspended in 20 µl DEPC water. These fractions were run on a nondenaturing 0,8% agarose gel for visualization.

2.4.6 Agarose gel electrophoresis

For RNA applications, nondenaturing 1,5% or 2% agarose in 1xTAE buffer were used. Add to 10 µl sample: 2 µl of RNA loading buffer, 1 µl of 1:100 diluted EtBr. Run for ca. 40 minutes at 80V.

2.4.7 Real-Time PCR

After collecting the supernatant of the Phylotrap-elution fraction, 10 µl were used for 1:10 dilution and Reverse Transcription and qPCR. Reverse Transcription was performed with iScript™ Reverse Transcription Supermix for RT-qPCR.

Premix calculation per sample:
4 µl 5x RT Reaction Mix
1 µl RT Enzyme Mix
10 µl Sample
15 µl

Temperature program: 25°C 5 min
42°C 30 min
85°C 5 min
4°C Hold

After RT reaction, add 185 µl H_2O to the 15 µl reaction and used for qRT-PCR:

Mix Biorad	10 µl
pF	2 µl
pR	2 µl
water	1 µl
template 5 µl	
	20 µl

PCR reaction and fluorescence data collection was performed in iCycler iQ™Real-Time PCR Detection System according to Instruction Manual by BioRad. Total *A.nidulans* and *R.terrigena* RNA was reverse transcribed and diluted to be used as standards in qPCR reactions. All reactions wer run in duplicates. Melting curve analysis was performed following qRT- PCR to identify the presence of primer dimers and analyze the specifity of the reaction.

2.4.8 Materials

Reagents:

DEPC (diethylpyrocarbonate)
Formamide (Sigma), frozen in aliquots to prevent oxidation
TRIzol®- Reagent (Invitrogen, Carlsbad, California 92008)
Chloroform (RNase- free)
Isopropanol (RNase- free)
70% Ethanol
H_2O (RNase- free)
Physiological saline: 0,85% (w/v) NaCl, autoclave
0,12M sodium phosphate buffer, pH 7.2, autoclave
5% (w/v) sodium dodecyl sulphate (SDS)
Polyethylene glycol (PEG) 8000 20% (w/v) in 1 % (w/v) potassium phosphate pH 7.2, autoclave
3M sodium acetate, pH 5.2, autoclave
Agarose (Sigma)
Ethidiumbromide (10 mg/ml stock, use 15 µl/l agarose gel) (Sigma)
Gene Ruler™ 100bp DNA Ladder (Fermentas)
Gene Ruler™ 1kb DNA Ladder (Fermentas)
Yeast-tRNA (Invitrogen) 10 mg/ml
RNA loading buffer (50% glycerol, bromphenolblue, xylencyanol)

Dynabeads® M- 280 Streptavidin (Invitrogen)

SolutionA :	0,1M NaOH
	0,05M NaCl
	DEPC treated
SolutionB :	0,1M NaCl
	DEPC treated
2xB&W Buffer:	10mM Tris- HCl (pH 7,5)
	1mM EDTA
	2M NaCl

Enzymes:

DNase I RNase free (Fermentas)
DNase I 10x reaction buffer with $MgCl_2$ (Fermentas)

Buffers:
TE buffer

50x TAE buffer:	242 g Tris (2M)
	57.1 ml glacial acetic acid (1M)
	100 ml 0,5M EDTA (pH 8.0)
	To 1000 ml with ddwater

Hybridization buffer:	5xSSC
	0,1% N-laurylsarcosine
	0,1% NaCl
	0,02% SDS
	DEPC treated
	(MacGregor *et al.*, 2002)

Materials:
RNeasy Kit (Promega)
Quartz kuvette
Photometer
StarPhoresis Horizontal Gel System (Starlab) + Power supply
iCycler (Biorad)
iScript™ Reverse Transcription Supermix for RT-qPCR (biorad)
iQ™ Supermix (Biorad)

Probe sequences:
Probes were 5'biotin labelled and contained a DNA linker sequence (shown in brackets). The target sequence was LNA™ enhanced by Exiqon, Denmark. Details on the probe sequences are available at probeBase (Loy *et al.*, 2007).

Probe name	Sequence 5'-3'	target
EUKb310-Y-bio	BIO-[aatactaa] TCA GGC BCC YTC TCC G	18S rRNA of nearly all eukarya
Bakt338_bio	BIO-[aaaaaaaaaaaa]GCTGCCTCCCGTAGGAGT	Most bacteria

Primer sequences for qPCR

Primer	**Sequence (5'-3')**	**Target**	**Gene**	**T(°C)**	**Reference**
SR7R	AGTTAAAAAGCTCGTAGTTG	eukarya	18S	56°C	http://sites.biology.duke.edu/fungi/mycolab/primers.htm
SR5	GTGCCCTTCCGTCAATT	Eukarya	18S	56°C	http://sites.biology.duke.edu/fungi/mycolab/primers.htm
Ctb6	GCATATCAATAAGCGGAGG	eukarya	28S	60°C	https://nature.berkeley.edu/brunslab/tour/primers.html
TW13	GGTCCGTGTTTCAAGACG	eukarya	28S	60°C	https://nature.berkeley.edu/brunslab/
EUBr1387	GCCCGGGAACGTATTCACCG	bacteria	16S	60°C	(Iwamoto *et al.*, 2000)
EUBf933	GCACAAGCGGTGGAGCATGTGG	bacteria	16S	60°C	(Iwamoto *et al.*, 2000)
fBACT23S	GCGATTTCYGAAYGGGGRAACCC [Y is C or T] [R is A or G]	bacteria	23S	67°C	(Anthony *et al.*, 2000)
rBact23S	TTCGCCTTTCCCTCACGGTACT	bacteria	23S	67°C	(Anthony *et al.*, 2000)

3 RESULTS

3.1 Fungal clone library results

Fungal clone library sequences were generated as described in 2.2.2. Beech litter from four different locations in Austria was incubated in microcosms for 2 and 14 days before DNA was extracted and clone libraries were constructed. In **Figure 39**, an example of a 2% Agarose Gel with RFLP patterns is shown. All other agarose gels can be found in Supplementary Material.

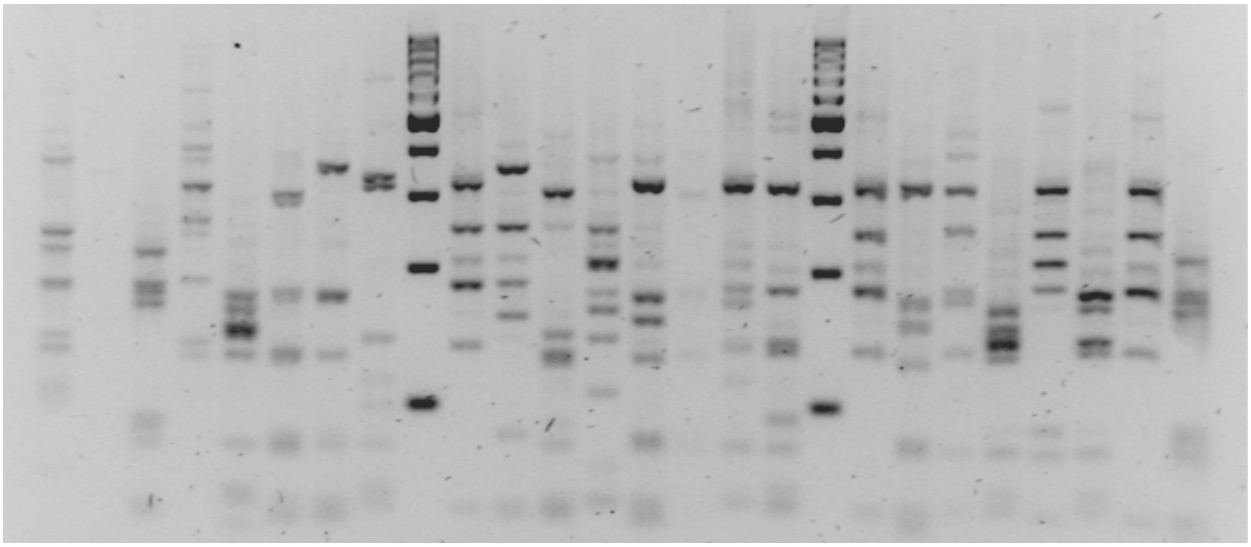

Figure 39: Agarose Gel showing RFLP patterns of SW at time point 2 weeks, row 1-3 A through H respectively.

AC_0	JF424278 - JF424358
AC_2	JF449454 - JF449493
AC_14	JF449494 - JF449563
OS_0	JF449639 - JF449665
OS_2	JF449666 - JF449703
OS_14	JF449704 - JF449748
KL_0	JF449564 - JF449587
KL_2	JF495179 - JF495259
KL_14	JF449588 - JF449638
SW_0	JF449749 - JF449776
SW_2	JF449777 - JF449847
SW_14	JF449848 - JF449892

By the combined approach of RFLP-typing and sequencing of fungal ITS/partial LSU regions a total of 120 ribotypes were detected in the four beech litter types at three different incubation times in microcosms. All sequences were of fungal origin and the majority (88 sequences) could be classified to species or genus level. All sequences are available on NCBI with accession numbers as shown in the table. No indications for an underestimation of species richness due to insufficient resolution of RFLP were found.

3.1.1 Species accumulation curves

Unified species accumulation curves for fungal clone libraries were constructed as described in (Colwell et al., 2012).

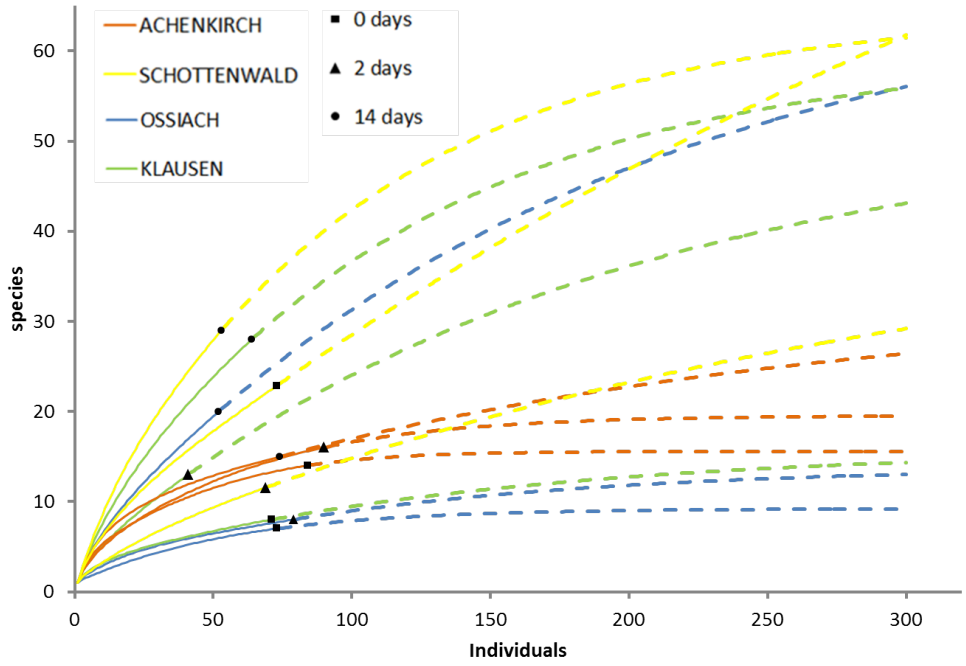

Figure 40: Species accumulation curves for fungal species richness on decaying beech litter, showing detected species (OTUs) vs analyzed individuals (clones). Interpolation (rarefaction, see **Fehler! Verweisquelle konnte nicht gefunden werden.**) and extrapolation (see 1.3.1.2) were integrated to produce unified species accumulation curves for empirically collected data, based on reference samples. This set of species accumulation curves was generated by EstimateS Version 9.1.0., using 'Sample-based input file Format 1' as explained in Estimate S User Guide (Colwell, 2013). Samples were randomized 100 times. Rarefaction curves were extrapolated to a total number of 300 samples. Curves were plotted with Excel for Windows. Different locations (Achenkirch AC, Schottenwald SW, Ossiach OS, Klausenleopoldsdorf KL) are shown with color code as explained in the figure. Reference samples for each assemblage are indicated by full squares, rectanges, and circles respectively. Full lines show rarefaction curves, dashed lines represent extrapolation up to 300 individuals per assemblage.

In **Figure 40**, the y-axis shows the number of detected species (i.e. individual OTUs) for fungal clone libraries, and the x-axis shows increased sampling effort. A lower curve slope indicates that the fungal community richness is more saturated, a higher curve slope shows that new species are detected much faster and richness reaches the asymptote (= true species richness) later. Maximum fungal species density was found at Schottenwald (SW) time point 14 days, lowest species density was found at Ossiach (OS) time point 0 days. For location Achenkirch (AC) shown in orange, all three timepoints flattened out asymptotically for the rarefied part of the curve (full

line), which indicates that fungal richness had been sampled sufficiently. Rarefaction curves for OS samples showed asymptotic behavior at 0 and 2 days, Klausenleopoldsdorf (KL) at 0 days, Schottenwald (SW) at 2 days. These samples can all be assumed to be sampled well enough to represent the actual species richness.

Curves for all samples at time point 14 days only started to flatten out after extrapolation up to 300 individuals (dashed line), location SW even merely started asymptotic flattening at 300 individuals. This indicates that these assemblages were not represented well by the applied sampling approach and might contain significant numbers of undetected species.

3.1.2 Fungal richness and diversity indices

Litter	days	clones	S_{obs}	Chao1	SD_{Chao1}	Chao2	SD_{Chao2}	H	1/D
AC	0	84	14	15,6	2,1	15,6	2,1	2,0	5,2
AC	2	90	16	19,6	3,8	19,6	3,8	1,9	3,6
AC	14	74	15	32,8	23,3	32,8	23,3	2,2	7,0
KL	0	71	8	15,9	11,5	15,9	11,5	1,1	2,0
KL	2	41	13	52,5	47,9	52,5	47,9	1,8	3,6
KL	14	64	28	59,9	21,5	59,9	21,5	2,9	10,2
OS	0	73	7	9,2	3,4	9,2	3,4	0,6	1,3
OS	2	79	8	13,9	7,0	13,9	7,0	0,9	1,6
OS	14	52	20	68,1	43,2	68,1	43,2	2,4	6,2
SW	0	69	22	125,5	55,4	125,5	55,4	2,4	5,8
SW	2	73	12	43,6	39,1	43,6	39,1	1,1	1,7
SW	14	53	29	64,4	23,5	64,4	23,5	3,1	17,9

Table 4: Fungal richness and diversity indices for beech litter fungal clone libraries as computed by EstimateS 9.1.0 (Colwell, 2013). AC= Achenkirch, KL= Klausenleopoldsdorf, OS=Ossiach, SW= Schottenwald. Time points 0, 2 and 14 days. Clones=number of analyzed clones for each sample. S_{obs}=number of observed species in clone library. Chao1=predicted species richness based on the Chao1 estimator (Chao, 1984). Chao2 = predicted species richness based on the Chao2 estimator (Chao, 1984). SD_{Chao1}, SD_{Chao2} = Standard deviation for respective richness estimators (Chao, 1987b). H = Shannon Diversity index. 1/D= Inverse Simpson Diversity Index.

Obtained data from each clone library were used to calculate species richness and diversity indices and estimates, applying the software EstimateS Version 9.1.0 (Colwell, 2013). Data Input Format 1 was used to compute Biodiversity Statistics for each sample

individually. Richness ranged from 7 to 29 of observed and from 9 to 125 for predicted species numbers (Chao1; Chao, 1987a) per sample (see **Table 4**). Richness and Diversity values for different locations and three time points are displayed graphically in **Figure 41**. The differences between observed species counts (S_{obs}) and estimated species richness (Chao1) accounted for coverages from 90% (AC_0) to 17% (SW_0).

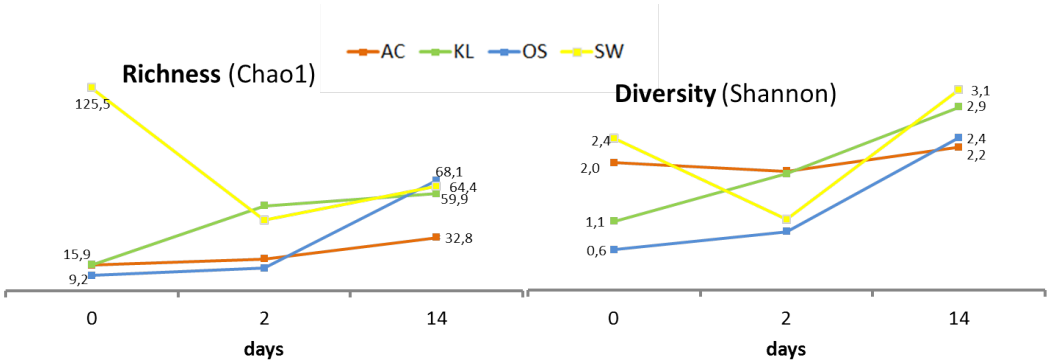

Figure 41: Chao1 richness estimators and Shannon diversity indices for beech litter fungal clone libraries as computed by EstimateS. AC= Achenkirch, KL= Klausenleopoldsdorf, OS=Ossiach, SW= Schottenwald. Time points 0, 2 and 14 days.

Richness values generally increased with time (**Figure 41**, left section) for locations AC, KL, and OS; but not for SW because of a very high richness at 0 days. Therefore no statistically significant richness differences could be found for the three timepoints (see below). Diversity is highest at the 14 days timepoint for all samples (**Figure 41**, right section).

A one-way Analysis of Variance (ANOVA) was performed with STATGRAPHICS Centurion XVI Version 16.0.09 using the Diversity (Shannon) and Richness (Chao1) values of for different sampling sites (AC, KL, OS, SW) at three different time points (0, 2 and 14 days) from **Table 4**. The results are plotted in **Figure 42**.

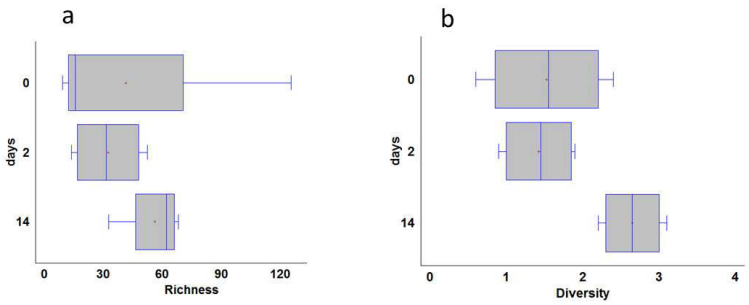

Figure 42: Box and Whisker plot for Diversity and Richness at different time points. Vertical line in the boxes show median, red cross marks the mean value. Four sampling sites are included per time point. (a) Diversity (Shannon), (b) Richness (Chao1).

According to the Multiple Range Test, Shannon diversity index data at time point 14 days are significantly different from all other time points at the 95% confidence level (See Figure **Figure 42b**). No statistically significant differences could be calculated for Richness data.

3.1.3 Rank abundance plots

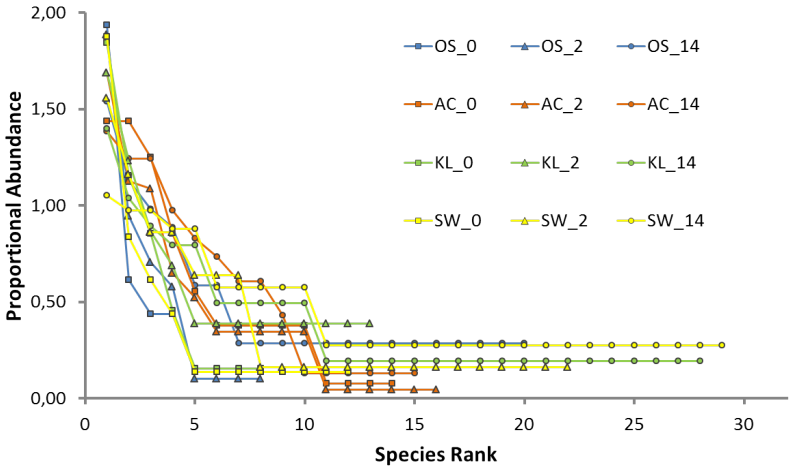

Figure 43: Rank-Abundance distributions of fungal species on beech litter, plotted by species rank. AC=Achenkirch, OS=Ossiach, KL=Klausenleopoldsdorf, SW=Schottenwald, time points 0, 2 and 14 days, respectively. The proportional abundance on the y-axis (on a logarithmic scale) was calculated by setting the sum of all species abundances to 100% for every sample individually.

Overall, rank abundance plots for fungal OTUs from clone libraries show a similar pattern, highlighting low evenness among fungal decomposer communities. There is a sharp drop in abundance for the highest ranking species (dominant OTUs), and a long tail representing rare species. OS_0 shows the lowest curve as well as the shortest curve, which means that both species evenness and species richness were lowest in this sample. Higher species richness in later time points, especially time point 14 days, is represented by the longer tails in the respective rank-abundance curves.

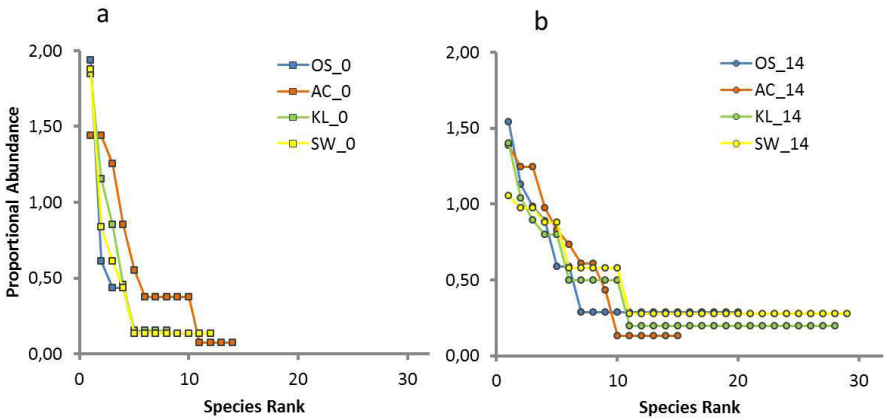

Figure 44: Rank-Abundance distributions of fungal species on beech litter, plotted by species rank. AC=Achenkirch, OS=Ossiach, KL=Klausenleopoldsdorf, SW=Schottenwald. The proportional abundance on the y-axis (on a logarithmic scale) was calculated by setting the sum of all species abundances to 100% for every sample individually. (a) Time point 0 days. (b) Time point 14 days.

The drop between the highest-ranking, dominant OTU and the following OTUs narrowed with incubation time, indicating the proliferation of subdominant species with time (**Figure 44**). The curve tail became longer as well, showing a higher number of rare species detected in the later time point.

3.1.4 Biotic similarity of fungal communities found on beech litter samples

To investigate the similarity between fungal communities in different locations and at different time points (β-diversity), the Morisita–Horn index was used. This index is based on the relative abundance of species by pairwise community comparisons (Chao *et al.*, 2008). Analysis of the fungal patterns for all sample combinations showed similarity indices covering a wide range from almost zero (no overlap of fungal species) to almost 1 (complete overlap of fungal species), see Figure 45.

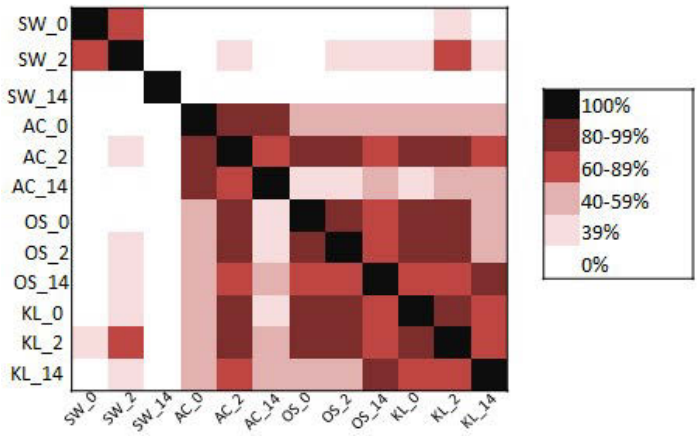

Figure 45: Morisita-Horn similarity indices for beech litter associated fungal species compositions in all combinations of locations and time points. Increasingly intense colors show higher similiarity. (AC=Achenkirch, OS=Ossiach, KL=Klausenleopoldsdorf, SW=Schottenwald), time points 0, 2 and 14 days, respectively. Indices based on shared species between any two communities, as calculated by EstimateS (Colwell, 2013). Analysis was based on fungal species abundance.

Comparing the biotic similarity of the three samples (0, 2 and 14 days) within each location, the OS location samples shared the most species with each other. (0.66-0.99). The SW location not only showed the lowest similarity with all other beech locations (0.0-0.61), but even the time course within the SW location shared the lowest amount of species with each other.

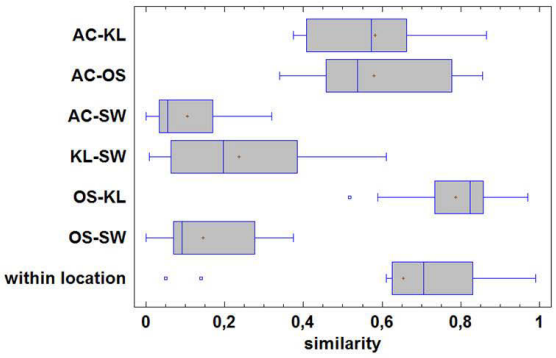

Figure 46: Fungal community similarity comparison among locations. Box plots are based on pairwise comparisons of Morisita-Horn fungal community similarity within each sample group. The box indicates the 25% quartile, median, and 75% quartile. Outside points, which are points more than 1.5 times the interquartile range (box width) above or below the box, are indicated by point symbols.

Regarding biotic similarity among locations, the samples from OS and KL locations showed the highest biotic similarity with similarity indices between 0.52-0.97. As shown in **Figure 46**, these values are in the same range as the similarity of the samples from within the same location.

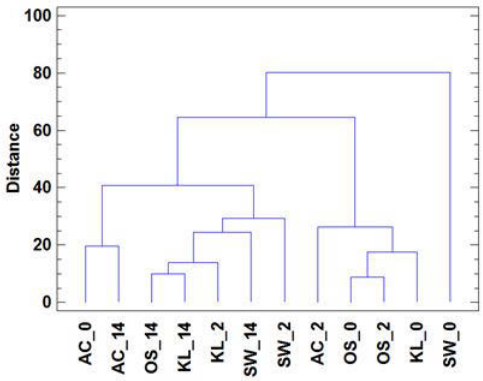

Figure 47: Dendrogram showing the results of cluster analysis for beech litter fungal clone libraries. 12 complete cases were used (AC=Achenkirch, OS=Ossiach, KL=Klausenleopoldsdorf, SW=Schottenwald, time points 0, 2 and 14 days, respectively), Furthest Neighbor Method, using Euclidean Distance Matrix. Indices based on shared species between any two communities. Analysis was based on fungal species abundance.

A cluster analysis revealed the SW_0 sample distinctively as an outgroup, and a tendency to clustering by time point. AC clustered together rather than with other samples, only AC_2 showed similarity indices above 0.5 with other samples.

3.1.5 Taxonomic and phylogenetic diversity

Fungal ITS/partial LSU sequences obtained by RFLP-typing and sequencing were all assigned to fungal sequences. Classification with the BLAST (Altschul *et al.*, 1990) algorithm led to classification down to genus or species level for the majority of sequences. Fungal communities on beech litter of different locations in Austria were identified with this approach, providing a snapshot of the very early stage of beech litter decay from 0 to 14 days after sample incubation.

3.1.5.1 Ratio of fungal phyla found on beech litter

a

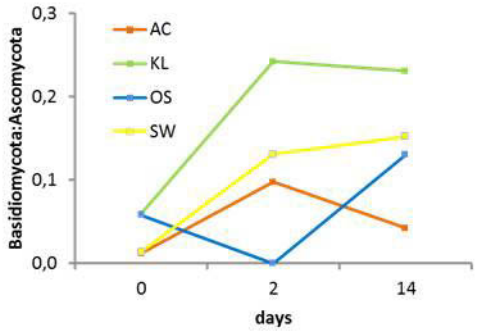

b

Litter	days	Asco-mycota %	Basidio-mycota %
AC	0	98,8	1,2
AC	2	91,1	8,9
AC	14	95,9	4,1
KL	0	94,4	5,6
KL	2	80,5	19,5
KL	14	81,3	18,8
OS	0	94,5	5,5
OS	2	100,0	0,0
OS	14	88,5	11,5
SW	0	98,6	1,4
SW	2	88,4	11,6
SW	14	86,8	13,2

Figure 48: Fungal taxonomic diversity for beech litter fungal clone libraries, shown as (a) ratio of encountered Basidiomycota versus Ascomycota and (b) total percentage of encountered Asco- and Basidiomycota species respectively, based on the total number of identified clones per sample. AC= Achenkirch, KL= Klausenleopoldsdorf, OS=Ossiach, SW= Schottenwald. Time points 0, 2 and 14 days.

All OTUs derived from fungal clone libraries of different beech litter samples were assigned to the Dikarya phyla of Ascomycota and Basidiomycota. By this DNA library

based approach, no members of the Glomeromycotina, Mucoromycotina or any other basal fungal lineage were detected. All tested litter communities were dominated by Ascomycota, which were represented by at least 80% of the clones in the respective libraries (see Figure 48b). The remaining clones belonged to the Basidiomycota. The only sample with no OTUs assigned to Basidiomycota was OS litter at time point 2 days; but generally on all litter types, ratios of Basidiomycota:Ascomycota increased with incubation time (see Figure 48a) . This pattern was most prominent on KL litter, here OTUs assigned to Basidiomycota showed the highest percentage of 19,5% at 2 days, and 18,8% at 2 weeks, respectively.

3.1.5.2 Fungal classes found on different locations

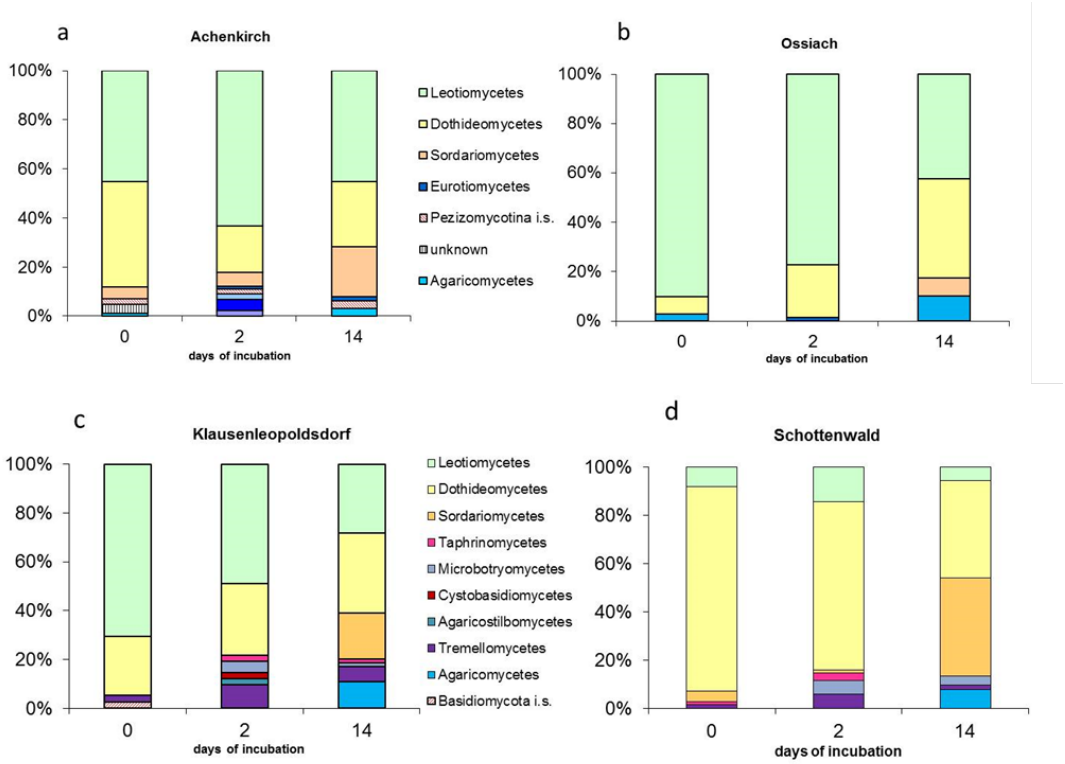

Figure 49: Taxonomic diversity of fungal clone libraries from decaying beech litter, sorted by class. a, b, c, d, showing different litter locations Achenkirch, Ossiach, Klausenleopoldsdorf, and Schottenwald. Time points 0, 2 and 14 days.

Most fungal OTUs on beech litter were assigned to the Ascomycota classes Leotiomycetes, Dothideomycetes and Sordariomycetes within the Pezizomycotina. On SW litter, Dothideomycetes started as the dominating species class (Figure 49d), whereas OS and KL were dominated by Leotiomycetes (Figure 49bc). AC showed Leotiomycetes and Dothideomycetes at almost similar dominance levels (Figure 49a). Later time points generally showed less dominance of single OTUs and more classes of fungi detected. Only a few OTUs were assigned to the Eurotiomycetes. The

ascomycetous subphylum of Taphrinomycotina was represented on KL and SW litter between 1,3 - 2,8% by some *Taphrinaceae* species (see also full species list

Figure 51). Main Basidiomycota classes were Agaricomycetes and Tremellomycetes of the Agaricomycotina. Pucciniomycotina (yeasts and rust fungi) were detected at low numbers on AC, KL and SW litter at time points 2 and 14 days only. No OTUs belonging to Ustilaginomycotina were detected.

3.1.5.3 Fungal OTU orders found at different time points

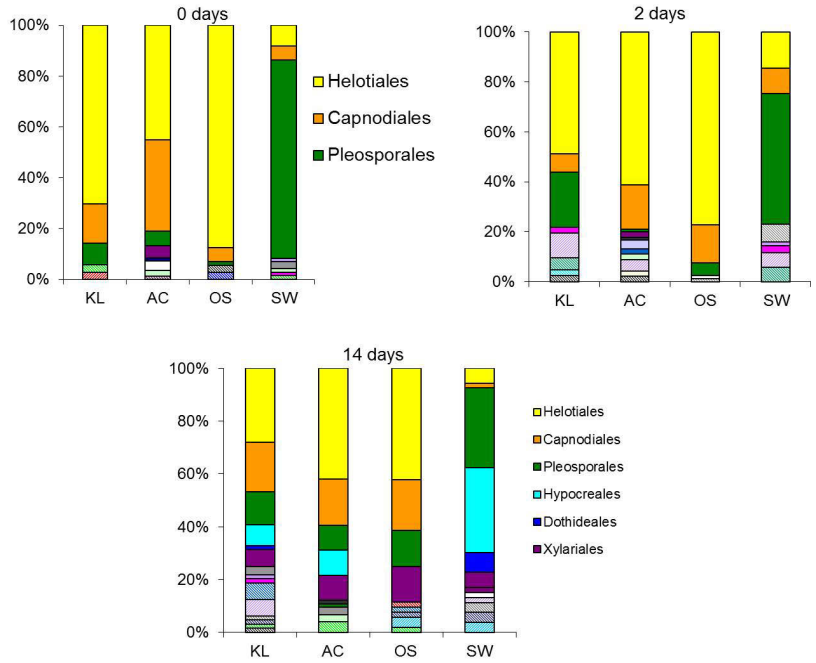

Figure 50: Taxonomic diversity of fungal clone libraries from decaying beech litter, sorted by orders on a time scale 1-14 days. AC= Achenkirch, KL= Klausenleopoldsdorf, OS=Ossiach, SW= Schottenwald. Time points 0, 2 and 14 days.

On beech litter of four different locations, the Ascomycete orders Helotiales, Capnodiales and Pleosporales were found to be the most abundant fungal OTUs. This is according to a recent study where these orders were associated with beech leaf litter (Unterseher *et al.*, 2013). Helotiales species were dominant on all locations except for SW, where Pleosporales species were dominant. A specific Helotiales OTU similar to *Lemonniera sp*. was found on beech litter of all locations and time points, being the dominant OTU on KL, AC, and OS locations at 0 and 2 days (see also

Figure 51). Dominance was highest on OS litter timepoint 0 with 86% of OTUs total. The dominant SW Pleosporales OTU was similar to an *Ampelomyces sp.*, accounting for 75% of OTUs on SW litter at timepoint 0. Other abundant OTUs in at least one litter

type were similar to species from the Capnodiales (*Cladosporium cladosporioides, Mycosphaerella punctiformis and Ramularia sp.*). A complete species list is given in Figure 51. Between 0 and 14 days, on all litter types the dominant species became gradually less dominant as species richness increased, showing Hypocreales, Dothideales and Xylariales species with growing abundances. Among the fungi that appeared only at the last sampling time point were two closely related *Discosia spp*. (order Xylariales) that were found in all four litter types only after two weeks incubation at abundances between 4 and 7.8%. On SW litter after two weeks of incubation, *Bionectria* (order Hypocreales) occured at frequencies of ca. 10%. *Aureobasidium pullulans* (order Dothideales) was only found at time points 2 days and/or 14 days on SW, OS and KL litter.

1

2 **3.1.5.4 Fungal clone library full taxonomic classification**

ID	days	soil	Identification	#	Genus	Family	Order	Class	Phylum
16	0	AC	Capnodiales sp. AC0_A03	1	Capnodiales	Capnodiales	Capnodiales	Dothideomycetes	Ascomycota
17	0	AC	Cylindrosympodium sp. AC0_B05	2	Cylindrosympodium	Venturiaceae	Pleosporales	Dothideomycetes	Ascomycota
18	0	AC	Dactylaria sp. AC0_A09	3	Dactylaria	Orbiliaceae	Orbiliales	Orbiliomycetes	Ascomycota
19	0	AC	Helotiales sp. AC0_A02	15	Helotiales	Helotiales i.s.	Helotiales	Leotiomycetes	Ascomycota
20	0	AC	Lemonniera sp. KL0_A01	23	Lemonniera	Helotiales i.s.	Helotiales	Leotiomycetes	Ascomycota
21	0	AC	Microdochium phragmitis	2	Microdochium	Xylariales i.s.	Xylariales	Sordariomycetes	Ascomycota
22	0	AC	Mycosphaerella punctiformis KL0_B03	6	Mycosphaerella	Mycosphaerellaceae	Capnodiales	Dothideomycetes	Ascomycota
23	0	AC	Myriangium sp. AC0_B12	1	Myriangium	Myriangiaceae	Myriangiales	Dothideomycetes	Ascomycota
24	0	AC	Pezizomycotina sp. AC0_E01	2	Pezizomycotina	Pezizomycotina i.s.	Pezizomycotina i.s.	Pezizomycotina i.s.	Ascomycota
25	0	AC	Phaeosphaeria sp. AC0_H10	1	Phaeosphaeria	Phaeosphaeriaceae	Pleosporales	Dothideomycetes	Ascomycota
26	0	AC	Pleosporales sp. AC0_C06	2	Pleosporales	Pleosporales incertae sedis	Pleosporales	Dothideomycetes	Ascomycota
27	0	AC	Ramularia sp. AC0_A06	23	Ramularia	Mycosphaerellaceae	Capnodiales	Dothideomycetes	Ascomycota
28	0	AC	Rosellinia corticium	2	Rosellinia	Xylariaceae	Xylariales	Sordariomycetes	Ascomycota
29	0	AC	Tricholomataceae sp. AC0_B02	1	Tricholomataceae	Tricholomataceae	Agaricales	Agaricomycetes	Basidiomycota
72	2	AC	Tremellales sp.AC2d_D09	4	Tremellales i.s.	Tremellales i.s.	Tremellales	Tremellomycetes	Basidiomycota
73	2	AC	Ramularia sp. AC0_A06	12	Ramularia	Mycosphaerellaceae	Capnodiales	Dothideomycetes	Ascomycota
74	2	AC	Polyscytalum fecundissimum	3	Sordariomycetes i.s.	Sordariomycetes i.s.	Sordariomycetes i.s.	Sordariomycetes	Ascomycota
75	2	AC	Pleosporales sp.AC2d_C05	1	Pleosporales i.s.	Pleosporales i.s.	Pleosporales	Dothideomycetes	Ascomycota
76	2	AC	Pezizomycotina sp. AC2d_B03	2	Pezizomycotina i.s.	Pezizomycotina i.s.	Pezizomycotina i.s.	Pezizomycotina i.s.	Ascomycota
77	2	AC	Mycosphaerella punctiformis KL0_B03	1	Mycosphaerella	Mycosphaerellaceae	Capnodiales	Dothideomycetes	Ascomycota
78	2	AC	Microdochium phragmitis	2	Microdochium	Xylariales i.s.	Xylariales	Sordariomycetes	Ascomycota
79	2	AC	Microbotryales sp.AC2d_D11	2	Microbotryales i.s.	Microbotryales i.s.	Microbotryales	Microbotryomycetes	Basidiomycota
80	2	AC	Leotiomycetes sp.AC2d_F08	2	Leotiomycetes i.s.	Leotiomycetes i.s.	Leotiomycetes i.s.	Leotiomycetes	Ascomycota

81	2	AC	Lemonniera sp. KL0_A01	44	Lemonniera	Helotiales i.s.	Helotiales	Leotiomycetes	Ascomycota
82	2	AC	Helotiales sp. AC0_A02	11	Helotiales i.s.	Helotiales i.s.	Helotiales	Leotiomycetes	Ascomycota
83	2	AC	Erythrobasidiales sp.AC2d_H09	2	Erythrobasidiales i.s.	Erythrobasidiales incertae sedis	Erythrobasidiales	Cystobasidiomycetes	Basidiomycota
84	2	AC	Emericella sp. AC2d_B11	1	Emericella	Trichocomaceae	Eurotiales	Eurotiomycetes	Ascomycota
85	2	AC	Davidiella sp. AC2d_H03	1	Davidiella	Davidiellaceae	Capnodiales	Dothideomycetes	Ascomycota
86	2	AC	Cladosporium cladosporioides	1	Cladosporium	Mycosphaerellaceae	Capnodiales	Dothideomycetes	Ascomycota
87	2	AC	Capnodiales sp.AC2d_C01	1	Capnodiales i.s.	Capnodiales i.s.	Capnodiales	Dothideomycetes	Ascomycota
85	14	AC	Alternaria sp. KL0_A04	1	Alternaria	Pleosporaceae	Pleosporales	Dothideomycetes	Ascomycota
86	14	AC	Rosellinia corticium	3	Rosellinia	Xylariaceae	Xylariales	Sordariomycetes	Ascomycota
87	14	AC	Ramularia sp. AC0_A06	13	Ramularia	Mycosphaerellaceae	Capnodiales	Dothideomycetes	Ascomycota
88	14	AC	Polyscytalum fecundissimum	2	Polyscytalum	Sordariomycetes i.s.	Sordariomycetes i.s.	Sordariomycetes	Ascomycota
89	14	AC	Pleosporales sp.AC2w_B11	5	Pleosporales incertae sedis	Pleosporales incertae sedis	Pleosporales	Dothideomycetes	Ascomycota
90	14	AC	Plectosphaerella cucumerina	1	Plectosphaerella	Phyllachoraceae	Phyllachorales	Sordariomycetes	Ascomycota
91	14	AC	Pezizomycotina sp.AC2w_C11	1	Pezizomycotina i.s.	Pezizomycotina i.s.	Pezizomycotina i.s.	Pezizomycotina i.s.	Ascomycota
92	14	AC	Pezizomycotina sp.AC2w_B10	1	Pezizomycotina i.s.	Pezizomycotina i.s.	Pezizomycotina i.s.	Pezizomycotina i.s.	Ascomycota
93	14	AC	Lemonniera sp. KL0_A01	13	Lemonniera	Helotiales incertae sedis	Helotiales	Leotiomycetes	Ascomycota
94	14	AC	Helotiales sp. AC0_A02	18	Helotiales i.s.	Helotiales i.s.	Helotiales	Leotiomycetes	Ascomycota
95	14	AC	Gibberella avenacea	7	Gibberella	Nectriaceae	Hypocreales	Sordariomycetes	Ascomycota
96	14	AC	Epicoccum nigrum	1	Epicoccum	Pleosporaceae	Pleosporales	Dothideomycetes	Ascomycota
97	14	AC	Efibulobasidium sp. AC2w_A05	3	Efibulobasidium	Sebacinaceae	Sebacinales	Agaricomycetes	Basidiomycota
98	14	AC	Discosia sp.AC2w_E02	4	Discosia	Amphisphaeriaceae	Xylariales	Sordariomycetes	Ascomycota
99	14	AC	Aspergillus fumigatus	1	Aspergillus	Trichocomaceae	Eurotiales	Eurotiomycetes	Ascomycota
8	0	KL	Ampelomyces sp. KL0_B12	5	Ampelomyces	Phaeosphaeriaceae	Pleosporales	Dothideomycetes	Ascomycota
9	0	KL	Basidiomycota sp. KL0_ A12	2	Basidiomycota	Basidiomycota	Basidiomycota	Basidiomycota	Basidiomycota
10	0	KL	Cryptococcus carnescens	1	Cryptococcus	Tremellaceae	Tremellales	Tremellomycetes	Basidiomycota
11	0	KL	Cryptococcus sp. KL0_H03	1	Cryptococcus	Tremellaceae	Tremellales	Tremellomycetes	Basidiomycota
12	0	KL	Helotiales sp. KL0_F05	1	Helotiales	Helotiales	Helotiales	Leotiomycetes	Ascomycota
13	0	KL	Lemonniera sp. KL0_A01	49	Lemonniera	Helotiales i.s.	Helotiales	Leotiomycetes	Ascomycota
14	0	KL	Mycosphaerella punctiformis KL0_B03	10	Mycosphaerella	Mycosphaerellaceae	Capnodiales	Dothideomycetes	Ascomycota
15	0	KL	Alternaria sp. KL0_A04	1	Alternaria	Pleosporaceae	Pleosporales	Dothideomycetes	Ascomycota

72	2	KL	Alternaria sp. KL0_A04	1	Alternaria	Pleosporaceae	Pleosporales	Dothideomycetes	Ascomycota
73	2	KL	Ampelomyces sp. KL0_B12	7	Ampelomyces	Phaeosphaeriaceae	Pleosporales	Dothideomycetes	Ascomycota
74	2	KL	Ascochyta sp.KL2d_D09	1	Ascochyta	Pleosporales i.s.	Pleosporales	Dothideomycetes	Ascomycota
75	2	KL	Bensingtonia yuccicola	1	Bensingtonia	Agaricostilbaceae	Agaricostilbales	Agaricostilbomycetes	Basidiomycota
76	2	KL	Bulleromyces albus	1	Bulleromyces	Tremellaceae	Tremellales	Tremellomycetes	Basidiomycota
77	2	KL	Cryptococcus tephrensis	1	Cryptococcus	Tremellaceae	Tremellales	Tremellomycetes	Basidiomycota
78	2	KL	Dioszegia hungarica	1	Dioszegia	Tremellaceae	Tremellales	Tremellomycetes	Basidiomycota
79	2	KL	Erythrobasidiales sp.KL2d_H09	1	Erythrobasidiales i.s.	Erythrobasidiales i.s.	Erythrobasidiales	Cystobasidiomycetes	Basidiomycota
80	2	KL	Lemonniera sp. KL0_A01	20	Lemonniera	Helotiales incertae sedis	Helotiales	Leotiomycetes	Ascomycota
81	2	KL	Mycosphaerella punctiformis KL0_B03	3	Mycosphaerella	Mycosphaerellaceae	Capnodiales	Dothideomycetes	Ascomycota
82	2	KL	Rhodotorula aurantiaca	2	Rhodotorula	Sporidiobolales i.s.	Sporidiobolales	Microbotryomycetes	Basidiomycota
83	2	KL	Taphrinaceae sp. KL2d_A06	1	Taphrinaceae i.s.	Taphrinaceae	Taphrinales	Taphrinomycetes	Ascomycota
84	2	KL	Tremellales sp. SW2d_A06	1	Tremellales i.s.	Tremellales i.s.	Tremellales	Tremellomycetes	Basidiomycota
100	14	KL	Waitea circinata	1	Waitea	Corticiaceae	Corticiales	Agaricomycetes	Basidiomycota
101	14	KL	Trichoderma sp.KL2w_E11	1	Trichoderma	Hypocreaceae	Hypocreales	Sordariomycetes	Ascomycota
102	14	KL	Tremellales sp.KL2w_G12	1	Tremellales i.s.	Tremellales i.s.	Tremellales	Tremellomycetes	Basidiomycota
103	14	KL	Taphrinaceae sp.KL2w_H08	1	Taphrinaceae	Taphrinaceae	Taphrinales	Taphrinomycetes	Ascomycota
104	14	KL	Rhodotorula aurantiaca	1	Rhodotorula	Sporidiobolales i.s.	Sporidiobolales	Microbotryomycetes	Basidiomycota
105	14	KL	Phaeosphaeriaceae sp.KL2w_A08	1	Phaeosphaeriaceae	Phaeosphaeriaceae	Pleosporales	Dothideomycetes	Ascomycota
106	14	KL	Phaeosphaeria sp.KL2w_E12	1	Phaeosphaeria	Phaeosphaeriaceae	Pleosporales	Dothideomycetes	Ascomycota
107	14	KL	Peniophora cinerea	1	Peniophora	Peniophoraceae	Russulales	Agaricomycetes	Basidiomycota
108	14	KL	Mycosphaerella punctiformis KL0_B03	5	Mycosphaerella	Mycosphaerellaceae	Capnodiales	Dothideomycetes	Ascomycota
109	14	KL	Lewia infectoria	1	Lewia	Pleosporaceae	Pleosporales	Dothideomycetes	Ascomycota
110	14	KL	Lemonniera sp. KL0_A01	16	Lemonniera	Helotiales i.s.	Helotiales	Leotiomycetes	Ascomycota
111	14	KL	Hypocreales sp.KL2w_D08	1	Hypocreales i.s.	Hypocreales i.s.	Hypocreales	Sordariomycetes	Ascomycota
112	14	KL	Hypocreales sp.KL2w_B06	1	Hypocreales i.s.	Hypocreales i.s.	Hypocreales	Sordariomycetes	Ascomycota
113	14	KL	Hypocreales sp. KL2w_B08	2	Hypocreales i.s.	Hypocreales i.s.	Hypocreales	Sordariomycetes	Ascomycota
114	14	KL	Helotiales sp.KL2w_E10	1	Helotiales i.s.	Helotiales i.s.	Helotiales	Leotiomycetes	Ascomycota
115	14	KL	Helotiales sp.KL2w_C04	1	Helotiales i.s.	Helotiales i.s.	Helotiales	Leotiomycetes	Ascomycota
116	14	KL	Epicoccum nigrum	1	Epicoccum	Pleosporaceae	Pleosporales	Dothideomycetes	Ascomycota

117	14	KL	Efibulobasidium albescens	1	Efibulobasidium	Sebacinaceae	Sebacinales	Agaricomycetes	Basidiomycota
118	14	KL	Discosia sp.AC2w_E02	4	Discosia	Amphisphaeriaceae	Xylariales	Sordariomycetes	Ascomycota
119	14	KL	Dictyochaeta sp. SW0_C11	2	Dictyochaeta	Chaetosphaeriaceae	Chaetosphaeriales	Sordariomycetes	Ascomycota
120	14	KL	Cryptococcus victoriae	2	Cryptococcus	Tremellaceae	Tremellales	Tremellomycetes	Basidiomycota
121	14	KL	Cryptococcus sp.KL2w_B07	1	Cryptococcus	Tremellaceae	Tremellales	Tremellomycetes	Basidiomycota
122	14	KL	Coprinellus micaceus	4	Coprinellus	Psathyrellaceae	Agaricales	Agaricomycetes	Basidiomycota
123	14	KL	Cladosporium cladosporioides	7	Cladosporium	Mycosphaerellaceae	Capnodiales	Dothideomycetes	Ascomycota
124	14	KL	Aureobasidium pullulans	1	Aureobasidium	Dothioraceae	Dothideales	Dothideomycetes	Ascomycota
125	14	KL	Apiognomonia errabunda	1	Apiognomonia	Gnomoniaceae	Diaporthales	Sordariomycetes	Ascomycota
126	14	KL	Alternaria sp.KL2w_B01	2	Alternaria	Pleosporaceae	Pleosporales	Dothideomycetes	Ascomycota
127	14	KL	Alternaria sp. KL0_A04	2	Alternaria	Pleosporaceae	Pleosporales	Dothideomycetes	Ascomycota
1	0	OS	Ceratobasidiaceae sp. OS0_A9	2	Ceratobasidiaceae	Ceratobasidiaceae	Cantharellales	Agaricomycetes	Basidiomycota
2	0	OS	Guehomyces pullulans	2	Guehomyces	Cystofilobasidiaceae	Cystofilobasidiales	Tremellomycetes	Basidiomycota
3	0	OS	Helotiales sp. OS0_C04	1	Helotiales	Helotiales	Helotiales	Leotiomycetes	Ascomycota
4	0	OS	Herpotrichia juniperi related	1	Herpotrichia	Lophiostomataceae	Pleosporales	Dothideomycetes	Ascomycota
5	0	OS	Lemonniera sp. KL0_A01	63	Lemonniera	Helotiales i.s.	Helotiales	Leotiomycetes	Ascomycota
6	0	OS	Mycosphaerella flageoletiana	1	Mycosphaerella	Mycosphaerellaceae	Capnodiales	Dothideomycetes	Ascomycota
7	0	OS	Mycosphaerella punctiformis KL0_B03	3	Mycosphaerella	Mycosphaerellaceae	Capnodiales	Dothideomycetes	Ascomycota
42	2	OS	Mycosphaerella punctiformis KL0_B03	4	Mycosphaerella	Mycosphaerellaceae	Capnodiales	Dothideomycetes	Ascomycota
43	2	OS	Lemonniera sp. KL0_A01	61	Lemonniera	Helotiales incertae sedis	Helotiales	Leotiomycetes	Ascomycota
44	2	OS	Herpotrichiellaceae sp. OS2d_B04	1	Herpotrichiellaceae	Herpotrichiellaceae	Chaetothyriales	Eurotiomycetes	Ascomycota
45	2	OS	Epicoccum nigrum	3	Epicoccum	Pleosporaceae	Pleosporales	Dothideomycetes	Ascomycota
46	2	OS	Cladosporium cladosporioides	7	Cladosporium	Mycosphaerellaceae	Capnodiales	Dothideomycetes	Ascomycota
47	2	OS	Aureobasidium pullulans	1	Aureobasidium	Dothioraceae	Dothideales	Dothideomycetes	Ascomycota
48	2	OS	Alternaria sp. KL0_A04	1	Alternaria	Pleosporaceae	Pleosporales	Dothideomycetes	Ascomycota
49	2	OS	Mycosphaerella flageoletiana	1	Mycosphaerella	Mycosphaerellaceae	Capnodiales	Dothideomycetes	Ascomycota
128	14	OS	Alternaria sp. KL0_A04	1	Alternaria	Pleosporaceae	Pleosporales	Dothideomycetes	Ascomycota
129	14	OS	Auriculariales sp.OS2w_F02	2	Auriculariales i.s.	Auriculariales i.s.	Auriculariales	Agaricomycetes	Basidiomycota
130	14	OS	Ceratobasidiaceae sp. OS0_D12	1	Ceratobasidiaceae	Ceratobasidiaceae	Cantharellales	Agaricomycetes	Basidiomycota
131	14	OS	Cladosporium cladosporioides	5	Cladosporium	Mycosphaerellaceae	Capnodiales	Dothideomycetes	Ascomycota
132	14	OS	Corticiales sp. OS2w_C06	1	Corticiales i.s.	Corticiales i.s.	Corticiales	Agaricomycetes	Basidiomycota
133	14	OS	Davidiella tassiana	1	Davidiella	Davidiellaceae	Capnodiales	Dothideomycetes	Ascomycota
134	14	OS	Discosia sp.AC2w_E02	7	Discosia	Amphisphaeriaceae	Xylariales	Sordariomycetes	Ascomycota

135	14	OS	Efibulobasidium albescens	1	Efibulobasidium	Sebacinaceae	Sebacinales	Agaricomycetes	Basidiomycota
136	14	OS	Epicoccum nigrum	4	Epicoccum	Pleosporaceae	Pleosporales	Dothideomycetes	Ascomycota
137	14	OS	Helotiales sp.OS2w_C03	1	Helotiales i.s.	Helotiales i.s.	Helotiales	Leotiomycetes	Ascomycota
138	14	OS	helotiales sp.OS2w_F01	1	Helotiales i.s.	Helotiales i.s.	Helotiales	Leotiomycetes	Ascomycota
139	14	OS	Helotiales sp.OS2w_E06	1	Helotiales i.s.	Helotiales i.s.	Helotiales	Leotiomycetes	Ascomycota
140	14	OS	Helotiales sp.OS2w_G09	1	Helotiales i.s.	Helotiales i.s.	Helotiales	Leotiomycetes	Ascomycota
141	14	OS	Hypholoma capnoides	1	Hypholoma	Strophariaceae	Agaricales	Agaricomycetes	Basidiomycota
142	14	OS	Lemonniera sp. KL0_A01	18	Lemonniera	Helotiales i.s.	Helotiales	Leotiomycetes	Ascomycota
143	14	OS	Mycosphaerella flageoletiana	1	Mycosphaerella	Mycosphaerellaceae	Capnodiales	Dothideomycetes	Ascomycota
144	14	OS	Mycosphaerella punctiformis KL0_B03	2	Mycosphaerella	Mycosphaerellaceae	Capnodiales	Dothideomycetes	Ascomycota
145	14	OS	Phoma exigua var. exigua	1	Phoma	Pleosporales i.s.	Pleosporales	Dothideomycetes	Ascomycota
146	14	OS	Pleurophoma cava	1	Pleurophoma	Pleosporales i.s.	Pleosporales	Dothideomycetes	Ascomycota
147	14	OS	Teratosphaeriaceae sp.OS2w_F09	1	Teratosphaeriaceae	Teratosphaeriaceae	Capnodiales	Dothideomycetes	Ascomycota
30	0	SW	Ampelomyces sp. KL0 B12	55	Ampelomyces	Phaeosphaeriaceae	Pleosporales	Dothideomycetes	Ascomycota
31	0	SW	Apiognomonia errabunda	1	Apiognomonia	Gnomoniaceae	Diaporthales	Sordariomycetes	Ascomycota
32	0	SW	Cryptococcus aff. amylolyticus	1	Cryptococcus	Tremellaceae	Tremellales	Tremellomycetes	Basidiomycota
33	0	SW	Davidiella tassiana	1	Davidiella	Davidiellaceae	Capnodiales	Dothideomycetes	Ascomycota
34	0	SW	Dictyochaeta sp. SW0_C11	2	Dictyochaeta	Chaetosphaeriaceae	Chaetosphaeriales	Sordariomycetes	Ascomycota
35	0	SW	Helotiales sp. SW0_C04	1	Helotiales	Helotiales	Helotiales	Leotiomycetes	Ascomycota
36	0	SW	Lemonniera sp. KL0_A01	5	Lemonniera	Helotiales i.s.	Helotiales	Leotiomycetes	Ascomycota
37	0	SW	Mycosphaerella punctiformis KL0_B03	3	Mycosphaerella	Mycosphaerellaceae	Capnodiales	Dothideomycetes	Ascomycota
38	0	SW	Pezizomycotina sp. SW0_G03	1	Pezizomycotina	Pezizomycotina	Pezizomycotina	Pezizomycotina	Ascomycota
39	0	SW	Phaeosphaeria sp. SW0_F12	1	Phaeosphaeria	Phaeosphaeriaceae	Pleosporales	Dothideomycetes	Ascomycota
40	0	SW	Pleurophoma cava	1	Pleurophoma	Pleosporales i.s.	Pleosporales	Dothideomycetes	Ascomycota
41	0	SW	Taphrina sp. SW0_A10	1	Taphrina	Taphrinaceae	Taphrinales	Taphrinomycetes	Ascomycota
50	2	SW	Alternaria brassicae	1	Alternaria	Pleosporaceae	Pleosporales	Dothideomycetes	Ascomycota
51	2	SW	Alternaria sp. KL0_A04	1	Alternaria	Pleosporaceae	Pleosporales	Dothideomycetes	Ascomycota
52	2	SW	Alternaria sp. SW2d_E01	1	Alternaria	Pleosporaceae	Pleosporales	Dothideomycetes	Ascomycota
53	2	SW	Ampelomyces sp. KL0_B12	25	Ampelomyces	Phaeosphaeriaceae	Pleosporales	Dothideomycetes	Ascomycota
54	2	SW	Apiognomonia errabunda	1	Apiognomonia	Gnomoniaceae	Diaporthales	Sordariomycetes	Ascomycota
55	2	SW	Aureobasidium pullulans	5	Aureobasidium	Dothioraceae	Dothideales	Dothideomycetes	Ascomycota
56	2	SW	Cladosporium cladosporioides	3	Cladosporium	Mycosphaerellaceae	Capnodiales	Dothideomycetes	Ascomycota

57	2	SW	Cryptococcus wieringae	1	Cryptococcus	Tremellaceae	Tremellales	Tremellomycetes	Basidiomycota
58	2	SW	Davidiella tassiana	1	Davidiella	Davidiellaceae	Capnodiales	Dothideomycetes	Ascomycota
59	2	SW	Epicoccum nigrum	5	Epicoccum	Pleosporaceae	Pleosporales	Dothideomycetes	Ascomycota
60	2	SW	Lemonniera sp. KL0_A01	10	Lemonniera	Helotiales i.s.	Helotiales	Leotiomycetes	Ascomycota
61	2	SW	Mycosphaerella punctiformis KL0_B03	3	Mycosphaerella	Mycosphaerellaceae	Capnodiales	Dothideomycetes	Ascomycota
62	2	SW	Phaeosphaeria sp. AC0_H10	1	Phaeosphaeria	Phaeosphaeriaceae	Pleosporales	Dothideomycetes	Ascomycota
63	2	SW	Pleosporales sp. SW2d_H02	1	Pleosporales	Pleosporales	Pleosporales	Dothideomycetes	Ascomycota
64	2	SW	Pleurophoma cava	1	Pleurophoma	Pleosporales i.s.	Pleosporales	Dothideomycetes	Ascomycota
65	2	SW	Rhodotorula aurantiaca	1	Rhodotorula	Sporidiobolales i.s.	Sporidiobolales	Microbotryomycetes	Basidiomycota
66	2	SW	Rhodotorula fujisanensis	1	Rhodotorula	Sporidiobolales i.s.	Sporidiobolales	Microbotryomycetes	Basidiomycota
67	2	SW	Rhodotorula pinicola	1	Rhodotorula	Sporidiobolales i.s.	Sporidiobolales	Microbotryomycetes	Basidiomycota
68	2	SW	Sporobolomyces coprosmae	1	Sporobolomyces	Sporidiobolales i.s.	Sporidiobolales	Microbotryomycetes	Basidiomycota
69	2	SW	Taphrina sp.SW0_A10	1	Taphrina	Taphrinaceae	Taphrinales	Taphrinomycetes	Ascomycota
70	2	SW	Taphrina vestergrenii	1	Taphrina	Taphrinaceae	Taphrinales	Taphrinomycetes	Ascomycota
71	2	SW	Tremellales sp. SW2d_A06	3	Tremellales i.s.	Tremellales i.s.	Tremellales	Tremellomycetes	Basidiomycota
148	14	SW	Acremonium strictum	1	Acremonium	Hypocreales i.s.	Hypocreales	Sordariomycetes	Ascomycota
149	14	SW	Alternaria sp. KL0_A04	4	Alternaria	Pleosporaceae	Pleosporales	Dothideomycetes	Ascomycota
150	14	SW	Ampelomyces sp. KL0_B12	1	Ampelomyces	Phaeosphaeriaceae	Pleosporales	Dothideomycetes	Ascomycota
151	14	SW	Aureobasidium pullulans	4	Aureobasidium	Dothioraceae	Dothideales	Dothideomycetes	Ascomycota
152	14	SW	Auriculariales sp.SW2w_A01	2	Auriculariales incertae sedis	Auriculariales i.s.	Auriculariales	Agaricomycetes	Basidiomycota
153	14	SW	Bionectria compactiuscula	5	Bionectria	Bionectriaceae	Hypocreales	Sordariomycetes	Ascomycota
154	14	SW	Bionectria sp. SW2w_A02	6	Bionectria	Bionectriaceae	Hypocreales	Sordariomycetes	Ascomycota
155	14	SW	Corticiales sp. SW2w_D05	2	Corticiales incertae sedis	Corticiales i.s.	Corticiales	Agaricomycetes	Basidiomycota
156	14	SW	Cryptococcus wieringae	1	Cryptococcus	Tremellaceae	Tremellales	Tremellomycetes	Basidiomycota
157	14	SW	Dactylaria sp. AC0_A09	1	Dactylaria	Orbiliaceae	Orbiliales	Orbiliomycetes	Ascomycota
158	14	SW	Davidiella tassiana	1	Davidiella	Davidiellaceae	Capnodiales	Dothideomycetes	Ascomycota
159	14	SW	Discosia sp.AC2w_E02	2	Discosia	Amphisphaeriaceae	Xylariales	Sordariomycetes	Ascomycota
160	14	SW	Fusarium sp.SW2w_H02	1	Fusarium	Nectriaceae	Hypocreales	Sordariomycetes	Ascomycota
161	14	SW	Helotiales sp.SW2w_E05	2	Helotiales i.s.	Helotiales i.s.	Helotiales	Leotiomycetes	Ascomycota
162	14	SW	Helotiales sp.SW2w_G11	1	Helotiales i.s.	Helotiales i.s.	Helotiales	Leotiomycetes	Ascomycota

163	14	SW	Hypocreales sp.SW2w_D03	1	Hypocreales i.s.	Hypocreales i.s.	Hypocreales	Sordariomycetes	Ascomycota
164	14	SW	Lewia infectoria	2	Lewia	Pleosporaceae	Pleosporales	Dothideomycetes	Ascomycota
165	14	SW	Nectria sp.SW2w_F03	1	Nectria	Nectriaceae	Hypocreales	Sordariomycetes	Ascomycota
166	14	SW	Pleosporales sp.SW2w_B05	1	Pleosporales i.s.	Pleosporales i.s.	Pleosporales	Dothideomycetes	Ascomycota
167	14	SW	Pleosporales sp.SW2w_C02	1	Pleosporales i.s.	Pleosporales i.s.	Pleosporales	Dothideomycetes	Ascomycota
168	14	SW	Pleosporales sp.SW2w_D07	1	Pleosporales i.s.	Pleosporales i.s.	Pleosporales	Dothideomycetes	Ascomycota
169	14	SW	Pleosporales sp.SW2w_H05	1	Pleosporales i.s.	Pleosporales i.s.	Pleosporales	Dothideomycetes	Ascomycota
170	14	SW	Pleurophoma cava	5	Pleurophoma	Pleosporales i.s.	Pleosporales	Dothideomycetes	Ascomycota
171	14	SW	Rhodosporidium lusitaniae	1	Rhodosporidium	Sporidiobolales i.s.	Sporidiobolales	Microbotryomycetes	Basidiomycota
172	14	SW	Rhodotorula aurantiaca	1	Rhodotorula	Sporidiobolales i.s.	Sporidiobolales	Microbotryomycetes	Basidiomycota
173	14	SW	Rosellinia corticium	1	Rosellinia	Xylariaceae	Xylariales	Sordariomycetes	Ascomycota
174	14	SW	Sordariales sp.SW2w_F04	1	Sordariales incertae sedis	Sordariales i.s.	Sordariales	Sordariomycetes	Ascomycota
175	14	SW	Trichoderma sp.SW2w_D04	1	Trichoderma	Hypocreaceae	Hypocreales	Sordariomycetes	Ascomycota
176	14	SW	Trichoderma sp.SW2w_H08	1	Trichoderma	Hypocreaceae	Hypocreales	Sordariomycetes	Ascomycota

Figure 51: Full taxonomic identification of beech litter fungal OTUs from clone libraries. AC= Achenkirch, KL= Klausenleopoldsdorf, OS=Ossiach, SW= Schottenwald.

3.1.6 Beech litter nutrient and trace element values

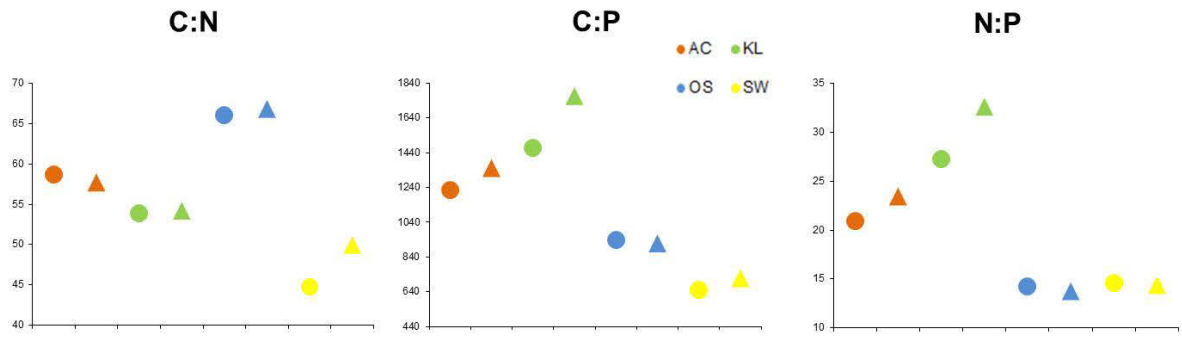

Figure 52: Beech litter nutrient ratios at different locations and time points. Carbon:Nitrogen ratio (C:N), Carbon: Phosphorus ratio (C:P) and Nitrogen:Phosphorus ratio (N:P) as measured. Locations: AC= Achenkirch, KL= Klausenleopoldsdorf, OS=Ossiach, SW= Schottenwald, indicated by color code. Rounds show nutrient ratios of native litter at 0 days (starting point), triangles show values after 14 days.

Ratios of major nutrients are within the range typical for litter from *Fagus sylvatica* (Berg & Mc Claugherty, 2008). The main differences between the four litter types were higher N, P and Mn contents and consequently lower C:N and C:P ratios in SW.

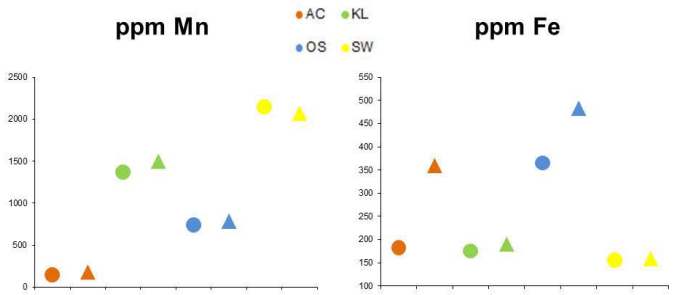

Figure 53: Beech litter trace element values (Manganese, Iron) at different locations and time points in ppm. Locations: AC= Achenkirch, KL= Klausenleopoldsdorf, OS=Ossiach, SW= Schottenwald, indicated by color code. Rounds show nutrient ratios of native litter at 0 days (starting point), Triangles show values after 14 days. No data available for time point 2 days.

3.1.7 Fungal community structure and sampling site interaction

A one-way Analysis of Variance (ANOVA) was performed with STATGRAPHICS Centurion XVI Version 16.0.09 using total percentage of Helotiales and Pleosporales (from **Figure 50**) at different sampling sites (AC, KL, OS, SW) and their respective elevation above sea level (ASL) in meters (from **Table 1**). Three different time points (0, 2 and 14 days) were averaged per sampling site.

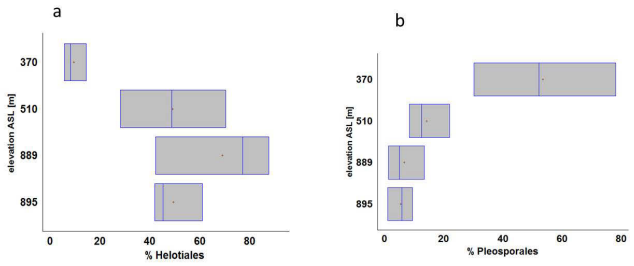

Figure 54: Box-and-Whisker Plots showing one-way ANOVAs for main Ascomycete classes at each level of elevation asl of the different sampling sites. Vertical line in the boxes shows median, red cross marks the mean value. (a) total percentage of Helotiales OTUs averaged over three time points. (b) Total percentage of Pleosporales OTUs averaged over three time points. Time points 0, 2 and 14 days respectively.

Box-and-Whisker Plots show a clear separation of phylogenetic fungal clone library data from the SW sampling site at 370 m elevation above sea level from all other locations. In Figure 54a, the percentage of Helotiales OTUs (calculated from total number of OTUs in the sample) at 370m (SW) ranges from 5,6 - 14,5% in the three different samples taken at 0, 2 and 14 days. This is significantly different from all other levels (510, 880 and 895 m elevation asl, i.e. KL, OS, AC), where the percentage of Helotiales OTUs ranged from 28,1 – 87,7 %. In Figure 54b, Box-and-Whisker Plot generated from one-way ANOVA data shows the total percentage of Pleosporales OTUs at 370m asl (SW) at 30,1 - 87,7 %, while the other three locations had Pleosporales OTU percentages of 1,1- 21,9%.

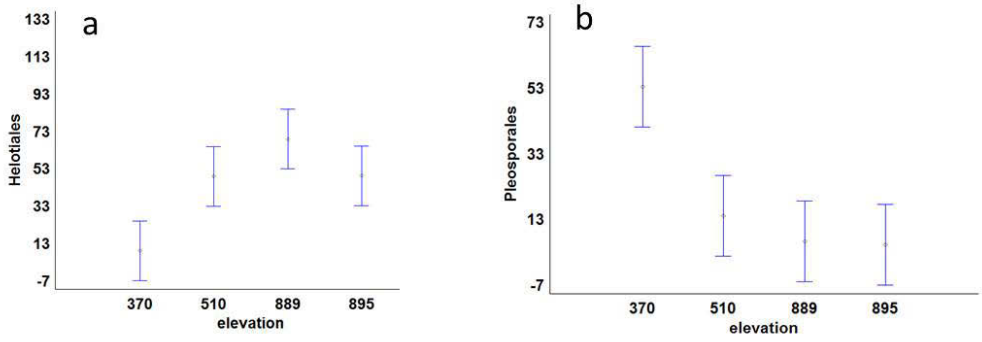

Figure 55: Means Plot and 95% LSD-Intervals for main Ascomycete classes at each level of elevation. Intervals are displayed as Fisher's least significant difference (LSD). (a) Means of Helotiales OTU total % at three different time points. (b) Means of Pleosporales OTU total % at three different time points. Time points 0, 2 and 14 days.

According to the Multiple Range Test, data for 370m (SW litter) elevation above sea level are significantly different from all other elevations at the 95% confidence level, this refers to both the percentage of Helotiales as well as the total percentage of Pleosporales.

3.1.8 Principal component analysis for main drivers of fungal community structure

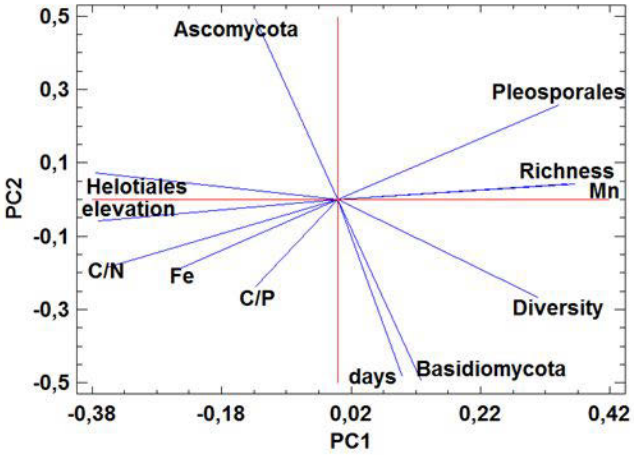

Figure 56: Principal component analysis (PCA) biplot of taxonomic community structure, richness, diversity and environmental factors. Data are from different sampling time points (0, 2 and 14 days) and four different locations (AC, KL, OS, SW). Nutrient level measurements and ratios were provided by Dr.Katharina Keiblinger.

In the PCA biplot shown in **Figure 56**, the principal components are calculated from different variables with relation to data variability. This was done to determine which variables can be regarded as drivers of change within the fungal decomposer community. On PCA1 (x-axis), elevation above sea level, C/N and C/P ratios, as well as Fe concentration are located together on the left, negative side, together with the percentage of Helotiales. On the positive side, Mn concentration, Richness and Diversity are allocated with %Pleosporales. PCA2 is dominated by the % Ascomycota vs. % Basidiomycota, which is also related to the incubation time (days).

3.2 Microbial community composition changes during beech litter decomposition in a mesocosm experiment

From a mesocosm experiment with sterilized and inoculated beech litter outlined in 2.3, samples of four different locations and 4 harvest time points (2.3.1.1) were generated, with 5 replicates each. DNA was extracted and qPCR with fungal and bacterial specific primers was performed in triplicates. Fungal/bacterial ratios were calculated and plotted on a time scale.

3.2.1 Fungal-specific RFLP and T-RFLP Analysis of E1 replicas

Since 5 replicates of each inoculated litter sample were used, it had to be tested if all replicas contained the same microbial community at the start of the experiment. To this end, a simple RFLP approach with two different restriction enzymes was performed.

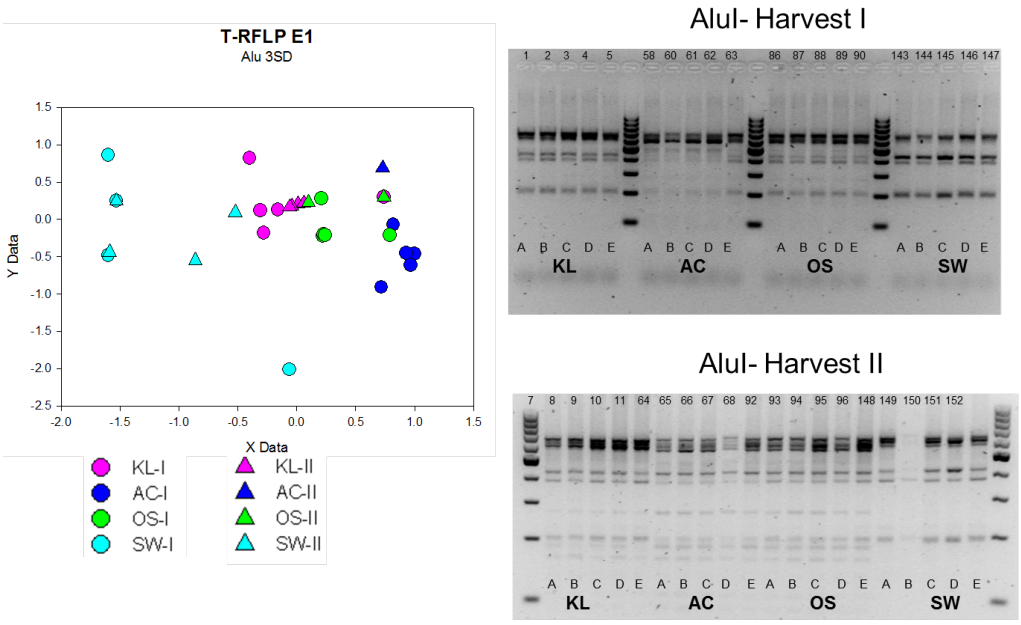

Figure 57: T-RFLP (left) and RFLP of E1 replicas from harvest I (2weeks) and Harvest II (2 months). Litter DNA PCR was performed with fungal specific primers ITS1R-ITS4 for 30 cycles at 54°C. PCR triplicates were pooled for RFLP with AluI. Numbers indicate internal sample code. AC= Achenkirch, KL= Klausenleopoldsdorf, OS=Ossiach, SW= Schottenwald. RFLP analysis was performed by Dragana Bandian.

According to the RFLP pattern produced by AluI, replicas of the locations KL, OS, and SW contained the same starting community and were therefore used for further experiments. Sample No.63 of the AC location showed a different RFLP pattern than the other four replicas of this location with this restriction enzyme. T-RFLP pattern

does not show a particular pattern for meaningful interpretation, however locations seem to cluster more or less together.

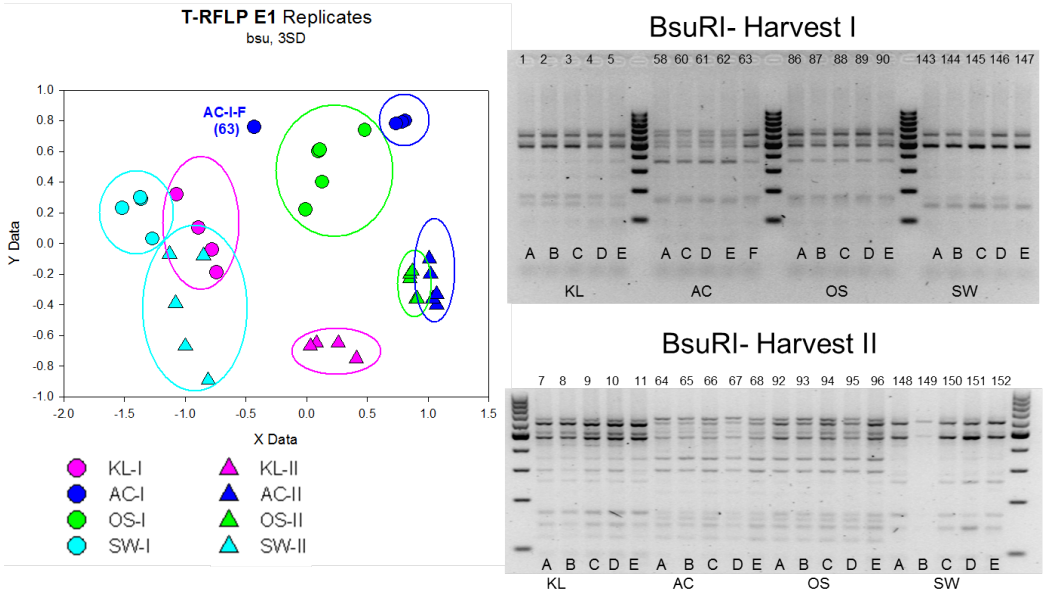

Figure 58: **T-RFLP (left) and RFLP (right) of E1 replicas from harvest I (2weeks) and Harvest II (2 months).** Litter DNA PCR was performed with fungal specific primers ITS1R-ITS4 for 30 cycles at 54°C. PCR triplicates were pooled for RFLP with BsuRI. Numbers indicate internal sample code. AC= Achenkirch, KL= Klausenleopoldsdorf, OS=Ossiach, SW= Schottenwald. RFLP analysis was performed by Dragana Bandian.

RFLP analysis with another restriction enzyme, BsuRI, showed the same AC mesocosm (no.63) of harvest I to contain a significantly different fungal community as represented by a different RFLP pattern on the gel. T-RFLP analysis (left section of Figure 58) revealed a clustering of locations as well as harvest time points, demonstrating similar fungal community behavior within the replicas. The result of RFLP was backed up by T-RFLP results, because AC-I-F (no.63) did not cluster together with the other mesocosm replicas of AC first harvest.

Harvest II did not show any indication of unpredictable replica behavior as backed up by both RLFP and T-RFLP analysis with two different enzymes. Because of dissimilar RFLP patterns (by two enzymes) and T-RFLP clustering with BsuRI, results from one particular mesocosm of the first harvest (AC-I-F, no.63) were excluded from later analyses.

3.2.2 Nutrient ratio changes during decomposition

The nutrient ratios of beech litter from four different locations in Austria were assessed in a mesocosm decomposition experiment. Experimental details are outlined in (Schneider *et al.*, 2012).

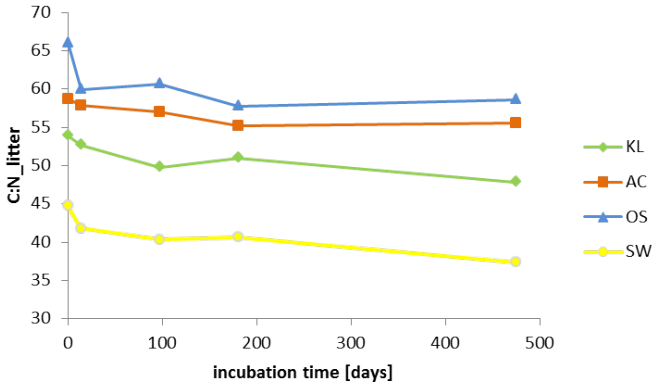

Figure 59: Litter nutrient ratios during decomposition in a mesocosm experiment. Experimental details and data provided by Dr.Katharina Keiblinger (BFW).

Results from litter biogeochemistry measurements are explained in detail here (Schneider *et al.*, 2012). Shortly, all four locations varied in their nutrient ratios as well as their behaviour during decomposition. SW has high nutrient status, represented by a low C:N ratio. OS and AC showed the highest C:N ratios and can therefore be considered low in nutrients. Ratios went down slightly as decomposition progressed.

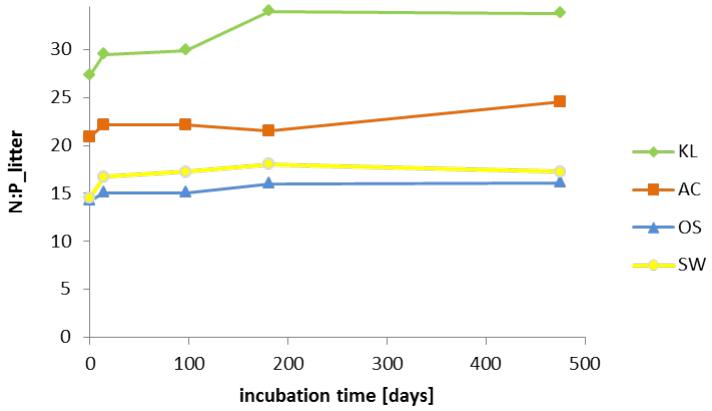

Figure 60: Litter nutrient ratios during decomposition in a mesocosm experiment. Experimental details and data provided by Dr.Katharina Keiblinger (BFW).

C:P ratios in litter present SW and OS with the narrowest ratio, i.e. highest P levels, and KL with the highest ratio. Ratios stayed more or less stable during the decomposition process.

3.2.3 Quantitative Real-Time PCR of E1 litter samples

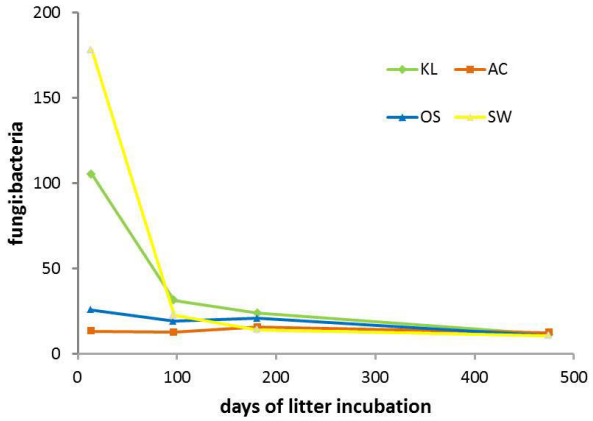

Figure 61: Fungal/bacterial ratios during beech litter composition obtained by qPCR. AC= Achenkirch, KL= Klausenleopoldsdorf, OS=Ossiach, SW= Schottenwald. Time points 14, 97, 181 and 475 days.

Fungal/bacterial ratios derived from qPCR data of litter DNA were highest at the first harvest time point (14 days) and decreased with time. At the first two timepoints, there were significant differences in fungal/bacterial ratios between the four locations, but these differences decreased during decomposition. Fungal/bacterial ratios at 14 days were highest for SW and KL locations (178 and 105). OS and AC fungal/bacterial ratios showed little change during decomposition: OS fungal/bacterial ratios started at 25 (14 days) and went down to 11 (475 days); AC started at 13 and went down to 12,5. The last time point showed very similar ratios for all locations (10,6 - 12,4).

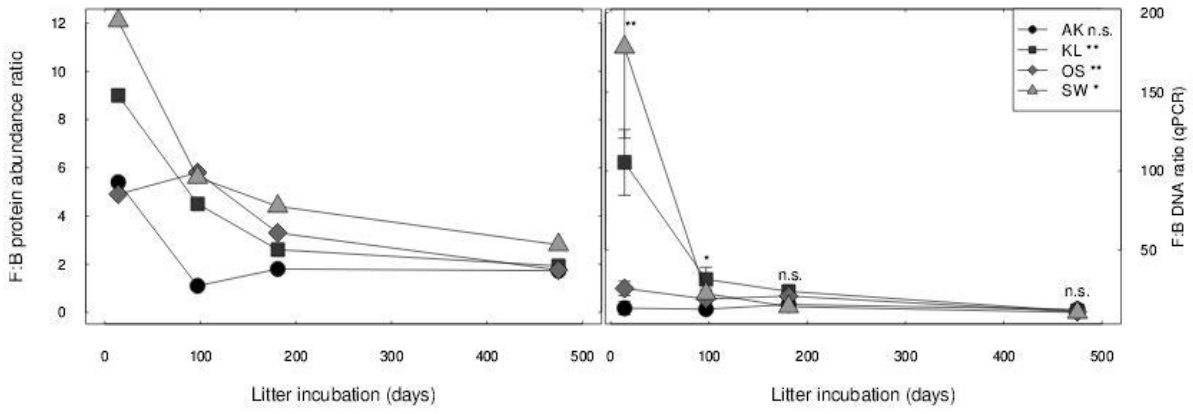

Figure 62: Fungi/Bacteria ratios by metaproteome and qPCR measurements, figure from Lukas Kohl (Kohl, 2011). Left: metaproteome data were generated by Lukas Kohl. Right: DNA-based qPCR data. Both analyses were performed from the same beech litter samples. AK= Achenkirch, KL= Klausenleopoldsdorf, OS=Ossiach, SW= Schottenwald. Time points 14, 97, 181 and 475 days. Error bars indicate standard errors (n=5)

The same beech litter samples were analyzed by metaproteomic analysis to generate another set of Fungi/Bacteria ratio data[3]. Figure 62 shows fungi/bacteria ratios from metaproteomics data as well as from qPCR data. Metaproteomics data were generated by Lukas Kohl, University of Vienna. The results both show a similar pattern between litter types and harvests: the earlier harvest points show much higher ratios than later time points. Fungal proteins were dominant on all samples, but like in the qPCR analysis, SW and KL showed the highest fungal dominance. Also, AC showed the lowest ratios of fungal/bacterial proteins. Overall, Fungi/bacteria ratios were highly correlated between protein- and DNA-based estimates.

3.2.4 Microbial community composition changes under various resource C:N ratios

Fungal/bacterial ratios derived from qPCR data of litter DNA were plotted against the C:N resource ratios of the litter. C/N resource ratios were measured and calculated by Dr.Katharina Keiblinger, BFW, and recently published here (Schneider *et al.*, 2012) and here (Mooshammer *et al.*, 2012).

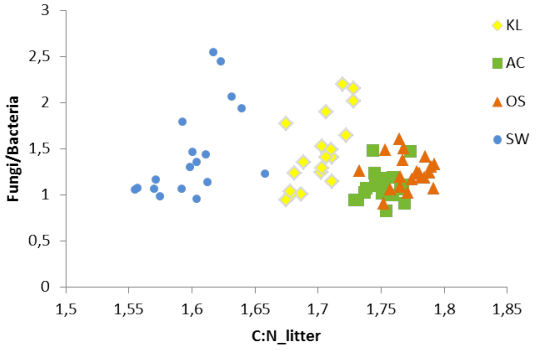

Figure 63: Litter C:N ratios plotted against Fungi/Bacteria ratios. Litter C/N mass ratios were calculated and measured by Dr.Katharina Keiblinger, BFW. Fungi/Bacteria ratios were obtained by qPCR as described above. Logarithmic values are shown. AC= Achenkirch, KL= Klausenleopoldsdorf, OS=Ossiach, SW= Schottenwald. Five repetitions and time points 14, 97, 181 and 475 days per location respectively.

Resource C:N ratio appears to have no relationship with the Ratio of Fungi/Bacteria, suggesting homeostatic behavior (see Figure 63). Because Fungal/Bacterial ratios only give a hint of underlying elemental ratios, biomass C:N ratios were used for the statistic calculation instead. When calculating the relation of resource C:N and biomass C:N, there was no statistically significant relationship found. The slope was not statistically different from zero on linear and logarithmic axes, which demonstrates C:N

[3] Metaproteomic Fungi/Bacteria ratio data were generated by Lukas Kohl, University of Vienna.

homeostasis according to (Sterner & Elser, 2002). Further proof for homeostatic behavior of the microbial communities in these samples has been published here (Mooshammer *et al.*, 2012).

3.2.5 Temperature perturbations

Beech litter of different locations was incubated in mesocosms as described above. Additionally, stress treatments were introduced to mimic climate change events, as described in detail in (Keiblinger *et al.*, 2012). Temperature treatments and harvesting procedure of mesocosms is described in 2.3.1.2. DNA was extracted and qPCR with fungal and bacterial specific primers was performed in triplicates as described in 2.3. Fungal/bacterial ratios were calculated and plotted on a time scale.

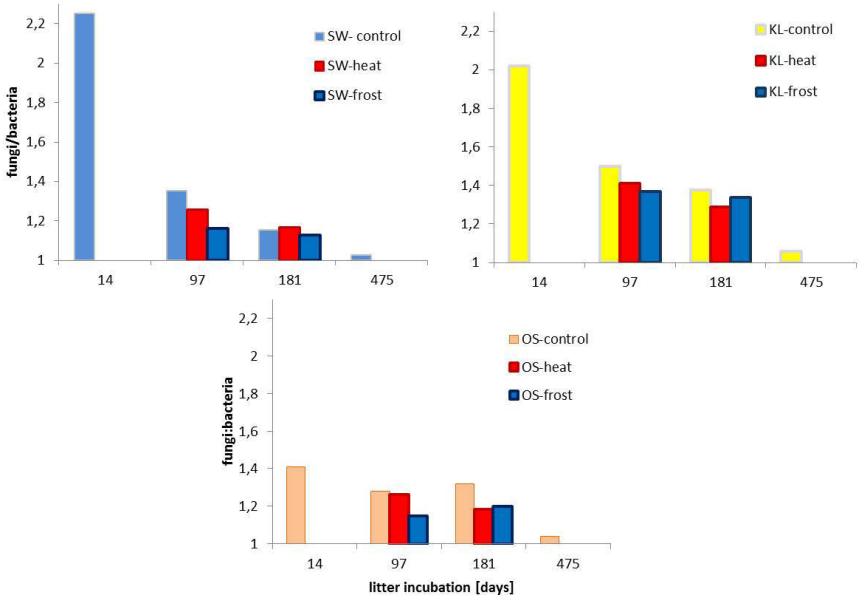

Figure 64: Fungal/bacterial ratios during beech litter composition under heat/frost treatments, obtained by qPCR. Beech leaf litter locations: OS=Ossiach, SW= Schottenwald, KL= Klausenleopoldsdorf. Time points 14, 97, 181 and 475 days. control= no temperature shift. heat=short period at 30°C before harvest. frost= short period at -4°C before harvest. Heat and freeze treatments were only applied before the 3 months (97days) harvest.

The stress treatments- heat and frost- did not cause an in increase in fungal/bacterial ratio compared to the unstressed condition. In SW, the location with the initially highest F/B ratio, there was a decrease in F/B ratio at the first sampling after the temperature stress (both heat and frost), which showed a slight overcompensation at the second sampling after stress for the heat condition. Frost stress caused the most pronounced decrease in F/B ratios for all three litter locations at the first sampling after stress. After 181 days, F/B ratios went back to match the unstressed conditions in SW and KL, but did not recover at the OS location, where F/B ratios stayed at a lower value.

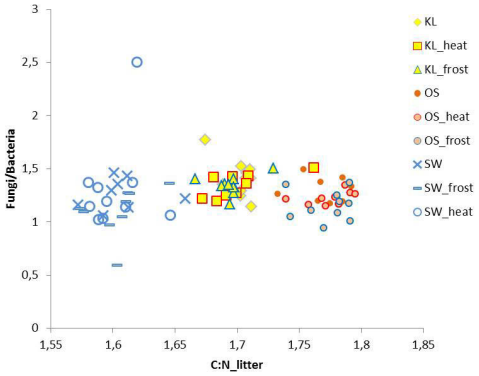

Figure 65: Litter C:N ratios plotted against Fungi/Bacteria ratios. Litter C/N mass ratios were calculated and measured by Dr.Katharina Keiblinger, BFW and published here (Keiblinger *et al.*, 2012). Fungi/Bacteria ratios were obtained by qPCR as described above. Logarithmic values are shown. heat=short period at 30°C before harvest. frost= short period at -4°C before harvest. Beech leaf litter locations: KL= Klausenleopoldsdorf, OS=Ossiach, SW= Schottenwald. Five repetitions, and time points 97 and 181 days per location respectively.

3.3 Improvement of the PhyloTrap

Starting from the protocol as outlined in 2.4.4, the following parameters were optimized with the use of LNA (locked nucleic acid) enriched probes: hybridization time, hybridization temperature, formamide concentration in hybridization buffer, washing conditions, elution temperature.

3.3.1 Bead-probe binding optimization

Custom LNA™ enriched probes were designed and manufactured by Exiqon using the same probe sequences as shown in 2.4.4.

	pmol	**180**	**200**	**250**	**300**
INPUT	µg/ml	7,74	8,54	10,63	12,55
	µg total	1,55	1,71	2,13	2,51

	pmol	**180**	**200**	**250**	**300**
UNBOUND	µg/ml	0,80	0,80	1,31	1,72
	µg total	**0,16**	**0,16**	**0,26**	**0,34**

BOUND	µg total	1,39	1,55	1,86	2,17
	%	**89,81**	**90,78**	**87,46**	**86,44**

Different amounts (180, 200, 250 and 300 pmol) of LNA- enhanced probe EUK-Y-bio were used on 100 µl Dynabeads, resuspended in 200 µl binding buffer. Binding was performed as described in 2.4.4. The unbound fraction of probe in found in the supernatant after washing the beads was determined by Quant-iT fluorometric quantitation. For further experiments, 200 pmol probe were used because of the highest binding efficiency of over 90%.

3.3.2 Protocol Troubleshooting: Washing and Blocking steps

Problem 1: unspecific binding of bacterial rRNA on LNA-euk probe

When using bacterial RNA on the LNA-euk probe, unspecific binding of both bacterial SSU and LSU were detected. The protocol as outlined in 2.4.4 was used, and some additional washing steps were added as shown below:

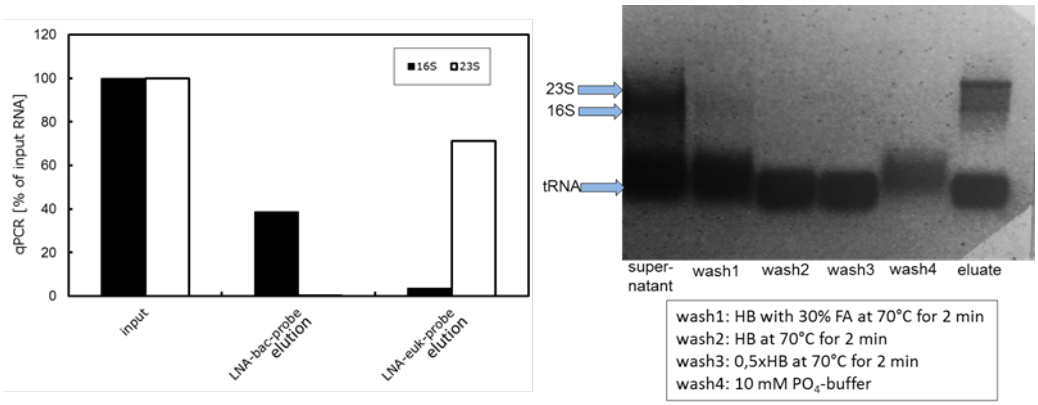

Figure 66: Unspecific binding of bacterial SSU and LSU to LNA-euk probe. qPCR (left) and gel (right) showing input and eluate fractions after Phylotrap protocol using 10 µg *R.terrigena* RNA on LNA-bac probe and LNA-euk probe respectively. Primers: Bacterial 16S (EUB f933; EUB r1387) and bacterial 23S (fBact23S; rBact23S). In this diagram, RNA amounts were normalized to the detected RNA amount in the input fraction.

After the hybridization step with *R.terrigena* RNA and LNA-euk probe coated Dynabeads, the eluate fraction showed both SSU and LSU bands on the gel. This binding was highly unspecific and subsequent experiments were conducted to increase specificity.

The unspecific binding of bacterial RNA to the LNA enhanced euk-probe was confirmed by qPCR-analysis of the elution fractions. The bacterial rRNA recovery by LNA-bac-probe was specific and detected only 16S rRNA. However the LNA-euk probe showed unspecific binding of high amounts of bacterial 23S rRNA.

Problem 2: unspecific fungal rRNA binding to LNA-bac probe

A.nidulans SSU RNA was found in eluate after hybridization with LNA-bac-probe coated Dynabeads using the Phylotrap protocol. Hybridization was performed in 30% Formamide at 40°C for 2 hours, washing steps were performed at 40°C.

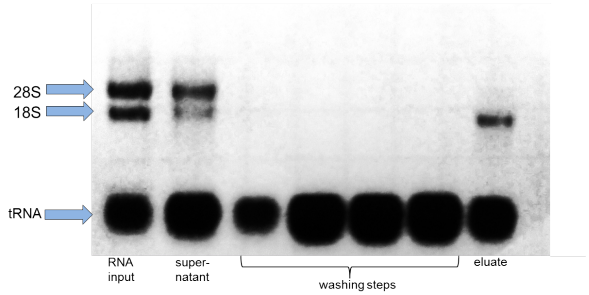

Figure 67: Unspecific binding of fungal SSU rRNA to LNA-bac probe. Washing steps were performed at 40°C.

The protocol had to be adjusted to make sure no unspecific rRNA would stick to the LNA probes. The first modification was the introduction of a 'stringent' washing step by increasing the washing temperature from 40°C to 70°C.

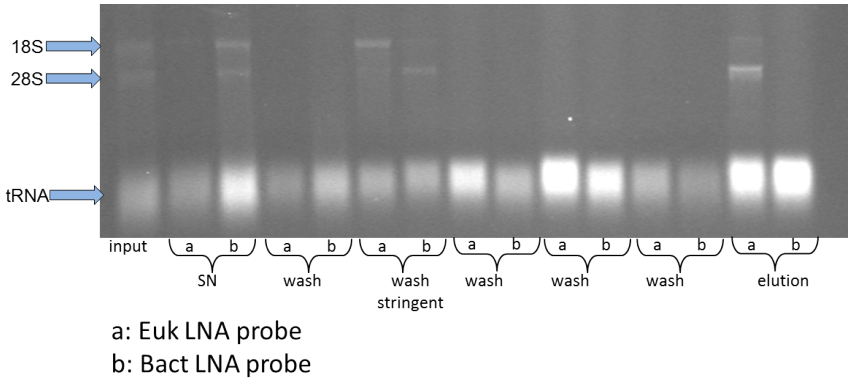

Figure 68: Introduction of a ‚stringent' washing step to the Phylotrap Protocol. 10 µg total *A.nidulans* RNA were used on (a)LNA-euk-probe and (b)LNA-bac-probe respectively. Stringent wash: wash with Hybridization buffer + 30% Formamide at 70°C for 2 minutes. Samples were run on a non-denaturing 2% Agarose gel with EtBr staining.

On the gel, it can be seen that this stringent washing step with 70°C removes not only the unspecific binding of *A.nidulans* LSU to the euk-LNA probe (stringent wash a), but also unspecific binding of fungal SSU to the LNA-euk-probe (wash stringent b). This protocol produced a fungal 18S band in the elution fraction for LNA-euk-probe (elution a), and no RNA in the elution fraction after phylotrap with LNA-bac-probe (elution b).

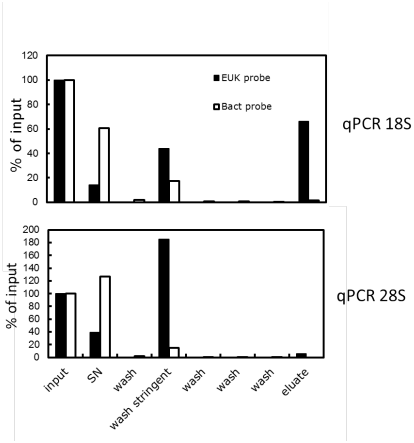

Figure 69: qPCR of Phylotrap experiment with *A.nidulans* RNA and introduction of a stringent washing step. Primers for 18S: SR7R-SR5. Primers for 28S: Ctb6-TW13. Stringent washing step was performed with hybridization buffer containing 30% Formamide for 2 minutes at 70°C. RNA amounts are shown as relative to the input. Black bars show LNA-euk-probe, white bars show LNA-bac-probe**.**

The fractions of the Phylotrap procedure (as shown above on the gel) were also reverse transcribed and measured by quantitative Real-Time PCR with specific primers for fungal 18S and 28S respectively. The stringent washing step was able to remove unspecific binding of fungal SSU to the LNA-bac-probe, and also completely wash off any unspecific binding of fungal LSU to both probes.

The specific SSU recovery by this method (in the eluate recovered by LNA-euk-probe) was estimated to be 66% of the input according to qPCR measurements.

Modifications:

- Hybridization performed at 65°C for 30 min (instead of 40°C)
- Hybridization buffer with higher Formamide concentrations (30%)
- All washing steps performed at 70°C for 2 minutes
- Additional washing step with 0.1x HB at 70°C for 2 min
- Blocking of beads with blocking solution before hybridization (MacGregor *et al.*, 2002).

The higher hybridization temperature of 65°C, as well as the stringent washing step using 0,1x Hybridization buffer were introduced into the PhyloTrap protocol to provide discrimination against specific targets. Additionally, beads were blocked with 0,1% Blocking Solution (Roche) in 0,5xSSC buffer for 1 hour prior to addition of probes, as recommended in (MacGregor *et al.*, 2002).

Modified protocol with specific rRNA yield:

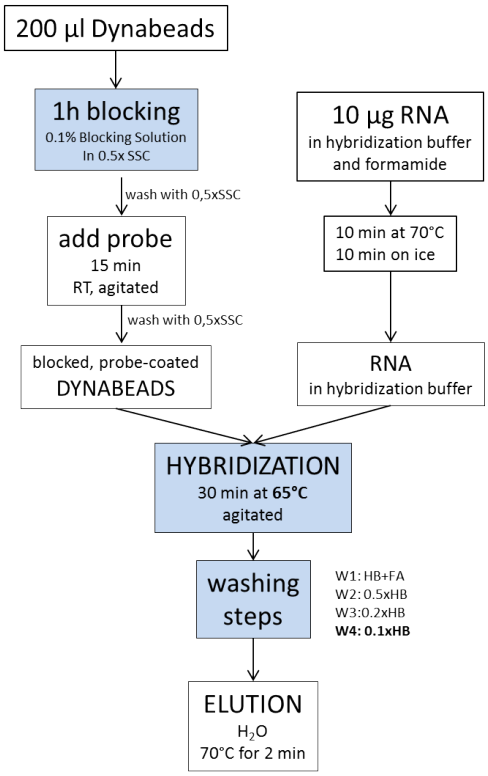

Figure 70: Flowchart of the modified Phylotrap Protocol. Modified steps are explained above and highlighted in blue boxes.

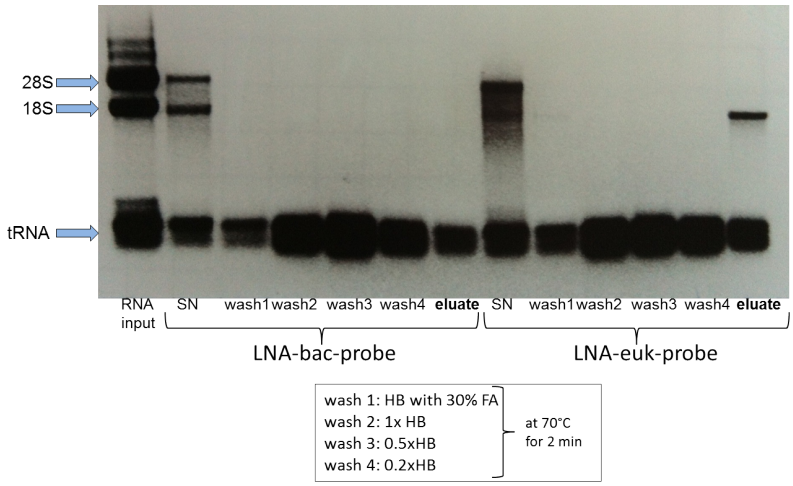

Figure 71: Fractions on the gel after using the modified PhyloTrap protocol, using *A.nidulans* RNA on LNA enhanced bacterial probe (left section) and LNA enhanced eukaryotic probe (right section).

Using the modifications as described above, specific fungal 18S rRNA could be recovered with LNA enhanced euk-probe, while no unspecific rRNA showed up in the eluate of bac-probe coated Dynabeads.

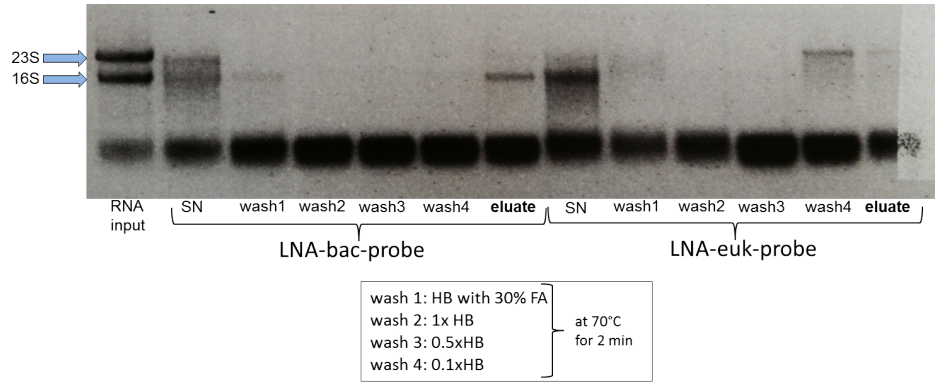

Figure 72: Fractions on the gel after using the modified PhyloTrap protocol, using *R.terrigena* RNA on LNA enhanced bacterial probe (left section) and LNA enhanced eukaryotic probe (right section).

Specific recovery of *R.terrigena* SSU rRNA is shown for LNA enhanced bac-probe in Figure 72. Washing step 4 (very low concentration) is crucial to remove unspecific binding of bacterial rRNA to the LNA-euk-probe.

3.3.3 Optimization of hybridization conditions

Using the general protocol outline as shown in Figure 70, several conditions were tested to finetune the Phylotrap method.

3.3.3.1 Formamide concentration

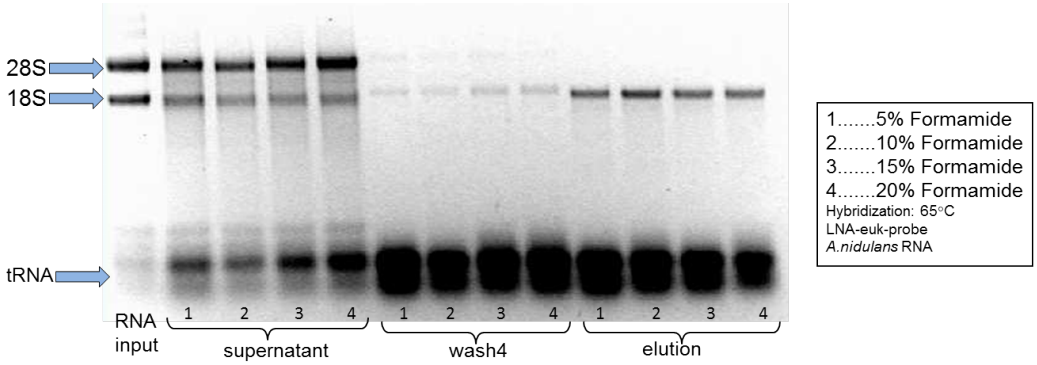

Figure 73: Phylotrap protocol (euk-probe) tested for four different Formamide concentrations in the hybridization buffer: 5, 10, 15 and 20%. *A.nidulans* RNA was used on LNA-euk probe, Hybridization was performed at 65°C for 30 minutes. wash4 = 0.1x Hybridization Buffer.

The Phylotrap method was tested with four different Formamide concentrations in the hybridization buffer. Upon using LNA-euk-probe coated Dynabeads with *A.nidulans* RNA, the 10%Formamide treatment resulted in the strongest SSU recovery in the elution fraction (see Figure 73, elution 2).

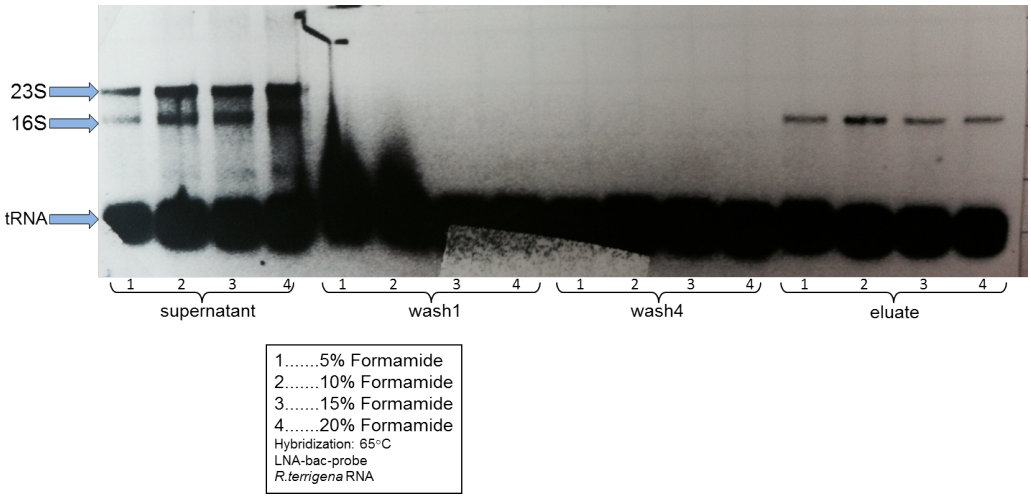

Figure 74: Phylotrap protocol (bac-probe) tested for four different Formamide concentrations in the hybridization buffer: 5, 10, 15 and 20%. *R.terrigena* RNA was used on LNA-bac probe. Hybridization was performed at 65°C for 30 minutes. Wash1 = 1xHybridization buffer (HB), wash4 = 0.2x Hybridization buffer.

As with the LNA-euk-probe, the 10% Formamide condition in the hybridization buffer also resulted in the strongest SSU rRNA yield with LNA-bac-probe coated Dynabeads using the specific target *R.terrigena* RNA (see Figure 74, eluate2).

3.3.3.2 Hybridization temperature

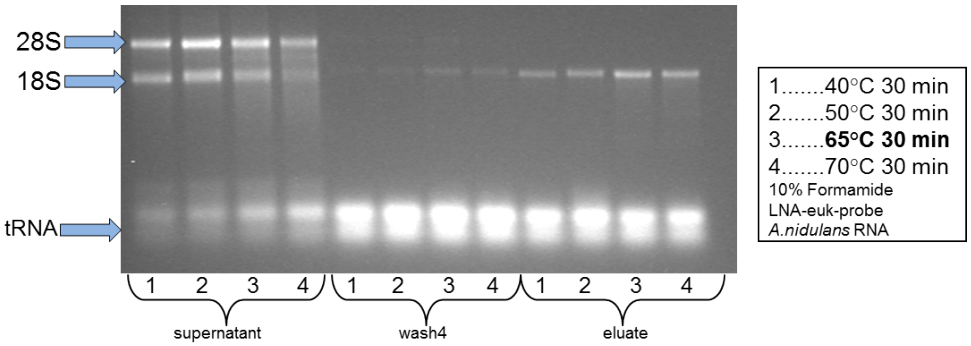

Figure 75: Phylotrap protocol (euk-probe) tested for four different hybridization temperatures: 40, 50, 65 and 70°C respectively. *A.nidulans* RNA was used on LNA-euk probe, using 10% formamide in the hybridization buffer. Supernatant after hybridization = unhybridized RNA. Wash4=0.1xHybridization buffer.

Hybridization temperatures were tested for the Phylotrap method using *A.nidulans* RNA and LNA-euk-probe coated Dynabeads. After 30 minutes of hybridization, the hybridization temperature of 65°C seemed to work best for fungal SSU yield (see Figure 75, eluate 3).

Since the 18S band in the supernatant after hybridization seemed to be even less prominent for the 70°C hybridization sample (Supernatant sample 4), which suggests higher amounts of hybridization, the 65°C and 70°C temperatures were tested again:

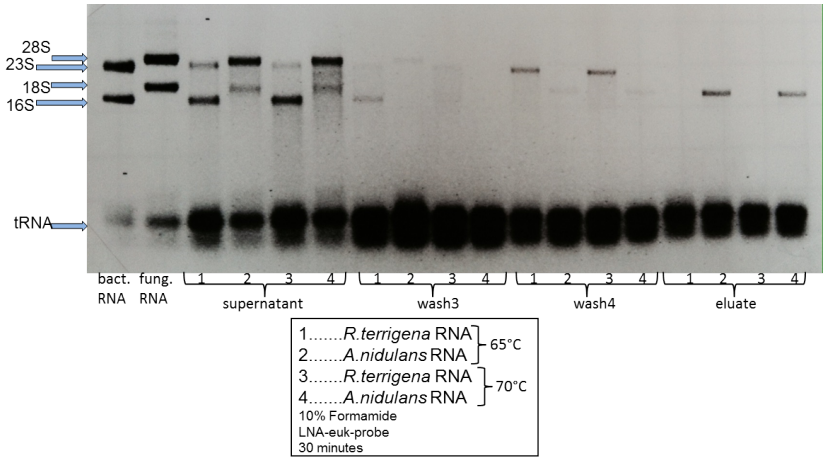

Figure 76: Phylotrap protocol tested with LNA-euk probe for two different hybridization temperatures: 65 and 70°C, with specific target (*A.nidulans* RNA) and unspecific target (*R.terrigena* RNA) respectively. 10% formamide was used in the hybridization buffer. Wash4=0.1xHybridization buffer.

According to the experiment with specific and unspecific target RNA and LNA-euk-probe coated Dynabeads, the fungal SSU capture after hybridization at 65°C was most satisfying (see Figure 76 , eluate 2). However the LSU of unspecific target RNA of *R.terrigena* did hybridize as well (see Figure 76 , supernatant 1 and 3), and was not reduced by a higher hybridization temperature. Only the stringent washing step wash4 with 0.1x HB (at 70°C for 2 minutes) was able to remove the unspecific rRNA before elution (wash4; bands 1 and 3).

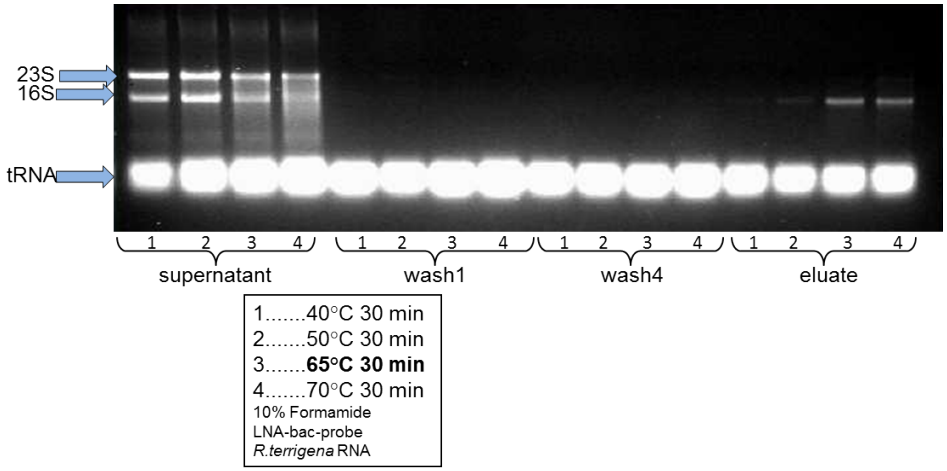

Figure 77: Phylotrap protocol (bac-probe) tested for four different hybridization temperatures: 40, 50, 65 and 70°C respectively. *R.terrigena* RNA was used on LNA-bac probe, using 10% formamide in the hybridization buffer. Wash1= 1xHybridization buffer. Wash4=0.2xHB.

Also the probe specific for bacterial SSU, LNA-bac-probe, was tested for the same temperature range with the specific target *R.terrigena* RNA. As shown in Figure 77, only hybridization temperatures of 65 and 70°C produced a significant bacterial SSU band in the eluate.

Overall, for both the bacterial and eukaryotic LNA enhanced probes, higher hybridization temperatures produced an increase in SSU rRNA yield using the Phylotrap method. The temperature of 70°C did not provide better rRNA yield than hybridization at 65°C, and together with the higher risk of RNA degradation, this was the reason to choose the hybridization temperature of 65°C for further experiments.

3.3.3.3 Hybridization time

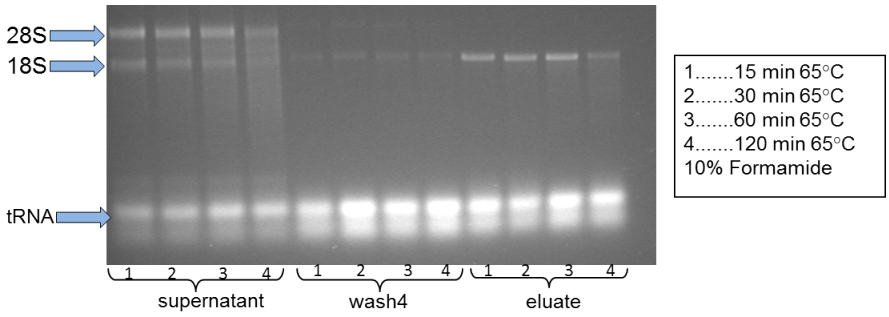

Figure 78: Phylotrap protocol tested with *A.nidulans* RNA on LNA-euk probe for different hybridization times: 15, 30, 60 and 120 minutes. Hybridization was performed in 10% Formamide at 65°C. Wash4=0.1x Hybridization buffer.

Different hybridization times were tested for the specific target *A.nidulans* RNA on LNA-euk-probe coated Dynabeads. When using 10% Formamide in the hybridization buffer at 65°C, the hybridization times 30 and 60 minutes resulted in the strongest SSU band on the gel. Because of a higher risk of RNA degradation with longer incubation times, the hybridization time of 30 minutes was chosen for further experiments.

3.3.3.4 Phylotrap optimized protocol

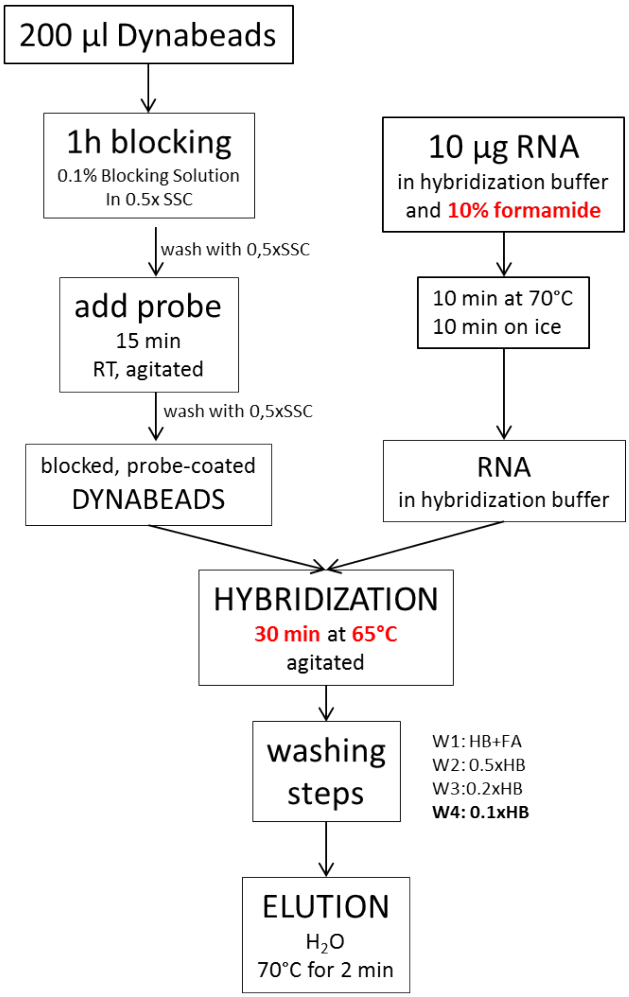

Figure 79: Phylotrap protocol including the optimized conditions highlighted in red.

Dynabeads:	50 µl/reaction		
RNA:	5 µg / reaction		
LNA probes:	12,5 pmol / reaction		
Formamide:	10%		
Hybridization:	Hybridization buffer (HB)		
	5xSSC		
	0,1% N-laurylsarcosine		
	0,1% NaCl		
	0,02% SDS		
	30 minutes		
	65°C		
Washing:	W1: 1xHB	70°C 2 min	
	W2: 0,5xHB	70°C 2 min	
	W3: 0,2xHB	70°C 2 min	
	W4: 0,2xHB	70°C 2 min	FOR BAC338
	W4: 0,1xHB	70°C 2 min	FOR EUKb310

Elution H_2O 70°C 2 min

3.3.4 Phylotrap with mixed RNAs

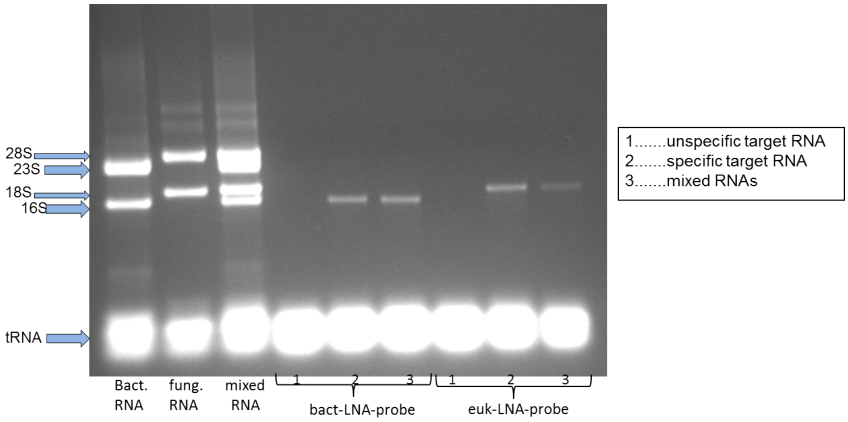

Figure 80: Phylotrap protocol with bacterial RNA (R.terrigena), fungal RNA (A.nidulans) and mixed RNA (R.terrigena + A.nidulans) using Dynabeads coated with LNA enhanced probes. Specific target for bact-LNA-probe: 5 µg R.terrigena RNA. specific target for euk-LNA-probe: 5 µg A.nidulans RNA. Mixed RNAs: 5 µg R.terrigena RNA + 5 µg A.nidulans RNA. Hybridization was performed in 10% Formamide at 65°C for 30 min.

Testing the Phylotrap protocol with *A.nidulans* and *R.terrigena* RNA mixed together, the specific target SSUs were recovered with no unspecific SSU or LSU showing on the gel. For bact-LNA-probe, the samples containing specific target (i.e. samples 2 and 3) showed clean bacterial SSU recovery bands with the same intensity for both mixed and single species RNA. Phylotrap performed with euk-LNA-probe coated Dynabeads also produced specific fungal SSU bands in sample 2 and 3 without unspecific contamination. However for the euk-LNA-probe, specific target fungal SSU rRNA could not be recovered from the mixed sample with the same yield as from the single species RNA sample (sample 2 vs sample 3).These samples were also tested with quantitative Real-Time PCR using primers for 18S and 28S rRNA, see Figure 81:

Figure 81: 18S capture from *A.nidulans* RNA with LNA-euk-probe coated Dynabeads, analyzed by qPCR. Primers: "SR7R-SR5" for 18S and "Ctb6-TW13" for 28 S. Specific target for euk-LNA-probe: 5 µg *A.nidulans* RNA. Mixed sample: 5 µg *A.nidulans* RNA + 5 µg *R.terrigena* RNA. Samples were reverse transcribed and analyzed by qRT- PCR with reverse transcribed *A.nidulans* RNA dilutions as standards. In this diagram, RNA amounts of elution fractions were normalized to the detected RNA amount in the input.

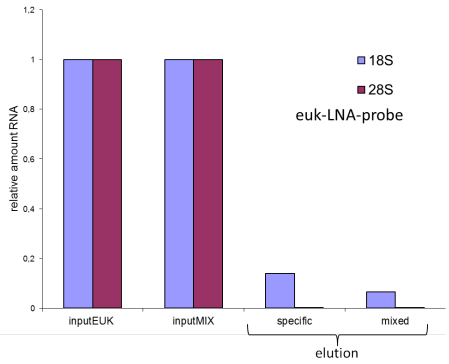

In mixed samples, the specific RNA capturing efficiency goes down by 53% compared to the clean RNA samples when using eukLNA probe-coated Dynabeads, from 14%

capture in the sample with specific target only (inputEUK), to 6% in the sample with mixed target (inputMIX) which contained *A.nidulans* as well as *R.terrigena* RNA.

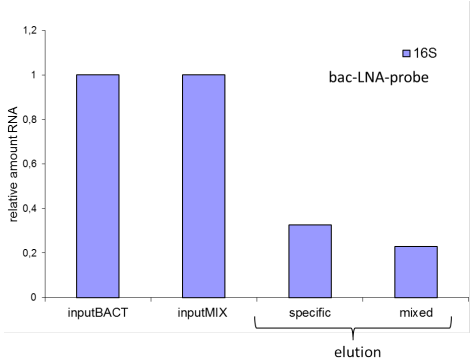

Figure 82: 16S capture from pure *R.terrigena* RNA and RNA mix (*A.nidulans and R.terrigena)* with LNA-bac-probe coated Dynabeads, analyzed by qPCR. Primers: "EUBf933-EUBr1387" for bacterial 16S. Specific target for bac-LNA-probe: 5 µg *R.terrigena* RNA. Mixed sample: 5 µg *A.nidulans* RNA + 5 µg *R.terrigena* RNA. Samples were reverse transcribed and analyzed by qRT- PCR with reverse transcribed *R.terrigena* RNA dilutions as standards. In this diagram, RNA amounts were normalized to the detected RNA amount in the input.

Real-time PCR with primers for bacterial 16S rRNA confirmed what the gels in Figure 80 suggested. The total specific rRNA yield by Phylotrap was higher using the bac-LNA-probe than the euk-LNA-probe, and the capturing efficiency decrease was lower when using the mixed RNA sample compared to the clean RNA sample. 16S rRNA capturing efficiency went down from 33% to 23% in the mixed sample which is a 30% decrease.

To test if higher stringency was needed to increase capturing efficiency with eukLNA-probes in mixed samples, different Formamide concentrations were tested with mixed RNA samples :

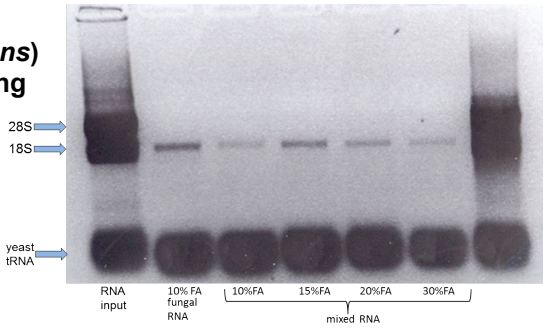

Figure 83: Phylotrap protocol fungal RNA (*A.nidulans*) and mixed RNA *(A.nidulans and R.terrigena)* using Dynabeads coated with LNA-euk-probe. Specific target for euk-LNA-probe: 5 µg *A.nidulans* RNA. Mixed RNAs: 5 µg *R.terrigena* RNA + 5 µg *A.nidulans* RNA. Hybridization was performed at 65°C for 30 min. Different formamide concentrations in the hybridization buffer were used: 10%, 15%, 20% and 30% as indicated in the figure.

As shown in Figure 83, the specific RNA yield from mixed RNA samples could be increased by using the higher formamide concentration of 15% instead of 10% in the hybridization buffer for the Phylotrap method. The formamide concentrations of 20% and 30% were not able to increase the specific yield significantly.

For phylotrap experiments using LNA-euk-probe coated Dynabeads and mixed RNA samples, the formamide concentration of 15% was therefore used for further

experiments in mixed RNA samples to match the yield of pure culture *A.nidulans* RNA that was achieved at 10% formamide.

To increase the total specific rRNA yield from mixed samples further, the supernatant after hybridization (i.e. the unhybridized fraction of RNA) was reused for another round of hybridization for a higher total yield from the same sample. One mixed RNA sample was divided, to be hybridized with both probes respectively (a and b).

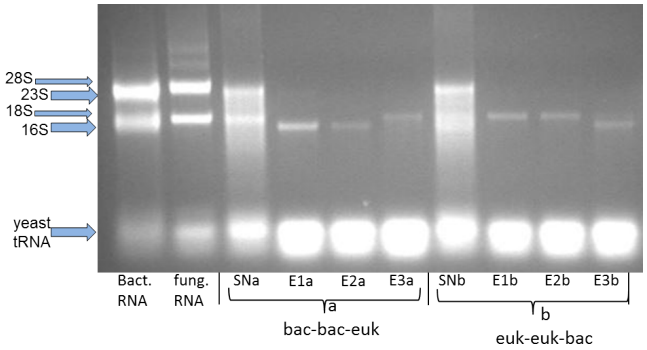

Figure 84: : Phylotrap protocol including multiple hybridizations. Mixed RNA *(A.nidulans and R.terrigena)* was hybridized with Dynabeads coated with LNA enhanced probes, reusing the supernatant for two more hybridizations. Mixed RNAs: 5 µg *R.terrigena* RNA + 5 µg *A.nidulans* RNA. Hybridization was performed in 65°C for 30 min with 15% Formamide. (a) Mixed RNA was hybridized with LNA-bac-probe, yielding eluate E1a. Supernatant was hybridized again with LNA-bac-probe, yielding eluate E2a. Then, supernatant was hybridized with LNA-euk-probe, yielding eluate E3a. (b) Mixed RNA was hybridized with LNA-euk-probe, yielding eluate E1b. Supernatant was hybridized again with LNA-euk-probe, yielding eluate E2b. Then, supernatant was hybridized with LNA-bac-probe, yielding eluate E3b.

The RNA eluates after multiple hybridizations were quantified with a fluorescence RNA quantitation kit (Invitrogen), see Figure 85.

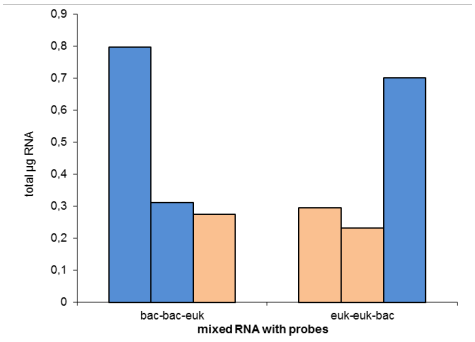

Figure 85: RNA quantification after mixed RNA Phylotrap capture, using multiple hybridizations from the same sample. 7 µg bacterial (*R.terrigena*) RNA and 7 µg fungal RNA *(A.nidulans*) were used in a mixed sample for specific SSU rRNA capture with LNA-euk-probe (euk) and LNA-bac probe (bac). Eluates were quantified with Quant-iT™ RNA Assay Kit. Left section: Mixed RNA sample was hybridized with LNA-bac-probe coated Dynabeads twice, and finally with LNA-euk-probe coated Dynabeads. Right section: Mixed RNA sample was hybridized with LNA-euk-probe coated Dynabeads twice, and finally with LNA-bac-probe coated Dynabeads.

The Phylotrap SSU rRNA capture using multiple hybridizations was able to capture a total of 1,8 µg bacterial and 0,8 µg fungal SSU RNA, which puts the total yield at 26% capture from one sample by the bacterial probe and 11% by the eukaryotic probe, respectively.

4 DISCUSSION

Beech litter from four different locations in Austria was used for a series of experiments, with the goal to describe fungal diversity during early stages of litter decomposition. After litterfall, plant residues like beech litter are decomposed by a variety of microbial activities, and extracellular enzyme activities make fungal communities the key decomposers in forest ecosystems (Kellner *et al.*, 2010). Even though there is an Austrian fungi database (http://www.austria.mykodata.net/), only few molecular data of local origin are available, especially on litter decomposition. Austrian studies focusing on molecular identification of fungi and yeast include (Klaubauf *et al.*, 2010b), a study on fungal communities in agricultural soils, and (Wuczkowski *et al.*, 2005), focused on fungi and yeast in soils and litter from the alluvial zone along the river Danube (Nationalpark Donauauen), however here only yeast strains were identified by molecular methods. One recent study focused on microbial decomposer structure (Schneider *et al.*, 2012) by metaproteomics, using beech litter from sampling sites in Austria similar to our study. Rhizosphere microbial community changes by PLFA were published by (Koranda *et al.*, 2011). A decomposition study of *Quercus petraea* litter in Czech Republic was published recently (Voriskova & Baldrian, 2013) providing sequencing data on fungal community succession.

Beech (*Fagus sylvatica*) is the most common broadleaf tree in Austria, growing preferably at 300-900 m above sea level (Schadauer *et al.*, 2006). Beech and mixed spruce-beech stands are mostly found on rendzic leptosols (Rendzina) and cambisols (Braunerde) which are among the prevalent Austrian soil types (Dämon & Krisai-Greilhuber, 2012). The four sampling locations used in this study were chosen due to their litter nutrient content as explained in (Schneider *et al.*, 2012): Klausenleopoldsdorf (KL) in Lower Austria, Achenkirch (AC) in Tyrol, Ossiach (OS) in Carinthia, and Schottenwald (SW) in Vienna. Within the framework of the MICDIF project (*Linking microbial diversity across scales and ecosystems,* national research network funded by the FWF, project S 100), beech litter samples were collected in 2009 as explained in detail here (Wanek et al., 2010) and here (Schneider et al., 2012). For details on the MICDIF project, see page 3.

4.1 Early fungal community succession on native beech litter in a microcosm experiment

Using aliquots of the collected litter samples from all four locations, a small microcosm experiment was conducted in the laboratory for two weeks, and to get an idea of the 'native' undisturbed fungal community on the litter becoming active upon increase of the water content, fungal SSU/partial LSU gene clone libraries were constructed for each location and time point, yielding a total of 12 libraries (4 locations, three time points). The three time points were: 0 days, 2 and 14 days respectively. The litter used for these experiments was dried and shredded, but not sterilized or inoculated prior to incubation, and can therefore be considered to contain the native fungal community at timepoint 0 days. Timepoints 2 and 14 days were taken after incubation at room temperature with a water content of 60% . Molecular genotyping of the native litter community in this study was done by DNA extraction, RFLP (Restriction fragment length polymorphism) analysis of the SSU/LSU region, followed by sequencing of clones with distinctive patterns. Among the nuclear ribosomal regions, the fungal ITS region is the most successful biomarker for species identification (Schoch *et al.*, 2012), and therefore was suggested as the universal barcode marker for fungi. This combination of RFLP genotyping and DNA sequencing is a common method for studying fungal populations (Xu, 2006).

Fungal litter communities were represented well by molecular genotyping at earlier time points. Species accumulation curves were plotted to find out if each particular sample was represented well enough by the constructed clone library. Not all of the samples showed asymptotic behaviour or flattening, due to the trend of higher species density at later time points which was obvious for all samples. Samples represented well by the generated clone libraries include all three timepoints of Achenkirch (AC), timepoints 0 and 2 days of Ossiach (OS), Klausenleopoldsdorf (KL) at 0 days, and Schottenwald at 2 days. Because none of the 4 curves for time point 14 days show asymptotic behaviour, it can be assumed that species density increases tremendously after 14 days of incubation, which leads to possible underrepresentation of rare species.

Fungal diversity and richness were related to incubation time. Richness as well as diversity both generally increased with time. Across all four locations, diversity at time point '14 days' was significantly higher than at earlier time points. This indicates that not only the number of species increased on dry litter upon wetting and start of the

decomposition process, but also the dominance of particular species became less prominent. Dry litter (sampling time point '0 days') may contain a considerable numer of fungi in dormant structures such as spores, and these might become activated upon wetting and start of the experiment. Since this experiment was based on DNA extraction, it must be kept in mind that high DNA content does not necessarily equal high activity of the respective species. However it does make sense that at the beginning of the decomposition process, more and more fungal species become active, grow and feed on the easily available carbon structures.

Highly uneven fungal community structures were found on Austrian beech litter. The observed community structures in this experiment can be categorized as highly uneven, the rank-abundance curves showing a long tail representing the rare species, and a few OTUs being dominant (highest rank). The tail became even longer at the later time point '14 days', which means that a higher number of rare species was detected. At the same time, the rank- abundance curve became less steep due to the proliferation of subdominant species with time. This pattern of one or two dominant OTUs together with a sharp drop in abundance from the top ranks in later phases is characteristic for decomposer communities and was also shown in a study focused on fungal communities in composts (De Gannes *et al.*, 2013). OS, KL and SW locations were strongly dominated by one OTU (up to 96%), whereas on AC litter, dominance was shared between two different OTUs. The fungal community found on AC litter was therefore not as uneven as on the KL and OS locations, where only one dominating species was found. This was also represented in a slightly less steep rank abundance curve.

Biotic similarity of fungal communities seemed to be influenced by nutrient ratios. Biotic similarity between the four sampling areas was assessed using the Morisita-Horn similarity measure. This calculation is based on species abundance and shared species between assemblages. The fungal community represented by OTU libraries from the SW location showed the lowest similarity to all other locations. Trying to find an explanation to this difference, beech litter nutrient ratios might be an answer. SW has already been characterized as a high nutrient site, with wet N deposition at 20.2 kg N $ha^{-1}y^{-1}$ (Kitzler *et al.*, 2006). SW litter presented the highest N, P and Mn contents, and therefore this site presented the lowest C/N and C/P ratios. This location's nutrient status and environmental parameters are discussed in detail by (Schneider *et al.*, 2012). KL and OS were found to be the biotically most similar locations- these locations both presented poor nutrient levels with OS showing the

highest C/P ratio and KL showing the highest C/N ratio respectively. So it seems likely that similar nutrient ratios make for a higher biotic similarity. Generally, substrate quality- also defined by C/N ratio of the litter- has been shown to influence litter decomposition (Berg & McClaugherty, 2014), therefore a higher biotic similarity would be expected for sites with similar nutrient status. However at the very early onset of decomposition, nutrient ratios cannot be the only determinant of biotic similarity because there is no mass loss involved and elemental ratio effects are therefore negligible, as demonstrated in a beech litter mesocosm experiment (Mooshammer *et al.*, 2012). So despite quite different C/N ratios of beech litter in the four different locations, nutrient variations cannot solely explain biotic similarities and dissimilarities in this study.

The elevation gradient of the sampling location could influence fungal community composition. Looking for another explanation for biotic variation, the elevation above sea level of the sampling location might be a candidate. SW is located at 370 m asl which is the lowest of all four locations. It has been shown that the composition of beech phyllosphere fungal communities varied between different elevation sites in the French Pyrénées (Cordier *et al.*, 2012). In that particular study it was concluded that climatic variables were the reason for different fungal species at different sites. According to (Schneider *et al.*, 2012), the SW site was the warmest site. Additionally, the SW site is close to the big city Vienna (Kitzler *et al.*, 2006), and therefore the climatic difference to the other locations might be even higher than solely explained by the lower elevation. Taken together, this might be one of the reasons as to why the fungal biota found at SW were significantly different from the other locations in the study.

Schottenwald (SW) fungal community was significantly different from all other locations. Even though there was a pattern of clustering by time point, it was shown by cluster analysis that SW_0 was distinctively an outgroup. SW samples shared the least OTUs, while time course samples of OS showed the highest similarity. Compared to the other locations, the fungal community of SW was significantly different from all other locations used in the study. This difference was obvious simply by pairwise comparisons of shared species. By taxonomic analysis, a *Lemonniera* OTU from the order Helotiales was identified as the dominant species on OS (up to 86%) and KL (up to 69%) litter, and was one of three dominating species on AC litter (up to 49%). It was found on SW, but not as a dominating species (up to 14%, but absent in SW_14). In SW samples however, not *Lemonniera* was found as the dominating species, but an

OTU assigned to the genus *Ampelomyces* of the Pleosporales. These are often saprobically associated with plant material, and also involve mycoparasites. According to (Zhang *et al.*, 2009), anamorphic *Ampelomyces* is polyphyletic, with some species placed within the *Didymellaceae*, and others in the *Phaeosphaeriaceae*. Some *Ampelomyces* species can be assigned morphologically to the coelomycetous fungi, others to hyphomycetes. The name coelomycete points out that these fungi produce their conidia in enclosed structures, in contrast to hyphomycetes with free conidia (Sutton, 1980).

Taxonomic analysis of the fungal community on Austrian beech litter revealed Ascomycota dominance. By taxonomic analysis of the clone library sequencing data, all OTUs were assigned to Ascomycota and Basidiomycota only, both of which comprise of a variety of saprotrophic fungal genera known to be important for litter decomposition. The absence of Glomeromycotina (arbuscular mycorrhizal fungi), Mucoromycotina or any other basal fungal lineage was not unexpected as these phyla are not known to inhabit the phyllosphere or exhibit endophytic behavior in leaves. All analysed microcosm communities were dominated by Ascomycota, accounting for at least 80% of the clones in the respective libraries. All other OTUs were assigned to the Basidiomycota. This is in accordance with metaproteomic studies of beech litter decay (Schneider *et al.*, 2012) where Ascomycota abundance and activity dominated the fungal decomposer community in early stages of litter decomposition. This dominance is due to the fact that Ascomycota efficiently degrade easily accessible polysaccharides rather than lignin.

Basidiomycota were preferably found in later time points. The ratios of Basidiomycota:Ascomycota found in this study generally increased with incubation time, and the highest ratio of 19,5% Basidiomycota was found on KL litter at 2 days. An increase in Basidiomycota species with time is in accordance with a study on decomposing oak leaves (Voriskova & Baldrian, 2013), where initially dominating Ascomycota were overruled by Basidiomycota after 2 years of decomposition. This follows a general decomposition pattern for ligninolytic fungi as suggested by (Osono, 2007), with Ascomycetes being abundant on freshly fallen leaves but gradually decrease in abundance during decomposition, concomitant with a rise in Basidiomycete abundancy. The differential abilities do degrade lignin efficiently were proposed as the main factors for these successional changes. Within the Basidiomycota, known plant pathogens from the rust fungi Pucciniomycotina like *Rhodotorula* and *Bensingtonia* were found, as well as wood inhabiting Agaricomycotina (e.g. jelly fungi like

Tremellales, Auriculariales) and basidiomycetous phylloplane yeast genera (e.g. *Dioszegia*, *Cryptococcus*). Many of the assigned species were also found in a beech litter decay study in Czech Republic (Voriskova & Baldrian, 2013), as well as a yeast study from Austria (Wuczkowski *et al.*, 2005). This shows that our taxonomic assignments based on this clone library based approach were able to produce data which are relatable to similar studies involving litter decay.

Common primary saprophytes and leaf parasites were found on Austrian beech litter. Within the Ascomycete OTUs, only a few sequences belong to the subphylum Taphriniomycotina, while the majority are assigned to Pezizomycotina. Within the Pezizomycotina, 5 classes and 14 orders are represented. Taphriniomycotina were represented by the Taphrinaceae family only, which is known to contain plant pathogens. Ascomycete species involved so-called 'common primary saprophytes' (Hudson, 1968), like *Alternaria alternata*, *Cladosporium cladosporioides*, *Epicoccum nigrum*, and *Aureobasidium pullulans*. These leaf surface-inhabiting fungi are often among the first saprophytic invaders after litterfall. *A.pullulans* and *C.cladosporioides* can ecologically be classified as sugar fungi, which means they have very low cellulolytic abilities and therefore depend on soluble carbohydrates (Osono & Takeda, 2006). This makes them successful primary colonizers in the onset of decomposition. Also present in higher numbers were OTUs similar to *Apiognomonia errabunda*, *Davidiella tassiana, Mycosphaerella punctiformis*, as well as its anamorph *Ramularia*. These are typical parasites on living beech leaves, and were also found in other studies on beech litter decomposition (Cordier *et al.*, 2012). One particular OTU called *M.punctiformis* KL0_B03 was found on almost all samples, being absent only in SW_14 and AC_14, which strongly indicates primary colonizer behavior. On AC litter only, one particular *Ramularia* OTU was among the three most abundant OTUs together with a *Lemonniera* sp. and a *Helotiales* sp., being present at 13-27%. *Ramularia* is a teleomorphic form of *Mycosphaerella* and associated with litter decomposition, together with other '*Cladosporium*-like hyphomycetes' within the Dothideomycetes. This group involves saprobic plant pathogens with pleomorphic behavior, which means they can occur in sexual (teleomorph) and asexual (anamorph) forms. Sometimes even more than one asexual morph is known (synanamorph) which makes morphological identification complicated (Wingfield *et al.*, 2012). This is the reason for dual naming for many genera, however thanks to PCR and DNA sequencing technology, many genera are already linked, for example *Cladosporium* and *Davidiella* (teleomorph form), *Mycosphaerella* and *Ramularia*, or *Alternaria-Lewia* (Wijayawardene *et al.*, 2014). All of

these genera were found in different abundances on almost all locations, as expected due to their known primary saprophytic lifestyle on plant litter.

Dynamics of aquatic hyphomycete occurrence pointed to a dual ecological lifestyle. As said before, a *Lemonniera* OTU from the order Helotiales was highly abundant and found on all samples and time points with the exception of SW_14. These high numbers of one particular OTU were mainly responsible for the pronounced uneven community structure as discussed earlier. *Lemonniera* belongs to the so-called 'Ingoldian Fungi' or Aquatic Hyphomycetes, known to be the main decomposers of deciduous leaves falling into streams (Bärlocher, 1992). Within this polyphyletic ecologically defined group, most fungi belong to the Ascomycota. They are also found on wet or submerged litter in terrestrial niches like treeholes (Gonczol & Revay, 2003). Since aquatic hyphomycetes are often found far away from their classic habitats, and also occur on different types of plant detritus, a dual ecological lifestyle has been suggested (Seena & Monroy, 2016) as endophytic aquatic hyphomycetes. A possible shift between saprotrophic and biotrophic lifestyle was proposed, which makes this group ecologically very interesting (Chauvet *et al.*, 2016). In the present study, *Lemonniera* dominance went down with time, for example from 86% to 34% in OS, and from 69% to 25% in KL. The high initial Lemonniera dominance (up to 86%) suggests endophytic behavior on live leaves, followed by fast sporulation and colonization upon litterfall as primary saprophytes. Successively this dominance declines because other saprophytic fungi can invade the litter. Most phyllosphere fungi are present on fresh litter, but only for a short period of time (Osono, 2006). This dynamic of initial high dominance followed by a decline together with detection of new species was confirmed within this study. This indicates a possible life cycle consisting of endophytic as well as saprophytic phases.

Rare species found only in later timepoints involved known beech litter saprobes. Some species found only in later time points at low abundance, but on several locations were *Lewia, Discosia, and Epicoccum.* The same Discosia OTU was found on all four locations at the 14 days timepoint. Discosia is known as a leaf pathogen but also found saprobically associated with beech (Li *et al.*, 2015).

The importance of environmental sequence collection databases was highlighted for the identification of unknown species. There were some OTUs which could not be assigned to a certain genus or even family level based on BLAST search at that time, and were therefore named 'uncultured Basidiomycota' or 'uncultured fungus'. But due to the growing amount of environmental sequences in online databases, there

might be more assignements possible soon. One example is a particular French study (Cordier *et al.*, 2012) which found two of our sequences published at GenBank (Benson *et al.*, 2003) matching two of their 12 most abundant OTUs by 100%:

GenBank accession no.	MOTU relative abundance	GenBank (environmental sequences excluded)			GenBank (environmental sequences included)			
		Closest match	Similarity/ coverage	Putative taxon	Closest match	Similarity/ coverage	Putative taxon	Source
JN906440	14.38	AY239214	86/96	*Lalaria inositophila*	**JF495183**	100/100	**Uncultured *Taphrina***	Austria, *Fagus sylvatica* leaf litter, S. R. Moll *et al.*, unpublished
JN904440	14.34	GQ411291	95/100	*Articulospora tetracladia*	**JF945438**	100/100	**Uncultured fungus**	France, *Fagus sylvatica* phyllosphere, Cordier *et al.* (2012)
JN906683	10.46	AY971723	76/94	Fungal sp.	**JF495199**	100/100	**Uncult. Pezizomycotina**	Austria, *Fagus sylvatica* leaf litter, S. R. Moll *et al.*, unpublished
JN905902	6.11	**AY239215**	100/100	***Taphrina carpini***	**AY239215**	100/100	***Taphrina carpini***	Portugal, *Quercus pyrenaica* phylloplane, Inácio *et al.* (2004)

Figure 86: Two of our unidentified fungal OTUs matching 100% with OTUs from beech phyllosphere fungal assemblages in the French Pyrenees, modified from (Cordier *et al.*, 2012)

This is a promising event which demonstrates again that even with a study design that did not involve a huge amount of samples or biological repetitions, we were still able to produce a meaningful dataset on beech phyllosphere fungal community composition. The publication in sequence databases is a huge help for future studies, especially with the application DNA metasystematic approaches like next generation sequencing and DNA barcoding for community ecology (Hajibabaei, 2012).

Influence of nutrient levels, ratios and environmental factors on fungal community structure. As a visual demonstration of the results discussed above, Principle component analysis (PCA) of the native litter dataset shows the influence of taxonomic community structure, nutrient levels and environmental factors. Generally it can be stated from looking at the PCA that litter with a different nutrient status potentially hosts a different fungal community. Since the experiment only involved a few samples and datapoints, the PCA can only give a few hints of possible relationships. Most strikingly, Ascomycota are located opposite to Basidiomycota, overall diversity and incubation time in days. This confirms again visually that the longer the samples were incubated, diversity indices were higher and more species were discovered, and Basidiomycota were detected at later time points only. On the y-axis, nutrient ratios C/N and C/P as well as Fe levels are allocated together with elevation of the sampling location and percentage of Helotiales. On the opposite, positive side, percentage of Pleosporales and Mn levels are located. This suggests that lower nutrient ratios, lower elevation and lower percentage of Helotiales- as it was the case for the SW location- are connected to a higher percentage of Pleosporales. Higher Mn levels seem to support a community with higher abundance of Pleosporales as well.

Manganese levels could have an influence on community composition. It is known that litter quality- that refers to nutrient ratios as well as lignin or Manganese content- has an influence on decomposition and mineralization rates (Couteaux *et al.*, 1995). A potential influence of initial Mn and K elemental contents on decomposition was also proposed in a beech litter decomposition experiment due to correlations with respiration activity (Brandstatter *et al.*, 2013). Even though there are many theories on functional redundancy of microbial communities (Andren *et al.*, 1995), there is also evidence that different communities are functionally dissimilar (Strickland *et al.*, 2009). It might therefore make sense that litter from a sampling location with different nutrient composition- in this study a high Mn content of SW- attracts a different fungal community, which could potentially result in decomposition rate differences. More specifically, it was demonstrated that Manganese levels have an influence on litter decomposition rates (Berg *et al.*, 2007), so the finding of a different fungal community composition in the Mn rich SW sampling site is not unexpected. However the sampling time points were very early and therefore only represent the initial fungal community at the onset of decomposition, far from actual mass loss. Therefore it is questionable if the Mn content of the litter can be the reason for drastic fungal community differences. But usually a good amount of the fungi from live leaves are also found on litter at the start of decomposition (Snajdr *et al.*, 2011), so stoichiometric differences of beech leaves at a sampling site can still be a determinant factor for fungal decomposer community assembly at early time points, because saprotrophic fungi at the forest ground are able to re-invade fresh leaves in the spring, fulfilling a life cycle consisting of both endophytism and saprotrophism. Mn and K elemental contents at the early stage of decomposition were also proposed to influence respiration levels in a beech litter decomposition study.

4.2 Microbial community composition changes during beech litter decomposition in a mesocosm experiment

The results discussed above are all based on a characterization of the fungal community on native, that means, unsterilized beech litter with different nutrient ratios. We were interested in the native fungal community on the undisturbed litter present at the start of the experiment. Within the framework of the MICDIF (see page 3), litter from the same four sites in Austria was used, however it was sterilized before the start of the experiment. An inoculum was generated from KL litter, and therefore the same 'window' of active microbes was reintroduced to litter with different nutrient ratios. Therefore it has to be kept in mind that these two studies cannot be compared, even though the litter sampling sites were the same.

Mesocosm study design and results of sister studies. To further investigate microbial decomposition on different beech litter samples over a longer period of time, a mesocosm experiment was conducted over the time course of six months under the main supervision of Dr.Katharina Keiblinger (BFW) and Dr.Ieda Hämmerle (University of Vienna) as explained here (Keiblinger *et al.*, 2012) and here (Leitner *et al.*, 2012). Litter samples were sterilized and inoculated as explained in 2.3.1. Upon harvesting after two weeks, three, six and fifteen months after inoculation, aliquots of the samples were distributed to different laboratories participating in the study. Each laboratory addressed different questions using the same litter sample material. To highlight a few, it was discovered that decomposition mass loss was negligible at three and six months of this experiment (Mooshammer *et al.*, 2012). Mass loss after 15 months was found highest in SW (10%) (Mooshammer *et al.*, 2012) which is still a slow decomposition rate. This was explained by the mesocosm conditions where leaching and litter fragmentation by invertebrate fauna were absent and the only processes were microbial (respiration, denitrification). Litter nutrient ratios were also shown to have an impact on fungal abundance (Keiblinger *et al.*, 2012).

The fungal/bacterial ratio of copy numbers was used to detect community shifts. In this study, the fungal/bacterial ratios in the time course of decomposition were assessed via qPCR (or Real-Time PCR). This was done to quantify microbial community composition changes, as opposed to the first experiment with native unsterilized litter, with the goal to describe the natural fungal community taxonomically. qPCR is commonly used for quantification of a fluorescent molecule accumulating

together with a PCR product of choice. For studying microbial communities, qPCR has been shown to help tremendously by making it easier and more straightforward to process a large number of samples at the same time and estimate gene copy numbers simultaneously (Fierer *et al.*, 2005). In this study, general primer sets for bacteria (101F-537R) as well as for fungi (NSI1-5.8S) were used that had already been tested and used for qPCR application (Inselsbacher *et al.*, 2010). The fungal/bacterial (F/B) ratio was calculated, which is the ratio of copy numbers measured with the fungal and bacterial qPCR assays respectively. The fractional copy numbers are more suitable to present an index of target abundances, because the goal was to only detect the community shift with time.

The microbial community was changing during decomposition. The fungal dominance in this mesocosm experiment that had already been published ((Schneider *et al.*, 2012) and (Keiblinger *et al.*, 2012)) was confirmed by qPCR F/B ratios. The F/B ratios overall were highest at the first sampling point (2 weeks), and went down with time. This shows that fungi were able to colonize the beech litter faster than bacteria, and the onset of litter decomposition was highly dominated by fungi. Fungal dominance was highest at the beginning of decomposition. This can be explained by the finding that many endophytic fungi infect live leaves and persist after litterfall acting as pioneer decomposers (Hirose *et al.*, 2013). The initial fungal dominance (especially at SW and KL) went down with decomposition time, until all four sites reached a similar F/B ratio. Rapid and dynamic changes in the litter-associated microbial community during decomposition are a common feature of microbial succession, which is mainly driven by nutritional changes within the litter. The production of extracellular enzymes is a very important fungal process during decomposition, and it could even be the prerequisite for bacteria gaining dominance in later stages, as it was discussed in a functional approach on the same litter mesocosms (Schneider *et al.*, 2012), where the bacteria were called ‘cheaters’.

Very distinctive microbial communities evolved from the same inoculum on nutritionally different beech litters. At 2 weeks, all 4 sampling locations showed very different F/B ratios. This is interesting because all samples started off with the very same inoculum and therefore presumably the same F/B ratios (no data available). As established before, there are different explanations for this finding. First, the nutrient levels of each site are very different, and therefore specifically adapted microbial communities are likely to be found. Secondly, it has been shown before that bacteria and fungi favour different nutrient ratios. Third, there is a so-called ‘home-field

advantage' (Fanin *et al.*, 2016) which might have an effect on microbial activity because litter inoculum was generated from one of the four litter types used in the study. All of these reasons are non-exclusive and may contribute to the microbial composition at a site during litter decomposition.

High nutrient ratios induced fungal dominance. In a microcosm decomposition experiment, it has already been established that bacterial cell counts were highest at an N:P ratio of 5, and fungal ergosterol content was highest at N:P ratios of 15-45 (Gusewell & Gessner, 2009). This leads to the assumption that substrates with high nutrient levels (narrow C:N) are preferred by bacteria, and low nutrient levels (wide C:N) favor fungi. Even though the site with the narrowest C:N ratio was SW (which would seem more suitable for bacteria), this was the site of the highest F/B ratio, i.e. highest fungal dominance, as detected by qPCR. However, all of the litter sites in the present study showed nutrient ratios above 40, so a fungal dominance in litter decomposition is likely for all litter locations, which has also been demonstrated here (Keiblinger *et al.*, 2012). SW was also the litter location that showed accelerated decomposition (Keiblinger *et al.*, 2012), which could potentially be promoted by the higher fungal contribution.

Fungi did not use their home-field advantage. The litter inoculum used in this mesocosm experiment was generated using KL litter, which presented a wider C:N ratio than SW. F/B ratios of the KL mesocosms started off second highest. This means that within a response time of only two weeks, fungi from the KL inoculum gained more dominance on the nutrient-rich SW litter than on the 'home-field' litter of KL. SW was also shown to have higher enzyme activities and faster decomposition in general (Keiblinger *et al.*, 2012), which fits to the model that early decomposition is usually N limited (Moorhead & Sinsabaugh, 2006), proposing accelerated decomposition in a N rich site like SW. It seems that the nutrient status of SW litter generally accelerates decomposition and at the same time, favors fungi.

Low nutrient locations were not dominated by fungi. AC and OS locations showed little to almost no change in F/B ratios. These two locations are characterized by wide C:N ratios (around 55-60) and are therefore not very favourable for microbial growth in general, however it was unexpected that fungi did not dominate. Additionally, also the N:P ratio of the AC site was wide. N:P ratios are most likely to determine N or P limitation (Elser *et al.*, 2007) especially early in decomposition, and together with a wide C:N ratio this points to a potential P limitation. According to the growth-rate hypothesis, fast-growing microorganisms have an increased P demand, and this would also point

towards fungal growth. From qPCR and nutrient ratios alone, the answer to why the AC site did not show a stronger fungal dominance remains unanswered.

Metaproteomic data showed similar community shift patterns. The use of unspecific fungal and bacterial primers can only provide information on microbial community structure at a very coarse level of taxonomic resolution. While this method could address more specific questions simply by using different primer sets with the very same DNA samples, it is also possible to link these results with a functional approach. From the same set of samples, F/B protein abundance ratios (the metaproteome) were measured by Lukas Kohl, University of Vienna. These results showed showed very similar patterns: while fungal proteins were dominant on all samples, dominance was most pronounced on SW and KL early harvests, and narrowest ratios were found on AC. The protein- and DNA- based approach both were able to characterize the succession of F/B ratios during this mesocosm decomposition experiment on two levels, with very correlated results.

Temperature stress did not show a huge impact on the microbial community. This experiment aimed at mimicking climate change events, as explained in (Keiblinger *et al.*, 2012), a study using the same litter samples. As assessed by qPCR ratios, neither of the stress temperatures- heat nor frost- did cause an in increase in fungal/bacterial ratio compared to the unstressed condition. These results are backed up by the sister study where the results of temperature stress were emphasized only at the enzyme activitiy level, but to a lesser extent at the microbial community level (Keiblinger *et al.*, 2012) by a metaproteomic approach. Generally, frost stress caused the most pronounced decrease in F/B ratios for all three litter locations at the first sampling after stress. Frost stress was also shown to have a stronger effect on microbial community than heat on a metaproteomic level (Keiblinger *et al.*, 2012). In SW, the location with the initially highest F/B ratio, there was a decrease in F/B ratio at the first sampling after the temperature stress (both heat and frost), which showed a slight overcompensation at the second sampling after heat stress. After 181 days, F/B ratios went back to match the unstressed conditions in SW and KL locations. Only the OS location, where F/B ratios did not change much over the whole duration of the decomposition experiment, F/B ratios stayed at a lower value than the unstressed samples.

4.3 Further development of a phylum-specific rRNA capture technique: the 'PhyloTrap'

Both experimental setups discussed before- the taxonomic identification of native fungal community (4.1), and the detection of microbial community shifts in mesocosms (4.2), were based on the same target molecule: DNA. Therefore it was another goal of this study to further develop the PhyloTrap method ((Böck, 2008),(Keuschnig, 2015)) with labelled rRNA as a target molecule, to have a novel method at hand to study environmental processes in detail. As explained before, this method has the potential to link structure (probe specificity) and function (stable isotope incorporation) in a straightforward way. Stable Isotope Probing (SIP) techniques are very popular in microbial ecology (Radajewski *et al.*, 2000), employing DNA, RNA or PLFA as target molecules. However the only method combining SIP with high phylogenetic resolution has been developed by (MacGregor *et al.*, 2002) using magnetic bead hybridization combined with SIP (termed Mag-SIP). This method has also been developed further to investigate bacterial substrate utilization in marine sediments (Miyatake *et al.*, 2009). To my knowledge, there is no study using this technique with eukaryotic probes, or for terrestrial ecosystems. The first study to combine SIP with metatranscriptomics was able to identify methylotrophy genes from forest soil (Dumont *et al.*, 2006). This shows the potential of SIP- related techniques to shed light on the black box of litter decomposition. The further testing and rRNA yield improvement of the PhyloTrap method with pure-culture RNAs was a main goal in this study, which is a prerequisite for application in environmental samples.

Optimization of the PhyloTrap protocol for the application of locked nucleic acid (LNA) enhanced probes due to hybridization issues. General probes for bacteria and eukaryotes targeting the SSU were enhanced with locked nucleic acids (LNA) and tested with the established PhyloTrap protocol with the goal to increase specific rRNA yield (Campbell & Wengel, 2011) with pure-culture RNAs. Unexpectedly, the new LNA probes did not work as well as expected with the protocol as developed in (Böck, 2008). The eluate showed highly unspecific bindings- not only within the target sample (i.e. bacterial RNA on bacterial probe), but also when bacterial RNA was used on the eukaryotic probe. Changes in the protocol (washing temperature, introduction of stringent washing steps) were able to produce specific elution fractions. Additionally, a blocking step of the beads was introduced as suggested in (MacGregor *et al.*, 2002), and formamide was added during hybridization to increase probe specificity. A thorough analysis of optimal formamide concentration, hybridization temperature and time was

able to produce an optimized Phylotrap protocol using LNA enhanced bacterial and eukaryotic probes.

The PhyloTrap was able to separate fungal and bacterial RNA from a mixed sample. With the optimized protocol, specific rRNA could be recovered both from the target sample, as well as from a mixed sample containing both fungal and bacterial RNA. However, there were still some problems with unspecific hybridization. Unspecific target RNA in the mix caused a 53% loss of specific SSU recovery with the eukaryotic probe, and a 30% decrease of specific target was detected for the bacterial probe. Even though the protocol optimization resulted in a clean target recovery, the hybridization itself was still compromised by competition with unspecific rRNA. A formamide concentration of 15% as opposed to 10% was able to increase the specific yield as shown on the gel. It was also demonstrated that the yield from a single sample could be increased by re-using the supernatant after hybridization for multiple rounds. By RNA quantification, it was shown that a total of 1,8µg bacterial and 0,8 µg fungal SSU RNA could be recovered. The total yield can be calculated at 26% for the bacterial probe, and 11% by the eukaryotic probe.

5 CONCLUSION AND OUTLOOK

With the overall goal of the MICDIF project in mind, 'linking microbial diversity and ecosystem functions', this pioneer study presents insights into the fungal community on Austrian beech litter samples under different nutrient conditions. The employed approach of approach of RFLP typing and clone library sequencing was state-of-the art and suited the project financially back in 2008 when the experiments were conducted, and even though these methods might seem outdated now, our chosen experimental conditions represented the fungal litter community well at earier timepoints within the experiment. We were able to put a name to the dominant Ascomycete species within the highly uneven communities of the four locations. The lack of biological repetitions is an obvious drawback of the native litter study, presenting only a 'snapshot in time' of the fungal community at the four different sampling locations. With newer, improved methods available nowadays, like next generation sequencing (NGS), it would be much easier to work with more samples at the same time. Deeper sequence information with more statistical significance would improve this native litter study tremendously.

The nutrient rich Schottenwald (SW) location exhibiting a very distinct resource stoichiometry was shown to stand out with a completely different fungal community, which is strongly supported by many other studies within the MICDIF framework. Even though our experiments were performed on unsterilized litter, and most of the MICDIF experiments used sterilized an re-inoculated litter, the SW location was still singled out and showed a very specific behaviour. Together with other results generated within MICDIF, the nutrient status of the SW site seems to generally accelerate decomposition and at the same time, favour fungi. This even happened when the same starting community was introduced on the sterilized litter.This highlights that nutrient conditions rather than the initial starting community have the main impact on decomposition.

Taking the MICDIF idea to the next level, this study documents the optimization of a novel method for microbial ecology, aimed at the phylogenetically specific recovery of stable isotope labelled SSU rRNA from environmental RNA samples. This could be the key to the much cited structure-function link by assigning assimilatory activities directly to different phyla. This study showed the recovery of fungal and bacterial rRNA seperately from a mixed sample of pure culture RNA. The use of locked nucleic acid probes (LNAs) was not able to improve the rRNA yield satisfyingly enough to proceed to

downstream analysis by IRMS within this study, which is why tracer incorporation and recovery experiments are not documented yet. The applicability of this method for natural samples is strongly dependent on probe specificity and rRNA yield, which was adressed in a follow-up study: alterations of DNA probe length together with addition of a T-linker increased capture efficiency significantly, and bacterial rRNA recovery from soil RNA was successful (Keuschnig, 2015). Together with the application of stable isotope tracers, this method has the potential to fully disentangle nutrient use pathways in complex nutrient cycles, answering the question who is doing what within ecosystem processes.

6 REFERENCES

Abdo, Z., U.M.E. Schuette, S.J. Bent, C.J. Williams, L.J. Forney & P. Joyce, (2006) Statistical methods for characterizing diversity of microbial communities by analysis of terminal restriction fragment length polymorphisms of 16S rRNA genes. *Environmental microbiology* **8**: 929-938.

Aber, J.D. & J.M. Melillo, (2001) Terrestrial Ecosystems, Second Edition. *Harcourt Academic Press USA*.

Adl, S.M., A.G. Simpson, M.A. Farmer, R.A. Andersen, O.R. Anderson, J.R. Barta, S.S. Bowser, G. Brugerolle, R.A. Fensome, S. Fredericq, T.Y. James, S. Karpov, P. Kugrens, J. Krug, C.E. Lane, L.A. Lewis, J. Lodge, D.H. Lynn, D.G. Mann, R.M. McCourt, L. Mendoza, O. Moestrup, S.E. Mozley-Standridge, T.A. Nerad, C.A. Shearer, A.V. Smirnov, F.W. Spiegel & M.F. Taylor, (2005) The new higher level classification of eukaryotes with emphasis on the taxonomy of protists. *The Journal of eukaryotic microbiology* **52**: 399-451.

Agren, G.I. & F.O. Andersson, (2012) Terrestrial ecosystem ecology: principles and applications. *Cambridge University Press*.

Alberts, B., A. Johnson & J. Lewis, (2002) Molecular Biology of the Cell, 4th Edition. *Garland Science, New York.*

Altschul, S.F., W. Gish, W. Miller, E.W. Myers & D.J. Lipman, (1990) Basic Local Alignment Search Tool. *J Mol Biol* **215**: 403-410.

Amend, A.S., K.L. Matulich & J.B. Martiny, (2015) Nitrogen addition, not initial phylogenetic diversity, increases litter decomposition by fungal communities. *Frontiers in microbiology* **6**: 109.

Andren, O., J. Bengtsson & M. Clarholm, (1995) Biodiversity and species redundancy among litter decomposers. *H.P. Collins, G.P. Robertson & M.J. Klug (eds.): The significance and regulation of soil biodiversity. 141-151, Kluwer Academic Publishers*.

Anthony, R.M., T.J. Brown & G.L. French, (2000) Rapid diagnosis of bacteremia by universal amplification of 23S ribosomal DNA followed by hybridization to an oligonucleotide array. *J Clin Microbiol* **38**: 781-788.

Arcondeguy, T., R. Jack & M. Merrick, (2001) P-II signal transduction proteins, pivotal players in microbial nitrogen control. *Microbiol Mol Biol R* **65**: 80-+.

Baas Becking, L.G.M., (1934) Geobiologie of inleiding tot de milieukunde. *W.P. Van Stockum & Zoon, The Hague, The Netherlands. (in Dutch)*.

Bailey, V.L., J.L. Smith & H. Bolton, (2002) Fungal-to-bacterial ratios in soils investigated for enhanced C sequestration. *Soil Biol Biochem* **34**: 997-1007.

Baker, G. & R. Conrad, (2011) Diversity, structure, and size of N2O-producing microbial communities in soils-what matters for their functioning? *Advances in Applied Microbiology* **75**: 33-70.

Bärlocher, F., (1992) The ecology of aquatic hyphomycetes. *Springer, Berlin*.

Begon, M., R.W. Howarth & C.R. Townsend, (2014) Essentials of Ecology, 4th Edition. *John Wiley & Sons*.

Begon, M., C.R. Townsend & J.L. Harper, (2005) Ecology: From Individuals to Ecosystems, 4th Edition. *Blackwell Science Publishing*.

Benson, D.A., I. Karsch-Mizrachi, D.J. Lipman, J. Ostell & D.L. Wheeler, (2003) GenBank. *Nucleic Acids Res* **31**: 23-27.

Berg, B. & C. Mc Claugherty, (2008) *Plant Litter: Decomposition, Humus Formation, Carbon Sequestration*. Springer, Berlin.

Berg, B. & C. McClaugherty, (2014) Plant Litter: Decomposition, Humus Formation, Carbon Sequestration. 3rd Edition. *Springer, New York*.

Berg, B., K.T. Steffen & C. McClaugherty, (2007) Litter decomposition rate is dependent on litter Mn concentrations. *Biogeochemistry* **82**: 29-39.

Blazewicz, S.J., R.L. Barnard, R.A. Daly & M.K. Firestone, (2013) Evaluating rRNA as an indicator of microbial activity in environmental communities: limitations and uses. *Isme Journal* **7**: 2061-2068.

Böck, S., (2008) Linking fungal Diversity with Function: Development of a species-specific rRNA capturing System. *Diploma thesis, Universität für Bodenkultur Wien*.

Bottomley, P.J. & D.D. Myrold, (2007) Biological N Inputs. *In Paul, Eldor A. (Ed.): Soil Microbiology, Ecology, and Biochemistry, Third Edition. Elsevier Academic Press*.

Brandstatter, C., K. Keiblinger, W. Wanek & S. Zechmeister-Boltenstern, (2013) A closeup study of early beech litter decomposition: potential drivers and microbial interactions on a changing substrate. *Plant Soil* **371**: 139-154.

Bruns, T., (2006) Evolutionary biology: a kingdom revised. *Nature* **443**: 758-761.

Butler, B.J. & R.L. Chazdon, (1998) Species richness, spatial variation, and abundance of the soil seed bank of a secondary tropical rain forest. *Biotropica* **30**: 214-222.

Butterbach-Bahl, K., E.M. Baggs, M. Dannenmann, R. Kiese & S. Zechmeister-Boltenstern, (2013) Nitrous oxide emissions from soils: how well do we understand the processes and their controls? *Philos T R Soc B* **368**.

Campbell, M.A. & J. Wengel, (2011) Locked vs. unlocked nucleic acids (LNA vs. UNA): contrasting structures work towards common therapeutic goals. *Chem Soc Rev* **40**: 5680-5689.

Cavalier-Smith, T., (1998) A revised six-kingdom system of life. *Biological reviews of the Cambridge Philosophical Society* **73**: 203-266.

Cavalier-Smith, T., (2004) Only six kingdoms of life. *Proceedings. Biological sciences / The Royal Society* **271**: 1251-1262.

Census of Marine Life, (2011) How many species on Earth? About 8.7 million, new estimate says. *Science Daily, 24 August 2011.* www.sciencedaily.com/releases/2011/08/110823180459.htm.

Chao, A., (1984) Non parametric estimation of the number of classes in a population. *Scandinavian Journal of Statistics*: 265-270.

Chao, A., (1987a) Estimating the population size for capture-recapture data with unequal catchability. *Biometrics* **43**: 783-791.

Chao, A., (1987b) Estimating the population size for capture-recapture data with unequal catchability. *Biometrics*: 783-791.

Chao, A., N.J. Gotelli, T.C. Hsieh, E.L. Sander, K.H. Ma, R.K. Colwell & A.M. Ellison, (2014) Rarefaction and extrapolation with Hill numbers: a framework for sampling and estimation in species diversity studies. *Ecol Monogr* **84**: 45-67.

Chao, A., L. Jost, S.C. Chiang, Y.H. Jiang & R.L. Chazdon, (2008) A Two-Stage Probabilistic Approach to Multiple-Community Similarity Indices. *Biometrics* **64**: 1178-1186.

Chapin III, F., P. Matson & P. Vitousek, (2011a) Decomposition and Ecosystem Carbon Budgets. *In: Principles of Terrestrial Ecosystem Ecology, Second Edition. Springer, New York*.

Chapin III, F.S., P.A. Matson & H.A. Mooney, (2002) Principles of Terrestrial Ecosystem Ecology. *Springer, New York*.

Chapin III, F.S., P.A. Matson & P. Vitousek, (2011b) Principles of Terrestrial Ecosystem Ecology, Second Edition. *Springer, New York* **2**.

Chauvet, E., J. Cornut, K.R. Sridhar, M.A. Selosse & F. Barlocher, (2016) Beyond the water column: aquatic hyphomycetes outside their preferred habitat. *Fungal Ecol* **19**: 112-127.

Cheng, Q., (2008) Perspectives in biological nitrogen fixation research. *J Integr Plant Biol* **50**: 786-798.

Cleveland, C.C. & D. Liptzin, (2007) C : N : P stoichiometry in soil: is there a "Redfield ratio" for the microbial biomass? *Biogeochemistry* **85**: 235-252.

Colwell, R.K., (2013) EstimateS: statistical estimation of species richness and shared species from samples. Version 9. *User's Guide and application at* http://purl.oclc.org/estimates.

Colwell, R.K., A. Chao, N.J. Gotelli, S.Y. Lin, C.X. Mao, R.L. Chazdon & J.T. Longino, (2012) Models and estimators linking individual-based and sample-based rarefaction, extrapolation and comparison of assemblages. *J Plant Ecol-Uk* **5**: 3-21.

Colwell, R.K. & J.A. Coddington, (1994) Estimating terrestrial biodiversity through extrapolation. *Philosophical transactions of the Royal Society of London. Series B, Biological sciences* **345**: 101-118.

Colwell, R.K. & J.E. Elsensohn, (2014) EstimateS turns 20: statistical estimation of species richness and shared species from samples, with non-parametric extrapolation. *Ecography* **37**: 609-613.

Colwell, R.K., C.X. Mao & J. Chang, (2004) Interpolating, extrapolating, and comparing incidence-based species accumulation curves. *Ecology* **85**: 2717-2727.

Cordier, T., C. Robin, X. Capdevielle, O. Fabreguettes, M.L. Desprez-Loustau & C. Vacher, (2012) The composition of phyllosphere fungal assemblages of European beech (Fagus sylvatica) varies significantly along an elevation gradient. *New Phytol* **196**: 510-519.

Cotgreave, P. & I. Forseth, (2002) Introductory Ecology. *Blackwell Science Publishing*.

Couteaux, M.M., P. Bottner & B. Berg, (1995) Litter Decomposition, Climate and Litter Quality. *Trends in ecology & evolution* **10**: 63-66.

Dämon, W. & I. Krisai-Greilhuber, (2012) Die Datenbank der Pilze Österreichs. *Stapfia*: 245-330.

Dashtban, M., H. Schraft, T.A. Syed & W. Qin, (2010) Fungal biodegradation and enzymatic modification of lignin. *International journal of biochemistry and molecular biology* **1**: 36-50.

De Boer, W. & G.A. Kowalchuk, (2001) Nitrification in acid soils: micro-organisms and mechanisms. *Soil Biol Biochem* **33**: 853-866.

De Gannes, V., G. Eudoxie & W.J. Hickey, (2013) Insights into fungal communities in composts revealed by 454-pyrosequencing: implications for human health and safety. *Frontiers in microbiology* **4**: 164.

Dixon, R. & D. Kahn, (2004) Genetic regulation of biological nitrogen fixation. *Nature reviews. Microbiology* **2**: 621-631.

Dumont, M.G., S.M. Radajewski, C.B. Miguez, I.R. McDonald & J.C. Murrell, (2006) Identification of a complete methane monooxygenase operon from soil by combining stable isotope probing and metagenomic analysis. *Environmental microbiology* **8**: 1240-1250.

Edgar, R.C., (2004) MUSCLE: a multiple sequence alignment method with reduced time and space complexity. *Bmc Bioinformatics* **5**: 1-19.

Elser, J.J., M.E.S. Bracken, E.E. Cleland, D.S. Gruner, W.S. Harpole, H. Hillebrand, J.T. Ngai, E.W. Seabloom, J.B. Shurin & J.E. Smith, (2007) Global analysis of nitrogen and phosphorus limitation of primary producers in freshwater, marine and terrestrial ecosystems. *Ecol Lett* **10**: 1135-1142.

Faith, D.P., C.A. Lozupone, D. Nipperess & R. Knight, (2009) The cladistic basis for the phylogenetic diversity (PD) measure links evolutionary features to environmental gradients and supports broad applications of microbial ecology's "phylogenetic beta diversity" framework. *International journal of molecular sciences* **10**: 4723-4741.

Falkowski, P.G., T. Fenchel & E.F. Delong, (2008) The microbial engines that drive Earth's biogeochemical cycles. *Science* **320**: 1034-1039.

Fanin, N., N. Fromin & I. Bertrand, (2016) Functional breadth and home-field advantage generate functional differences among soil microbial decomposers. *Ecology* **97**: 1023-1037.

Fierer, N., J.A. Jackson, R. Vilgalys & R.B. Jackson, (2005) Assessment of soil microbial community structure by use of taxon-specific quantitative PCR assays. *Applied and environmental microbiology* **71**: 4117-4120.

Forsythe, W.G., M.D. Garrett, C. Hardacre, M. Nieuwenhuyzen & G.N. Sheldrake, (2013) An efficient and flexible synthesis of model lignin oligomers. *Green Chem* **15**: 3031-3038.

Fowler, D., M. Coyle, U. Skiba, M.A. Sutton, J.N. Cape, S. Reis, L.J. Sheppard, A. Jenkins, B. Grizzetti, J.N. Galloway, P. Vitousek, A. Leach, A.F. Bouwman, K. Butterbach-Bahl, F. Dentener, D. Stevenson, M. Amann & M. Voss, (2013) The global nitrogen cycle in the twenty-first century. *Philos T R Soc B* **368**.

Franklin, O., E.K. Hall, C. Kaiser, T.J. Battin & A. Richter, (2011) Optimization of Biomass Composition Explains Microbial Growth-Stoichiometry Relationships. *Am Nat* **177**: E29-E42.

Fujii, T. & N. Takaya, (2008) Denitrification by the fungus Fusarium oxysporum involves NADH-nitrate reductase. *Bioscience, biotechnology, and biochemistry* **72**: 412-420.

Galloway, J.N., J.D. Aber, J.W. Erisman, S.P. Seitzinger, R.W. Howarth, E.B. Cowling & B.J. Cosby, (2003) The nitrogen cascade. *Bioscience* **53**: 341-356.

Galloway, J.N., A.M. Leach, A. Bleeker & J.W. Erisman, (2013) A chronology of human understanding of the nitrogen cycle. *Philosophical transactions of the Royal Society of London. Series B, Biological sciences* **368**: 20130120.

Galloway, J.N. & G.E. Likens, (1981) Acid Precipitation - the Importance of Nitric-Acid. *Atmos Environ* **15**: 1081-1085.

Gardes, M. & T.D. Bruns, (1993) ITS Primers with Enhanced Specificity for Basidiomycetes - Application to the Identification of Mycorrhizae and Rusts. *Mol Ecol* **2**: 113-118.

Gentsch, N., R. Mikutta, O. Shibistova, B. Wild, J. Schnecker, A. Richter, T. Urich, A. Gittel, H. Santruckova, J. Barta, N. Lashchinskiy, C.W. Mueller, R. Fuss & G. Guggenberger, (2015) Properties and bioavailability of particulate and mineral-associated organic matter in Arctic permafrost soils, Lower Kolyma Region, Russia. *Eur J Soil Sci* **66**: 722-734.

Gonczol, J. & A. Revay, (2003) Treehole fungal communities: aquatic, aero-aquatic and dematiaceous hyphomycetes. *Fungal diversity* **12**: 19-34.

Gotelli, N.J. & A. Chao, (2013) Measuring and Estimating Species Richness, Species Diversity, and Biotic Similarity from Sampling Data. *Levin S.A. (Ed.) Encyclopedia of Biodiversity, Second Edition, Volume 5, pp.195-211, Waltham MA: Academic Press*: 195-211.

Gotelli, N.J. & R.K. Colwell, (2010) Estimating species richness. *Magurran A.E. & McGill B.J. (eds.): Biological Diversity: Frontiers in Measurement and Assessment. Chapter 4. Oxford Univ.Press, Oxford UK.*

Groffman, P.M., (2012) Terrestrial denitrification: Challenges and opportunities. *Ecological Processes* **1**: 11.

Guerriero, G., J.F. Hausman, J. Strauss, H. Ertan & K.S. Siddiqui, (2015) Destructuring plant biomass: focus on fungal and extremophilic cell wall hydrolases. *Plant science : an international journal of experimental plant biology* **234**: 180-193.

Gusewell, S. & M.O. Gessner, (2009) N : P ratios influence litter decomposition and colonization by fungi and bacteria in microcosms. *Funct Ecol* **23**: 211-219.

Hagen, J.B., (1996) Robert Whittaker and the Classification of Kingdoms. *Hagen JB, Allchin D, Singer F (Eds.): Doing Biology. Addison Wesley Pub Co Inc*.

Hajibabaei, M., (2012) The golden age of DNA metasystematics. *Trends Genet* **28**: 535-537.

Hall, E.K., K. Besemer, L. Kohl, C. Preiler, K. Riedel, T. Schneider, W. Wanek & T.J. Battin, (2012) Effects of resource chemistry on the composition and function of stream hyporheic biofilms. *Frontiers in microbiology* **3**.

Hall, E.K., F. Maixner, O. Franklin, H. Daims, A. Richter & T. Battin, (2011) Linking Microbial and Ecosystem Ecology Using Ecological Stoichiometry: A Synthesis of Conceptual and Empirical Approaches. *Ecosystems* **14**: 261-273.

Henschler, G., (1988) Analysen im biologischen Material. *VCH Verlagsgesellschaft mbH, Weinheim*.

Hibbett, D.S., M. Binder, J.F. Bischoff, M. Blackwell, P.F. Cannon, O.E. Eriksson, S. Huhndorf, T. James, P.M. Kirk, R. Lucking, H. Thorsten Lumbsch, F. Lutzoni, P.B. Matheny, D.J. McLaughlin, M.J. Powell, S. Redhead, C.L. Schoch, J.W. Spatafora, J.A. Stalpers, R. Vilgalys, M.C. Aime, A. Aptroot, R. Bauer, D. Begerow, G.L. Benny, L.A. Castlebury, P.W. Crous, Y.C. Dai, W. Gams, D.M. Geiser, G.W. Griffith, C. Gueidan, D.L. Hawksworth, G. Hestmark, K. Hosaka, R.A. Humber, K.D. Hyde, J.E. Ironside, U. Koljalg, C.P. Kurtzman, K.H. Larsson, R. Lichtwardt, J. Longcore, J. Miadlikowska, A. Miller, J.M. Moncalvo, S. Mozley-Standridge, F. Oberwinkler, E. Parmasto, V. Reeb, J.D. Rogers, C. Roux, L. Ryvarden, J.P. Sampaio, A. Schussler, J. Sugiyama, R.G. Thorn, L. Tibell, W.A. Untereiner, C. Walker, Z. Wang, A. Weir, M. Weiss, M.M. White, K. Winka, Y.J. Yao & N. Zhang, (2007) A higher-level phylogenetic classification of the Fungi. *Mycological research* **111**: 509-547.

Hill, M.O., (1973) Diversity and Evenness: A Unifying Notation and Its Consequences. *Ecology* **54**: 427-432.

Hirose, D., S. Matsuoka & T. Osono, (2013) Assessment of the fungal diversity and succession of ligninolytic endophytes in Camellia japonica leaves using clone library analysis. *Mycologia* **105**: 837-843.

Hori, C., J. Gaskell, K. Igarashi, M. Samejima, D. Hibbett, B. Henrissat & D. Cullen, (2013) Genomewide analysis of polysaccharides degrading enzymes in 11 white- and brown-rot Polyporales provides insight into mechanisms of wood decay. *Mycologia* **105**: 1412-1427.

Horn, H.S., (1966) Measurement of Overlap in Comparative Ecological Studies. *Am Nat* **100**: 419-&.

Horwath, W., (2007) Carbon Cycling and Formation of Soil Organic Matter. *In Paul, Eldor A. (Ed.): Soil Microbiology, Ecology, and Biochemistry, Third Edition. Elsevier Academic Press*.

Huber, T., G. Faulkner & P. Hugenholtz, (2004) Bellerophon: a program to detect chimeric sequences in multiple sequence alignments. *Bioinformatics* **20**: 2317-2319.

Hudson, H.J., (1968) Ecology of Fungi on Plant Remains above Soil. *New Phytol* **67**: 837-&.

Hughes, J.B., J.J. Hellmann, T.H. Ricketts & B.J. Bohannan, (2001) Counting the uncountable: statistical approaches to estimating microbial diversity. *Applied and environmental microbiology* **67**: 4399-4406.

Hughes, K.W., R.H. Petersen & E.B. Lickey, (2009) Using heterozygosity to estimate a percentage DNA sequence similarity for environmental species' delimitation across basidiomycete fungi. *New Phytol* **182**: 795-798.

Hurlbert, S.H., (1971) Nonconcept of Species Diversity - Critique and Alternative Parameters. *Ecology* **52**: 577-&.

Inselsbacher, E., N. Hinko-Najera Umana, F.C. Stange, M. Gorfer, E. Schuller, K. Ripka, S. Zechmeister-Boltenstern, R. Hood-Novotny, J. Strauss & W. Wanek, (2010) Short-term competition between crop plants and soil microbes for inorganic N fertilizer. *Soil Biol Biochem* **42**: 360-372.

Inselsbacher, E., K. Ripka, S. Klaubauf, D. Fedosoyenko, E. Hackl, M. Gorfer, R. Hood-Novotny, N. Von Wirén, A. Sessitsch, S. Zechmeister-Boltenstern, W. Wanek & J. Strauss, (2009) A cost-effective high-throughput microcosm system for studying nitrogen dynamics at the plant-microbe-soil interface. *Plant Soil* **317**: 293-307.

IPCC, (2014) Summary for Policymakers. *In: Climate Change 2014: Mitigation of Climate Change. Contribution of Working Group III to the Fifth Assessment Report of the Intergovernmental Panel on Climate Change [Edenhofer, O., R. Pichs-Madruga, Y. Sokona, E. Farahani, S. Kadner, K. Seyboth, A. Adler, I. Baum, S. Brunner, P. Eickemeier, B. Kriemann, J. Savolainen, S. Schlömer, C. von Stechow, T. Zwickel and J.C. Minx (eds.)]. Cambridge University Press, Cambridge, United Kingdom and New York, NY, USA.*

Iwamoto, T., K. Tani, K. Nakamura, Y. Suzuki, M. Kitagawa, M. Eguchi & M. Nasu, (2000) Monitoring impact of in situ biostimulation treatment on groundwater bacterial community by DGGE. *FEMS microbiology ecology* **32**: 129-141.

James, T.Y., F. Kauff, C.L. Schoch, P.B. Matheny, V. Hofstetter, C.J. Cox, G. Celio, C. Gueidan, E. Fraker, J. Miadlikowska, H.T. Lumbsch, A. Rauhut, V. Reeb, A.E. Arnold, A. Amtoft, J.E. Stajich, K. Hosaka, G.H. Sung, D. Johnson, B. O'Rourke, M. Crockett,

M. Binder, J.M. Curtis, J.C. Slot, Z. Wang, A.W. Wilson, A. Schussler, J.E. Longcore, K. O'Donnell, S. Mozley-Standridge, D. Porter, P.M. Letcher, M.J. Powell, J.W. Taylor, M.M. White, G.W. Griffith, D.R. Davies, R.A. Humber, J.B. Morton, J. Sugiyama, A.Y. Rossman, J.D. Rogers, D.H. Pfister, D. Hewitt, K. Hansen, S. Hambleton, R.A. Shoemaker, J. Kohlmeyer, B. Volkmann-Kohlmeyer, R.A. Spotts, M. Serdani, P.W. Crous, K.W. Hughes, K. Matsuura, E. Langer, G. Langer, W.A. Untereiner, R. Lucking, B. Budel, D.M. Geiser, A. Aptroot, P. Diederich, I. Schmitt, M. Schultz, R. Yahr, D.S. Hibbett, F. Lutzoni, D.J. McLaughlin, J.W. Spatafora & R. Vilgalys, (2006) Reconstructing the early evolution of Fungi using a six-gene phylogeny. *Nature* **443**: 818-822.

Jan, M.T., P. Roberts, S.K. Tonheim & D.L. Jones, (2009) Protein breakdown represents a major bottleneck in nitrogen cycling in grassland soils. *Soil Biol Biochem* **41**: 2272-2282.

Janna Olmos, J.D. & J. Kargul, (2015) A quest for the artificial leaf. *The international journal of biochemistry & cell biology* **66**: 37-44.

Johnson, J.M.F., A.J. Franzluebbers, S.L. Weyers & D.C. Reicosky, (2007) Agricultural opportunities to mitigate greenhouse gas emissions. *Environ Pollut* **150**: 107-124.

Jones, S.E. & J.T. Lennon, (2010) Dormancy contributes to the maintenance of microbial diversity. *Proceedings of the National Academy of Sciences of the United States of America* **107**: 5881-5886.

Jørgensen, S., (2008) Ecosystem Ecology, 1st Edition. *Elsevier*.

Jost, L., A. Chao & R.L. Chazdon, (2010) Compositional similarity and β (beta) diversity. *Magurran A.E. & McGill B.J. (eds.): Biological Diversity: Frontiers in Measurement and Assessment. Chapter 6. Oxford Univ.Press, Oxford UK.*

Kaiser, C., M. Koranda, B. Kitzler, L. Fuchslueger, J. Schnecker, P. Schweiger, F. Rasche, S. Zechmeister-Boltenstern, A. Sessitsch & A. Richter, (2010) Belowground carbon allocation by trees drives seasonal patterns of extracellular enzyme activities by altering microbial community composition in a beech forest soil. *New Phytol* **187**: 843-858.

Keiblinger, K.M., E.K. Hall, W. Wanek, U. Szukics, I. Hammerle, G. Ellersdorfer, S. Bock, J. Strauss, K. Sterflinger, A. Richter & S. Zechmeister-Boltenstern, (2010) The effect of resource quantity and resource stoichiometry on microbial carbon-use-efficiency. *FEMS microbiology ecology* **73**: 430-440.

Keiblinger, K.M., T. Schneider, B. Roschitzki, E. Schmid, L. Eberl, I. Hammerle, S. Leitner, A. Richter, W. Wanek, K. Riedel & S. Zechmeister-Boltenstern, (2012) Effects of stoichiometry and temperature perturbations on beech leaf litter decomposition, enzyme activities and protein expression. *Biogeosciences* **9**: 4537-4551.

Kellner, H., D.R. Zak & M. Vandenbol, (2010) Fungi Unearthed: Transcripts Encoding Lignocellulolytic and Chitinolytic Enzymes in Forest Soil. *PloS one* **5**.

Keuschnig, C., (2015) PhyloTrap - Separate Capture of Bacterial and Fungal Small Subunit Ribosomal RNAs using Magnetic Beads. *Diploma thesis, Universität für Bodenkultur Wien*.

Kindt, R. & R. Coe, (2005) Tree diversity analysis. A manual and software for common statistical methods for ecological and biodiversity studies. *World Agroforestry Centre (ICRAF), Nairobi, Kenya*.

Kitzler, B., S. Zechmeister-Boltenstern, C. Holtermann, U. Skiba & K. Butterbach-Bahl, (2006) Nitrogen oxides emission from two beech forests subjected to different nitrogen loads. *Biogeosciences* **3**: 293-310.

Klaubauf, S., E. Inselsbacher, S. Zechmeister-Boltenstern, W. Wanek, R. Gottsberger, J. Strauss & M. Gorfer, (2010a) Molecular diversity of fungal communities in agricultural soils from Lower Austria. *Fungal Divers.* **44**: 65-75.

Klaubauf, S., E. Inselsbacher, S. Zechmeister-Boltenstern, W. Wanek, R. Gottsberger, J. Strauss & M. Gorfer, (2010b) Molecular diversity of fungal communities in agricultural soils from Lower Austria. *Fungal diversity* **44**: 65-75.

Kobayashi, M., Y. Matsuo, A. Takimoto, S. Suzuki, F. Maruo & H. Shoun, (1996) Denitrification, a novel type of respiratory metabolism in fungal mitochondrion. *J Biol Chem* **271**: 16263-16267.

Kögel-Knabner, I., (2002) The macromolecular organic composition of plant and microbial residues as inputs to soil organic matter. *Soil Biol Biochem*: 139-162.

Kohl, L., (2011) High molecular weight compounds in beech litter decomposition. *Diploma thesis, University of Vienna.*

Koops, H.P. & A. Pommerening-Roser, (2001) Distribution and ecophysiology of the nitrifying bacteria emphasizing cultured species. *FEMS microbiology ecology* **37**: 1-9.

Koranda, M., J. Schnecker, C. Kaiser, L. Fuchslueger, B. Kitzler, C.F. Stange, A. Sessitsch, S. Zechmeister-Boltenstern & A. Richter, (2011) Microbial processes and community composition in the rhizosphere of European beech - The influence of plant C exudates. *Soil Biol Biochem* **43**: 551-558.

Koshkin, A.A., S.K. Singh, P. Nielsen, V.K. Rajwanshi, R. Kumar, M. Meldgaard, C.E. Olsen & J. Wengel, (1998) LNA (Locked Nucleic Acids): Synthesis of the adenine, cytosine, guanine, 5-methylcytosine, thymine and uracil bicyclonucleoside monomers, oligomerisation, and unprecedented nucleic acid recognition. *Tetrahedron* **54**: 3607-3630.

Krivtsov, V., (2008) Indirect Effects in Ecology. *Jørgensen, SE (Ed.): Fundamental Laws in Ecology, 1st Edition. Elsevier*.

Lal, R., (2004) Soil carbon sequestration to mitigate climate change. *Geoderma* **123**: 1-22.

Lam, H.M., K.T. Coschigano, I.C. Oliveira, R. MeloOliveira & G.M. Coruzzi, (1996) The molecular-genetics of nitrogen assimilation into amino acids in higher plants. *Annu Rev Plant Phys* **47**: 569-593.

Laughlin, R.J. & R.J. Stevens, (2002) Evidence for fungal dominance of denitrification and codenitrification in a grassland soil. *Soil Sci Soc Am J* **66**: 1540-1548.

Leigh, J.A., (2000) Nitrogen fixation in methanogens: the archaeal perspective. *Current issues in molecular biology* **2**: 125-131.

Leitner, S., W. Wanek, B. Wild, I. Haemmerle, L. Kohl, K.M. Keiblinger, S. Zechmeister-Boltenstern & A. Richter, (2012) Influence of litter chemistry and stoichiometry on glucan depolymerization during decomposition of beech (Fagus sylvatica L.) litter. *Soil Biol Biochem* **50**: 174-187.

Li, W.J., J.K. Liu, D.J. Bhat, E. Camporesi, D.Q. Dai, P.E. Mortimer, J.C. Xu, K.D. Hyde & P. Chomnunti, (2015) Molecular phylogenetic analysis reveals two new species of Discosia from Italy. *Phytotaxa* **203**: 37-46.

Liebig, J.v., (1840) Liebigs law of the minimum. *In: Michael Allaby: A Dictionary of Ecology (2004), Retrieved August 18, 2015 from* http://www.encyclopedia.com/doc/1O14-Liebigslawoftheminimum.html.

Lindeman, R.L., (1942) The trophic-dynamic aspect of ecology. *Ecology* **23**: 399-418.

Lonsdale, D., M. Pautasso & O. Holdenrieder, (2008) Wood-decaying fungi in the forest: conservation needs and management options. *Eur J Forest Res* **127**: 1-22.

Loy, A., F. Maixner, M. Wagner & M. Horn, (2007) probeBase - an online resource for rRNA-targeted oligonucleotide probes: new features 2007. *Nucleic Acids Res* **35**: D800-D804.

Lozupone, C., M. Hamady & R. Knight, (2006) UniFrac - An online tool for comparing microbial community diversity in a phylogenetic context. *Bmc Bioinformatics* **7**.

Lundell, T.K., M.R. Makela & K. Hilden, (2010) Lignin-modifying enzymes in filamentous basidiomycetes--ecological, functional and phylogenetic review. *Journal of basic microbiology* **50**: 5-20.

Luyssaert, S., E.D. Schulze, A. Borner, A. Knohl, D. Hessenmoller, B.E. Law, P. Ciais & J. Grace, (2008) Old-growth forests as global carbon sinks. *Nature* **455**: 213-215.

Lynch, M.D.J. & J.D. Neufeld, (2015) Ecology and exploration of the rare biosphere. *Nature Reviews Microbiology* **13**: 217-229.

Ma, W.K., R.E. Farrell & S.D. Siciliano, (2008) Soil Formate Regulates the Fungal Nitrous Oxide Emission Pathway. *Applied and environmental microbiology* **74**: 6690-6696.

MacGregor, B.J., V. Bruchert, S. Fleischer & R. Amann, (2002) Isolation of small-subunit rRNA for stable isotopic characterization. *Environmental microbiology* **4**: 451-464.

Makela, M.R., N. Donofrio & R.P. de Vries, (2014) Plant biomass degradation by fungi. *Fungal genetics and biology : FG & B* **72**: 2-9.

Martin, K.J. & P.T. Rygiewicz, (2005) Fungal-specific PCR primers developed for analysis of the ITS region of environmental DNA extracts. *Bmc Microbiol* **5**.

Martinez-Argudo, I., R. Little, N. Shearer, P. Johnson & R. Dixon, (2004) The NifL-NifA system: a multidomain transcriptional regulatory complex that integrates environmental signals. *J Bacteriol* **186**: 601-610.

Martinez, D., R.M. Berka, B. Henrissat, M. Saloheimo, M. Arvas, S.E. Baker, J. Chapman, O. Chertkov, P.M. Coutinho, D. Cullen, E.G. Danchin, I.V. Grigoriev, P. Harris, M. Jackson, C.P. Kubicek, C.S. Han, I. Ho, L.F. Larrondo, A.L. de Leon, J.K. Magnuson, S. Merino, M. Misra, B. Nelson, N. Putnam, B. Robbertse, A.A. Salamov, M. Schmoll, A. Terry, N. Thayer, A. Westerholm-Parvinen, C.L. Schoch, J. Yao, R. Barabote, M.A. Nelson, C. Detter, D. Bruce, C.R. Kuske, G. Xie, P. Richardson, D.S. Rokhsar, S.M. Lucas, E.M. Rubin, N. Dunn-Coleman, M. Ward & T.S. Brettin, (2008) Genome sequencing and analysis of the biomass-degrading fungus Trichoderma reesei (syn. Hypocrea jecorina). *Nature biotechnology* **26**: 553-560.

Martinez, D., J. Challacombe, I. Morgenstern, D. Hibbett, M. Schmoll, C.P. Kubicek, P. Ferreira, F.J. Ruiz-Duenas, A.T. Martinez, P. Kersten, K.E. Hammel, A. Vanden Wymelenberg, J. Gaskell, E. Lindquist, G. Sabat, S.S. Bondurant, L.F. Larrondo, P. Canessa, R. Vicuna, J. Yadav, H. Doddapaneni, V. Subramanian, A.G. Pisabarro, J.L. Lavin, J.A. Oguiza, E. Master, B. Henrissat, P.M. Coutinho, P. Harris, J.K. Magnuson, S.E. Baker, K. Bruno, W. Kenealy, P.J. Hoegger, U. Kues, P. Ramaiya, S. Lucas, A. Salamov, H. Shapiro, H. Tu, C.L. Chee, M. Misra, G. Xie, S. Teter, D. Yaver, T. James, M. Mokrejs, M. Pospisek, I.V. Grigoriev, T. Brettin, D. Rokhsar, R. Berka & D. Cullen, (2009) Genome, transcriptome, and secretome analysis of wood decay fungus Postia placenta supports unique mechanisms of lignocellulose conversion. *Proceedings of the National Academy of Sciences of the United States of America* **106**: 1954-1959.

Martinez, D., L.F. Larrondo, N. Putnam, M.D. Gelpke, K. Huang, J. Chapman, K.G. Helfenbein, P. Ramaiya, J.C. Detter, F. Larimer, P.M. Coutinho, B. Henrissat, R. Berka, D. Cullen & D. Rokhsar, (2004) Genome sequence of the lignocellulose degrading fungus Phanerochaete chrysosporium strain RP78. *Nature biotechnology* **22**: 695-700.

Maurer, B.A. & B.J. McGill, (2010) Measurement of species diversity. *Magurran A.E. & McGill B.J. (eds.): Biological Diversity: Frontiers in Measurement and Assessment. Chapter 5. Oxford Univ.Press, Oxford UK*.

McClain, M.E., E.W. Boyer, C.L. Dent, S.E. Gergel, N.B. Grimm, P.M. Groffman, S.C. Hart, J.W. Harvey, C.A. Johnston, E. Mayorga, W.H. McDowell & G. Pinay, (2003) Biogeochemical hot spots and hot moments at the interface of terrestrial and aquatic ecosystems. *Ecosystems* **6**: 301-312.

McLaughlin, D.J., D.S. Hibbett, F. Lutzoni, J.W. Spatafora & R. Vilgalys, (2009) The search for the fungal tree of life. *Trends in microbiology* **17**: 488-497.

Merrick, M.J. & R.A. Edwards, (1995) Nitrogen Control in Bacteria. *Microbiol Rev* **59**: 604-&.

Miyatake, T., B.J. MacGregor & H.T.S. Boschker, (2009) Linking Microbial Community Function to Phylogeny of Sulfate-Reducing Deltaproteobacteria in Marine Sediments by Combining Stable Isotope Probing with Magnetic-Bead Capture Hybridization of 16S rRNA. *Applied and environmental microbiology* **75**: 4927-4935.

Moorhead, D.L. & R.L. Sinsabaugh, (2006) A theoretical model of litter decay and microbial interaction. *Ecol Monogr* **76**: 151-174.

Mooshammer, M., W. Wanek, I. Hammerle, L. Fuchslueger, F. Hofhansl, A. Knoltsch, J. Schnecker, M. Takriti, M. Watzka, B. Wild, K.M. Keiblinger, S. Zechmeister-Boltenstern & A. Richter, (2014a) Adjustment of microbial nitrogen use efficiency to carbon: nitrogen imbalances regulates soil nitrogen cycling. *Nat Commun* **5**.

Mooshammer, M., W. Wanek, J. Schnecker, B. Wild, S. Leitner, F. Hofhansl, A. Blochl, I. Hammerle, A.H. Frank, L. Fuchslueger, K.M. Keiblinger, S. Zechmeister-Boltenstern & A. Richter, (2012) Stoichiometric controls of nitrogen and phosphorus cycling in decomposing beech leaf litter. *Ecology* **93**: 770-782.

Mooshammer, M., W. Wanek, S. Zechmeister-Boltenstern & A. Richter, (2014b) Stoichiometric imbalances between terrestrial decomposer communities and their resources: mechanisms and implications of microbial adaptations to their resources. *Frontiers in microbiology* **5**.

Mora, C., D.P. Tittensor, S. Adl, A.G. Simpson & B. Worm, (2011) How many species are there on Earth and in the ocean? *PLoS biology* **9**: e1001127.

Morris, S.J. & C.B. Blackwood, (2007) The Ecology of Soil Organisms. *in Paul, Eldor A. (Ed.): Soil Microbiology, Ecology, and Biochemistry, Third Edition. Elsevier Academic Press*.

Morris, S.J. & C.B. Blackwood, (2014) The Ecology of the Soil Biota and their Function. *In Paul, Eldor A. (Ed.): Soil Microbiology, Ecology, and Biochemistry, Fourth Edition. Elsevier Academic Press*.

Nakahara, K., T. Tanimoto, K. Hatano, K. Usuda & H. Shoun, (1993) Cytochrome-P-450-55a1 (P-450dnir) Acts as Nitric-Oxide Reductase Employing Nadh as the Direct Electron-Donor. *J Biol Chem* **268**: 8350-8355.

Nelson, M.S. & M.J. Sadowsky, (2015) Secretion systems and signal exchange between nitrogen-fixing rhizobia and legumes. *Front Plant Sci* **6**.

Nikoh, N., N. Hayase, N. Iwabe, K. Kuma & T. Miyata, (1994) Phylogenetic relationship of the kingdoms Animalia, Plantae, and Fungi, inferred from 23 different protein species. *Molecular biology and evolution* **11**: 762-768.

Nilsson, T., G. Daniel, T.K. Kirk & J.R. Obst, (1989) Chemistry and Microscopy of Wood Decay by Some Higher Ascomycetes. *Holzforschung* **43**: 11-18.

Nomura, M., R. Gourse & G. Baughman, (1984) Regulation of the Synthesis of Ribosomes and Ribosomal Components. *Annu Rev Biochem* **53**: 75-117.

Osono, T., (2006) Role of phyllosphere fungi of forest trees in the development of decomposer fungal communities and decomposition processes of leaf litter. *Can J Microbiol* **52**: 701-716.

Osono, T., (2007) Ecology of ligninolytic fungi associated with leaf litter decomposition. *Ecol Res* **22**: 955-974.

Osono, T. & H. Takeda, (2006) Fungal decomposition of Abies needle and Betula leaf litter. *Mycologia* **98**: 172-179.

Paul, E.A., H.P. Collins & S.W. Leavitt, (2001) Dynamics of resistant soil carbon of midwestern agricultural soils measured by naturally occurring C-14 abundance. *Geoderma* **104**: 239-256.

Paustian, K. & J. Schnurer, (1987) Fungal Growth-Response to Carbon and Nitrogen Limitation - a Theoretical-Model. *Soil Biol Biochem* **19**: 613-620.

Pedros-Alio, C., (2006) Marine microbial diversity: can it be determined? *Trends in microbiology* **14**: 257-263.

Peet, R.K., (1974) The measurement of species diversity. *Annual Review of Ecology and Systematics* **5**: 285-307.

Porter, T.M., C.W. Schadt, L. Rizvi, A.P. Martin, S.K. Schmidt, L. Scott-Denton, R. Vilgalys & J.M. Moncalvo, (2008) Widespread occurrence and phylogenetic placement of a soil clone group adds a prominent new branch to the fungal tree of life. *Molecular phylogenetics and evolution* **46**: 635-644.

Radajewski, S., P. Ineson, N.R. Parekh & J.C. Murrell, (2000) Stable-isotope probing as a tool in microbial ecology. *Nature* **403**: 646-649.

Ramette, A., (2007) Multivariate analyses in microbial ecology. *FEMS microbiology ecology* **62**: 142-160.

Rayner, A.D.M. & L. Boddy, (1988) Fungal decomposition of wood: It's biology and ecology. *John Wiley & Sons*.

Redfield, A., (1934) On the proportions of organic derivations in sea water and their relation to the composition of plankton. *James Johnstone Memorial Volume, Editor: R.Daniel, Publisher: University Press of Liverpool*.

Reinhold-Hurek, B. & T. Hurek, (1998) Life in grasses: diazotrophic endophytes. *Trends in microbiology* **6**: 139-144.

Reznick, D., M.J. Bryant & F. Bashey, (2002) r- and K-selection revisited: The role of population regulation in life-history evolution. *Ecology* **83**: 1509-1520.

Richter, A., (2006) MICDIF project proposal. www.micdif.net.

Riley, R., A.A. Salamov, D.W. Brown, L.G. Nagy, D. Floudas, B.W. Held, A. Levasseur, V. Lombard, E. Morin, R. Otillar, E.A. Lindquist, H. Sun, K.M. LaButti, J. Schmutz, D. Jabbour, H. Luo, S.E. Baker, A.G. Pisabarro, J.D. Walton, R.A. Blanchette, B. Henrissat, F. Martin, D. Cullen, D.S. Hibbett & I.V. Grigoriev, (2014) Extensive

sampling of basidiomycete genomes demonstrates inadequacy of the white-rot/brown-rot paradigm for wood decay fungi. *Proceedings of the National Academy of Sciences of the United States of America* **111**: 9923-9928.

Robertson, G. & P. Groffman, (2007) Nitrogen Transformations. *In Paul, Eldor A. (Ed.): Soil Microbiology, Ecology, and Biochemistry, Third Edition. Elsevier Academic Press*.

Robertson, G. & P. Groffman, (2015) Nitrogen transformations. *in Paul, Eldor A. (Ed.): Soil Microbiology, Ecology, and Biochemistry, Fourth Edition. Elsevier Academic Press*.

Rosling, A., F. Cox, K. Cruz-Martinez, K. Ihrmark, G.A. Grelet, B.D. Lindahl, A. Menkis & T.Y. James, (2011) Archaeorhizomycetes: Unearthing an Ancient Class of Ubiquitous Soil Fungi. *Science* **333**: 876-879.

Ruggiero, M.A., D.P. Gordon, T.M. Orrell, N. Bailly, T. Bourgoin, R.C. Brusca, T. Cavalier-Smith, M.D. Guiry & P.M. Kirk, (2015) A higher level classification of all living organisms. *PloS one* **10**: e0119248.

Sagar, R. & G. Sharma, (2012) Measurement of alpha diversity using Simpson index (1/D): the jeopardy. *Environmental Sceptics and Critics* **1**: 23-24.

Sala, O.E., F.S. Chapin, 3rd, J.J. Armesto, E. Berlow, J. Bloomfield, R. Dirzo, E. Huber-Sanwald, L.F. Huenneke, R.B. Jackson, A. Kinzig, R. Leemans, D.M. Lodge, H.A. Mooney, M. Oesterheld, N.L. Poff, M.T. Sykes, B.H. Walker, M. Walker & D.H. Wall, (2000) Global biodiversity scenarios for the year 2100. *Science* **287**: 1770-1774.

Schadauer, K., R. Büchsenmeister & H. Schodterer, (2006) Aktuelle und potenzielle Verbreitung der Buche in Österreich. *BFW-Praxisinformation*: 8-9.

Schimel, J.P. & J. Bennett, (2004) Nitrogen mineralization: Challenges of a changing paradigm. *Ecology* **85**: 591-602.

Schmalenberger, A., F. Schwieger & C.C. Tebbe, (2001) Effect of primers hybridizing to Different evolutionarily conserved regions of the small-subunit rRNA gene in PCR-based microbial community analyses and genetic profiling. *Applied and environmental microbiology* **67**: 3557-3563.

Schneider, T., B. Gerrits, R. Gassmann, E. Schmid, M.O. Gessner, A. Richter, T. Battin, L. Eberl & K. Riedel, (2010) Proteome analysis of fungal and bacterial involvement in leaf litter decomposition. *Proteomics* **10**: 1819-1830.

Schneider, T., K.M. Keiblinger, E. Schmid, K. Sterflinger-Gleixner, G. Ellersdorfer, B. Roschitzki, A. Richter, L. Eberl, S. Zechmeister-Boltenstern & K. Riedel, (2012) Who is who in litter decomposition? Metaproteomics reveals major microbial players and their biogeochemical functions. *The ISME journal* **6**: 1749-1762.

Schoch, C.L., K.A. Seifert, S. Huhndorf, V. Robert, J.L. Spouge, C.A. Levesque, W. Chen, E. Bolchacova, K. Voigt, P.W. Crous, A.N. Miller, M.J. Wingfield, M.C. Aime, K.D. An, F.Y. Bai, R.W. Barreto, D. Begerow, M.J. Bergeron, M. Blackwell, T. Boekhout, M. Bogale, N. Boonyuen, A.R. Burgaz, B. Buyck, L. Cai, Q. Cai, G. Cardinali, P. Chaverri, B.J. Coppins, A. Crespo, P. Cubas, C. Cummings, U. Damm, Z.W. de Beer, G.S. de Hoog, R. Del-Prado, D. B, J. Dieguez-Uribeondo, P.K. Divakar, B. Douglas, M. Duenas, T.A. Duong, U. Eberhardt, J.E. Edwards, M.S. Elshahed, K. Fliegerova, M. Furtado, M.A. Garcia, Z.W. Ge, G.W. Griffith, K. Griffiths, J.Z. Groenewald, M. Groenewald, M. Grube, M. Gryzenhout, L.D. Guo, F. Hagen, S. Hambleton, R.C. Hamelin, K. Hansen, P. Harrold, G. Heller, G. Herrera, K. Hirayama, Y. Hirooka, H.M. Ho, K. Hoffmann, V. Hofstetter, F. Hognabba, P.M. Hollingsworth, S.B. Hong, K. Hosaka, J. Houbraken, K. Hughes, S. Huhtinen, K.D. Hyde, T. James,

E.M. Johnson, J.E. Johnson, P.R. Johnston, E.B. Jones, L.J. Kelly, P.M. Kirk, D.G. Knapp, U. Koljalg, K. GM, C.P. Kurtzman, S. Landvik, S.D. Leavitt, A.S. Liggenstoffer, K. Liimatainen, L. Lombard, J.J. Luangsa-Ard, H.T. Lumbsch, H. Maganti, S.S. Maharachchikumbura, M.P. Martin, T.W. May, A.R. McTaggart, A.S. Methven*, et al.*, (2012) Nuclear ribosomal internal transcribed spacer (ITS) region as a universal DNA barcode marker for Fungi. *Proceedings of the National Academy of Sciences of the United States of America* **109**: 6241-6246.

Schulten, H.R. & M. Schnitzer, (1997) The chemistry of soil organic nitrogen: a review. *Biol Fert Soils* **26**: 1-15.

Seena, S. & S. Monroy, (2016) Preliminary insights into the evolutionary relationships of aquatic hyphomycetes and endophytic fungi. *Fungal Ecol* **19**: 128-134.

Shannon, C. & W. Weaver, (1949) The Mathematical Theory of Communication. *University of Illinois Press, Urbana USA*.

Shoun, H., S. Fushinobu, L. Jiang, S.W. Kim & T. Wakagi, (2012) Fungal denitrification and nitric oxide reductase cytochrome P450nor. *Philos T R Soc B* **367**: 1186-1194.

Shoun, H. & T. Tanimoto, (1991) Denitrification by the Fungus Fusarium-Oxysporum and Involvement of Cytochrome-P-450 in the Respiratory Nitrite Reduction. *J Biol Chem* **266**: 11078-11082.

Silver, W.L., D.J. Herman & M.K. Firestone, (2001) Dissimilatory nitrate reduction to ammonium in upland tropical forest soils. *Ecology* **82**: 2410-2416.

Simpson, E.H., (1949) Measurement of Diversity. *Nature* **163**: 688-688.

Sinsabaugh, R.L., C.L. Lauber, M.N. Weintraub, B. Ahmed, S.D. Allison, C. Crenshaw, A.R. Contosta, D. Cusack, S. Frey, M.E. Gallo, T.B. Gartner, S.E. Hobbie, K. Holland, B.L. Keeler, J.S. Powers, M. Stursova, C. Takacs-Vesbach, M.P. Waldrop, M.D. Wallenstein, D.R. Zak & L.H. Zeglin, (2008) Stoichiometry of soil enzyme activity at global scale. *Ecol Lett* **11**: 1252-1264.

Snajdr, J., T. Cajthaml, V. Valaskova, V. Merhautova, M. Petrankova, P. Spetz, K. Leppanen & P. Baldrian, (2011) Transformation of Quercus petraea litter: successive changes in litter chemistry are reflected in differential enzyme activity and changes in the microbial community composition. *FEMS microbiology ecology* **75**: 291-303.

Sterner, R. & J. Elser, (2002) Ecological Stoichiometry:The Biology of Elements from Molecules to the Biosphere. *Princeton University Press*.

Strickland, M.S., C. Lauber, N. Fierer & M.A. Bradford, (2009) Testing the functional significance of microbial community composition. *Ecology* **90**: 441-451.

Sutton, B.C., (1980) The Coelomycetes. Fungi imperfecti with pycnidia, acervuli and stromata. *Commonwealth Mycological Institute, Kew UK*.

Svistoonoff, S., V. Hocher & H. Gherbi, (2014) Actinorhizal root nodule symbioses: what is signalling telling on the origins of nodulation? *Current opinion in plant biology* **20**: 11-18.

Takaya, N., (2009) Response to Hypoxia, Reduction of Electron Acceptors, and Subsequent Survival by Filamentous Fungi. *Biosci Biotech Bioch* **73**: 1-8.

Takaya, N., S. Kuwazaki, Y. Adachi, S. Suzuki, T. Kikuchi, H. Nakamura, Y. Shiro & H. Shoun, (2003) Hybrid respiration in the denitrifying mitochondria of Fusarium oxysporum. *J Biochem* **133**: 461-465.

Talbot, J.M. & K.K. Treseder, (2012) Interactions among lignin, cellulose, and nitrogen drive litter chemistry-decay relationships. *Ecology* **93**: 345-354.

Tamura, K., D. Peterson, N. Peterson, G. Stecher, M. Nei & S. Kumar, (2011) MEGA5: Molecular Evolutionary Genetics Analysis Using Maximum Likelihood, Evolutionary Distance, and Maximum Parsimony Methods. *Molecular biology and evolution* **28**: 2731-2739.

Tansley, A.G., (1935) The use and abuse of vegetational concepts and terms. *Ecology* **16**: 284-307.

Taylor, D.L. & T.D. Bruns, (1999) Community structure of ectomycorrhizal fungi in a *Pinus muricata* forest: minimal overlap between the mature forest and resistant propagule communities. *Mol. Ecol.* **8**: 1837-1850.

Tielens, A.G.M., C. Rotte, J.J. van Hellemond & W. Martin, (2002) Mitochondria as we don't know them. *Trends Biochem Sci* **27**: 564-572.

Underhill, D.M. & L.D. Lliev, (2014) The mycobiota: interactions between commensal fungi and the host immune system. *Nat Rev Immunol* **14**: 405-416.

Unterseher, M., D. Persoh & M. Schnittler, (2013) Leaf-inhabiting endophytic fungi of European Beech (Fagus sylvatica L.) co-occur in leaf litter but are rare on decaying wood of the same host. *Fungal diversity* **60**: 43-54.

Urban, A., M. Puschenreiter, J. Strauss & M. Gorfer, (2008) Diversity and structure of ectomycorrhizal and co-associated fungal communities in a serpentine soil. *Mycorrhiza* **18**: 339-354.

Vane-Wright, R., C. Humphries & P. Williams, (1991) What to protect: Systematics and the agony of choice. *Biological Conservation* **55**: 235-254.

Vitousek, P.M., J.D. Aber, R.W. Howarth, G.E. Likens, P.A. Matson, D.W. Schindler, W.H. Schlesinger & D. Tilman, (1997) Human alteration of the global nitrogen cycle: Sources and consequences. *Ecol Appl* **7**: 737-750.

Voriskova, J. & P. Baldrian, (2013) Fungal community on decomposing leaf litter undergoes rapid successional changes. *Isme Journal* **7**: 477-486.

Wanek, W., M. Mooshammer, A. Blochl, A. Hanreich, K. Keiblinger, S. Zechmeister-Boltenstern & A. Richter, (2011) Determination of gross rates of amino acid production and immobilization in decomposing leaf litter by a novel N-15 isotope pool dilution technique (vol 42, pg 1293, 2010). *Soil Biol Biochem* **43**: 221-221.

Wanek, W., M. Mooshammer, A. Blochl, A. Hanreich & A. Richter, (2010) Determination of gross rates of amino acid production and immobilization in decomposing leaf litter by a novel N-15 isotope pool dilution technique. *Soil Biol Biochem* **42**: 1293-1302.

Wardle, D.A. & P. Lavelle, (1997) Linkages between Soil Biota, Plant Litter Quality and Decomposition. *in: Cadisch, G. and Giller, K.E. (Eds.): Driven by Nature: Plant Litter Quality and Decomposition. CAB International*.

White, T., T. Bruns, S. Lee & J. Taylor, (1990a) Amplification and direct sequencing of fungal ribosomal RNA genes for phylogenetics. . *In: PCR Protocols: a guide to methods and applications (Innis MA, Gelfand DH, Sninsky JJ, White TJ, eds), Academic Press, New York,USA*: 315–322.

White, T.J., T.D. Bruns, S. Lee & J.W. Taylor, (1990b) Amplification and direct sequencing of fungal ribosomal RNA genes for phylogenetics. *M.A. Innis, D.H. Gelfand, J.Sninsky, T.J. White (Eds.): PCR Protocols: a Guide to Methods and Applications. Academic Press, San Diego.*

Whittaker, R.H., (1969) New concepts of kingdoms or organisms. Evolutionary relations are better represented by new classifications than by the traditional two kingdoms. *Science* **163**: 150-160.

Whittaker, R.H., (1972) Evolution and measurement of species diversity. *Taxon*: 213-251.

Wijayawardene, N.N., P.W. Crous, P.M. Kirk, D.L. Hawksworth, S. Boonmee, U. Braun, D.Q. Dai, M.J. D'souza, P. Diederich, A. Dissanayake, M. Doilom, S. Hongsanan, E.B.G. Jones, J.Z. Groenewald, R. Jayawardena, J.D. Lawrey, J.K. Liu, R. Lucking, H. Madrid, D.S. Manamgoda, L. Muggia, M.P. Nelsen, R. Phookamsak, S. Suetrong, K. Tanaka, K.M. Thambugala, D.N. Wanasinghe, S. Wikee, Y. Zhang, A. Aptroot, H.A. Ariyawansa, A.H. Bahkali, D.J. Bhat, C. Gueidan, P. Chomnunti, G.S. De Hoog, K. Knudsen, W.J. Li, E.H.C. McKenzie, A.N. Miller, A.J.L. Phillips, M. Piatek, H.A. Raja, R.S. Shivas, B. Slippers, J.E. Taylor, Q. Tian, Y. Wang, J.H.C. Woudenberg, L. Cai, W.M. Jaklitsch & K.D. Hyde, (2014) Naming and outline of Dothideomycetes-2014 including proposals for the protection or suppression of generic names. *Fungal diversity* **69**: 1-55.

Williams, T.A., P.G. Foster, C.J. Cox & T.M. Embley, (2013) An archaeal origin of eukaryotes supports only two primary domains of life. *Nature* **504**: 231-236.

Wingfield, M.J., Z.W. De Beer, B. Slippers, B.D. Wingfield, J.Z. Groenewald, L. Lombard & P.W. Crous, (2012) One fungus, one name promotes progressive plant pathology. *Mol Plant Pathol* **13**: 604-613.

Woese, C.R., O. Kandler & M.L. Wheelis, (1990) Towards a natural system of organisms: proposal for the domains Archaea, Bacteria, and Eucarya. *Proceedings of the National Academy of Sciences of the United States of America* **87**: 4576-4579.

Wuczkowski, M., E. Metzger, K. Sterflinger & H. Prillinger, (2005) Diversity of yeasts isolated from litter and soil of different natural forest sites in Austria. *Die Bodenkultur* **56**: 201-208.

Xu, J., (2006) Fundamentals of fungal molecular population genetic analyses. *Current issues in molecular biology* **8**: 75-89.

Zechmeister-Boltenstern, S., K.M. Keiblinger, M. Mooshammer, J. Penuelas, A. Richter, J. Sardans & W. Wanek, (2015) The application of ecological stoichiometry to plant-microbial-soil organic matter transformations. *Ecol Monogr* **85**: 133-155.

Zhang, Y., C.L. Schoch, J. Fournier, P.W. Crous, J. de Gruyter, J.H.C. Woudenberg, K. Hirayama, K. Tanaka, S.B. Pointing, J.W. Spatafora & K.D. Hyde, (2009) Multi-locus phylogeny of Pleosporales: a taxonomic, ecological and evolutionary re-evaluation. *Stud Mycol*: 85-102.

Zumft, W.G., (1997) Cell biology and molecular basis of denitrification. *Microbiol Mol Biol R* **61**: 533-+.

7 SUPPLEMENTARY MATERIAL

Gel pictures of RFLP analyses (see 3.1)

ACHENKIRCH 0 days

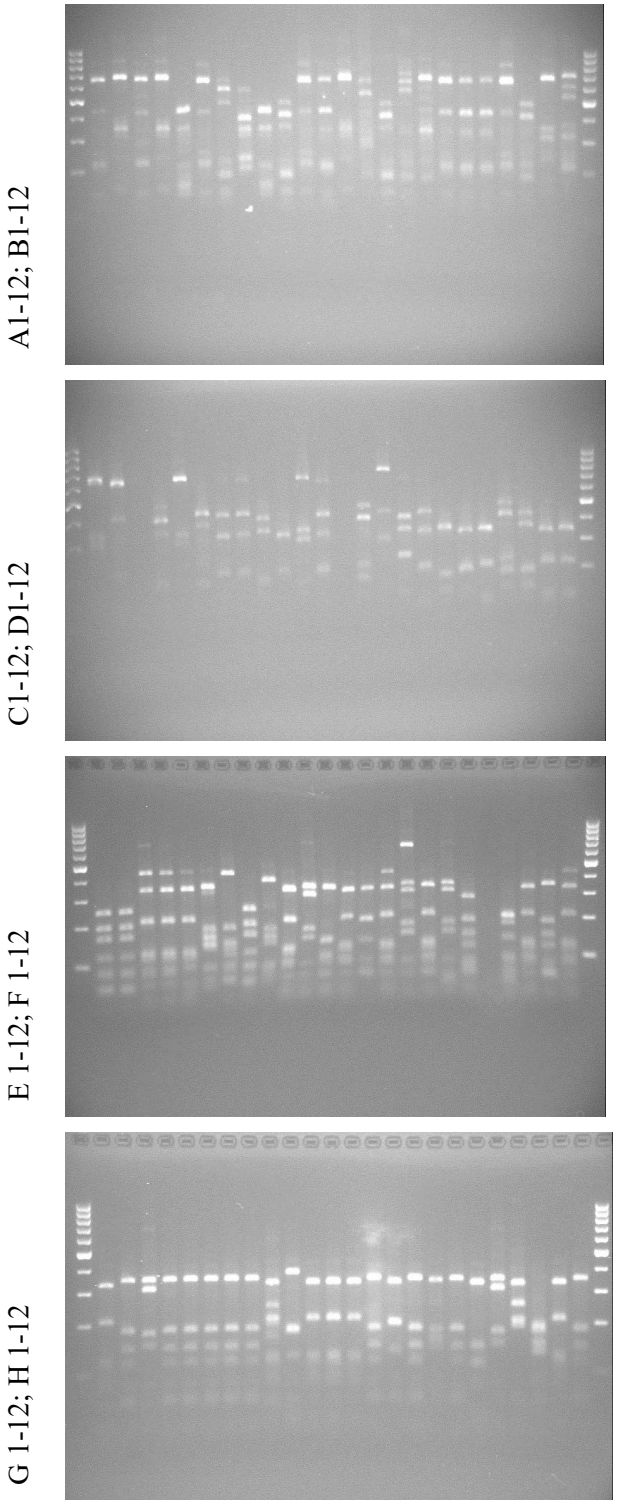

ACHENKIRCH 2 days

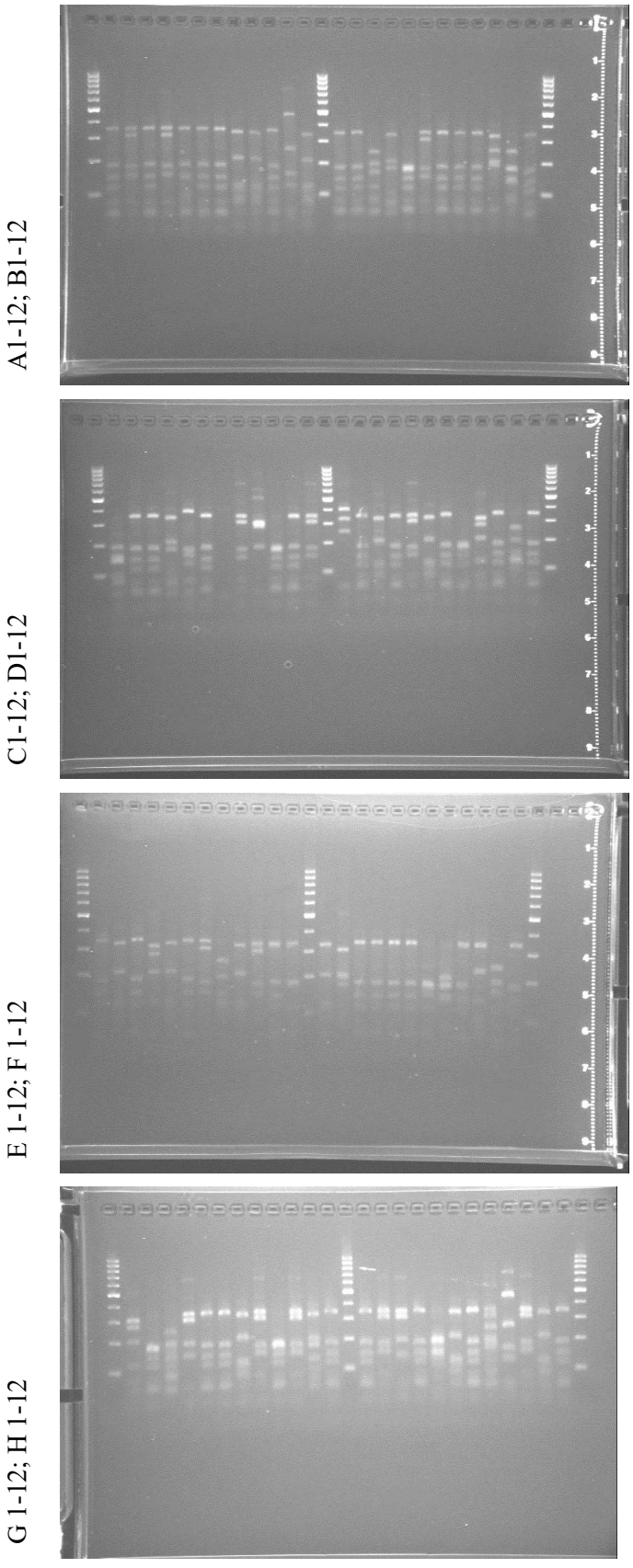

KLAUSENLEOPOLDSDORF 0 days

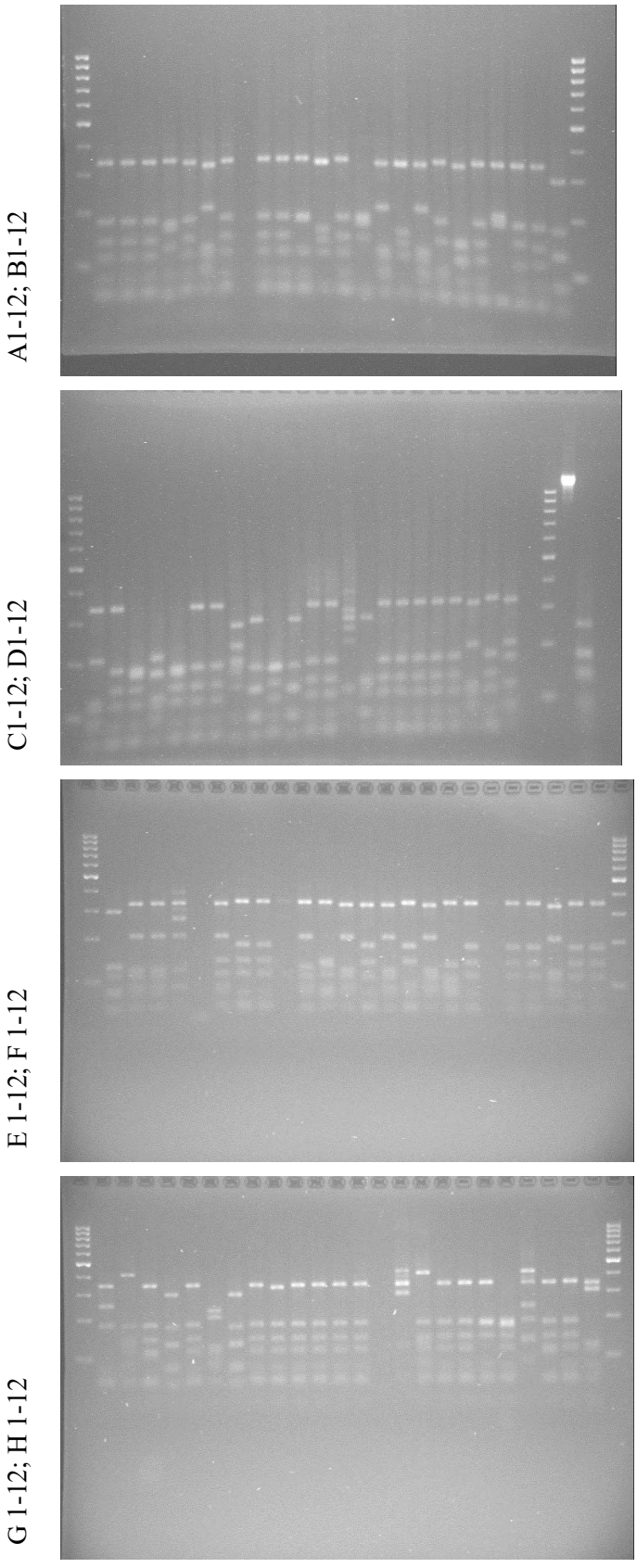

KLAUSENLEOPOLDSDORF 2 days

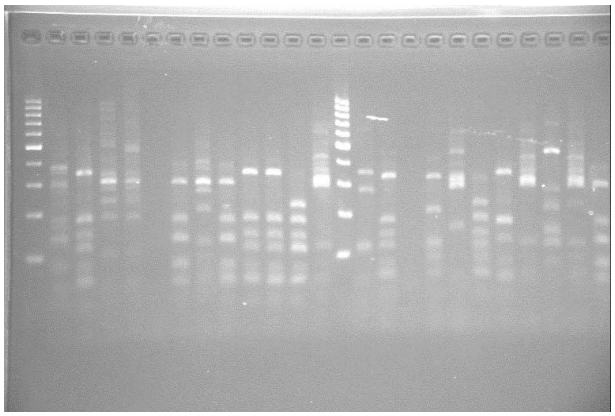

A1-12; B1-12

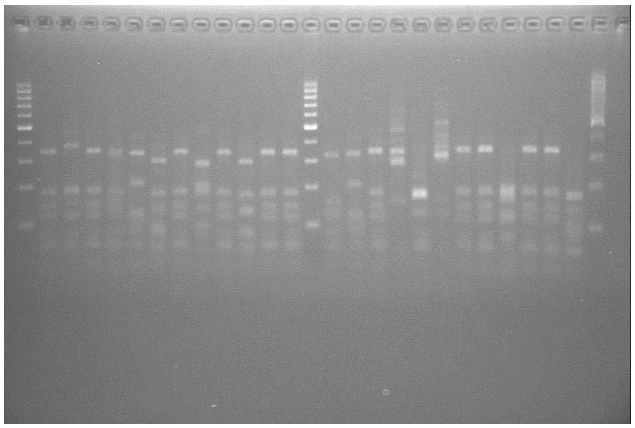

C1-12; D1-12

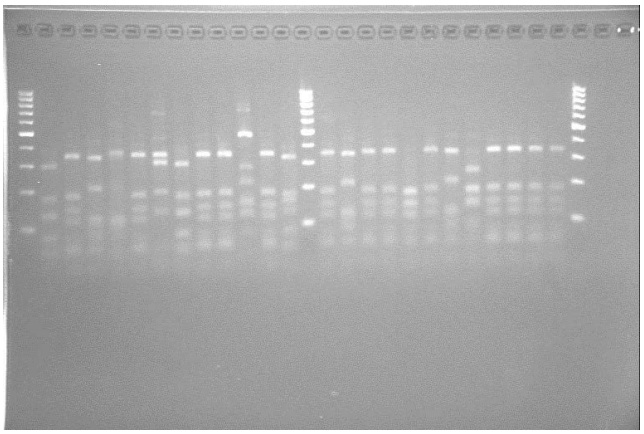

E 1-12; F 1-12

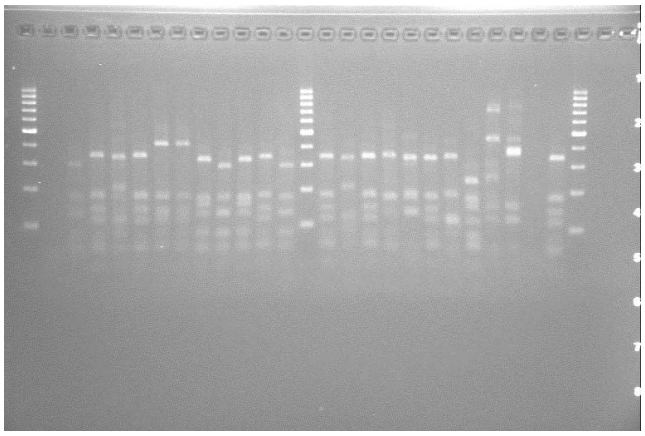

G 1-12; H 1-12

OSSIACH 0 days

1-30

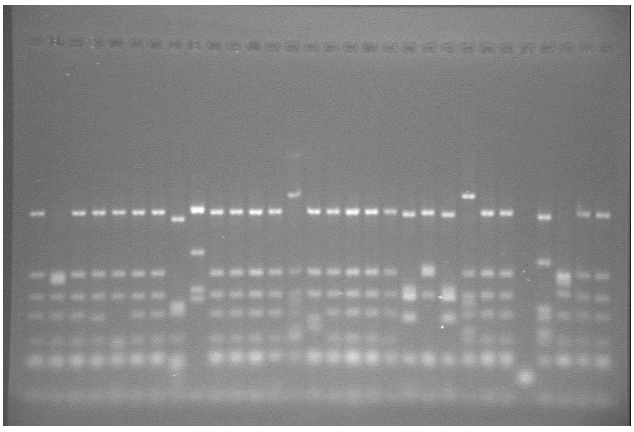

31-59

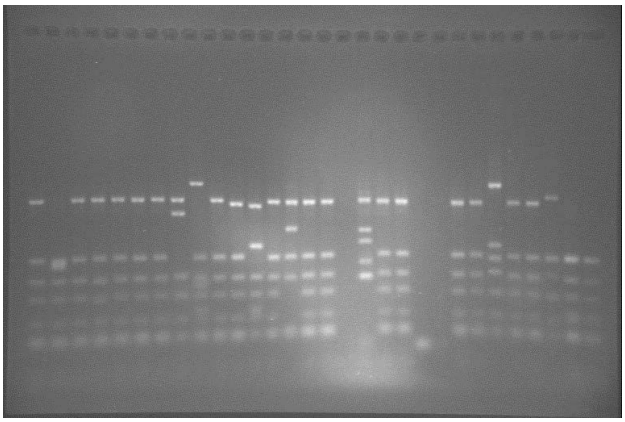

60-89

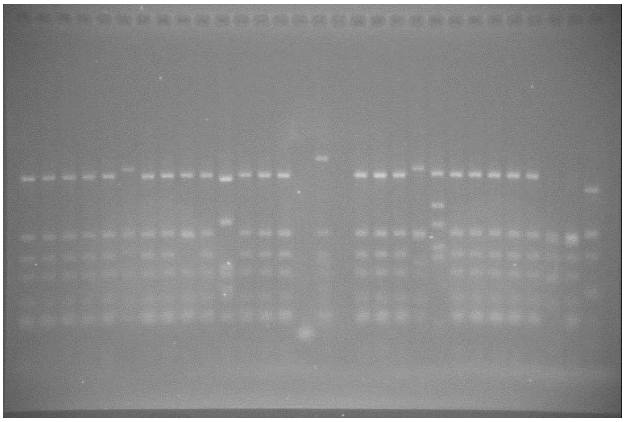

90-96

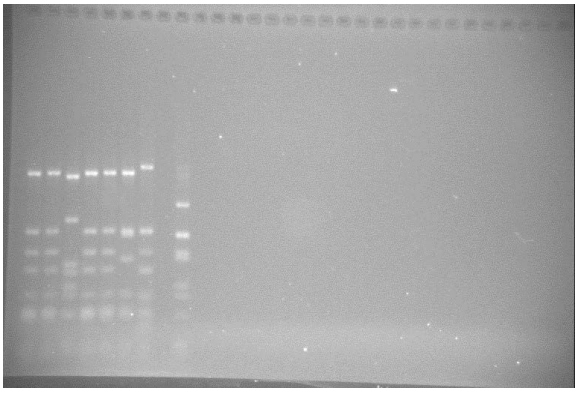

OSSIACH 2 days

A1-12; B1-12

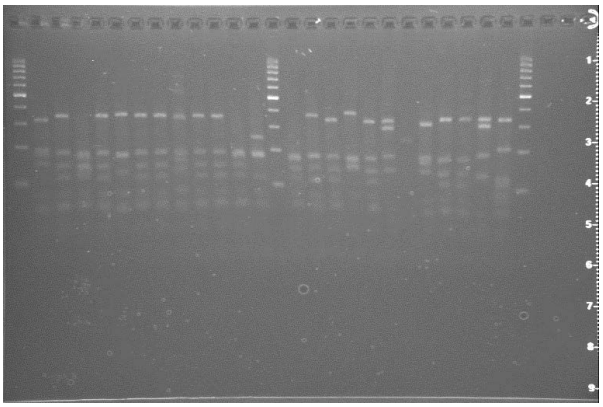

C1-12; D1-12

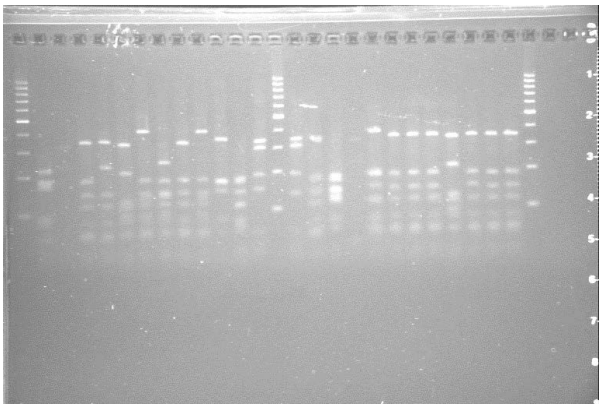

E 1-12; F 1-12

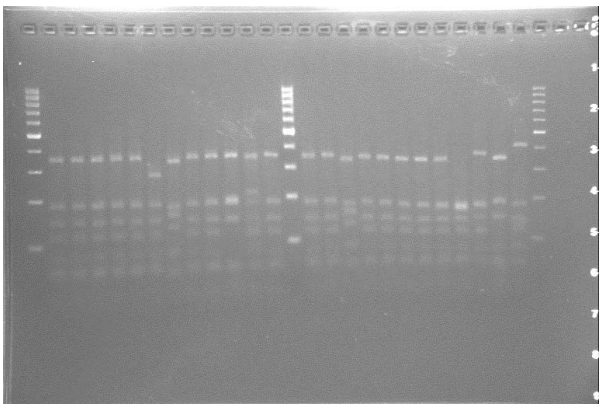

G 1-12; H 1-12

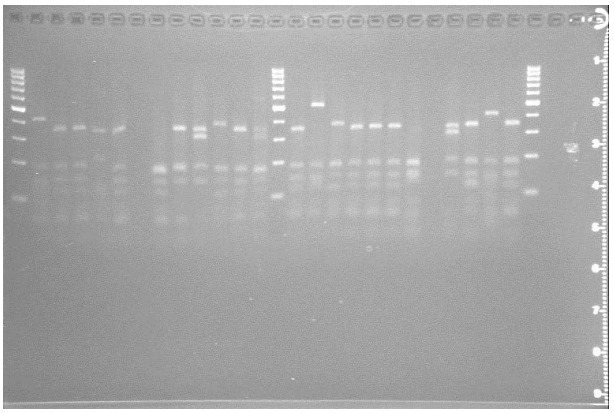

SCHOTTENWALD 0 days

A1-12; B1-12

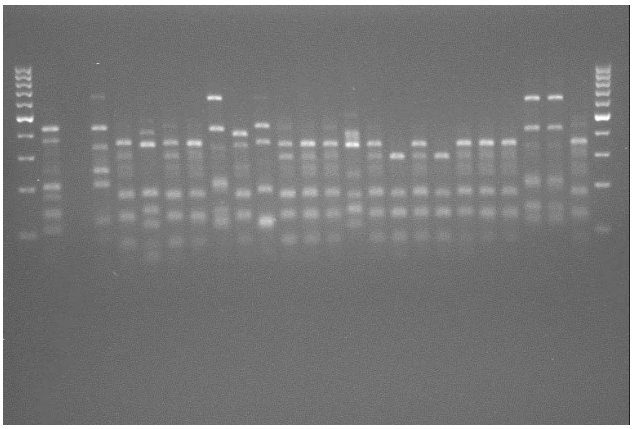

C1-12; D1-12

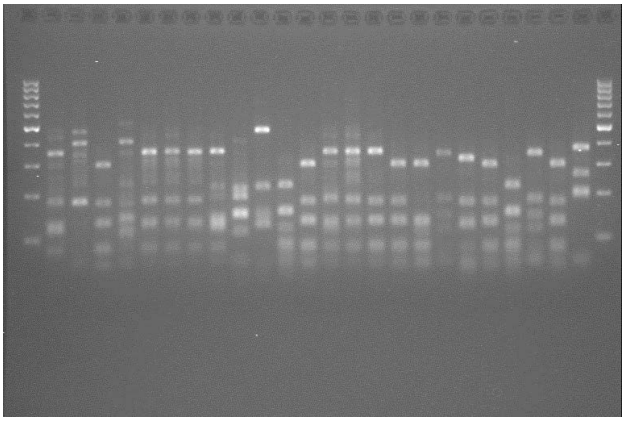

E 1-12; F 1-12

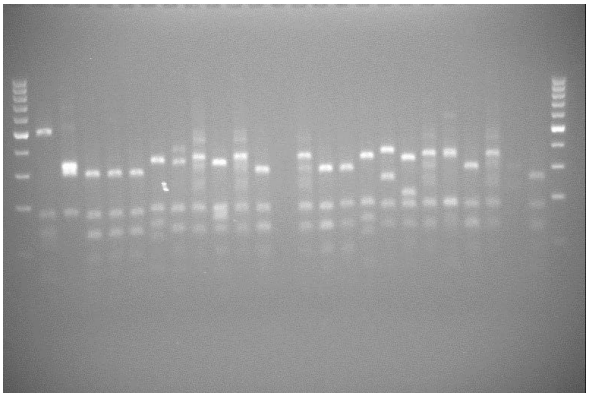

G 1-12; H 1-12

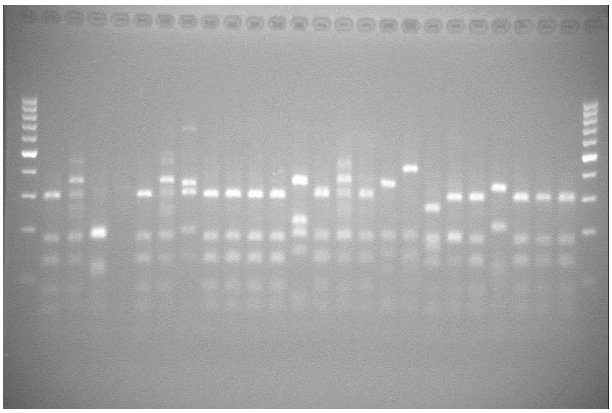

SCHOTTENWALD 2 days

A1-12; B1-12

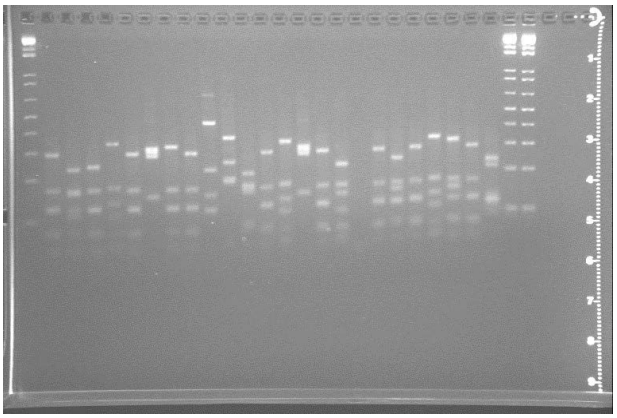

C1-12; D1-12

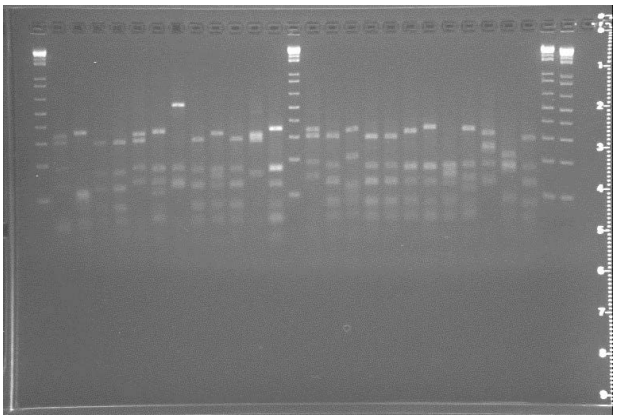

E 1-12; F 1-12

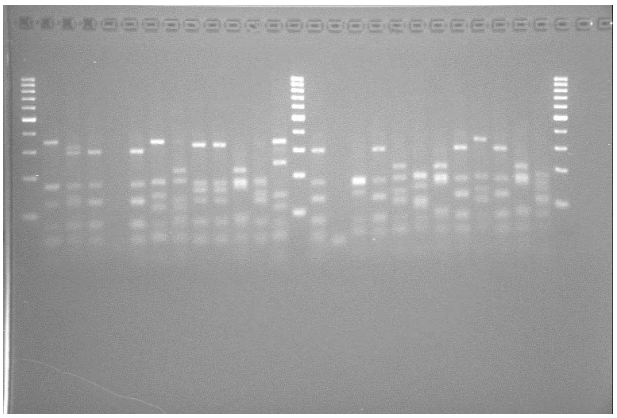

G 1-12; H 1-12

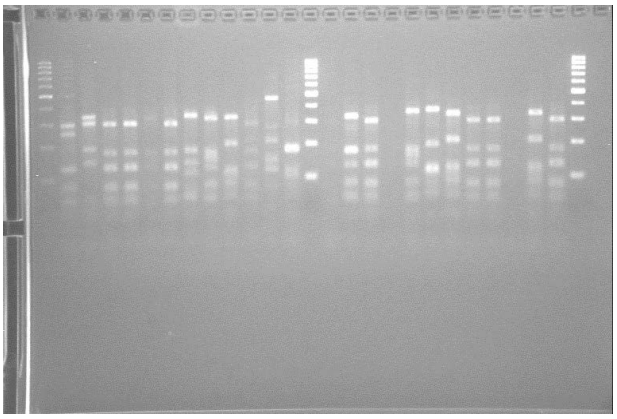

CURRICULUM VITAE

Dipl.Ing. Sandra Renate MOLL, BEd

DOB	Feb.01,1984
citizenship	Austria
personal information	married, maiden name: Böck 2 children: Edmund John (Nov.23,2011) and Liselotte Vienna (Sept.26,2013)
E-Mail	sandrarenatemoll@gmail.com

Education

since 01.2015	University of Natural Resources and Life Sciences Vienna Writing of PhD thesis
08.2011-12.2014	maternity leave, family management resident in Boston, USA
09.2008-11.2012	University of Natural Resources and Life Sciences Vienna **PhD project assistant** position at the Department of Applied Genetics and Cell Biology (DAGZ), division of microbial genetics Supervisor: Univ.-Prof. Dr. Joseph Strauss
09.2009-09.2010	Hochschule für Agrar- und Umweltpädagogik Ober St.Veit Bachelor program Agrarpädagogik, graduated as Bachelor of Education. **Bachelor thesis:** „Bewegter Unterricht an landwirtschaftlichen Fachschulen. Unterrichtsversuche zur Überprüfung der Anwendbarkeit sowie des Umsetzungspotentials.“ Supervisor: Mag. Katharina Salzmann-Schojer
09.2006 – 07.2008	University of Natural Resources and Life Sciences Vienna Master program: Biotechnology, graduated with distinction as Master of Science (Dipl.Ing.) **Master thesis**: Linking Fungal Diversity with Function: Development of a species-specific rRNA capturing system. Supervisor: Univ.-Prof. Dr. Joseph Strauss
09.2002-09.2006	University of Natural Resources and Life Sciences Vienna Bachelor program Food Science and Biotechnology **Bachelor thesis:** “Starvation Induced Chromatin Modification in Aspergillus nidulans” Supervisor: Univ.Prof.Dr. Joseph Strauss, BOKU Wien
09.1994 – 06.2002	High school BG/BRG Stockerau Graduated with distinction in June 2002

Work experience

since 09.2016	Chemistry teacher at BG/BRG Josefstraße, St.Pölten, Austria
09.2008-07.2011	Project assistant at University of Natural Resources and Life Sciences Vienna. Involved in the project „MICDIF: Linking microbial diversity and functions across scales and ecosystems" , funded by „FWF- Austrian Science Fonds" in a NRN (National Research Network) project.
04.2010; 12.2009	Teacher Training at Landwirtschaftliche Fachschule Hollabrunn Advisory teacher: DI Harald Summerer
since 2008	Group fitness instructor
06.2006-06.2008	Tutor at University of Natural Resources and Life Sciences Vienna: Laboratory Course in Molecular Biology
2002-2004	Jugendgruppenleiterin bei der Katholischen Jugend Stockerau
08.2005	Kuchen Peter Backwaren GmbH, Hagenbrunn- quality management and product development trainee
07.2005	Brau Union Österreich, Brauerei Schwechat- chemical and microbiological quality management trainee
08/09.2004	Hubertus Bräu, Laa/Thaya- chemical and microbiological quality management trainee
08.2002	Franz Haas Waffel- und Keksanlagen- Industrie GmbH, Wien
07.2001	Bank Austria, Stockerau

Fellowships

03.2011	Forschungsstipendium für Graduierte University of Natural Resources and Life Sciences Vienna

Other Qualifications

Languages	German (native), English (advanced), French
EDV	MS Office (Word, Excel, Power Point, Access), Photoshop Bioinformatics (EstimateS, R, VectorNTI) Statgraphics
Driving licence	B

Publications

Keiblinger, KM; Hall, EK; Wanek, W; Szukics, U; Hammerle, I; Ellersdorfer, G; **Böck, S**; Strauss, J; Sterflinger, K; Richter, A; Zechmeister-Boltenstern, S (2010): The effect of resource quantity and resource stoichiometry on microbial carbon-use-efficiency. FEMS MICROBIOL ECOL. 2010; 73(3): 430-440.

Harald Berger, Asjad Basheer, **Sandra Böck,** Thomas Dalik, Friedrich Altmann, and Joseph Strauss (2008). Dissecting individual steps of nitrogen transcription factor cooperation in the Aspergillus nidulans nitrate cluster. Mol. Microbiol 69: 1385 -1398

Presentations

Moll, S., Keiblinger, KM., Zechmeister-Boltenstern, S., Bandian, D., Richter, A., Strauss, J., Gorfer, M.: Fungal succession at early stages of beech litter decay. 15th International Biodeterioration and Biodegradation Symposium, Sept 19-24, 2011, Vienna, Austria

University of Natural Resources and Applied Life Sciences, Vienna

Affidavit

I hereby declare that I am the sole author of this work; no assistance other than that permitted has been used and all quotes and concepts taken from unpublished sources, published literature or the internet in wording or in basic content have been identified by footnotes or with precise source citations.

I further declare that all persons and institutions that have directly or indirectly helped me with the preparation of the thesis have been acknowledged and that this thesis has not been submitted, wholly or substantially, as an examination document at any other institution.

Date	Signature

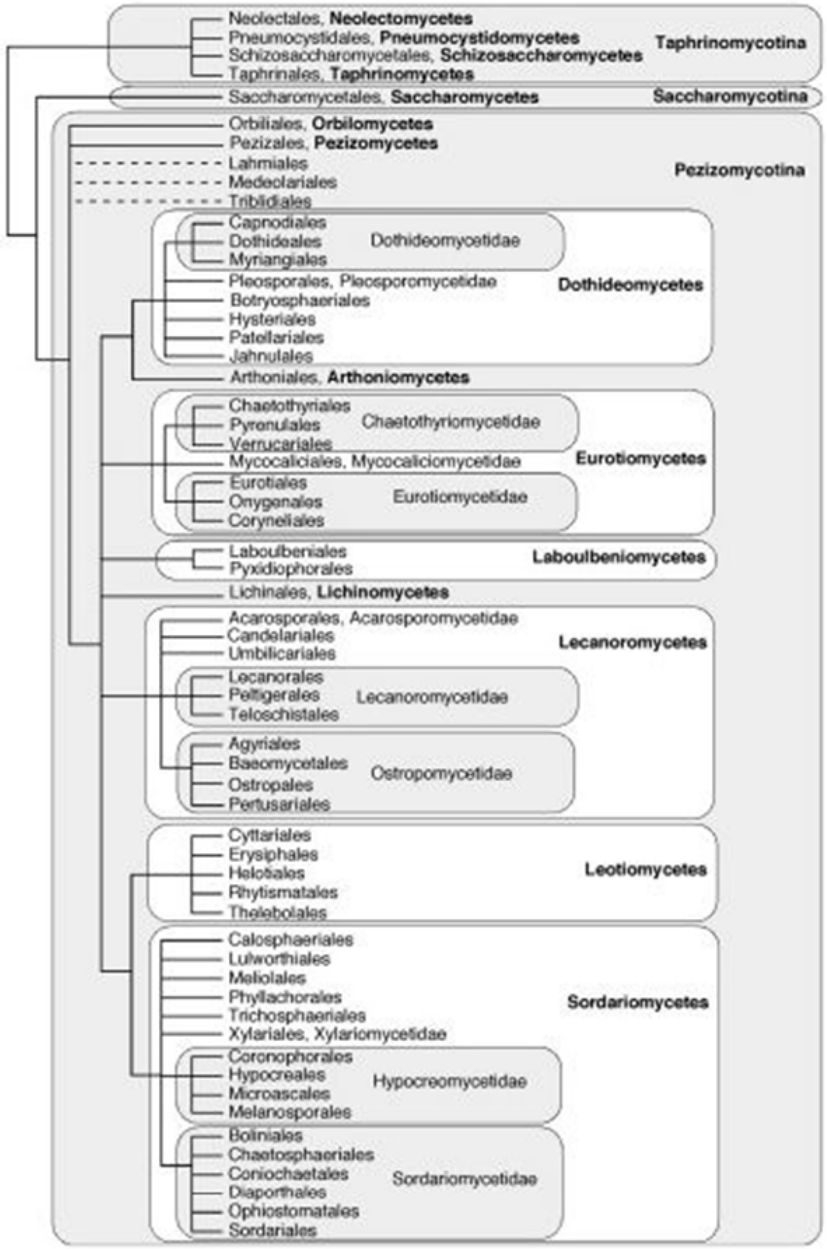

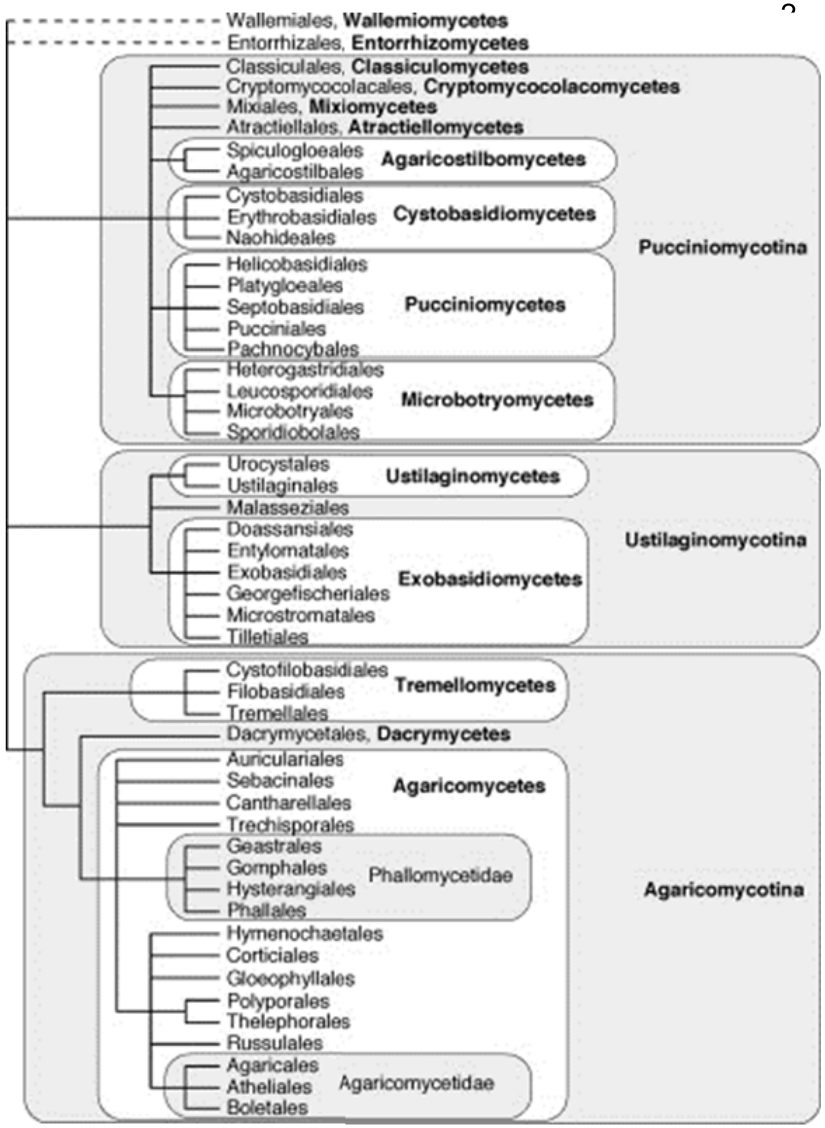

Figure 21: **Phylogeny and classification of *Ascomycota* (left) and *Basidiomycota* (right), from (Hibbett *et al.*, 2007)**

Within bacterial and eukaryotic cells, SSU rRNAs serve as a part of the ribosome complex, together with other rRNAs and proteins. Millions of ribosomes are readily available in the cytoplasm where they perform protein synthesis from mRNAs. Every cell contains multiple copies of the necessary rRNA genes to be able to produce enough ribosomes. The eukaryotic rRNA cistron contains 18S, 28S and 5.8S rRNA genes which are transcribed together as a precursor rRNA molecule. Figure 23 shows the posttranslational modifications occurring within the nucleus of eukaryotic cells, producing the rRNA molecules needed for assembly of ribosomes.

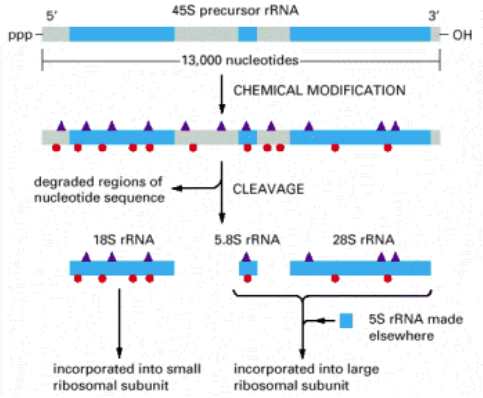

Figure 23: Processing of eukaryotic rRNA molecules in the nucleus, from (Alberts *et al.*, 2002)**.**

In Figure 24, the assembly of small and large ribosomal subunits are shown. Procaryotic and eukaryotic SSU rRNAs differ in their S- values (Svedberg unit), which refers to their sedimentation rate in an ultracentrifuge: 16S prokaryotic rRNA and 18S eukaryotic rRNA. Large subunit (LSU) sequences are also available in most databases for 28S (eukaryotic) and 23S (prokaryotic) rRNA sequences.

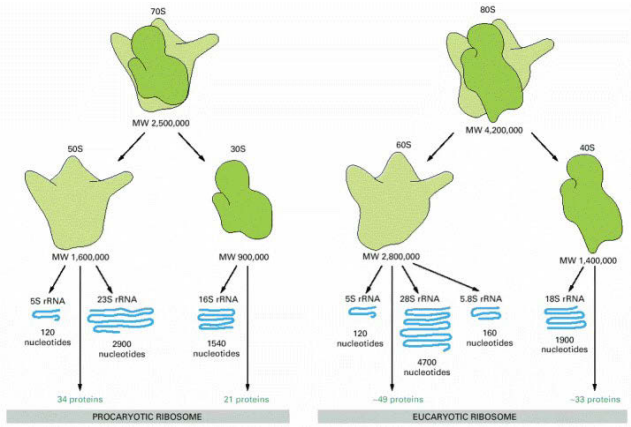

Figure 24: Structural comparison of procaryotic and eukaryotic ribosomes, from (Alberts *et al.*, 2002).

Depending on the level of resolution needed for a study, SSU rRNA can be used as a valuable and robust phylogenetic marker in prokaryotic as well as eukaryotic systems,

2013). Metaproteomics comes one step closer, but lacks evidence of enzyme activities. A very promising tool is therefore the application of stable isotopes which provide direct proof of activity. This coupling of metabolic activity (isotope incorporation) and rRNA analysis makes it possible to address a major gap in understanding microbial communities. Similar to the bacterial rRNA isolation published a while ago (MacGregor *et al.*, 2002), the idea was to combine stable isotope labelling on RNA basis and subsequent measure of ^{13}C and ^{15}N tracer incorporation, with the specific capture of rRNA of different phylogenetic origin. This method could be used to determine active carbon and nitrogen assimilating fungal and bacterial phyla (or even classes) because the isotopic ratio of stable isotopes ($\delta^{13}C$) of the carbon source has been shown to be reflected in total RNA and SSU rRNA of *E.coli* pure cultures (MacGregor *et al.*, 2002).

In vivo incorporation of substrates such as ^{13}C glucose or ^{15}N- nitrate, together with the use of SSU rRNA as diversity (sequence-based phylogenetic separation) as well as functional (isotope incorporation) biomarker, has the potential to gain insight into C and N flow in natural microbial communities.

In my diploma thesis “Linking fungal Diversity with Function: Development of a species-specific rRNA capturing System” (Böck, 2008), the PhyloTrap method was developed and its capability of highly specific SSU- rRNA separation on different phylogenetic levels was shown for pure culture RNA of a bacterial (*R.terrigena*) and three fungal species (*A.nidulans, S.pulverulentum, T.harzianum*).

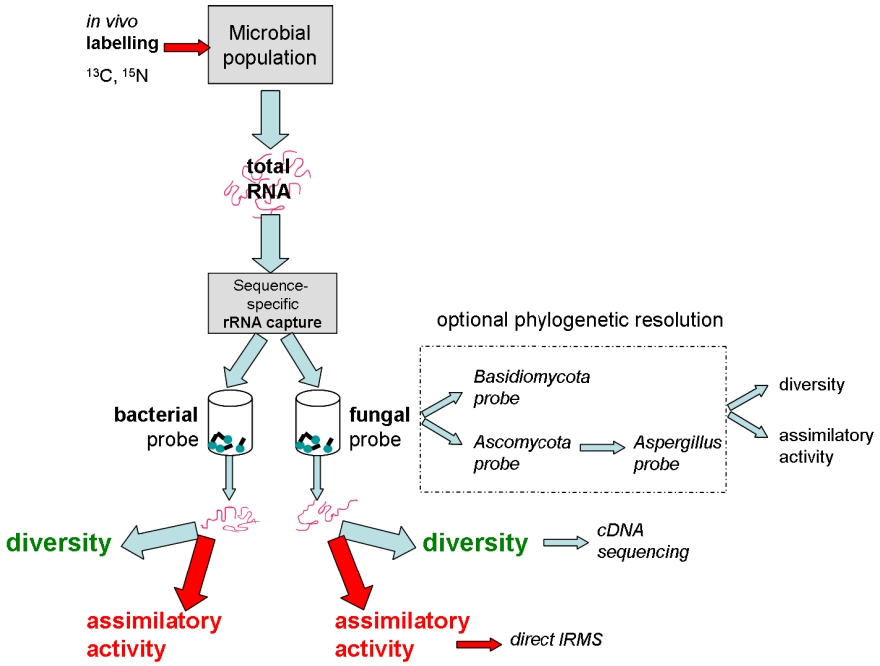

Figure 26: Conceptual development of the ‘PhyloTrap’, a magnetic- bead- based rRNA capture method with labelling of assimilatory active species. Figure from (Böck, 2008).

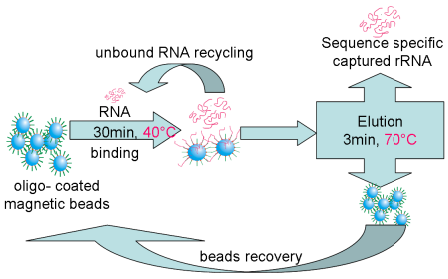

Figure 27: Final flowchart of the rRNA capturing method, as developed in (Böck, 2008).

This stringent protocol, as developed in my diploma thesis, provides exclusion of bacterial RNA and sequence- specific rRNA isolation from three fungal species with a eukaryotic probe targeting the 18S rRNA subunit of nearly all eukarya. However total RNA yield was not only too low, but also contaminated with an unknown, high-N chemical compound (most likely Guanidinium-thiocyanate from QIAquick cleaning procedure), that made IRMS measurements of the enriched rRNA unsatisfying. Therefore, the method had to be refined and developed further in order to address purification and RNA yield issues as discussed in detail in (Böck, 2008).

1.8.1 Improving rRNA yield with LNA probes

In order to improve the oligonucleotide-probe based PhyloTrap technique, it was important to increase target rRNA-probe hybridization. LNAs (locked nucleic acids) are oligonucleotides with increased binding affinity, containing one or more LNA monomers with structurally rigid modifications. The latter are very similar to native nucleic acids, but have an extra bridge connecting the 2' and 4' carbons which locks the furanose ring in the 3'-endo structural conformation (Koshkin *et al.*, 1998), see Figure 28.

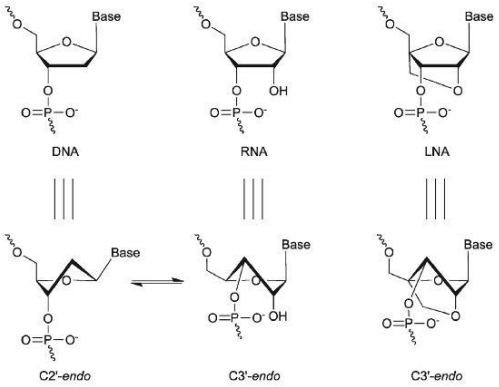

Figure 28: Structures of DNA, RNA and LNA monomers and their furanose conformation, from (Campbell & Wengel, 2011).

2.4.4 Phylotrap initial protocol

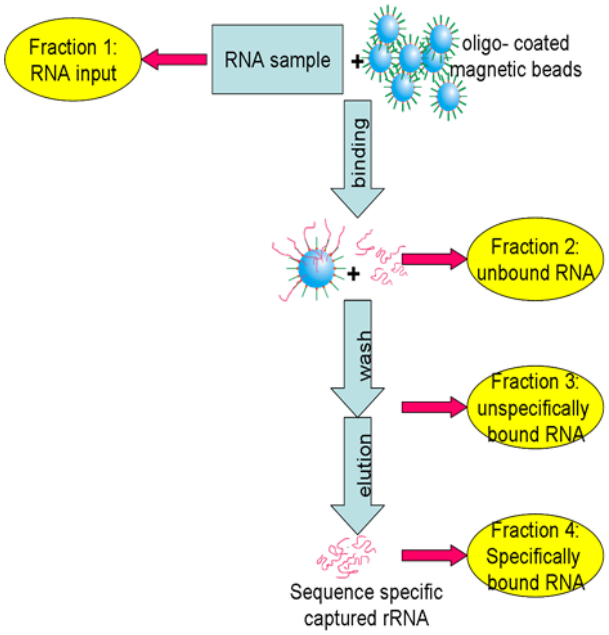

Figure 38: Flow chart of indirect sequence- specific rRNA capture with magnetic beads and obtained fractions 1-4 that were analyzed after the experiment, as developed in (Böck, 2008).

Bead coating: For RNA applications, 100 µl Dynabeads were washed twice with SolutionA for 2 minutes, and then with Solution B. For immobilization of the probe on the beads, beads were washed with 2xB&W buffer and resuspended in 1xB&W buffer to a final concentration of 5 µg/ml (twice the original volume). Biotinylated oligos (200 pmol) are added to the beads and incubated at RT for 15 minutes using gentle rotation. After immobilization, beads were washed 2-3 times with 1xB&W buffer and used for downstream applications or stored at 4°C.

RNA pre- treatment: Mix sample RNA (10 µg), Hybridization buffer (5xSSC, 0,1% N-laurylsarcosine, 0,1% NaCl, 0,02% SDS) and Formamide (15%) to a final volume of 450 µl. Incubate at 70°C for 10 min, then 30 min at RT. The mixture was divided: 200 µl were taken (→ Fraction 1: RNA input), 200 µl were used for the capturing step.

RNA capture: Add 200 µl RNA mixture to 1mg of probe- coated beads and incubate at 40°C for 30 min with agitation. Supernatant → Fraction 2

Washing step: Wash the beads with 0,5x SSC. Supernatant = Fraction 3: wash.

Elution: add 200 µl DEPC- water and incubate for 10 min at RT. Then incubate at 70°C for 3 min. Supernatant = Fraction 4: Eluate.

3.1.1 Species accumulation curves

Unified species accumulation curves for fungal clone libraries were constructed as described in (Colwell et al., 2012).

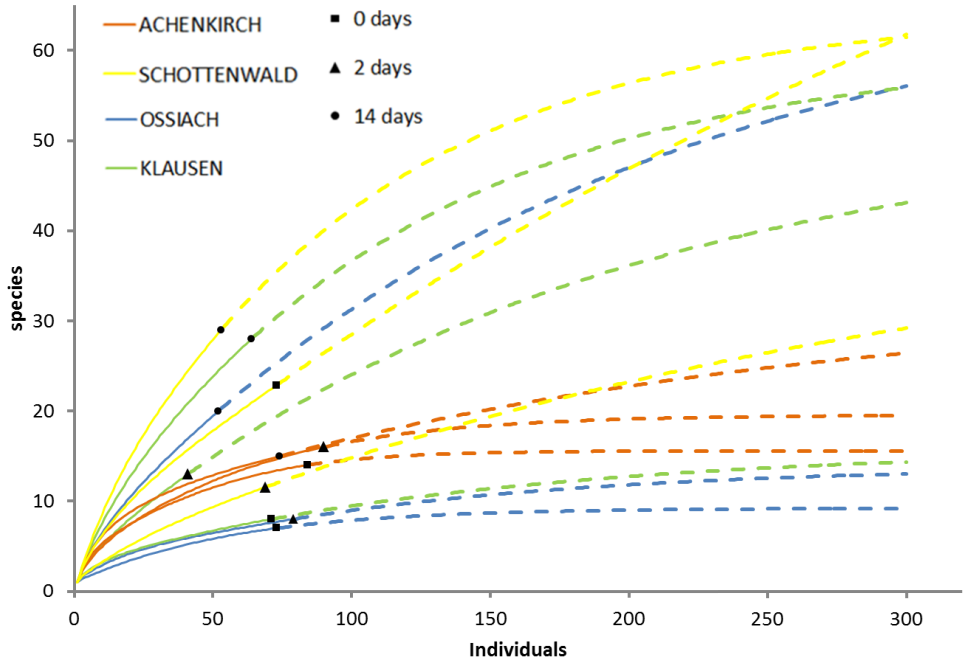

Figure 40: Species accumulation curves for fungal species richness on decaying beech litter, showing detected species (OTUs) vs analyzed individuals (clones). Interpolation (rarefaction, see **Fehler! Verweisquelle konnte nicht gefunden werden.**) and extrapolation (see 1.3.1.2) were integrated to produce unified species accumulation curves for empirically collected data, based on reference samples. This set of species accumulation curves was generated by EstimateS Version 9.1.0., using 'Sample-based input file Format 1' as explained in Estimate S User Guide (Colwell, 2013). Samples were randomized 100 times. Rarefaction curves were extrapolated to a total number of 300 samples. Curves were plotted with Excel for Windows. Different locations (Achenkirch AC, Schottenwald SW, Ossiach OS, Klausenleopoldsdorf KL) are shown with color code as explained in the figure. Reference samples for each assemblage are indicated by full squares, rectanges, and circles respectively. Full lines show rarefaction curves, dashed lines represent extrapolation up to 300 individuals per assemblage.

In **Figure 40**, the y-axis shows the number of detected species (i.e. individual OTUs) for fungal clone libraries, and the x-axis shows increased sampling effort. A lower curve slope indicates that the fungal community richness is more saturated, a higher curve slope shows that new species are detected much faster and richness reaches the asymptote (= true species richness) later. Maximum fungal species density was found at Schottenwald (SW) time point 14 days, lowest species density was found at Ossiach (OS) time point 0 days. For location Achenkirch (AC) shown in orange, all three timepoints flattened out asymptotically for the rarefied part of the curve (full

individually. Richness ranged from 7 to 29 of observed and from 9 to 125 for predicted species numbers (Chao1; Chao, 1987a) per sample (see **Table 4**). Richness and Diversity values for different locations and three time points are displayed graphically in **Figure 41**. The differences between observed species counts (S_{obs}) and estimated species richness (Chao1) accounted for coverages from 90% (AC_0) to 17% (SW_0).

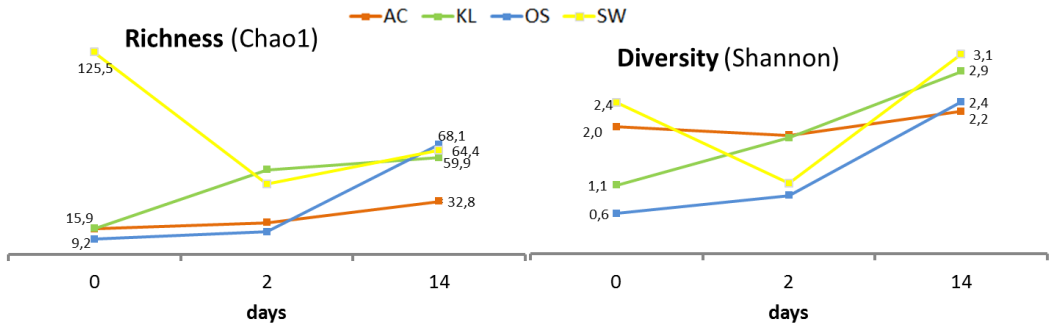

Figure 41: Chao1 richness estimators and Shannon diversity indices for beech litter fungal clone libraries as computed by EstimateS. AC= Achenkirch, KL= Klausenleopoldsdorf, OS=Ossiach, SW= Schottenwald. Time points 0, 2 and 14 days.

Richness values generally increased with time (**Figure 41**, left section) for locations AC, KL, and OS; but not for SW because of a very high richness at 0 days. Therefore no statistically significant richness differences could be found for the three timepoints (see below). Diversity is highest at the 14 days timepoint for all samples (**Figure 41**, right section).

A one-way Analysis of Variance (ANOVA) was performed with STATGRAPHICS Centurion XVI Version 16.0.09 using the Diversity (Shannon) and Richness (Chao1) values of for different sampling sites (AC, KL, OS, SW) at three different time points (0, 2 and 14 days) from **Table 4**. The results are plotted in **Figure 42**.

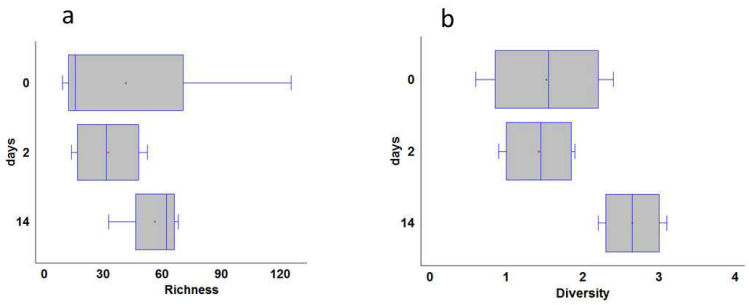

Figure 42: Box and Whisker plot for Diversity and Richness at different time points. Vertical line in the boxes show median, red cross marks the mean value. Four sampling sites are included per time point. (a) Diversity (Shannon), (b) Richness (Chao1).

According to the Multiple Range Test, Shannon diversity index data at time point 14 days are significantly different from all other time points at the 95% confidence level (See Figure **Figure 42b**). No statistically significant differences could be calculated for Richness data.

3.1.3 Rank abundance plots

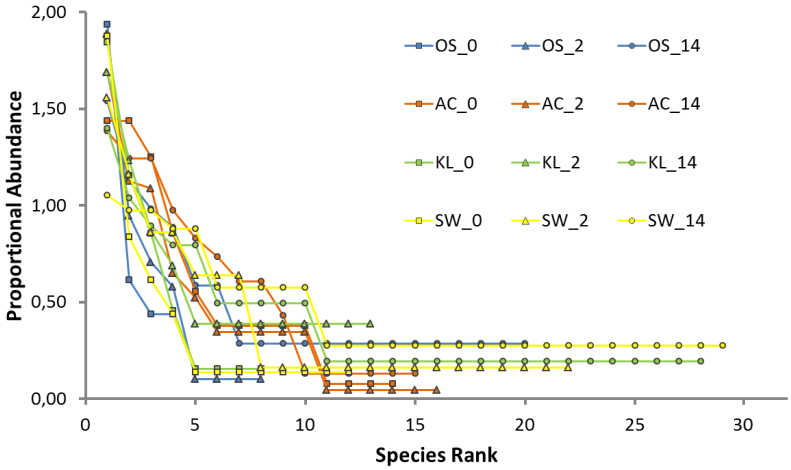

Figure 43: Rank-Abundance distributions of fungal species on beech litter, plotted by species rank. AC=Achenkirch, OS=Ossiach, KL=Klausenleopoldsdorf, SW=Schottenwald, time points 0, 2 and 14 days, respectively. The proportional abundance on the y-axis (on a logarithmic scale) was calculated by setting the sum of all species abundances to 100% for every sample individually.

Overall, rank abundance plots for fungal OTUs from clone libraries show a similar pattern, highlighting low evenness among fungal decomposer communities. There is a sharp drop in abundance for the highest ranking species (dominant OTUs), and a long tail representing rare species. OS_0 shows the lowest curve as well as the shortest curve, which means that both species evenness and species richness were lowest in this sample. Higher species richness in later time points, especially time point 14 days, is represented by the longer tails in the respective rank-abundance curves.

based approach, no members of the Glomeromycotina, Mucoromycotina or any other basal fungal lineage were detected. All tested litter communities were dominated by Ascomycota, which were represented by at least 80% of the clones in the respective libraries (see Figure 48b). The remaining clones belonged to the Basidiomycota. The only sample with no OTUs assigned to Basidiomycota was OS litter at time point 2 days; but generally on all litter types, ratios of Basidiomycota:Ascomycota increased with incubation time (see Figure 48a) . This pattern was most prominent on KL litter, here OTUs assigned to Basidiomycota showed the highest percentage of 19,5% at 2 days, and 18,8% at 2 weeks, respectively.

3.1.5.2 Fungal classes found on different locations

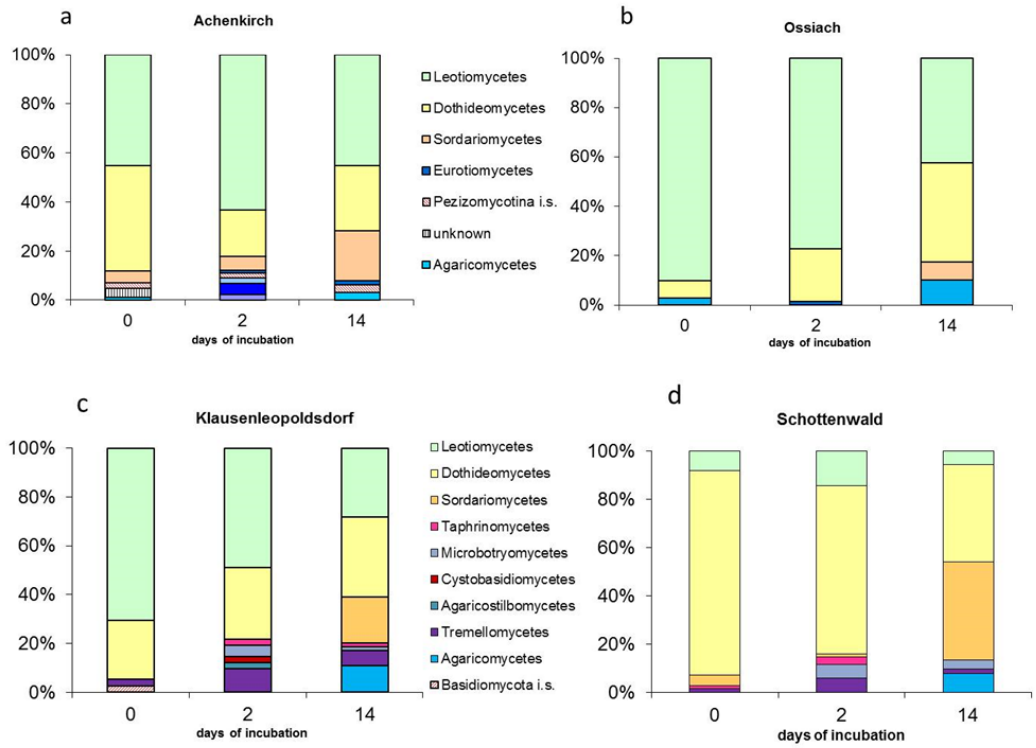

Figure 49: Taxonomic diversity of fungal clone libraries from decaying beech litter, sorted by class. a, b, c, d, showing different litter locations Achenkirch, Ossiach, Klausenleopoldsdorf, and Schottenwald. Time points 0, 2 and 14 days.

Most fungal OTUs on beech litter were assigned to the Ascomycota classes Leotiomycetes, Dothideomycetes and Sordariomycetes within the Pezizomycotina. On SW litter, Dothideomycetes started as the dominating species class (Figure 49d), whereas OS and KL were dominated by Leotiomycetes (Figure 49bc). AC showed Leotiomycetes and Dothideomycetes at almost similar dominance levels (Figure 49a). Later time points generally showed less dominance of single OTUs and more classes of fungi detected. Only a few OTUs were assigned to the Eurotiomycetes. The

3.2 Microbial community composition changes during beech litter decomposition in a mesocosm experiment

From a mesocosm experiment with sterilized and inoculated beech litter outlined in 2.3, samples of four different locations and 4 harvest time points (2.3.1.1) were generated, with 5 replicates each. DNA was extracted and qPCR with fungal and bacterial specific primers was performed in triplicates. Fungal/bacterial ratios were calculated and plotted on a time scale.

3.2.1 Fungal-specific RFLP and T-RFLP Analysis of E1 replicas

Since 5 replicates of each inoculated litter sample were used, it had to be tested if all replicas contained the same microbial community at the start of the experiment. To this end, a simple RFLP approach with two different restriction enzymes was performed.

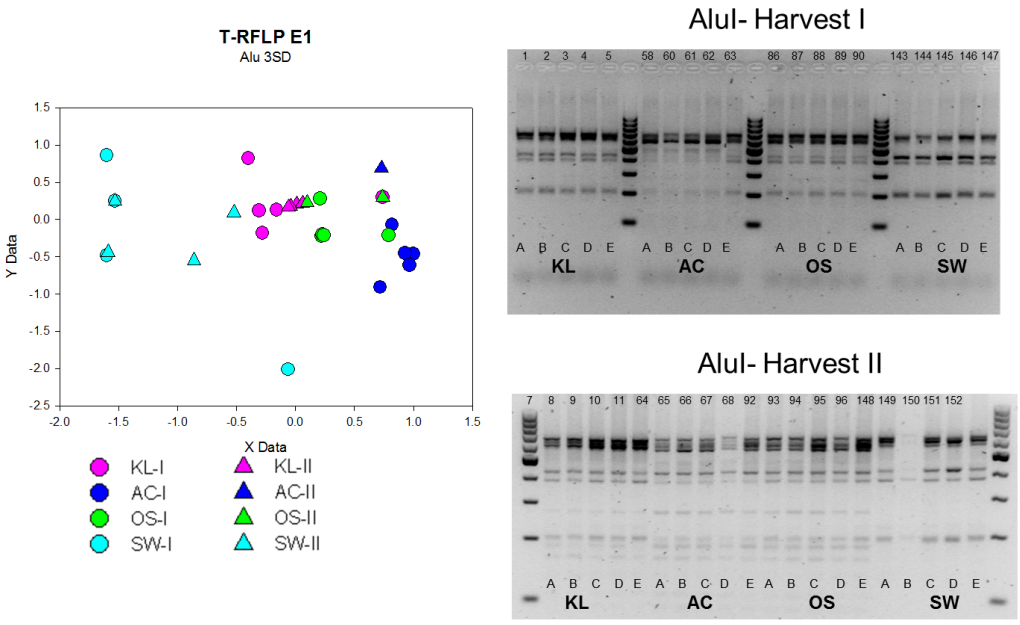

Figure 57: T-RFLP (left) and RFLP of E1 replicas from harvest I (2weeks) and Harvest II (2 months). Litter DNA PCR was performed with fungal specific primers ITS1R-ITS4 for 30 cycles at 54°C. PCR triplicates were pooled for RFLP with AluI. Numbers indicate internal sample code. AC= Achenkirch, KL= Klausenleopoldsdorf, OS=Ossiach, SW= Schottenwald. RFLP analysis was performed by Dragana Bandian.

According to the RFLP pattern produced by AluI, replicas of the locations KL, OS, and SW contained the same starting community and were therefore used for further experiments. Sample No.63 of the AC location showed a different RFLP pattern than the other four replicas of this location with this restriction enzyme. T-RFLP pattern

does not show a particular pattern for meaningful interpretation, however locations seem to cluster more or less together.

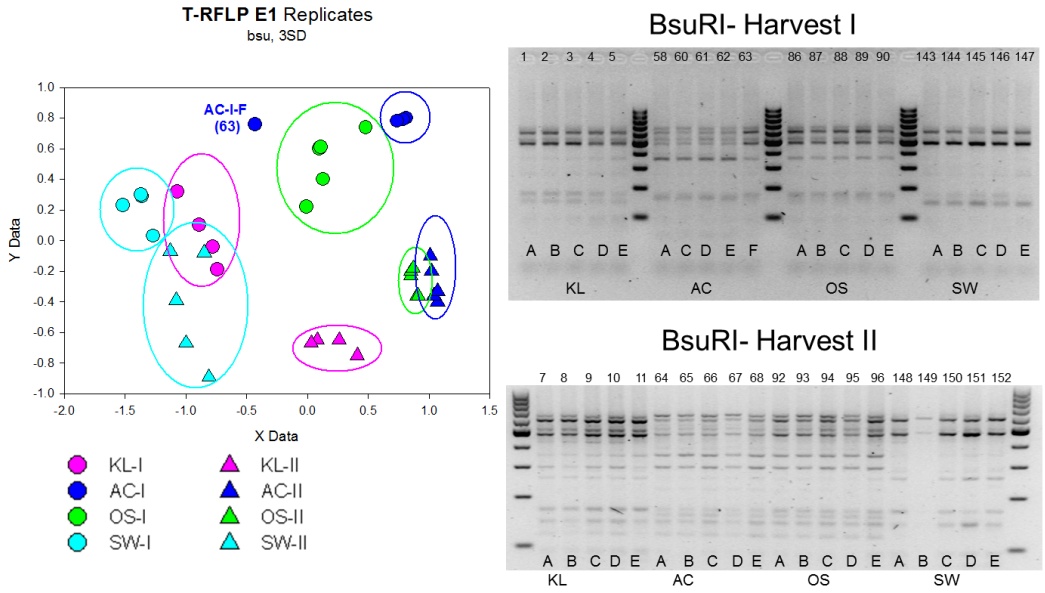

Figure 58: **T-RFLP (left) and RFLP (right) of E1 replicas from harvest I (2weeks) and Harvest II (2 months).** Litter DNA PCR was performed with fungal specific primers ITS1R-ITS4 for 30 cycles at 54°C. PCR triplicates were pooled for RFLP with BsuRI. Numbers indicate internal sample code. AC= Achenkirch, KL= Klausenleopoldsdorf, OS=Ossiach, SW= Schottenwald. RFLP analysis was performed by Dragana Bandian.

RFLP analysis with another restriction enzyme, BsuRI, showed the same AC mesocosm (no.63) of harvest I to contain a significantly different fungal community as represented by a different RFLP pattern on the gel. T-RFLP analysis (left section of Figure 58) revealed a clustering of locations as well as harvest time points, demonstrating similar fungal community behavior within the replicas. The result of RFLP was backed up by T-RFLP results, because AC-I-F (no.63) did not cluster together with the other mesocosm replicas of AC first harvest.

Harvest II did not show any indication of unpredictable replica behavior as backed up by both RLFP and T-RFLP analysis with two different enzymes. Because of dissimilar RFLP patterns (by two enzymes) and T-RFLP clustering with BsuRI, results from one particular mesocosm of the first harvest (AC-I-F, no.63) were excluded from later analyses.

3.2.2 Nutrient ratio changes during decomposition

The nutrient ratios of beech litter from four different locations in Austria were assessed in a mesocosm decomposition experiment. Experimental details are outlined in (Schneider *et al.*, 2012).

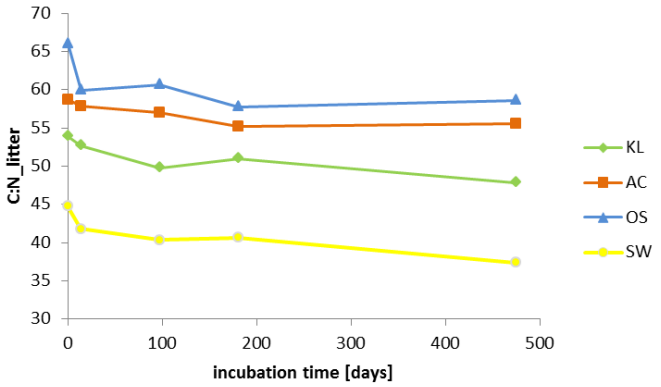

Figure 59: Litter nutrient ratios during decomposition in a mesocosm experiment. Experimental details and data provided by Dr.Katharina Keiblinger (BFW).

Results from litter biogeochemistry measurements are explained in detail here (Schneider *et al.*, 2012). Shortly, all four locations varied in their nutrient ratios as well as their behaviour during decomposition. SW has high nutrient status, represented by a low C:N ratio. OS and AC showed the highest C:N ratios and can therefore be considered low in nutrients. Ratios went down slightly as decomposition progressed.

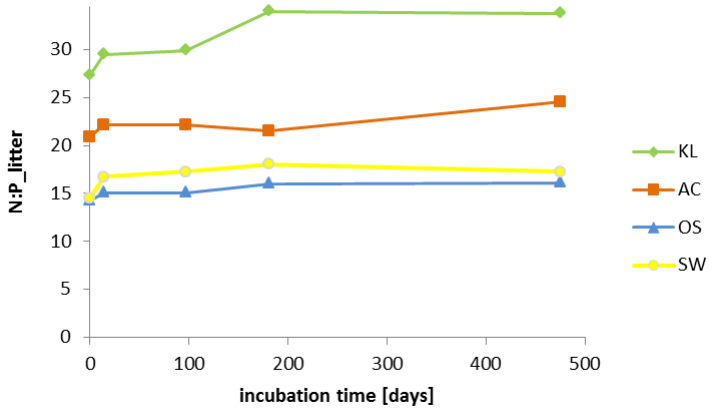

Figure 60: Litter nutrient ratios during decomposition in a mesocosm experiment. Experimental details and data provided by Dr.Katharina Keiblinger (BFW).

C:P ratios in litter present SW and OS with the narrowest ratio, i.e. highest P levels, and KL with the highest ratio. Ratios stayed more or less stable during the decomposition process.

The same beech litter samples were analyzed by metaproteomic analysis to generate another set of Fungi/Bacteria ratio data[3]. Figure 62 shows fungi/bacteria ratios from metaproteomics data as well as from qPCR data. Metaproteomics data were generated by Lukas Kohl, University of Vienna. The results both show a similar pattern between litter types and harvests: the earlier harvest points show much higher ratios than later time points. Fungal proteins were dominant on all samples, but like in the qPCR analysis, SW and KL showed the highest fungal dominance. Also, AC showed the lowest ratios of fungal/bacterial proteins. Overall, Fungi/bacteria ratios were highly correlated between protein- and DNA-based estimates.

3.2.4 Microbial community composition changes under various resource C:N ratios

Fungal/bacterial ratios derived from qPCR data of litter DNA were plotted against the C:N resource ratios of the litter. C/N resource ratios were measured and calculated by Dr.Katharina Keiblinger, BFW, and recently published here (Schneider *et al.*, 2012) and here (Mooshammer *et al.*, 2012).

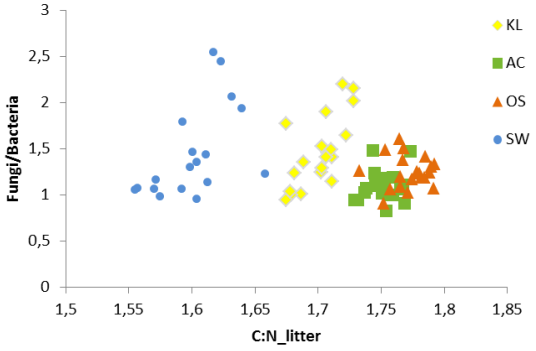

Figure 63: Litter C:N ratios plotted against Fungi/Bacteria ratios. Litter C/N mass ratios were calculated and measured by Dr.Katharina Keiblinger, BFW. Fungi/Bacteria ratios were obtained by qPCR as described above. Logarithmic values are shown. AC= Achenkirch, KL= Klausenleopoldsdorf, OS=Ossiach, SW= Schottenwald. Five repetitions and time points 14, 97, 181 and 475 days per location respectively.

Resource C:N ratio appears to have no relationship with the Ratio of Fungi/Bacteria, suggesting homeostatic behavior (see Figure 63). Because Fungal/Bacterial ratios only give a hint of underlying elemental ratios, biomass C:N ratios were used for the statistic calculation instead. When calculating the relation of resource C:N and biomass C:N, there was no statistically significant relationship found. The slope was not statistically different from zero on linear and logarithmic axes, which demonstrates C:N

[3] Metaproteomic Fungi/Bacteria ratio data were generated by Lukas Kohl, University of Vienna.

Different amounts (180, 200, 250 and 300 pmol) of LNA- enhanced probe EUK-Y-bio were used on 100 µl Dynabeads, resuspended in 200 µl binding buffer. Binding was performed as described in 2.4.4. The unbound fraction of probe in found in the supernatant after washing the beads was determined by Quant-iT fluorometric quantitation. For further experiments, 200 pmol probe were used because of the highest binding efficiency of over 90%.

3.3.2 Protocol Troubleshooting: Washing and Blocking steps

Problem 1: unspecific binding of bacterial rRNA on LNA-euk probe

When using bacterial RNA on the LNA-euk probe, unspecific binding of both bacterial SSU and LSU were detected. The protocol as outlined in 2.4.4 was used, and some additional washing steps were added as shown below:

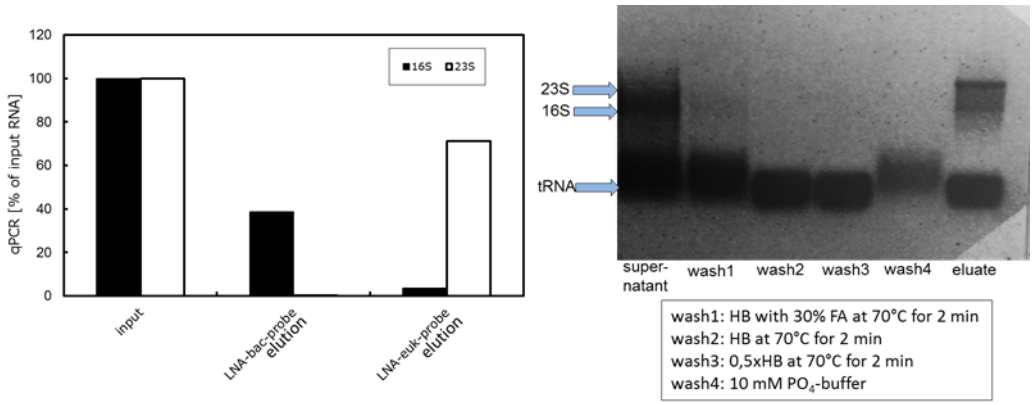

Figure 66: Unspecific binding of bacterial SSU and LSU to LNA-euk probe. qPCR (left) and gel (right) showing input and eluate fractions after Phylotrap protocol using 10 µg *R.terrigena* RNA on LNA-bac probe and LNA-euk probe respectively. Primers: Bacterial 16S (EUB f933; EUB r1387) and bacterial 23S (fBact23S; rBact23S). In this diagram, RNA amounts were normalized to the detected RNA amount in the input fraction.

After the hybridization step with *R.terrigena* RNA and LNA-euk probe coated Dynabeads, the eluate fraction showed both SSU and LSU bands on the gel. This binding was highly unspecific and subsequent experiments were conducted to increase specificity.

The unspecific binding of bacterial RNA to the LNA enhanced euk-probe was confirmed by qPCR-analysis of the elution fractions. The bacterial rRNA recovery by LNA-bac-probe was specific and detected only 16S rRNA. However the LNA-euk probe showed unspecific binding of high amounts of bacterial 23S rRNA.

Problem 2: unspecific fungal rRNA binding to LNA-bac probe

A.nidulans SSU RNA was found in eluate after hybridization with LNA-bac-probe coated Dynabeads using the Phylotrap protocol. Hybridization was performed in 30% Formamide at 40°C for 2 hours, washing steps were performed at 40°C.

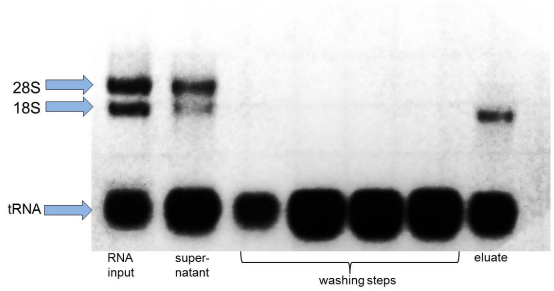

Figure 67: Unspecific binding of fungal SSU rRNA to LNA-bac probe. Washing steps were performed at 40°C.

The protocol had to be adjusted to make sure no unspecific rRNA would stick to the LNA probes. The first modification was the introduction of a 'stringent' washing step by increasing the washing temperature from 40°C to 70°C.

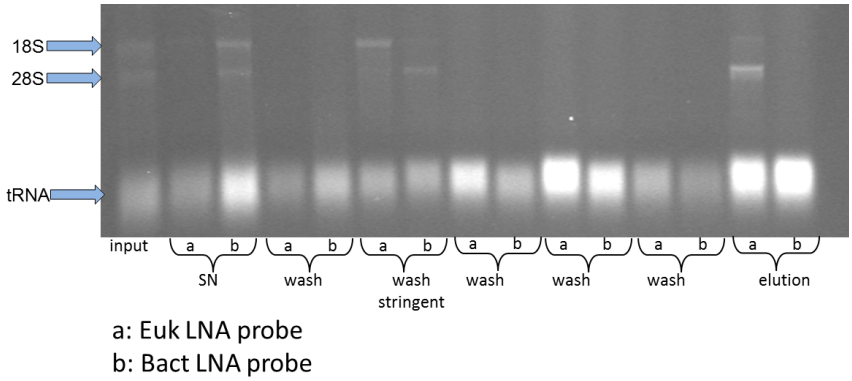

Figure 68: Introduction of a ‚stringent' washing step to the Phylotrap Protocol. 10 µg total *A.nidulans* RNA were used on (a)LNA-euk-probe and (b)LNA-bac-probe respectively. Stringent wash: wash with Hybridization buffer + 30% Formamide at 70°C for 2 minutes. Samples were run on a non-denaturing 2% Agarose gel with EtBr staining.

On the gel, it can be seen that this stringent washing step with 70°C removes not only the unspecific binding of *A.nidulans* LSU to the euk-LNA probe (stringent wash a), but also unspecific binding of fungal SSU to the LNA-euk-probe (wash stringent b). This protocol produced a fungal 18S band in the elution fraction for LNA-euk-probe (elution a), and no RNA in the elution fraction after phylotrap with LNA-bac-probe (elution b).

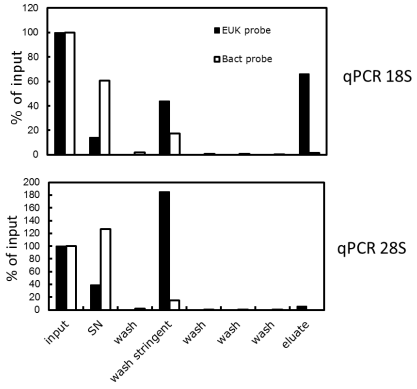

Figure 69: qPCR of Phylotrap experiment with *A.nidulans* RNA and introduction of a stringent washing step. Primers for 18S: SR7R-SR5. Primers for 28S: Ctb6-TW13. Stringent washing step was performed with hybridization buffer containing 30% Formamide for 2 minutes at 70°C. RNA amounts are shown as relative to the input. Black bars show LNA-euk-probe, white bars show LNA-bac-probe**.**

The fractions of the Phylotrap procedure (as shown above on the gel) were also reverse transcribed and measured by quantitative Real-Time PCR with specific primers for fungal 18S and 28S respectively. The stringent washing step was able to remove unspecific binding of fungal SSU to the LNA-bac-probe, and also completely wash off any unspecific binding of fungal LSU to both probes.

The specific SSU recovery by this method (in the eluate recovered by LNA-euk-probe) was estimated to be 66% of the input according to qPCR measurements.

Modifications:

- Hybridization performed at 65°C for 30 min (instead of 40°C)
- Hybridization buffer with higher Formamide concentrations (30%)
- All washing steps performed at 70°C for 2 minutes
- Additional washing step with 0.1x HB at 70°C for 2 min
- Blocking of beads with blocking solution before hybridization (MacGregor *et al.*, 2002).

The higher hybridization temperature of 65°C, as well as the stringent washing step using 0,1x Hybridization buffer were introduced into the PhyloTrap protocol to provide discrimination against specific targets. Additionally, beads were blocked with 0,1% Blocking Solution (Roche) in 0,5xSSC buffer for 1 hour prior to addition of probes, as recommended in (MacGregor *et al.*, 2002).

Modified protocol with specific rRNA yield:

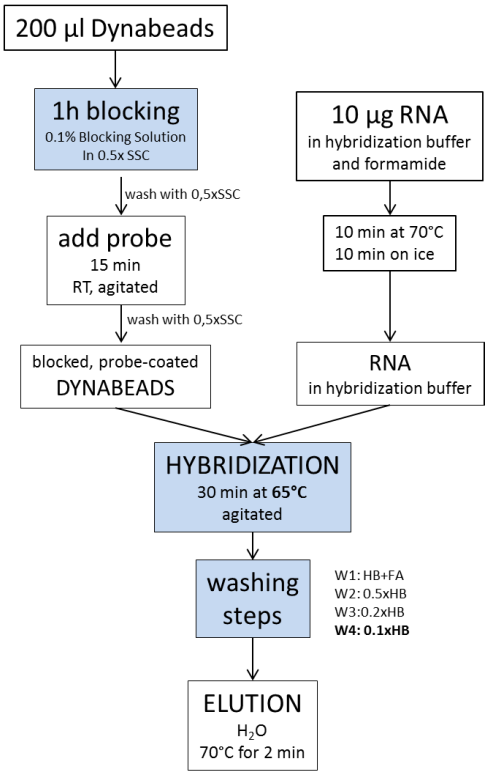

Figure 70: Flowchart of the modified Phylotrap Protocol. Modified steps are explained above and highlighted in blue boxes.

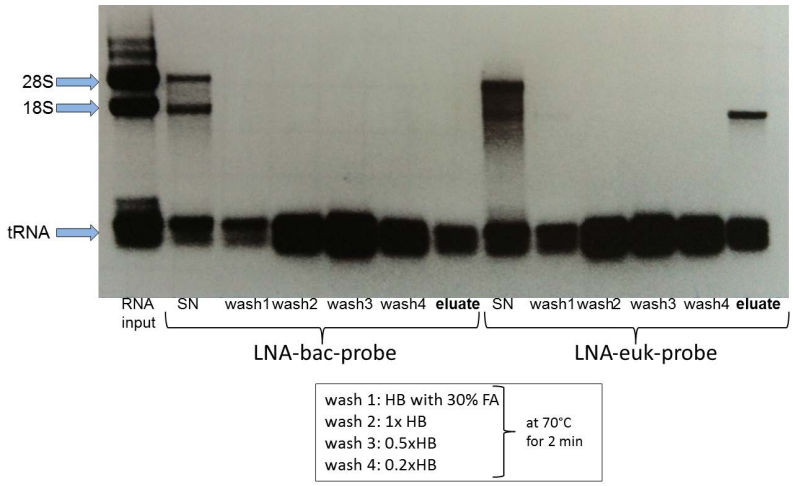

Figure 71: Fractions on the gel after using the modified PhyloTrap protocol, using *A.nidulans* RNA on LNA enhanced bacterial probe (left section) and LNA enhanced eukaryotic probe (right section).

Using the modifications as described above, specific fungal 18S rRNA could be recovered with LNA enhanced euk-probe, while no unspecific rRNA showed up in the eluate of bac-probe coated Dynabeads.

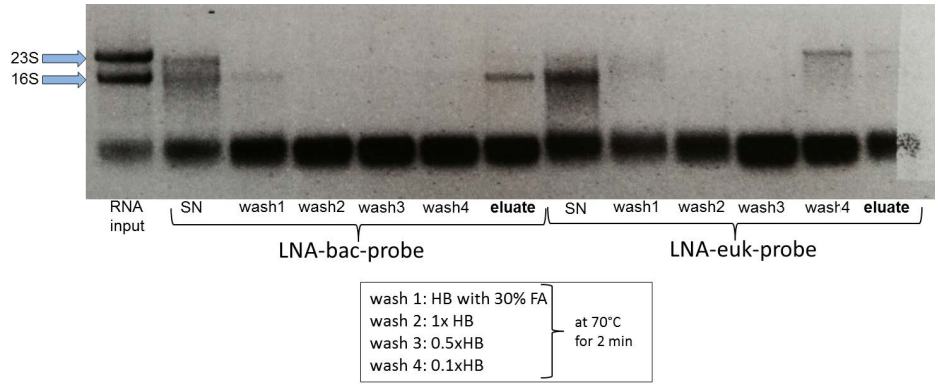

Figure 72: Fractions on the gel after using the modified PhyloTrap protocol, using *R.terrigena* RNA on LNA enhanced bacterial probe (left section) and LNA enhanced eukaryotic probe (right section).

Specific recovery of *R.terrigena* SSU rRNA is shown for LNA enhanced bac-probe in Figure 72. Washing step 4 (very low concentration) is crucial to remove unspecific binding of bacterial rRNA to the LNA-euk-probe.

3.3.3 Optimization of hybridization conditions

Using the general protocol outline as shown in Figure 70, several conditions were tested to finetune the Phylotrap method.

3.3.3.1 Formamide concentration

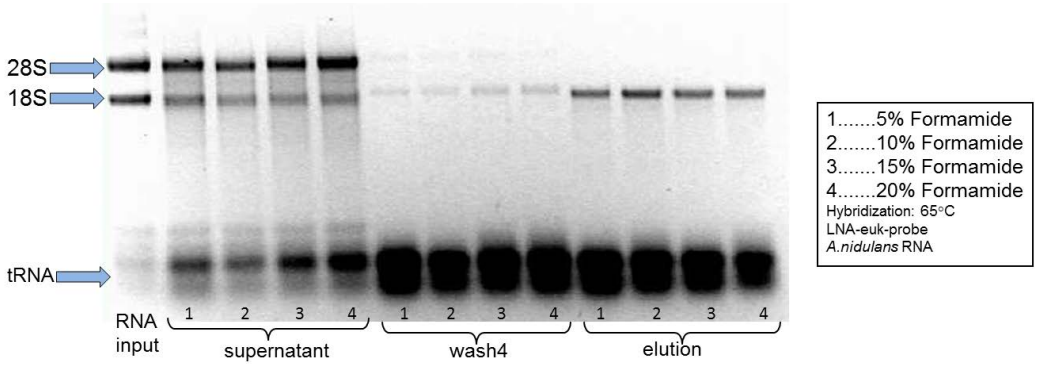

Figure 73: Phylotrap protocol (euk-probe) tested for four different Formamide concentrations in the hybridization buffer: 5, 10, 15 and 20%. *A.nidulans* RNA was used on LNA-euk probe, Hybridization was performed at 65°C for 30 minutes. wash4 = 0.1x Hybridization Buffer.

The Phylotrap method was tested with four different Formamide concentrations in the hybridization buffer. Upon using LNA-euk-probe coated Dynabeads with *A.nidulans* RNA, the 10%Formamide treatment resulted in the strongest SSU recovery in the elution fraction (see Figure 73, elution 2).

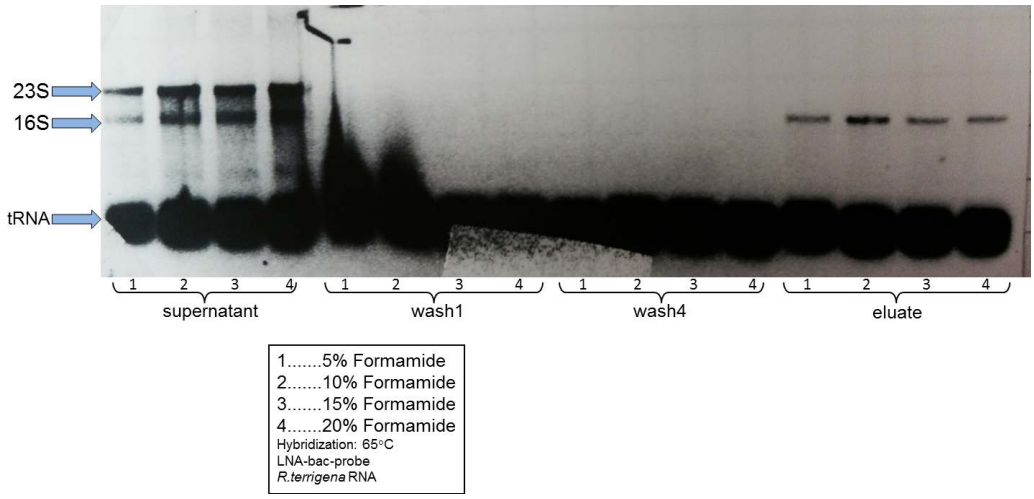

Figure 74: Phylotrap protocol (bac-probe) tested for four different Formamide concentrations in the hybridization buffer: 5, 10, 15 and 20%. *R.terrigena* RNA was used on LNA-bac probe. Hybridization was performed at 65°C for 30 minutes. Wash1 = 1xHybridization buffer (HB), wash4 = 0.2x Hybridization buffer.

As with the LNA-euk-probe, the 10% Formamide condition in the hybridization buffer also resulted in the strongest SSU rRNA yield with LNA-bac-probe coated Dynabeads using the specific target *R.terrigena* RNA (see Figure 74, eluate2).

3.3.3.2 Hybridization temperature

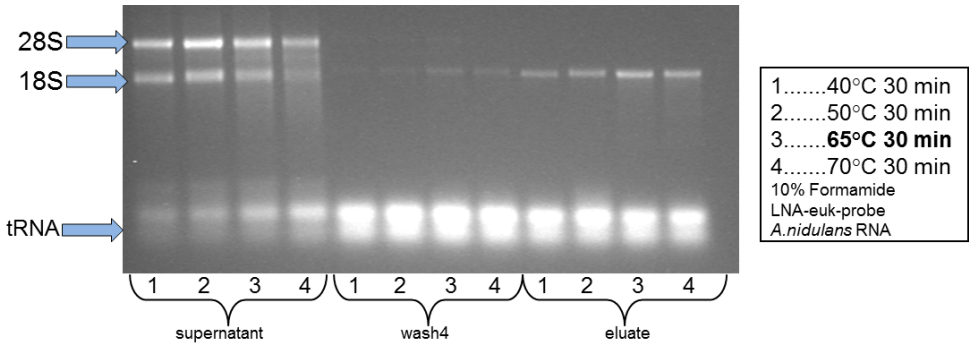

Figure 75: Phylotrap protocol (euk-probe) tested for four different hybridization temperatures: 40, 50, 65 and 70°C respectively. *A.nidulans* RNA was used on LNA-euk probe, using 10% formamide in the hybridization buffer. Supernatant after hybridization = unhybridized RNA. Wash4=0.1xHybridization buffer.

Hybridization temperatures were tested for the Phylotrap method using *A.nidulans* RNA and LNA-euk-probe coated Dynabeads. After 30 minutes of hybridization, the hybridization temperature of 65°C seemed to work best for fungal SSU yield (see Figure 75, eluate 3).

Since the 18S band in the supernatant after hybridization seemed to be even less prominent for the 70°C hybridization sample (Supernatant sample 4), which suggests higher amounts of hybridization, the 65°C and 70°C temperatures were tested again:

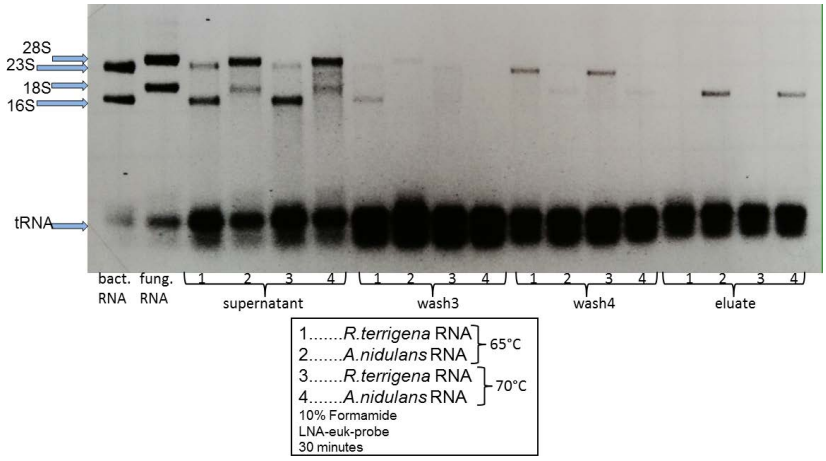

Figure 76: Phylotrap protocol tested with LNA-euk probe for two different hybridization temperatures: 65 and 70°C, with specific target (*A.nidulans* RNA) and unspecific target (*R.terrigena* RNA) respectively. 10% formamide was used in the hybridization buffer. Wash4=0.1xHybridization buffer.

According to the experiment with specific and unspecific target RNA and LNA-euk-probe coated Dynabeads, the fungal SSU capture after hybridization at 65°C was most satisfying (see Figure 76 , eluate 2). However the LSU of unspecific target RNA of *R.terrigena* did hybridize as well (see Figure 76 , supernatant 1 and 3), and was not reduced by a higher hybridization temperature. Only the stringent washing step wash4 with 0.1x HB (at 70°C for 2 minutes) was able to remove the unspecific rRNA before elution (wash4; bands 1 and 3).

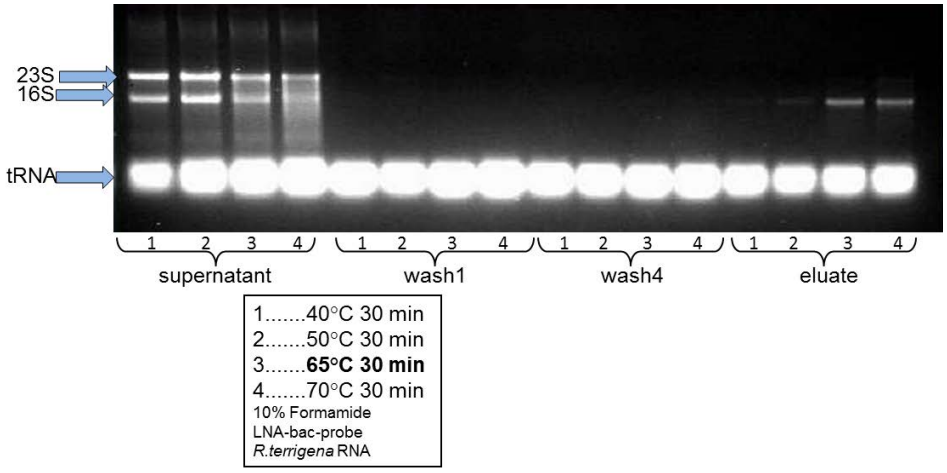

Figure 77: Phylotrap protocol (bac-probe) tested for four different hybridization temperatures: 40, 50, 65 and 70°C respectively. *R.terrigena* RNA was used on LNA-bac probe, using 10% formamide in the hybridization buffer. Wash1= 1xHybridization buffer. Wash4=0.2xHB.

Also the probe specific for bacterial SSU, LNA-bac-probe, was tested for the same temperature range with the specific target *R.terrigena* RNA. As shown in Figure 77, only hybridization temperatures of 65 and 70°C produced a significant bacterial SSU band in the eluate.

Overall, for both the bacterial and eukaryotic LNA enhanced probes, higher hybridization temperatures produced an increase in SSU rRNA yield using the Phylotrap method. The temperature of 70°C did not provide better rRNA yield than hybridization at 65°C, and together with the higher risk of RNA degradation, this was the reason to choose the hybridization temperature of 65°C for further experiments.

3.3.3.3 Hybridization time

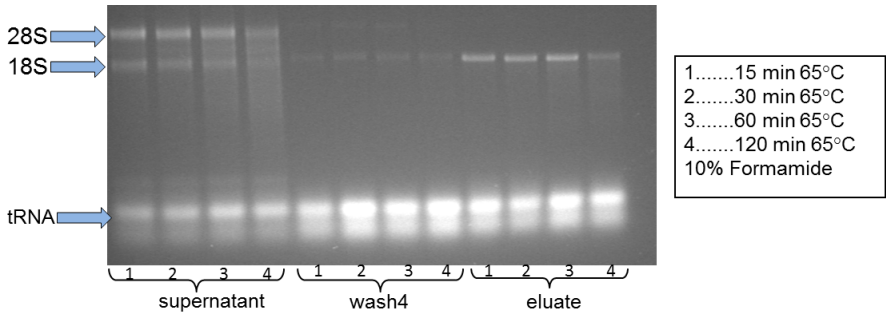

Figure 78: Phylotrap protocol tested with *A.nidulans* RNA on LNA-euk probe for different hybridization times: 15, 30, 60 and 120 minutes. Hybridization was performed in 10% Formamide at 65°C. Wash4=0.1x Hybridization buffer.

Different hybridization times were tested for the specific target *A.nidulans* RNA on LNA-euk-probe coated Dynabeads. When using 10% Formamide in the hybridization buffer at 65°C, the hybridization times 30 and 60 minutes resulted in the strongest SSU band on the gel. Because of a higher risk of RNA degradation with longer incubation times, the hybridization time of 30 minutes was chosen for further experiments.

3.3.3.4 Phylotrap optimized protocol

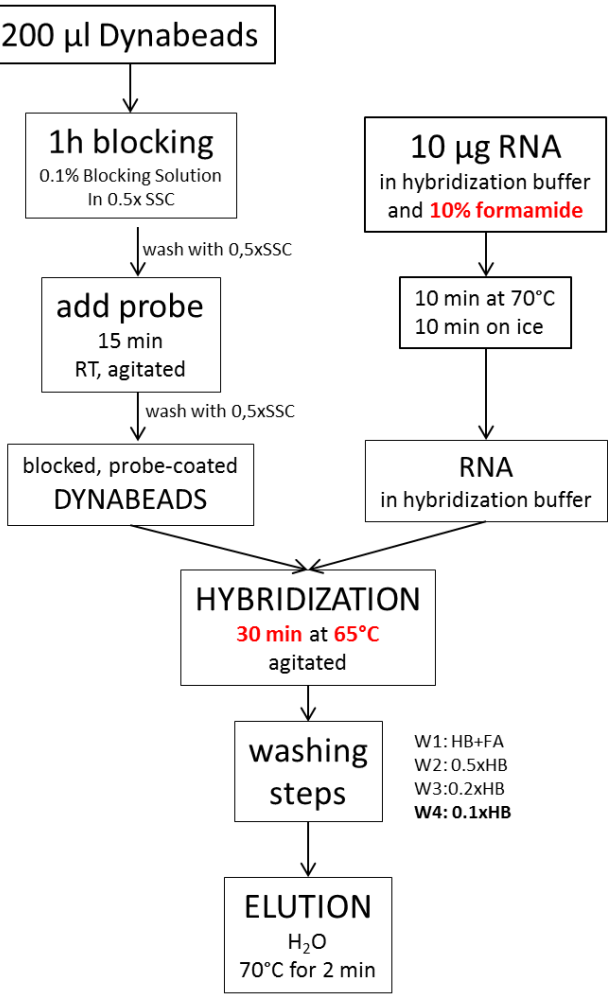

Figure 79: Phylotrap protocol including the optimized conditions highlighted in red.

Dynabeads:	50 µl/reaction		
RNA:	5 µg / reaction		
LNA probes:	12,5 pmol / reaction		
Formamide:	10%		
Hybridization:	Hybridization buffer (HB)		
	5xSSC		
	0,1% N-laurylsarcosine		
	0,1% NaCl		
	0,02% SDS		
	30 minutes		
	65°C		
Washing:	W1: 1xHB	70°C 2 min	
	W2: 0,5xHB	70°C 2 min	
	W3: 0,2xHB	70°C 2 min	
	W4: 0,2xHB	70°C 2 min	FOR BAC338
	W4: 0,1xHB	70°C 2 min	FOR EUKb310

Elution H_2O 70°C 2 min

3.3.4 Phylotrap with mixed RNAs

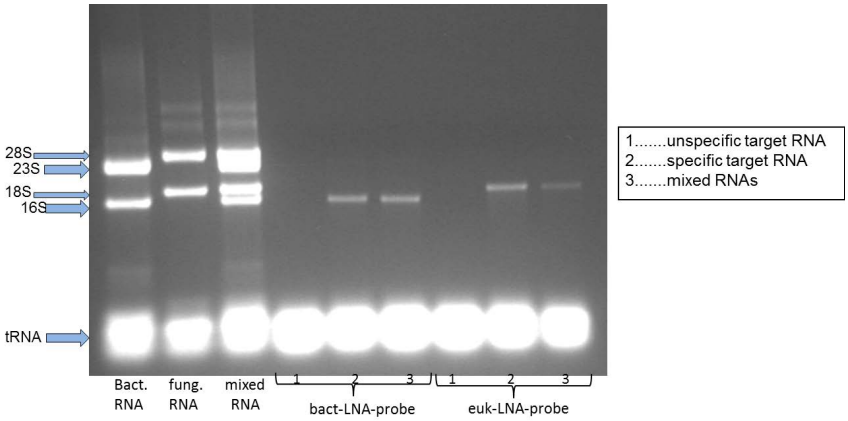

Figure 80: Phylotrap protocol with bacterial RNA (R.terrigena), fungal RNA (A.nidulans) and mixed RNA (R.terrigena + A.nidulans) using Dynabeads coated with LNA enhanced probes. Specific target for bact-LNA-probe: 5 µg R.terrigena RNA. specific target for euk-LNA-probe: 5 µg A.nidulans RNA. Mixed RNAs: 5 µg R.terrigena RNA + 5 µg A.nidulans RNA. Hybridization was performed in 10% Formamide at 65°C for 30 min.

Testing the Phylotrap protocol with *A.nidulans* and *R.terrigena* RNA mixed together, the specific target SSUs were recovered with no unspecific SSU or LSU showing on the gel. For bact-LNA-probe, the samples containing specific target (i.e. samples 2 and 3) showed clean bacterial SSU recovery bands with the same intensity for both mixed and single species RNA. Phylotrap performed with euk-LNA-probe coated Dynabeads also produced specific fungal SSU bands in sample 2 and 3 without unspecific contamination. However for the euk-LNA-probe, specific target fungal SSU rRNA could not be recovered from the mixed sample with the same yield as from the single species RNA sample (sample 2 vs sample 3).These samples were also tested with quantitative Real-Time PCR using primers for 18S and 28S rRNA, see Figure 81:

Figure 81: 18S capture from *A.nidulans* RNA with LNA-euk-probe coated Dynabeads, analyzed by qPCR. Primers: "SR7R-SR5" for 18S and "Ctb6-TW13" for 28 S. Specific target for euk-LNA-probe: 5 µg *A.nidulans* RNA. Mixed sample: 5 µg *A.nidulans* RNA + 5 µg *R.terrigena* RNA. Samples were reverse transcribed and analyzed by qRT- PCR with reverse transcribed *A.nidulans* RNA dilutions as standards. In this diagram, RNA amounts of elution fractions were normalized to the detected RNA amount in the input.

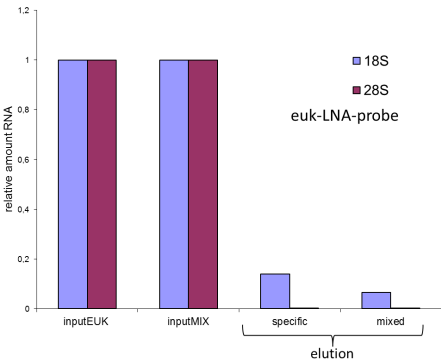

In mixed samples, the specific RNA capturing efficiency goes down by 53% compared to the clean RNA samples when using eukLNA probe-coated Dynabeads, from 14%

capture in the sample with specific target only (inputEUK), to 6% in the sample with mixed target (inputMIX) which contained *A.nidulans* as well as *R.terrigena* RNA.

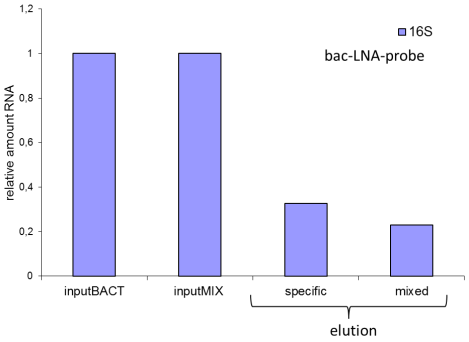

Figure 82: 16S capture from pure *R.terrigena* RNA and RNA mix (*A.nidulans and R.terrigena)* with LNA-bac-probe coated Dynabeads, analyzed by qPCR. Primers: "EUBf933-EUBr1387" for bacterial 16S. Specific target for bac-LNA-probe: 5 µg *R.terrigena* RNA. Mixed sample: 5 µg *A.nidulans* RNA + 5 µg *R.terrigena* RNA. Samples were reverse transcribed and analyzed by qRT- PCR with reverse transcribed *R.terrigena* RNA dilutions as standards. In this diagram, RNA amounts were normalized to the detected RNA amount in the input.

Real-time PCR with primers for bacterial 16S rRNA confirmed what the gels in Figure 80 suggested. The total specific rRNA yield by Phylotrap was higher using the bac-LNA-probe than the euk-LNA-probe, and the capturing efficiency decrease was lower when using the mixed RNA sample compared to the clean RNA sample. 16S rRNA capturing efficiency went down from 33% to 23% in the mixed sample which is a 30% decrease.

To test if higher stringency was needed to increase capturing efficiency with eukLNA-probes in mixed samples, different Formamide concentrations were tested with mixed RNA samples :

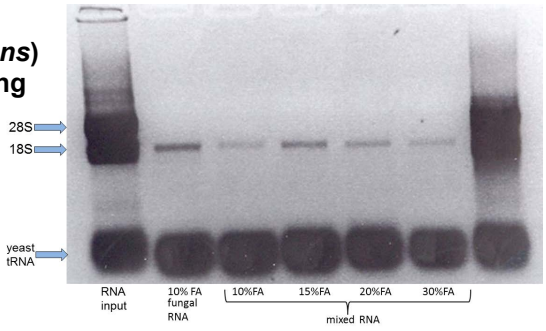

Figure 83: Phylotrap protocol fungal RNA (*A.nidulans*) and mixed RNA *(A.nidulans and R.terrigena)* using Dynabeads coated with LNA-euk-probe. Specific target for euk-LNA-probe: 5 µg *A.nidulans* RNA. Mixed RNAs: 5 µg *R.terrigena* RNA + 5 µg *A.nidulans* RNA. Hybridization was performed at 65°C for 30 min. Different formamide concentrations in the hybridization buffer were used: 10%, 15%, 20% and 30% as indicated in the figure.

As shown in Figure 83, the specific RNA yield from mixed RNA samples could be increased by using the higher formamide concentration of 15% instead of 10% in the hybridization buffer for the Phylotrap method. The formamide concentrations of 20% and 30% were not able to increase the specific yield significantly.

For phylotrap experiments using LNA-euk-probe coated Dynabeads and mixed RNA samples, the formamide concentration of 15% was therefore used for further

experiments in mixed RNA samples to match the yield of pure culture *A.nidulans* RNA that was achieved at 10% formamide.

To increase the total specific rRNA yield from mixed samples further, the supernatant after hybridization (i.e. the unhybridized fraction of RNA) was reused for another round of hybridization for a higher total yield from the same sample. One mixed RNA sample was divided, to be hybridized with both probes respectively (a and b).

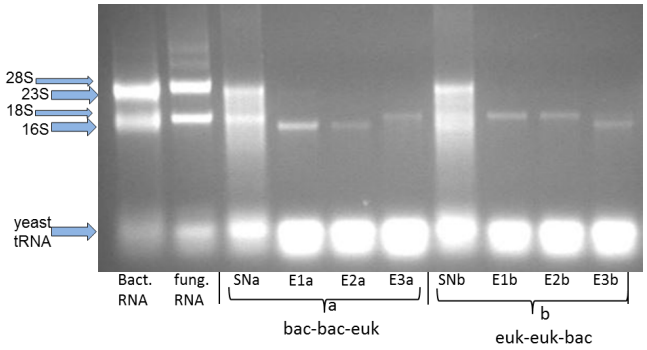

Figure 84: : Phylotrap protocol including multiple hybridizations. Mixed RNA *(A.nidulans and R.terrigena)* was hybridized with Dynabeads coated with LNA enhanced probes, reusing the supernatant for two more hybridizations. Mixed RNAs: 5 µg *R.terrigena* RNA + 5 µg *A.nidulans* RNA. Hybridization was performed in 65°C for 30 min with 15% Formamide. (a) Mixed RNA was hybridized with LNA-bac-probe, yielding eluate E1a. Supernatant was hybridized again with LNA-bac-probe, yielding eluate E2a. Then, supernatant was hybridized with LNA-euk-probe, yielding eluate E3a. (b) Mixed RNA was hybridized with LNA-euk-probe, yielding eluate E1b. Supernatant was hybridized again with LNA-euk-probe, yielding eluate E2b. Then, supernatant was hybridized with LNA-bac-probe, yielding eluate E3b.

The RNA eluates after multiple hybridizations were quantified with a fluorescence RNA quantitation kit (Invitrogen), see Figure 85.

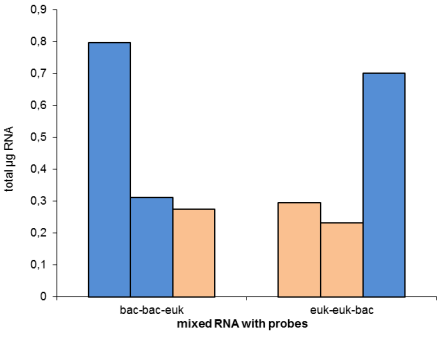

Figure 85: RNA quantification after mixed RNA Phylotrap capture, using multiple hybridizations from the same sample. 7 µg bacterial (*R.terrigena*) RNA and 7 µg fungal RNA *(A.nidulans*) were used in a mixed sample for specific SSU rRNA capture with LNA-euk-probe (euk) and LNA-bac probe (bac). Eluates were quantified with Quant-iT™ RNA Assay Kit. Left section: Mixed RNA sample was hybridized with LNA-bac-probe coated Dynabeads twice, and finally with LNA-euk-probe coated Dynabeads. Right section: Mixed RNA sample was hybridized with LNA-euk-probe coated Dynabeads twice, and finally with LNA-bac-probe coated Dynabeads.

The Phylotrap SSU rRNA capture using multiple hybridizations was able to capture a total of 1,8 µg bacterial and 0,8 µg fungal SSU RNA, which puts the total yield at 26% capture from one sample by the bacterial probe and 11% by the eukaryotic probe, respectively.

University of Natural Resources
and Applied Life Sciences, Vienna

Affidavit

I hereby declare that I am the sole author of this work; no assistance other than that permitted has been used and all quotes and concepts taken from unpublished sources, published literature or the internet in wording or in basic content have been identified by footnotes or with precise source citations.

I further declare that all persons and institutions that have directly or indirectly helped me with the preparation of the thesis have been acknowledged and that this thesis has not been submitted, wholly or substantially, as an examination document at any other institution.

Date	Signature